

BTIC FILE COPY

(1)

AGARD-CP-449

AGARD-CP-449

AD-A214 462

AGARD CONFERENCE PROCEEDINGS No.449

# Application of Advanced Material for Turbomachinery and Rocket Propulsion

DISTRIBUTION STATEMENT A  
Approved for public release  
Distribution Unlimited

DTIC  
ELECTE  
MAY 15 1989  
S D



DISTRIBUTION AND AVAILABILITY  
ON BACK COVER

89 5 15 091

NORTH ATLANTIC TREATY ORGANIZATION  
ADVISORY GROUP FOR AEROSPACE RESEARCH AND DEVELOPMENT  
(ORGANISATION DU TRAITE DE L'ATLANTIQUE NORD)

AGARD Conference Proceedings No.449  
**APPLICATION OF ADVANCED MATERIAL FOR TURBOMACHINERY  
AND ROCKET PROPULSION**

Accession For	
NTIS	CRA&I <input checked="" type="checkbox"/>
DTIC	TAB <input type="checkbox"/>
Unannounced <input type="checkbox"/>	
Justification	
By _____	
Distribution / _____	
Availability Codes	
Dist	Aval. and/or Special
A-1	



Papers presented at the Propulsion and Energetics Panel 72nd A Specialists' Meeting,  
held in Bath, United Kingdom, 3-5 October 1988.

## **THE MISSION OF AGARD**

According to its Charter, the mission of AGARD is to bring together the leading personalities of the NATO nations in the fields of science and technology relating to aerospace for the following purposes:

- Recommending effective ways for the member nations to use their research and development capabilities for the common benefit of the NATO community;
- Providing scientific and technical advice and assistance to the Military Committee in the field of aerospace research and development (with particular regard to its military application);
- Continuously stimulating advances in the aerospace sciences relevant to strengthening the common defence posture;
- Improving the co-operation among member nations in aerospace research and development;
- Exchange of scientific and technical information;
- Providing assistance to member nations for the purpose of increasing their scientific and technical potential;
- Rendering scientific and technical assistance, as requested, to other NATO bodies and to member nations in connection with research and development problems in the aerospace field.

The highest authority within AGARD is the National Delegates Board consisting of officially appointed senior representatives from each member nation. The mission of AGARD is carried out through the Panels which are composed of experts appointed by the National Delegates, the Consultant and Exchange Programme and the Aerospace Applications Studies Programme. The results of AGARD work are reported to the member nations and the NATO Authorities through the AGARD series of publications of which this is one.

Participation in AGARD activities is by invitation only and is normally limited to citizens of the NATO nations.

The content of this publication has been reproduced  
directly from material supplied by AGARD or the authors.

**Published March 1989**

**Copyright © AGARD 1989**  
**All Rights Reserved**

**ISBN 92-835-0498-4**



*Printed by Specialised Printing Services Limited  
40 Chigwell Lane, Loughton, Essex IG10 3TZ*

**RECENT PUBLICATIONS OF THE PROPULSION AND ENERGETICS PANEL**

**Conference Proceedings**

- Testing and Measurement Techniques in Heat Transfer and Combustion  
AGARD Conference Proceedings No.281, 55th A Meeting, May 1980
- Centrifugal Compressors, Flow Phenomena and Performance  
AGARD Conference Proceedings No.282, 56th B Meeting, May 1980
- Turbine Engine Testing  
AGARD Conference Proceedings No.293, 56th Meeting, Sep/October 1980
- Helicopter Propulsion Systems  
AGARD Conference Proceedings No.302, 57th Meeting, May 1981
- Ramjets and Ramrockets for Military Applications  
AGARD Conference Proceedings No.307, 58th Meeting, October 1981
- Problems in Bearings and Lubrication  
AGARD Conference Proceedings No.323, 59th Meeting, May/June 1982
- Engine Handling  
AGARD Conference Proceedings No.324, 60th Meeting, October 1982
- Viscous Effects in Turbomachines  
AGARD Conference Proceedings No.351, 61st A Meeting, June 1983
- Auxiliary Power Systems  
AGARD Conference Proceedings 352, 61st B Meeting, May 1983
- Combustion Problems in Turbine Engines  
AGARD Conference Proceedings 353, 62nd Meeting, October 1983
- Hazard Studies for Solid Propellant Rocket Motors  
AGARD Conference Proceedings 367, 63rd A Meeting, May/June 1984
- Engine Cyclic Durability by Analysis and Testing  
AGARD Conference Proceedings No.368, 63rd B Meeting, May/June 1984
- Gears and Power Transmission Systems for Helicopters and Turboprops  
AGARD Conference Proceedings No.369, 64th Meeting October 1984
- Heat Transfer and Cooling in Gas Turbines  
AGARD Conference Proceedings No.390, 65th Meeting, May 1985
- Smokeless Propellants  
AGARD Conference Proceedings No.391, 66th A Meeting, September 1985
- Interior Ballistics of Guns  
AGARD Conference Proceedings No.392, 66th B Meeting, September 1985
- Advanced Instrumentation for Aero Engine Components  
AGARD Conference Proceedings No.399, 67th Meeting, May 1986
- Engine Response to Distorted Inflow Conditions  
AGARD Conference Proceedings No.400, 68th A Meeting, September 1986
- Transonic and Supersonic Phenomena in Turbomachines  
AGARD Conference Proceedings No.401, 68th B Meeting, September 1986
- Advanced Technology for Aero Engine Components  
AGARD Conference Proceedings No.421, 69th Meeting, September 1987
- Combustion and Fuels in Gas Turbine Engine  
AGARD Conference Proceedings No.422, 70th Meeting, October 1987
- Engine Condition Monitoring -- Technology and Experience  
AGARD Conference Proceedings No.448, 71st Meeting, May/June 1988

#### **Working Group Reports**

##### **Aircraft Fire Safety**

AGARD Advisory Report 132, Vol.1 and Vol.2. Results of WG 11 (September and November 1979)

##### **Turbulent Transport Phenomena (in English and French)**

AGARD Advisory Report 150. Results of WG 09 (February 1980)

##### **Through Flow Calculations in Axial Turbomachines**

AGARD Advisory Report 175. Results of WG 12 (October 1981)

##### **Alternative Jet Engine Fuels**

AGARD Advisory Report 181. Vol.1 and Vol.2. Results of WG 13 (July 1982)

##### **Suitable Averaging Techniques in Non-Uniform Internal Flows**

AGARD Advisory Report 182 (in English and French). Results of WG 14 (June/August 1983)

##### **Producibility and Cost Studies of Aviation Kerosines**

AGARD Advisory Report 227. Results of WG 16 (June 1985)

##### **Performance of Rocket Motors with Metallized Propellants**

AGARD Advisory Report 230. Results of WG 17 (September 1986)

#### **Lecture Series**

##### **Non-Destructive Inspection Methods for Propulsion Systems and Components**

AGARD LS 103 (April 1979)

##### **The Application of Design to Cost and Life Cycle Cost to Aircraft Engines**

AGARD LS 107 (May 1980)

##### **Microcomputer Applications in Power and Propulsion Systems**

AGARD LS 113 (April 1981)

##### **Aircraft Fire Safety**

AGARD LS 123 (June 1982)

##### **Operation and Performance Measurement of Engines in Sea Level Test Facilities**

AGARD LS 132 (April 1984)

##### **Ramjet and Ramrocket Propulsion Systems for Missiles**

AGARD LS 136 (September 1984)

##### **3-D Computation Techniques Applied to Internal Flows in Propulsion Systems**

AGARD LS 140 (June 1985)

##### **Engine Airframe Integration for Rotorcraft**

AGARD LS 148 (June 1986)

##### **Design Methods Used in Solid Rocket Motors**

AGARD LS 150 (April 1987)

AGARD LS 150 (Revised) (April 1988)

#### **Other Publications**

##### **Airbreathing Engine Test Facility Register**

AGARD AG 269 (July 1981)

##### **Rocket Altitude Test Facility Register**

AGARD AG 297 (March 1987)

##### **Manual for Aeroelasticity in Turbomachines**

AGARD AG 298/1 (March 1987)

AGARD AG 298/2 (June 1988)

##### **Application of Modified Loss and Deviation Correlations to Transonic Axial Compressors**

AGARD Report 745 (November 1987)

### THEME

In the last few years, advances have been made in the field of materials to be applied in the hot parts of aerospace propulsion systems. The purpose of the Specialists' Meeting was to provide a forum for users of the new materials in the fields of turbomachinery and rockets, to report on recent achievements and to discuss the various applications. The scope of the Specialists' Meeting included the interaction between the properties of new materials and their potential applications; coatings, refractory metals; superalloys; composites and insulation. *(Keywords: composite materials; metal matrix composites; Symposium; (\*\*) — \*\*\**

Au cours des dernières années, des progrès notables ont été réalisés dans le domaine des matériaux qui composent la partie chaude des systèmes de propulsion des véhicules aéronautiques. Cette réunion de spécialistes a servi de forum aux utilisateurs des nouveaux matériaux dans les domaines de la turbomachinerie et des moteurs-fusées, en leur fournissant l'occasion de rendre compte des réalisations récentes et de discuter de différentes applications possibles. Le programme de la réunion comprenait les thèmes suivants: l'interaction entre les caractéristiques des nouveaux matériaux et leurs applications potentielles; les revêtements, les métaux réfractaires, les superalliages; les matériaux composites et la protection thermique.

## **PROPULSION AND ENERGETICS PANEL**

<b>Chairman:</b> Dr W.L.Macmillan EHF Communication Satellite Defence Research Establishment Ottawa, Ontario K1A 0Z4 Canada	<b>Deputy Chairman:</b> M. l'Ing. Princ. de l'Armement P.Ramette Société Européen de Propulsion Attaché au Directeur Technique pour les Activités Spatiales Boite Postal 303 92156 Suresnes Cedex France
---	--

## **PROGRAMME COMMITTEE**

Dr D.E.Colbourne (Chairman) Assistant Director, Engines 1 MOD (PE) St Giles Court 1-13 St Giles High Street London WC2H 8LD, UK	Dr-Ing. G.Maoli FIAT s.p.a. Direzione Via L.Bissolatti 57 00157 Roma, Italy
Prof. R.Jacques Ecole Royale Militaire 30 Avenue de la Renaissance 1040 Bruxelles, Belgium	Mr D.M.Rudnitski Division of Mechanical Engineering National Research Council of Canada Ottawa, Ontario K1A 0R6, Canada
Mr P.Lamicq Société Européenne de Propulsion Etablissements de Bordeaux Le Haillan — BP 37 33165 Saint Médard en Jalles, France	Mr W.W.Wagner Technical Director Naval Air Propulsion Center PO Box 7176 Trenton, New Jersey 08628-0176, USA
Dr-Ing. H.Lichtfuss Motoren und Turbinen Union Dachauerstrasse 665 8000 München 50, Germany	

## **HOST NATION COORDINATOR**

Dr D.E.Colbourne

## **PANEL EXECUTIVE**

Dr E.Riester  
AGARD-NATO-PEP  
7 rue Ancelle  
92200 Neuilly sur Seine  
France

## **ACKNOWLEDGEMENT**

The Propulsion and Energetics Panel wishes to express its thanks to the National Delegates from the United Kingdom for the invitation to hold this meeting in Bath, and for the facilities and personnel which made the meeting possible.

## CONTENTS

	Page
<b>RECENT PUBLICATIONS OF PEP</b>	iii
<b>THEME</b>	v
<b>PROPULSION AND ENERGETICS PANEL</b>	vi
<b>TECHNICAL EVALUATION REPORT</b> by N.M.Tallan	ix
	<b>Reference</b>
<b><u>SESSION I – OVERVIEW AND COMBINED APPLICATIONS</u></b>	
<b>APPLICATION OF ADVANCED MATERIALS FOR TURBOMACHINERY AND ROCKET PROPULSION</b> by J.B.Moore	1
<b>MONOLITHIC AND FIBER CERAMIC COMPONENTS FOR TURBO-ENGINES AND ROCKETS</b> by R.Kochendörfer	2
<b>CVD AND DIFFUSION COATINGS FOR HIGH TEMPERATURE APPLICATIONS IN TURBOMACHINERY AND ROCKET MOTORS</b> by S.P. Field, J.E.Restall, C.D.Chalk and C.Hayman	3
<b><u>SESSION II – GAS TURBINE APPLICATIONS</u></b>	
<b>FUTURE ADVANCED AERO-ENGINES – THE MATERIALS CHALLENGE</b> by D.R.Higton and W.J.Chrispin	4
<b>NEW METALLIC MATERIALS FOR GAS TURBINES</b> by M.A.Hicks	5
<b>DAMAGE TOLERANCE CONCEPTS FOR ADVANCED MATERIALS AND ENGINES</b> by T.E.Farmer and M.C.VanWanderham	6
<b>MATERIAL/MANUFACTURING PROCESS INTERACTION IN ADVANCED MATERIAL TECHNOLOGIES</b> by G.W.Meetham	7
<b>DEVELOPMENT OF STRESS AND LIFING CRITERIA FOR SINGLE CRYSTAL TURBINE BLADES</b> by S.Salvano, M.Stanisci and E.Campo	8
<b>ADVANCED MATERIALS TO COMBAT THE HIGH TEMPERATURE DEGRADATION PROCESSES IN TURBOMACHINERY</b> by P.Hancock and J.E.Restall	9
<b>THE DEMONSTRATION OF MONOLITHIC AND COMPOSITE CERAMICS IN AIRCRAFT GAS TURBINE COMBUSTORS</b> by F.G.Davis and D.A.Hudson	10
<b>COMPOSITE MATERIAL SYSTEMS FOR HIGH TEMPERATURE APPLICATIONS</b> by E.R.Thompson	11
<b>UTILISATION DES COMPOSITES HAUTES TEMPERATURES DANS LES TURBOREACTEURS</b> par R.Mestre	12
<b>INITIAL RESULTS OF TESTS ON METAL-CERAMIC GUIDE VANES</b> by W.Hüther and W.Krüger	13
<b>INTERACTION OF COATINGS WITH BASE METALS AT HIGH TEMPERATURE</b> by H.W.Gründling, K.Schneider and L.Singheiser	14

**Reference**

**SESSION III -- ROCKET APPLICATIONS**

**Paper 15 withdrawn**

**Paper 16 withdrawn**

**VACUUM PLASMA SPRAY COATING**  
by R.R.Holmes and T.N.McKechnie

**17**

**THRUST CHAMBER THERMAL BARRIER COATING TECHNIQUES**  
by R.J.Quentmeyer

**18**

**SILICON-CARBIDE COATED CARBON-CARBON – AN ADVANCED MATERIAL  
FOR ROCKET SYSTEMS**  
by E.v.Geilhorn, U.Gruber and H.Leis

**19**

**FIBER REINFORCED SUPERALLOYS FOR ROCKET ENGINES**  
by D.W.Petrasek and J.R.Stephens

**20**

**BEHAVIOUR OF TUNGSTEN, MOLYBDENUM AND ALLOYS UNDER UNUSUAL HEATING  
CONDITIONS**  
by R.Eck, H.Bilstein, F.Simader, R.Stickler and J.Tinzl

**21**

**LES MATERIAUX COMPOSITES REFRACTAIRES A HAUTE PERFORMANCE**  
par A.Hordonneau

**22**

**HIGH TEMPERATURE COMPOSITE MATERIALS FOR ROCKET PROPULSION**  
by P.Donguy and J.Broca

**23**

**SESSION IV – SPECIAL APPLICATIONS**

**ECHANGEURS DE CHALEUR ET AUBES DE TURBINE EN CERAMIQUE – THEORIE ET  
RESULTATS EXPERIMENTAUX**  
par P.Avran et S.Boudigues

**24**

**CRYOGENIC TURBOPUMP BEARING MATERIALS**  
by B.N.Bhat

**25**

**DEVELOPMENT OF AN ASBESTOS-FREE INSULANT FOR ROCKET MOTORS**  
by D.Sanschagrin and G.Couture

**26**

**METALLURGICAL STUDY OF SUPERALLOY BRAZING ALLOYS**  
by Ch.Lecomte-Mertens and W.Bex

**27**

TECHNICAL EVALUATION REPORT

by

Norman M. Tallan  
Metals & Ceramics Division  
AFWAL Materials Laboratory  
Wright-Patterson Air Force Base  
Dayton, Ohio 45433

1. INTRODUCTION

The 72nd-A Propulsion and Energetics Panel Specialists' Meeting on Application of Advanced Material for Turbomachinery and Rocket Propulsion was held in Bath, the United Kingdom, from 3-5 October 1988.

The development of airbreathing turbine engines and rocket propulsion systems, from their inception, have been paced primarily by the availability of materials strong or stiff enough, and durable enough under the harsh conditions of the engine to meet the requirements of emerging designs. This is especially true today, and many experts in the field now believe that the next major revolution in propulsion will be primarily the result of new materials capabilities, and the new structural design concepts they will allow.

The objectives of this meeting were to bring together the designers, developers and users of aerospace propulsion systems and the developers and producers of aerospace materials to provide a forum in which the material requirements of both current and future propulsion systems and the ability of emerging new materials to meet those requirements could be reviewed. The scope of the Specialists' Meeting included the properties and potential applications of superalloys, refractory metals, advanced intermetallic alloys, and metal matrix composites based on them; carbon-carbon and ceramic matrix composites; coatings and the processes used to prepare them; bearing and insulation materials; braze and weld repair methods; innovative design approaches to the use of these new materials; and the damage tolerance and life prediction of these materials and their implications with regard to damage tolerant design and applications to real propulsion systems.

A special effort was made, by including both airbreathing turbine and rocket propulsion systems in the program, to bring these two communities of propulsion system and materials developers together to explore and take advantage of the many similarities of problems and accomplishments in these two closely related fields.

The technical program was arranged by a committee under the chairmanship of Dr. D.E. Colbourne. The papers provided an excellent balance between the various types of materials involved, the materials producibility issues, the materials behavior issues, and the design factors involved. Of the twenty-five papers presented, ten were primarily turbine engine and nine primarily rocket engine oriented, eight dealt with metals and nine with

ceramic or carbon-carbon composites, and while most dealt primarily with the materials themselves, six dealt to a major extent with aspects of behavior, design and manufacturing.

## 2. GENERAL SUMMARY

The keynote paper by Moore [1] provided a general overview of material requirements for current and future airbreathing turbine engines and liquid fuel rocket propulsion systems. He pointed out that at least half of the advances in turbine engine performance envisioned by the engine industry for engines of the decades beyond the 1990's will come from improved materials and processes. Advanced engines of the 1990's will depend on improved superalloys for turbine disks, blades and vanes; thermal barrier coatings and improved cooling to allow still higher combustor exit temperatures; higher temperature, non-burning titanium-based alloys for static and rotating parts of the compressor and exhaust nozzle; and new component designs and fabrication methods such as integrally bladed rotors and dual alloy disks. The engines under consideration by the designers for the next century, however, will rely on aerodynamic advances, higher combustor and turbine temperatures, and especially innovative design concepts made possible by new classes of high temperature, lightweight materials. He pointed out further that a characteristic of most of the new higher temperature titanium-based and intermetallic alloys, the intermetallic matrix composites, and the carbon-carbon and ceramic matrix composites that will be needed will be their relatively low ductilities, low fracture toughnesses, and their process sensitivity, requiring that the material developer, designer and manufacturer work closer together, preferably from the very beginning, than ever before.

Mr. Moore [1] suggested that the requirements for materials for liquid fuel rocket applications, particularly in the case of rocket engine turbopumps, will largely be the same as those for gas turbines. One special requirement for advanced rocket engines, however, would be materials better able to withstand the very high heat fluxes characteristic of the throat region of the thrust chamber.

The dependence of major turbine engine advances on new materials was strongly endorsed by Higton and Chrispin [4]. They pointed out that the UK Advanced Core Military Engine (ACME) program has come to the same conclusion as the US Integrated High Performance Turbine Engine Technology (IHPTET) program, i.e. that about 70% of the doubling of the thrust-to-weight ratio of these very advanced engines will come about by taking weight out of the engine, a feat made possible primarily by the development of new materials. Much of the rest will come about by increases in cycle temperature, also made possible by radically new materials. They also, however, pointed out the need for emphasis on cost and durability in these endeavors.

Of the papers dealing with advanced metals and metal matrix composites, several were particularly noteworthy. Hicks [5] pointed out the continuing advances being made in both superalloys and titanium alloys through the integration of alloy design, microstructural engineering, and processing and manufacturing technologies, and predicted that these 'conventional' materials would continue to play a major role in turbine engine development for a number of years still to come. He also pointed out the major contribution that process modeling can make to microstructural control, and used the example of forging models for nickel-base superalloy parts to demonstrate the importance of such simulations in achieving exceptional product quality, and the ability to get it 'right the first time' rather than through a process of trial and error.

Meetham [7] provided several examples that demonstrated the importance of processing and manufacturing in getting the most out of a material, particularly as the material matures in its development cycle. He noted, for example, that when superalloys were first introduced, compositional advances alone led to significant property enhancements, but that now that their use temperatures are approaching the inherent limits of nickel-based alloy systems, manufacturing control of their microstructures and properties is playing a more and more dominant role in current superalloy development. He noted too that in the case of organic composites and the emerging ceramic and carbon-carbon composites, manufacturing plays an even greater role in defining the materials themselves and in determining the key fiber-matrix interfacial properties, and that manufacturing can therefore be expected to play a dominant role even earlier in their development cycle.

Petrasek and Stephens' paper [20] on fiber reinforced superalloys showed some of the significant gains that could be achieved in a composite in even a mature metallic system, and in so doing also highlighted some of the significant differences between aircraft gas turbines and the high pressure turbopumps used in liquid fuel rockets. They showed that superalloy composites can offer a several fold increase in life and over a 200°C increase in service temperature over materials currently used in the US space shuttle main engine turbopumps. Since these tungsten fiber reinforced superalloys are better especially in thermal shock resistance, where they are two to nine times better than currently used materials, and in resistance to hydrogen embrittlement, they are especially well suited to turbopump use. Turbopumps generally require materials that can withstand the very rapid thermal transients characteristic of start-up and shut-down, hydrogen embrittlement, and relatively short-time but high stress fatigue and creep conditions.

Eck, Bildstein, Simader, Stickler and Tinzl [21] presented a state-of-the art review of refractory metal capabilities and some of their potential applications. They pointed out, however, that there has still been very limited success in the development of coatings to protect these materials from oxidation for long times and high temperatures.

A number of papers dealt with emerging ceramic and carbon-carbon composites for turbine engine and rocket propulsion use. The use of fiber reinforcement to overcome the low toughness, brittle behavior of conventional high strength ceramics and the potential for engineeringly useful damage tolerance in the resultant ceramic matrix composites have received increasing attention in recent years. Thompson [11] showed that in fact graphite and silicon carbide fiber reinforced glass or glass-ceramic composites are available now, in at least a laboratory stage of development and quantities, and that they have crack growth resistances comparable to those of the graphite epoxy composites and potential use temperatures in the 500-1300°C range. Hudson [10], Mestre [12], Avran and Boudigues [24], and Donguy and Broca [23], in fact, presented very promising preliminary test results for even higher temperature, silicon carbide fiber reinforced silicon carbide matrix ceramic composites in turbine engine combustor, afterburner and exhaust nozzle parts, in turbine blades, and in small combustion chambers for satellite liquid rocket thruster motors.

Another very interesting aspect of the discussion of the use of ceramics was introduced very early in the meeting by Kochendorfer [2], who pointed out that even brittle monolithic ceramics can be used very successfully in these applications if the designer is very careful to use combinations of materials, separation of functions, and knowledge of the geometrical scaling effects on the properties of ceramics to limit the tensile stresses in the ceramic components. He thus suggested strongly that the use of ceramics be considered not just as a material development problem, but as a combined material and appropriate design issue. He, Ruther and Kruger [13], and Avran and Boudigues

[24] all presented extremely interesting examples of blade and vane designs in which a thin ceramic shell was used in conjunction with an underlying metal spar to minimize both tensile stresses in the ceramic and thermal loads in the metal.

The use of silicon carbide coated carbon-carbon composites, especially in rocket propulsion applications, was also vividly demonstrated. A paper by Gellhorn, Gruber and Leis [19] covered short-term, very high temperature applications in gas generators, hot gas valves and combustion chambers for high speed, tactical solid rocket motors. Hordonneau [22] showed current applications to the throats and inlet and exit sections of large strategic solid rocket nozzles and the increasing likelihood of use for both hot structure and propulsion components in advanced hypersonic vehicles such as Hermes and future space transportation systems such as STS 2000. Donguy and Broca [23] showed similar, very optimistic projections for the use of these protected carbon-carbon composites and new, more thermally stable graphite fiber reinforced ceramic matrix composites and thermostructural insulators, not only in solid rocket nozzles but in hot gas valves and small liquid rocket combustion chambers as well. The importance of matching the design and properties of the coating to the thermophysical properties of the substrate in striving for oxidation resistant carbon-carbon systems was emphasized by Thompson [11].

A pervasive feature of most of the discussions of advanced materials and their application to more and more stressful propulsion environments was, in fact, the need for improved protective coatings and coating processes. Field, Restall, Chalk and Hayman [3] provided an excellent overall review of coating processes and applications. Hancock and Restall [9] pointed out that it is often the very drive toward optimization of the mechanical properties of materials during the advanced stages of their development that compromises their oxidation and hot corrosion resistance, and they cautioned that the kind of interaction kinetics normally treated by the oxidation behavior and coating community are likely to play a key role in the behavior of fiber-matrix interfaces in high temperature composites. Examples of interaction effects between coatings and the underlying alloys in metallic components were treated as a specific case by Grunling, Schneider and Singheiser [14].

Many participants noted the contributions that advanced cooling technologies have played in advancing engine performance in cases where materials capabilities alone have not been adequate to meet system requirements, and the role that thermal barrier coatings can play in reducing the surface temperatures of underlying materials. Holmes and McKechnie [17] showed the dramatic effect that low pressure plasma sprayed thermal barrier coatings can have on the durability and life of turbopump blades subjected to cycles in which they are heated and cooled from cryogenic temperatures to full operating temperatures within a second during start-up and shut-down. Quentmeyer [18] showed a similarly dramatic application of thermal barrier coatings to the hot gas side walls of rocket thrust chambers to significantly reduce the heat transfer in high heat flux regions.

A number of papers, in addition to emphasizing the importance of design considerations in utilizing new materials to their fullest extent to meet advanced propulsion requirements, emphasized also the importance of a more complete understanding of their behavior and life prediction. Farmer and Van Wenderham [6] described the US damage tolerant design program, which requires that life assessments include analyses of the life remaining in critical components and locations after crack initiation. They also described its impact on current engine designs and its potential impact on the introduction of new, if any cases less forgiving materials. They provided some excellent examples of design reconfigurations, spurred by the application of damage

tolerance criteria, that significantly enhanced durability, reliability and inspectability relative to earlier low cycle fatigue-based designs. Both they and Hicks [5] emphasized also that we will need a better understanding of the behavior of new materials and more accurate life prediction methods if we want to avoid undue conservatism and weight penalties in future designs. An excellent example was provided by Campo [8], who showed recent results for the stress analysis and life prediction of anisotropic single crystal turbine blades in just such an attempt to take full advantage of their properties.

Finally, several papers were devoted to frequently overlooked, but very important topics, including a paper by Bhat [25] on bearing materials for cryogenic turbopumps that have to withstand conditions quite different from those encountered in gas turbine engines, a paper by Sanschagrin and Couture [26] on the development of insulants containing non-toxic fillers for use in rocket motors as replacements for asbestos-based materials, and a paper by Lecomte-Mertens and Bex [27] on the understanding and development of braze repair techniques for turbine engine parts. The latter was a particularly good example of the contribution a detailed metallurgical study can make to a complex, practical problem like component repair.

### 3. OVERALL EVALUATION

#### 3.1 General Comments

Several important themes emerged in the meeting as central points that recurred frequently in the formal presentations, in the discussions that followed them, and in conversations with the participants between sessions.

##### 3.1.1 The Potential for Growth in Propulsion Systems

The development of aircraft gas turbine engines has been characterized by a series of sequential growth curves. In each phase of their development, one or more technological advances, typically new sets of materials or process improvements, new advanced cooling techniques, or new structural design concepts, have spurred an initial period of rapid growth in performance. That initial growth has then been followed by a series of smaller and smaller incremental gains over the ensuing years until the infusion of a new set of technologies has given rise to a new growth curve. Turbine engine performance has more than doubled through a series of these growth curves over the past fifty years.

These very advances, however, have led some to suggest that propulsion technology is so mature now that the engine industry is approaching a 'sunset' status, and that little more can be done technologically. That view has been clearly challenged by recent studies that have shown that in fact with new materials, new structural concepts, and aerodynamic advances made possible by new computational techniques, there is no question that significant performance, reliability and durability improvements lie ahead. Indeed, based on such studies, research efforts are underway in the US and the UK aimed at the acceleration of those advances. The US Integrated High Performance Turbine Engine Technology (IHPTET) program, for example, has as its goal the development of technologies that could double turbine engine performance over today's most advanced baseline values, with no compromise in reliability or durability, within the next twenty years. The UK Advanced Core Military Engine (ACME) program has very similar goals.

Advanced materials, and the innovative components and structures they will allow, are absolutely key to the very large, rapid advances in propulsion capability envisioned in these programs. Several papers referred to the new,

advanced materials being responsible for at least 50%, and perhaps as much as 70% or more of all of the gains to be made.

These new materials are not only technically feasible but, in many cases at least, their development seems quite likely. Their development is being spurred worldwide by their pervasive role not only in future propulsion systems, but in future hot structures required for hypersonic vehicles, high performance rockets, survivable space structures, and a variety of other military and commercial applications.

### 3.1.2. The Risks Associated with the Introduction of New Materials

There were many expressions of caution throughout the meeting regarding how difficult it will be to sensibly and reliably introduce these new, perhaps higher risk materials into real production engines. This will indeed be a challenge to be faced by the materials and propulsion communities, but it can be done. The prize to be won, a more vital free-world engine industry and a military capability far surpassing anything available now, will drive substantial investments in research and development to produce these materials and provide the technologies needed to make revolutionary advances in engines possible. In pursuing this path, we should strive to accelerate the development of the materials and processes we need and to accelerate their validation in technology demonstrator engines, but the overall sense of the meeting was certainly that they should be introduced into real production engines sensibly and cautiously, only when ready, and in many cases by gradual steps in more and more demanding applications.

It was frequently said that the materials required will not just be new, in many cases they will behave quite differently from the relatively ductile, forgiving materials we've used in the past. Many speakers emphasized that

1) we must characterize and understand the behavior and failure modes of these new materials under realistic loads and environments

2) we must know how to predict and assure their life

and 3) the materials engineer, the designer, and the material and component manufacturer will all have to work more closely together than ever before, and they ought to do it from the very beginning of the effort.

It was clear throughout that these advanced new materials will not be used in production unless the risks associated with their introduction can be reduced to acceptable levels, and we should not expect otherwise of the system developer.

### 3.1.3 The Variety of New Materials Needed

It is sometimes said that current high temperature materials, and especially high temperature metals, are so near their development limits that engines of the future will be made entirely of non-metals, or entirely of ceramics or carbon-carbon composites. There are many, many new materials on the horizon, however, both metal and non-metal, and many processes available to make them. Just as today's engines are not made entirely of superalloys, so future engines will not be made entirely of ceramics or carbon-carbon. From the relatively cool front of the engine to the hottest parts of the back, from high performance static and rotating aerodynamic components to more efficient structural components, future engines will require many different material and component design options.

### 3.2 High Priority Areas for Material Development

#### 3.2.1 High Temperature Metals and Metal Matrix Composites

It was very clear from many of the papers and most of the discussions that the development of metals is far from dead. In fact, new, higher temperature, lighter weight metals will be critically needed in many parts of the engines of the future.

Superalloys will continue to play a major role in engines derived from today's advanced designs to provide incremental improvements in performance and in the engines likely to be in field use over the next 20-30 years. They are too good a class of materials, too highly developed, and too well understood to be readily dismissed. It is true that they are near the limits of their inherent capabilities, and indeed many are operating to within an astonishing fraction of their melting point. Still, with further alloy and process development, further advances in cooling effectiveness, better coatings, and perhaps with fiber reinforcement as discussed by Petrasek and Stephens [20], they will continue to serve us well. They will not, however, meet the long-term, high temperature, light-weight material goals of the IHPET or ACME engines of the future.

As noted by several authors, titanium and titanium-based materials are vitally needed for the higher performance, innovative, lightweight compressor structures of future engines. A typical IHPET design, for example, generally shows compressors of the future operating with many fewer stages, each stage doing more work and usually rotating at higher speeds, and with unique, diskless constructions that eliminate much of the weight of current designs. These compressors will also likely be operating at temperatures much higher than those characteristic of today's compressors. Many studies indicate compressor exit temperatures of 650 to 870°C, or more. These cannot be built without advanced titanium-based alloys and reinforced composites.

Fortunately, many researchers believe there is a lot of room for further development of titanium-based materials. Studies are underway that could well extend the service temperatures of titanium-based alloys and composites from today's 570 to 600°C range to the 750 or 800°C range. The titanium aluminide alloys and titanium aluminide composites may well be made to operate in the 850 to 1000°C range, and relatively soon, since they are also critically needed for use in lightweight hypersonic vehicles such as the US National Aerospace Plane. As noted frequently in the meeting, however, it should be borne in mind that for large, man-rated turbine engine use these titanium-based materials would also have to be thermally stable for long times, they would have to be fire-resistant, and in fact to operate at these extreme temperatures they may well need coatings for oxidation protection.

There were a number of comments about the potential usefulness of refractory metals in future turbine engines. Columbium alloys have not been looked at seriously for a number of years, and it may be possible now, using powder alloy and rapid solidification techniques, to process some of the higher strength, more oxidation resistant compositions that were identified in the past but dropped because at the time they were considered to be unprocessable. With the exception of coated columbium, which might be useful in some turbine blade and vane applications, perhaps to about 1300°C, refractory metals are not likely to be candidates for general use in future aircraft engines because of their high densities and poor oxidation resistance. They may, of course, be useful in other, short-term, specialty applications.

Unfortunately there was not much discussion within the meeting of a new, emerging class of metallic materials based on the advanced intermetallic

compounds. These are intermetallics with melting temperatures, and therefore potential use temperatures, much higher than those of the titanium aluminides and the nickel aluminides. While research in this area is still in its infancy, these materials, in either monolithic form or as matrices for very high temperature metal matrix composites, could be useful to temperatures as high as 1400 or even 1650°C. Although their use might well be as far off in the future as the very high temperature ceramic matrix composites, they should have significant service and fabrication advantages and, since they may well be the ultimate in metal matrix composites, their development should be thoroughly explored.

### 3.2.2 High Temperature Non-Metallics

#### 3.2.2.1 Carbon-Carbon Composites

A number of the papers and a substantial part of the discussions dealt with carbon-carbon composites for turbine engines and the difficult task of providing oxidation protection to a material with no inherent oxidation resistance of its own. One school of thought says that protection of high strength carbon-carbon at future turbine temperatures for thousands of hours is probably impossible. Still, progress in protection systems, often involving internal fiber, interface, and matrix inhibitor treatments as well as multi-layer external coatings, has been reported. Impressive results were shown at this meeting, in fact, with at least tens of hours of satisfactory performance at temperatures well above 1600°C. With their potential for use in static components and exhaust ducts even in large engines, and in many components in small, limited-life engines, there is strong justification in continuing the search for effective protection schemes.

#### 3.2.2.2 Ceramics and Ceramic Matrix Composites

A number of expressions of caution were voiced with regard to the potential risks and difficulties involved in the development and application of ceramics and ceramic matrix composites, but there was also a lot of evidence of success and a lot of promise for the future. A number of specific examples of successful component tests using both monolithic and composite ceramics were reported. An intermediate temperature, perhaps 1000 to 1300°C glass-ceramic matrix composite with useful strength at least in the 300 MPa range cross-plied, about 0.2% strain to failure, and an engineeringly useful level of fracture toughness was reported. That ought to be a usable material even now, once it is well characterized and capable of being produced reliably and reproducibly. There were examples of higher temperature, graphite and silicon carbide fiber reinforced silicon carbide composites that have potential for use to perhaps 1300 to 1500°C. Ultra-high temperature ceramic composites, those for use above about 1700°C, clearly will require the invention of adequate fibers, matrices, and interface control schemes.

In the meantime, there are two ways we can capitalize on the advantages of ceramics and ceramic matrix composites as they become available. We can introduce them, carefully and very conservatively, at first at very modest temperatures and in very low risk applications, to start the very important engineering design and manufacturing learning processes. Alternatively, as pointed out in several outstanding examples in the course of this meeting, we can introduce the ceramics in innovative designs that take advantage of at least some of their potential strengths and avoid their major current weaknesses. Some of the German and French papers at this meeting were especially interesting in this regard.

### 3.3 Other Related Technologies

Although there were only a few papers specifically devoted to life prediction and damage tolerant design with these new, advanced materials, the

importance of their message cannot be overemphasized. As noted so many times during the meeting, these materials must be introduced intelligently, and we cannot do that without precise, accurate characterization, life prediction and damage tolerant design methods and data.

A number of papers dealt with coatings and coating processes, an appropriate reminder that coatings should not be viewed only as a solution to material or component design problems when they arise in practice, but as a powerful tool in engine design that can significantly enhance the performance and/or durability of a material-component system.

Similarly, the several papers that dealt with such topics as joining and repair, bearings and lubrication, and insulation were a valuable reminder of the many such topics that must also be included, especially in any program aimed at overall new design concepts. They are often understated, but a real engine cannot be built without them.

Finally, it was interesting to see several references to process modeling and process simulation used not only to provide the fabrication of complex components with new, process-sensitive materials, and to get it 'right the first time', but also to control the microstructure and properties of our materials in the failure-critical parts of those components. The ability to do smart processing will probably be especially critical in the case of these new, advanced materials. We must learn to make our materials and components right, and not depend on inspection to find our mistakes.

#### 3.4 Materials for Rocket Propulsion

It was unfortunate that there was not more discussion of the unique requirements for materials in heavy launch, space transportation system, and tactical rocket motors. The papers that were presented in the rocket propulsion area, however, clearly testified to the progress being made in coatings, in carbon-carbon composites, and even in ceramic matrix composites in this area. When we consider the component sizes, the high heat fluxes, and the rapid thermal excursions characteristic of many of these rocket applications, the advances are very impressive. Hopefully these two communities, the turbine engine materials people and the rocket propulsion materials people, will continue to interact and communicate in the future in the Propulsion and Energetics Panel as they did at this meeting.

#### 3.5 MANAGEMENT CONSIDERATIONS

A very interesting point was made by Higton and Chrispin [4]. They talked about the need to 'manage for change'. Clearly in an area as technically complex as materials and processes for turbine engines and rocket propulsion, especially where attempts are made to rapidly accelerate development and application cycles, difficult technical decisions are to be expected. However in this case the need for exceptional management and leadership will probably go even further.

Managers of the changes envisioned here will have to provide a balance between the optimism for what we all hope will be possible in the engines of the future and the concern that we head in that direction prudently and wisely. Considering the magnitude of the job to be done and the restrictions on available resources that most of us face, it is critically important that good judgement be exercised in selecting both research paths and wise applications for the technologies we develop.

At the research end of the spectrum, innovation in new materials and processes is crucial and should not be stifled. On the other hand, expensive

investments in advanced development leading to production and use should be predicated on corporate commitment to the practicality and real need for the technology.

The management challenge in bringing about the material and engine revolutions discussed here must not be overlooked.

#### 4. CONCLUSIONS

1. Detailed engineering studies show that tremendous further improvements can still be made in the performance of aircraft gas turbine engines, and that these improvements would provide huge benefits in both the military capabilities of tactical and strategic aircraft and commercial competitiveness for our engine producers.

2. These studies also show that the key to these major advances in engine capability will be new materials and the new structural concepts that they will allow. Stronger, stiffer, higher temperature, lighter materials will be responsible for at least 50%, and probably 70% or more of the gains to be made.

3. While the material and process developments required for this next revolution in turbine engine capability will be difficult, and will require major national research investments and long-term commitments, they can be done. Indeed, many are already underway as parts of major national initiatives that have defined these advanced materials as pervasive keys to industrial competitiveness for the future.

4. As a general rule these new, advanced, high performance materials are likely to behave differently than the more familiar, more forgiving materials used in the past. Their development, their validation in technology demonstrator engines, and ultimately their introduction into real production engines will have to be done sensibly and with careful preparation to manage the risks involved.

5. This will require thorough knowledge and understanding of the behavior and life prediction of these advanced materials in realistic engine environments, and in many cases the materials and component designs will have to be optimized simultaneously. The material developers, material and component producers, and engine designers will have to work more closely together than ever before.

6. The development of these advanced engines will require a wide variety of materials, each used where their capabilities provide the best balance of properties for a given component. There are both great needs and significant opportunities for the development of higher temperature titanium-based alloys, advanced intermetallics, and very high temperature metal matrix composites based on them, oxidation resistant carbon-carbon composites, and both ceramics and ceramic matrix composites.

7. Nearer-term engine development opportunities and requirements will continue to place emphasis on the further development of superalloys, refractory metals, coatings, and a number of related technologies such as bearings and lubricants, joining and repair, etc.

8. Materials requirements for rocket propulsion have many features in common with those for aircraft gas turbines, but they also have many unique features since the lifetimes, pressures, heat fluxes, temperatures and temperature transients, and so on may be quite different for solid and liquid rockets intended for tactical and strategic applications.

Still, this meeting showed the remarkable synergism possible between the turbine and rocket materials communities and the impressive progress being made in carbon-carbon and ceramic composites, thermal barrier coatings, and a number of other technologies for rocket motor use.

9. While the technical challenges in developing these new materials and engines are the ones most often addressed, the management challenges must not be overlooked. To realize the full potential of these technological opportunities, long-term commitments will have to be made, government-industry-material supplier alliances will have to be forged, successful material and component developments along the way will have to be transitioned to near-term applications, difficult decisions between competing technologies will have to be made, and wherever possible cooperative programs will have to be sought to conserve resources and manage risks.

#### RECOMMENDATIONS

This meeting amply demonstrated the strong mutual interest and high level of current activity in all of the member nations in advanced materials for turbine engine and rocket propulsion applications. In view of the technological opportunities and huge potential military payoffs in this area, it is strongly recommended that

1. High level consideration be given to substantial, sustained support to materials and process research and development efforts in the areas described in this report, and to the component development and test activities required to transition the advances made into usable system capabilities.
2. The cooperative exchange of ideas and information in these areas evidenced in this meeting be continued, to accelerate the development of these crucial technologies, to conserve critical resources, and to minimize the risks that may be associated with the rapid development and application of these new materials.
3. Future meetings on this topic be scheduled within the Propulsion and Energetics Panel at appropriate intervals to again bring together materials and manufacturing experts, designers, and system developers in both the gas turbine and rocket propulsion areas to review progress and stimulate closer cooperation.

## APPLICATION OF ADVANCED MATERIALS FOR TURBOMACHINERY &amp; ROCKET PROPULSION /

by  
 Joseph B. Moore  
 Director, Materials Engineering  
 M. S. 706-04  
 Pratt & Whitney  
 P. O. Box 109600  
 West Palm Beach, FL 33410-9600, U.S.A.

SUMMARY

Gas turbine engines of the 1980's and 1990's will require improved nickel and titanium alloys as well as certain intermetallic compounds and low temperature composites. Engines of the 2000's with significantly higher thrust to weight ratios will require lighter weight, higher temperature non-conventional materials including aluminum alloys, titanium metal matrix composites, intermetallic compounds, and ceramic matrix composites. Major concerns once these materials are developed will be the design, manufacture, inspection, and repair of required components at affordable cost.

Current or near-term liquid rocket engines having technology levels equivalent to those being studied for the space transportation and advanced launch systems can benefit from improved materials for turbo machinery, high heat flux throat regions of the thrust chamber, high strength, hydrogen resistant materials for cases and ducts, and refractory materials for uncooled or partially cooled nozzle extensions.

To meet the far term goals for advanced rocket engines required for single-stage-to-orbit (SSTO) vehicles material requirements are not unlike those described above for 21st century gas turbine engines.

Materials are the key to increasing the performance of both aircraft gas turbine engines and rocket engines of the future. FIGURE 1 shows that at least 50% of the improvement in performance capability of aircraft turbojet engines will come from improved materials and processes. Reduced leakage contributing another 25% will also rely heavily on better materials. FIGURE 2 shows how military and commercial engine performance has risen since the inception of the J57 turbojet engine in the early 1950's. This increase is compared to an ideal core horsepower performance curve. It indicates that improved performance is possible through increasing turbine temperatures and a projection is made of what we believe can be achieved in the 1990 and 2000 year regimes. Both projections, if realized, represent significant opportunities for increasing aircraft performance. Both projections ride on the ability to develop new materials with greatly improved capability over those that are available today. The name of the game for future propulsion, both gas turbine and rocket engines, is summarized in FIGURE 3 - these are the characteristics of materials and components made from them that must be improved if we are to realize our visions of advanced aircraft and rocket engine vehicles of the next two decades.

Being more specific, materials requirements for engines of the late 1980's and 1990's, which will power aircraft such as the Advanced Tactical Fighter (FIGURE 4), will include improved nickel superalloys for turbine disks, blades and vanes, engine cases and exhaust nozzle liners. (FIGURE 5) Thermal barrier coatings will be needed for the airfoils so that the combustor exit temperature can be raised beyond that possible with airfoil cooling technology alone. High temperature non-burning titanium alloys, and intermetallic compounds, will be required for static and rotating parts of the compressor and nozzle components. New fabrication methods, such as integrally bladed rotors and dual alloy concepts will go hand-in-hand with the introduction of these new materials. In addition, light weight and stiff organic and metal matrix composites will be required for fan and compressor static hardware, as well as exhaust nozzle components. In this figure are depicted some of these new materials and processes that are being projected.

Now turning to Advanced Aircraft of the 2000's (FIGURE 6), with significantly higher thrust-to-weight engines, still newer classes of heat resistant, light weight materials will be required, including aluminum alloys, titanium alloys and metal matrix composites for fan and compressor parts. (FIGURE 7) High temperature intermetallic compounds, refractory alloys, and refractory composites will be needed for the combustor, turbine, and exhaust nozzle parts.

Nearly all of the candidate high temperature materials now being considered for engines of the 1990's and 2000's have one thing in common - they have relatively low ductility and low fracture toughness and are very process sensitive. Never before has it been so important for the materials developer, the designer, and the

manufacturer to work together in close concert, if components that will do the job are to be produced.

Major concerns for the utilization of these above mentioned materials, especially those for engine of the 2000's, are numerous. New system approaches are needed for designing components that will meet durability requirements utilizing ENSIP (Engine Structures Integrity Program) criteria. Innovative, intelligent processing methods (i.e. forming, joining, machining) will be required for manufacturing engine components at an affordable cost, and component repair methods must be developed. Also, inspection techniques that will insure part integrity during operation must be upgraded. (FIGURE 8) The challenges in these areas, as well as in the area of basic material development, are staggering.

Turning to rocket propulsion, (FIGURE 9) liquid rocket engines will continue to provide the major propulsive force for projected launch vehicles. If you will pardon the commercial, in FIGURE 10 is shown the RL10 developed by Pratt & Whitney in 1963. It was the world's first liquid hydrogen rocket engine and has compiled a record of which we are most proud. This engine has been, and is being used, for the Atlas-Centaur and Titan-Centaur programs involving a broad spectrum of payloads and missions. Basically, current liquid rocket engines of this type, as well as those of the future, will rely on materials and processes that have been developed for gas turbines. (FIGURE 11) However, rocket engines having technology levels equivalent to those being studied for the Space Transportation System and/or the Advanced Launch System can benefit from improved materials for the throat regions of the thrust chamber. These have extremely high heat fluxes, almost thirty times higher than experienced by jet engine turbine airfoils. With this high heat flux level, combined with combustion temperatures above 5000 degrees F copper, with its high thermal conductivity, is now the only material which satisfies combustion chamber requirement. Major improvements in material heat resistance, with no sacrifice of thermal conductivity, are needed as the heat flux moves still higher. Also, improved strength and hydrogen resistant materials are needed for cases and ducts, as well as refractory materials for uncooled or partially cooled nozzle extensions. Lower cost processing techniques involving the casting of injectors and turbine hardware is mandated for affordability.

The similarity between rocket engine turbopumps and gas turbine engines is shown in FIGURE 12. The Alternate Turbopump that Pratt & Whitney is developing for the Space Shuttle Main Engine is nearly the same size as the T800 gas turbine that is being developed for advanced helicopter applications. FIGURE 13 shows similarities in the T800 and ATD system. Both have centrifugal compressor stages and axial turbine stages - both have similar rotational and tip speeds. FIGURE 14 shows the kind of materials that Pratt & Whitney is considering for advanced rocket engine turbopumps. The pumps operate at cryogenic temperature levels and the turbine inlet temperature is generally less than that of the gas turbine. The materials stipulated are all of proven jet engine vintage, with the exception of the carbon/carbon composite material, which is now under intensive study and evaluation for applications in both gas turbine and rocket engines.

To meet the far term 2000+ year goals for advanced rocket engines required for Single-Stage-To-Orbit vehicles, materials requirements are not unlike those previously described for 21<sup>st</sup> century aircraft gas turbine engines. The performance requirements of these engines likewise drive the design toward high temperature composites and ceramics for the turbo-machinery and combustion components.

In conclusion, referring back to FIGURE 2, we are very optimistic about our collective ability to significantly upgrade the performance of aircraft gas turbines through improved materials and processes. When many of us started in the jet engine business, the J47 and J57 were regarded by many as the "ultimate" machines. As the chart shows, we have seen significant improvement over the years, doubling the core power of those early engines. The "1990's line" is what our current demonstrator engines are showing. This is a substantial improvement over our front line fighter engine, the F100. We're working hard to improve core engine power into the year 2000 and beyond. Even the stoichiometric limit, which is shown for JP fuel, can be overcome with the introduction of hydrogen or enhanced hydrocarbon fuels. As has been indicated, significant gains in jet engine materials will directly impact rocket turbomachinery performance. Considering the chart, we feel that we have yet to tap the full potential of the jet engine. Nobody has said that it will be easy to exploit. It will require vision, a lot of hard work, persistence, and perhaps a little luck.

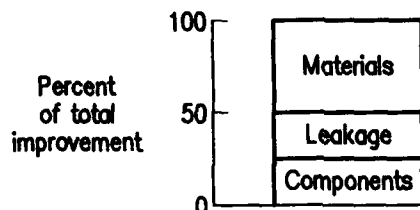


Figure 1. Materials are Key to Advances in Engine Technology

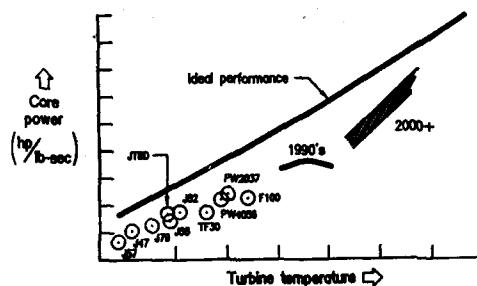


Figure 2. Improved Performance Possible

- Very high temperature capability
- Low density
- Durable
- Innovative manufacturing methods
- Inspectable
- Repairable
- Affordable

Figure 3. Materials and Components for Future Propulsion

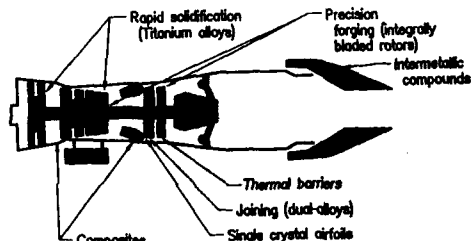


Figure 5. Materials and Process Innovation for the 1990's Engine



Figure 4. Advanced Tactical Fighter Concept (ATF)



Figure 6. Advanced Aircraft Concept

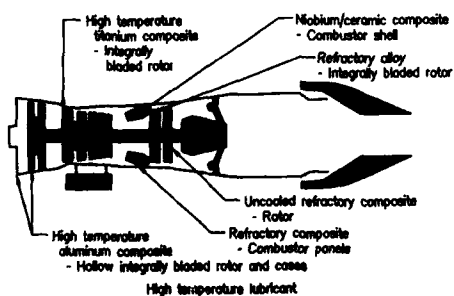


Figure 7. Advanced Technology Engine Materials for 2000 and Beyond

- Designing components that meet durability requirements
- Innovative, intelligent processing
- Components at affordable cost
- Component inspectability
- Cost effective, logically adaptable repair techniques

Figure 8. Major Concerns for Advanced Materials



Figure 9. Liquid Rocket Engine on Test

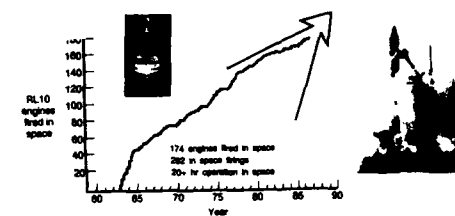


Figure 10. RL10 Liquid Hydrogen Rocket Engine



Advanced launch system  
Payloads to 2 times shuttle  
Payload cost - 1/10 shuttle



Figure 11. Launch System Propulsion

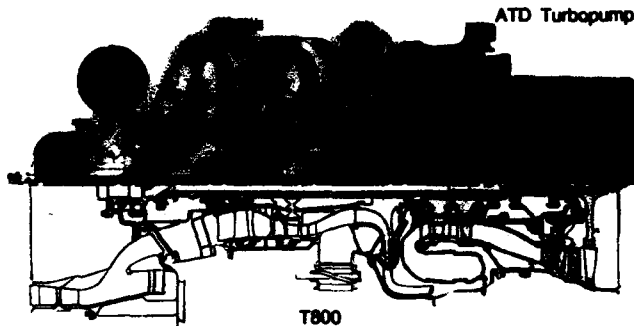


Figure 12. Physical Comparison Between T800 and ATD Turbopump

	T800	ATD	(Desired properties)
Pump/compressor stages	2 axial 1 centrifugal	3 centrifugal	Bearings (M-50)
Turbine stages	2	2	Shaftless impeller (Forged A110)
Turbine inlet temp, °F	2,340	1,430	Inducer (Cast A110)
Rotational speed, rpm	50,000	37,000	
Tip speed, ft/sec	1,950	1,950	
Materials			
Rotor	In100	In100	Turbine liner (Carbo/carbon)
Turb airfoils	Single crystal	Single crystal	Thrust platen (Inco 718 - leaded bronze)
Centrifugal stages	Titanium	Titanium	Blades (MAR-M-247)

Figure 13. Key Similarities

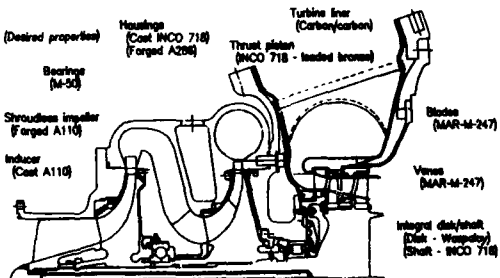


Figure 14. Rocket Engine - Hydrogen Turbopump

### DISCUSSION

R. Holmes, NASA-Marshall, US. I'm very interested in MAR-M-247 for rocket engines. Do you have any data on how it compares to MAR-M-246 in terms of hydrogen embrittlement?

J. Moore, Pratt & Whitney, US. We have some data that shows that it is susceptible to high temperature, high pressure hydrogen and that it does show some degradation.

N. Tallan, US Air Force, US. Your chart for core power vs. turbine inlet temperature includes a curve for the 1990's in which there is a maximum. After an initial increase with increasing temperature, the curve shows a downturn, in absolute terms and particularly relative to ideal performance. Could you comment on the reason?

Tom Farmer, Pratt & Whitney, US. The curve assumes that the materials available will have a service temperature limitation, so as turbine inlet temperature increases, there is an offsetting requirement for cooling. Above some point the performance improvement with increasing turbine temperature is more than offset by the increasing requirement for additional cooling.

D. Colbourne, MOD, UK. Are you suggesting that materials will not catch up in that timeframe to push the curve back up?

T. Farmer, Pratt & Whitney, US. At each point on the curve you optimize a material and a system or design combination. For a given set of materials, there is an optimum configuration and cooling efficiency associated with that set of materials and their capabilities. You optimize your design at a turbine inlet temperature condition and system match. That's the point of the maximum in the curve. For each material there will always be some limit, and as you take the system past that there will be that downturn.

D. Colbourne, MOD, UK. So the downturn is a matter of materials. If higher capability materials were available, there would be no need to increase the cooling flows with increased turbine inlet temperature and one would avoid increasing the parasitic losses in the cycle.

W. Wagner, US Navy, US. You show titanium and titanium matrix composites in the turbomachinery compressor sections for the engines of the 2000's. How do you see us avoiding or minimizing the risk of titanium fires resulting from incidents of titanium rubs?

J. Moore, Pratt & Whitney, US. We've had an internal effort for some time now to develop high strength titanium alloys that will not burn, and we have been successful to some degree, but it's a very tough problem. We actually started the alloy development program by screening candidates on the basis of fire resistance, using various combinations of materials in our test rig. That rig unfortunately doesn't go to high enough temperatures and pressures, but we will have a facility by the end of the year that will allow us to pretty closely simulate what goes on in the engine. Using the rig we had, we went through a very extensive screening program, and we were very successful. We came up with some alloys that had excellent resistance to burning based on the rig test results. There was only one problem, they weren't very strong. As so often happens, as we push these materials to more stressing conditions we find that criteria seesaw with respect to strength. We can get increases in fire resistance, but then the strength drops off. We can improve the strength, but then the fire resistance drops off. Still, we have had some success in getting a reasonable combination of both, and we're still pursuing it. But it's not an easy problem, at least not for us operating in the regimes we've been working in.

W. Chrispin, MOD, UK. I've noticed that on Figures 5 and 7, we're you are talking about materials for the early 2000's, you don't show any material innovations associated with the afterburner or exhaust duct components. Could you comment on that? Do you expect these areas to benefit from some of the metal matrix or ceramic composites?

J. Moore, Pratt & Whitney, US. Yes we do. New materials are shown in Fig. 5 and they should have been shown on Fig. 7 too.

**MONOLITHIC AND FIBER CERAMIC COMPONENTS  
FOR TURBOENGINES AND ROCKETS**

R. Kochendörfer

INSTITUTE FOR STRUCTURES AND DESIGN  
DFVLR - STUTTGART  
Pfaaffenwaldring 38/40  
7 Stuttgart - 80  
FRG

**Summary**

From the design point of view, the paper will review whether or not the existing experience gained during the automotive ceramic turbine development can be transferred to aero jet engines. It is well known that design considerations strongly influence the failure tolerance of ceramic structures. Following material adequate design concepts will increase component reliability. Focussing these topics, the future application of ceramics for thermally and/or mechanically high-loaded structures within the propulsion system will be discussed. Actual available data of emerging materials as C/C, C/SiC, SiC/SiC will be presented. The material's behaviour, their potential for structural applications as well as design consequences will be evaluated.

**Introduction**

Today's advanced aircraft engines are operating at the limits of present material technology. New, lighter, stronger and more durable materials are needed to meet the requirements of coming generations of engines. The development of conventional materials will lead to a step by step improvement of engine performance - as it was demonstrated in the past. High risk material technology may offer the availability of high temperature resistant exotic materials such as ceramics, however a revolution in materials should coincide with a revolution in design to guarantee the high reliability achieved with conventional materials. Whereas metals can reduce local overstresses by plastic deformation, ceramic materials do have only one mechanism to reduce stresses, that is cracking.

If this is accepted as a typical ceramic behaviour there are two ways to increase reliability of ceramic engine components:

1. Realize crack stopping effects, e. g. mechanisms which occur in zirconia toughened ceramics or in fiber ceramic composites to stop a critical crack, or to reduce crack propagation velocity.
2. Realize design concepts such as a combination of materials and separation of functions to minimize the tensile stress level within a ceramic component by an appropriate design approach.

In the following sections these ideas will be discussed on the basis of hitherto gained experience from different ceramic engine programs.

**Experience gained from automotive ceramic turbine programs**

Government sponsored programs were initiated in Germany as well as in the US. The total budget of the German Ceramic Turbine Program during the years 1974 to 1986 was about 140 Mio DM /1/. The US-Advanced Gas Turbine Programs AGT 100 (General Motors, Allison) and AGT 101 (Ford/Garrett) amounted to about 250 Mio DM, during the fiscal years 1980 to 1987. The results may be summarised as follows:

- A ceramic turbine in the 100 kW power range seems to be feasible to proof the concept. The today status however is far away from serial production.
- The static ceramic components as combustion chamber, stator, inlet cone etc. were much easier to realize than rotating components due to the fact that the geometry is more simple and tensile stresses are more or less induced thermal stresses. In all programs static ceramic components successfully passed fired engine tests. They do have a great potential for future serial application.
- As expected, the ceramic rotors were the most critical components. Within the German Program the design was focussed to axially bladed integral rotors. AGT 100 as well as AGT 101 had radially bladed integral rotors. Despite the fact that AGT 100 as well as AGT 101 were bench proof-tested for several hours /2/ and the Mercedes Benz turbine is installed for testing purpose in a serial car and road tested already, both rotor concepts are not fully qualified under severe design conditions and with guaranteed reliability. The engines have to be handled very carefully.

Rotors with ceramic single blades inserted into a metal disc did not successfully pass hot spin testing. The main reasons for premature failures were local overstresses at the contact areas as well as variations of contact angle and pressure during cycling.

Two problem areas of ceramic components should be mentioned before relating these results to larger size engines: (a) the volume effect on the allowable tensile stress level and (b) the internal stress level within a ceramic component due to fabrication.

- (a) Assuming a constant tensile stress field within a brittle material (or a component) the failure will start at the largest flaw, which may be inside the volume or at the surface: the larger the flaw the lower the failure strength. The probability of a failure critical flaw increases with increasing size of the component, thus the strength level decreases. The reduction of the allowable stress level with increasing volume is shown in Fig. 1. Weibull modulus is used as a parameter. It can be related to the scatter of strength values, the higher the value the lower the scatter. Test bars cut from AGT 100 ceramic rotors showed a modulus of about 10, e.g., increasing the volume of a rotor by a factor of 10 will reduce the calculated allowable stress level to 80%. In reality, a volume increase will coincide with a reduction in homogeneity of the material and consequently with a lower Weibull modulus m.
- (b) Scaling up the ceramic component size will also increase the internal stress level. At a certain point during the ceramic manufacturing process there will occur material shrinkage. The amount of shrinkage differs with different processes. Generally, high strength material means high shrinkage and that means danger from high internal stress level. This effect is pronounced especially in components where small volumes (blades) are connected to sections with large volume (hub/disc). The internal stress level can reach such high values, that the component will crack without applying an external load, starting at a failure critical flaw. Today no established method exists to measure the internal stress level of ceramic structures by nondestructive testing. The only way to get a fast answer to the question whether a structure has an acceptable status or not, is proof testing of every individual component.

As a consequence the upscaling factor of integrally bladed ceramic rotors for large turboengines seems to be very limited and design concepts where ceramic blades are inserted individually into a metal disk also create problems, already found at the small size engines. Thus, new design concepts are required to realize reliable large size turbine rotors with ceramic components. This is true also for the static parts of a large size engine. The experimental results during small size engine testing showed that the designer should voluntarily divide large ceramic structures into smaller components with a "crack pattern" the design can endure, rather than to wait until thermal stresses will crack the ceramic structure into a non acceptable crack pattern.

All these problems are related to the brittleness of ceramics, or more precisely, to the fact that a tensile stress field, perpendicular to a crack, will lead to a catastrophic failure as soon as the crack is larger than the critical crack length. Each phenomenon which can help to diverge a crack, or split a crack into a crack pattern, or reduce local stresses at the crack tip down to zero, will stop a crack or at least reduce the crack growth velocity.

#### **Applicability of ceramic materials offering crack stopping effects**

Partially stabilized zirconia (PSZ) and fiber reinforced ceramics are the key-words concerning that topic.

PSZ-materials and newer systems on the basis of PSZ offer the highest fracture toughness within the bulk ceramic family, however, the toughening effect decreases with increasing temperature, the thermal conductivity is low and the thermal expansion coefficient high, e.g., this material category is very susceptible to thermoshock conditions. It is a prime choice for thermal barrier coatings of metal substructures but it is very unlikely that it will be useful as a stand-alone structural ceramic in the hot sections of a turboengine.

Fiber reinforced ceramics may be suitable materials for these high temperature applications. Including fiber reinforced glass and carbon/carbon there exists a twenty year's experimental background for this group of materials. Today, several companies are able to manufacture three-dimensional reinforced carbon/carbon (3D-C/C) nozzles and exit cones for rocket engines up to 1.5 meter in diameter and 1.5 m length, and even larger 2D-C/C-molds for superplastic forming of titanium structures. US-Space Shuttle has a nose-cone and wing leading edge structures made of 2D-C/C with SiC surface protection to reduce oxidation /3/. However, all these structures are short time applications, compared to 10 000 hrs for a turboengine. During the short component life time, a certain amount of degradation (strength, mass loss etc.) due to oxidation has to be accepted, otherwise Carbon/Carbon can't be used. There is no protection scheme available up to now which can guarantee long time, high temperature operation of C/C components in oxidative environment without degradation.

The question is whether or not ceramic fibers such as SiC or Al<sub>2</sub>O<sub>3</sub> with an inherent higher oxidation resistance are able to solve the problems /12/. In Fig. 2 short time fiber strength values are summarized for different types of fibers. The highest values are published for 140 µm SiC-fibers from AVCO, manufactured by chemical vapor deposition (CVD)

on a carbon substrate. The values for 10 µm SiC-fibers made on the basis of Polycarbosilane (PCS-SiC) by Nippon Carbon and sold under the trade name Nicalon differ widely, depending on testing conditions and stage of fiber development. However, the fiber strength obviously drops drastically above 900°C to 1000°C. This is also true for a high temperature grade Al<sub>2</sub>O<sub>3</sub> fiber Nextel 480 manufactured by 3M-Company. Fig. 3 summarizes thermal exposure values in air up to 1000 hrs for Nicalon fibers and Al<sub>2</sub>O<sub>3</sub>-fibers from Sumitomo Comp. The RT-tensile strength of these fibers after exposure decreases with increasing time and temperature. The reason is not only oxidation, as can be seen in Fig. 4. Nicalon fibers of "standard" grade and "ceramic" grade (high temperature stable) were exposed at elevated temperatures in air and argon. Even in argon, where oxidation can be excluded, a fiber strength reduction occurs. The explanation was a change of the fiber microstructure at elevated temperatures.

The trends visible in Figs. 2 to 4, the creep results published in /4, 5, 7, 11/, the oxidation stability and microstructure analysis shown in /5, 6, 8, 9, 11/, indicate that:

- CVD-SiC-fibers offer the highest potential for temperature application up to 1200°C - 1300°C, however, they are hard to handle and not available in woven preform. At 1400°C creep occurs due to 1 % of free Silicon.
- PCS-SiC-fibers showed pronounced creep behaviour above 1100°C /5/. Between 1200°C and 1300°C drastic changes in microstructure occur /9/, in combination with reactions between the fiber constituents. Long time application seems to be limited to temperatures up to 1000°C.
- Al<sub>2</sub>O<sub>3</sub>-fiber strength degradation starts at 900°C. At 1150°C Nextel 480 showed 1 % creep after 100 hrs at a stress level corresponding to 10 % of RT failure stress.

This summary, based on today's fiber properties, indicates that fiber reinforced ceramics will not be a prime candidate for long time applications (10 000 hrs) at temperatures well above 1000°C. According to our own experience with fiber ceramic we would suggest, that even advanced fiber ceramic materials with improved high temperature stable fibers will have their advantageous applications and their big market in the field of limited life structures which are extremely weight sensitive, which cannot be cooled, which can not be manufactured in bulk ceramic due to size or geometry restrictions, etc. Today, C/SiC or SiC/SiC materials offer almost the same mechanical values as C/C, Fig. 5, their oxidation resistance, however, is extremely higher. They will be improved and new fiber/matrix combinations will certainly emerge in future.

#### Design considerations to increase the reliability of ceramic structures

As it is not possible to achieve high temperature stability and long time behaviour with failure tolerant fiber ceramics, the reliability of bulk ceramic components has to be guaranteed by design. Knowing the problems created by up-scaling and high tensile stress levels, the designer should follow ideas like:

- small volumes
- simple shapes
- constant wall thickness
- free thermal expansion
- compression stress state, etc.

In general, this cannot be realized without changing the existing metal design. Metals are predestinated to carry tensile loads, ceramics are not. Consequently, the design should change when replacing metals by ceramic. Most designers are hesitating to do so, because all of their experience and design feeling is based on metal design and fixed in specifications which are valid for metals only. Generations of designers were educated in an "iron and steel" design mentality, rather than in "bricks and stone" design, which is a much more adequate design philosophy for ceramics.

Just to demonstrate the feasibility of such an idea even for the highest tensile stressed structure within a turbine, we made a complete redesign for a turbine wheel, Fig. 6. To suppress tensile stresses, the ceramic blading as well as the ceramic hub is kept under compression by shrinkage rings.

For these rings the only material category which offered the required high values of weight related strength and stiffness were fiber reinforced composites. Tensile stressed composites and compression stressed ceramics is an ideal material combination - with an inherent mismatch in thermal stability. Consequently, the composite rings have to be separated from the hot gas flow ceramic components by a cooling ring. The individual ceramic components were fabricated in a low cost process, e. g. injection molded RBSN, and integrated to the wheel without additional material. The joining technique is based on form-locking and shrinkage mechanisms only. So we had no problems in combining different types of ceramic materials, e. g. RBSN blades and Al<sub>2</sub>TiO<sub>5</sub> cooling rings.

Altogether, five wheels were integrated to proof the feasibility of this design concept in cold spin tests. The burst speeds were between 28 000 rpm and 38 000 rpm, corresponding to a maximum blade tip speed of 300 m/s. Although the design speed of 56 000 rpm was not reached within the first five trials, the failure tolerance and the ability "to live with cracks in a ceramic structure" could be clearly demonstrated, Fig. 7. Compared to the first generation wheels, the second generation wheels showed a less pronounced cracking. Due to

a break of the driving spindle one wheel dropped at a speed of 40 000 rpm into the test facility, and survived. After rebalancing, the wheel could be even spin-tested up to 20000 rpm without complete failure, a result which proofed the failure tolerance of the design concept.

A design approach to realize a compression stress state in a ceramic airfoil without requiring a change of the engine concept is the tie rod design /15,13/, Fig. 8. Each blade of a turbine wheel consists of a hollow ceramic airfoil and an aircooled metal tie rod. Both are connected at the blade tip in a form-locking manner, whereas relative motion in radial direction is allowed in the blade root area. With increasing speed the contact pressure at the blade tip, the compression stress level within the ceramic airfoil and the tensile stress level within the tie rod are increasing. In this ceramic/metal combination is a synergistic effect. Each partner can survive within the harsh environment by using an advantageous property of the other material. The hollow ceramic airfoil protects the metal substructure due to a low thermal conductivity from superheating as well as from corrosive gases. The ceramic component can be seen as a self-supporting thermal barrier coating which does not crack by induced stresses due to the mismatch of thermal elongation with the metal substructure. On one hand, the hollow ceramic airfoil acts as an additional mass to the metal tie rod thus increasing its tensile stress level. On the other hand, due to the thermal protection and cooling effects, the temperature level of the tie rod is lower, and the allowable design stress is higher.

Thus, a combination of tensile stressed metal and compression stressed ceramic offers an advantageous solution. Some problems have to be solved regarding the contact areas, but difficulties are expected to be lower than for an all ceramic turbine wheel. Furthermore, it is a single blade solution with a conventional metal root. No attachment problem to a metal disc arises and no redesign of neighbouring components is required.

This idea was first published by Onera /16/ in 1979 and realized in the following years up to hot spin test qualification of simplified hollow elliptically shaped airfoils (long axis 30 mm, short axis 6 mm, span 30 mm, constant wall thickness 1.2 mm). Fig. 9 shows the test set-up for first static tests in a hot free gas stream. The results are summarized in /17/.

#### **Quotation:**

Either monolithic material such as silicon carbide manufactured by "Société Céramiques et Composites" or composite materials such as SIC canvas, C10 tissue, SIC satin by "Société Européenne de Propulsion" were used.

#### Test Results at Ambient Pressure Conditions

Sleeve blades, monolithic or composites, were first tested on a static bench in a hot free stream either as isolated blades or as blade cascades, with or without angles of attack (up to 45°).

The flow temperature was 2173 K (1900°C) and a good thermomechanical behaviour was detected for all the materials tested. The thermal shock resistance, tested through several firings and extinctions of a combustion chamber, was fully satisfactory. Cooling or ventilating air mass flow rate is controlled by means of three thermocouples placed in the metallic strut and the ceramic sleeve wall temperature is recorded by infrared pyrometry on suction and pressure side. The blade surface temperature distribution is thus well known.

In the above test conditions and with only a slight ventilating air flow at the pressure side the temperature did not exceed 1450 K with a temperature difference higher than 400 degrees between pressure and suction side.

No serious damage of the blades was noticed after several hours of operation.

#### Tests Results under Pressure Conditions

Series of tests on a pressurized fixed blade cascade were made at a slightly lower flow temperature of 1800 K and at a pressure of 6 atm.

For the same flow temperature and mass flow rate and for the same ventilating mass flow an increase in transfer coefficient was noted, the blade surface temperature being only 300 degrees lower than the flow temperature for an inlet total pressure of 6 atm, whereas it was 650 degrees at ambient pressure conditions. No effect was observed on the difference between blade and strut temperature (300 degrees).

After several hours of testing at full temperature, no changes in the thermomechanical properties and the thermal shock resistance of the silicon carbide sleeve blades were noticed. Yet a progressive surface erosion was detected on the blades with sleeves made of one of the composite materials listed above. Thus, apparently, in the present state of composite material technique, this kind of blades is not well suited for long duration tests.

#### Tests on Rotating Blade Set-up

A last series of tests was made on a rotating blade test set-up in order to check the effect on centrifugal forces on the behaviour of the blades.

The test facility used is simply made of a disk with two blades placed on the two ends of the same diameter. The disk is mounted between two roller bearings and due to the 60 degrees stagger angle of the blades an uniform rotation of the blades is obtained.

Test conditions are:

- flow total temperature 1800 K
- flow total pressure 1.3 atm
- blade tip speed 270 m/sec

No effect of the centrifugal forces on the thermomechanical properties of the various materials used (silicon, carbide, composite materials) was noticed. (End of quotation).

Corresponding to these successful results published by ONERA also MTU, Munich, is reporting fully satisfying results gained during hot gas testing of a hybrid design for stator vanes, Fig. 10, /18/. A metallic air cooled core carries the loads, hollow ceramic airfoils are mounted at this core allowing free axial movement between the components. In static tests at ambient pressure the stator blading sustained 1800 K for 200 hrs, and 1900 K for another 100 hrs without damage. Even after 100 cycles between 800 K and 1900 K over 25 hrs, no failure was visible.

Both concepts (ONERA and MTU) realize ceramic adequate design principles:

- material combination: air cooled metal core, hollow ceramic airfoils
- separation of function: load carrying metallic structure, minimized tensile stressed or compression stressed ceramic
- small size volume ceramic components: individual blades.
- constant wall thickness: hollow airfoils, thus low thermally induced stresses.
- free thermal expansion.

#### **Future aspects and conclusive remarks**

The manufacturing technology of bulk ceramic components certainly will be improved in future with the aim to reduce number and size of defects and increase homogeneity as well as allowable stress levels.

Ceramic turbochargers are in serial production since 1985 (Nissan Motor Co.). The turbine rotor outside diameter is 62 mm, operating at 390 m/sec tip speed /19/. Today, an improved second generation concept is under development not only at Nissan but also at Mitsubishi, Fig. 11. Successful tests of a 85 mm diameter ceramic rotor at 600 m/sec tip speed and 1200°C TIT are reported, /20/. The even larger AGT 100 rotor with 156 mm diameter was cold spin proof tested up to 720 m/sec tip speed. However, from the economic point of view, there will be a limit in size increase, and the question is still controversially discussed, whether or not a ceramic turbocharger is superior to a metal version, especially regarding efficiency and cost effectiveness.

As far as an automotive ceramic gas turbine is concerned there are worldwide activities to realize an all ceramic engine. In the US a following-on programme to the AGT-project started in 1987. It is estimated that DOE will fund within this Advanced Turbine Technology Application Project (ATTAP) about 80 Mio. DM up to 1991, /21/. Within the European Commission as well as in Japan new projects are emerging.

For aerojet engines the US government started the Integrated High Performance Turbine Engine Technology Initiative (IHPTET) to validate the technology for future aircraft propulsion systems from fundamental research up to full-scale engine demonstration. It is planned to use bulk ceramic as well as fiber ceramic, Fig. 12, in the areas of combustors, turbine vanes, high temperature bearings as well as in the exhaust systems to realize convergent flaps and multi-axis vectoring nozzle flaps. Especially in this weight sensitive and easy accessible area, where limited life components can easily be exchanged, fiber ceramics are favourable materials.

The experimental results will show whether the designers will follow ceramic adequate design principles or not. Manufacturing technology and material quality has to be and will be improved in future, but it is the task of the designers to pave the way to success.

#### **References**

- /1/ Bunk, W.; Böhmer, M., Herausgeber.  
Keramische Komponenten für Fahrzeug-Gasturbinen I bis III, Springer Verlag  
1978, 1981 und 1984.
- /2/ Carruthers, D.; Wimmer, J.,  
Gasturbines challenge ceramic technology.  
Aerospace America, May 1988.
- /3/ Curry, D.M.; Scott, H.C.; Webster, C.N.,  
Material Characteristics of Space Shuttle Reinforced Carbon-Carbon.  
SAMPE Vol. 24, p. 1524 ff, May 1979, San Francisco.
- /4/ Di Carlo, J.A.,  
Fibers for Structurally Reliable Metal and Ceramic Composites.  
Journal of Metals, June 1985, p. 44 ff.

- /5/ Bunsell, A.R.; Simon, G.,  
Mechanical and Structural Characterisation of Nicalon SiC-Fibers up to 1300°C.  
Composites Science and Technology 27, 1986, p. 157 ff.
- /6/ Andersson, C.H.; Warren, R.,  
Silicon Carbide Fibres and their Potential Use in Composite Materials.  
Composites, Volume 15 No. 1, Jan. 1984, p. 16 ff.
- /7/ Johnson, D.D.; Holtz, A.R.; Grether, M.F.,  
Properties of Nextel 480 Ceramic Fibers.  
11th Annual Conference on Composites and Advanced Ceramic Materials, Cocoa  
Beach, Jan. 1987.
- /8/ Clark, T.J.; Arons, R.M.; Stamatoff, J.B.,  
Thermal Degradation of Nicalon SiC Fibers.  
Ceram. Eng. Sci. Proc. Vol. 6 (7/8), 1985.
- /9/ Gadow, R.,  
Die Silizierung von Kohlenstoff.  
Dissertation bei der Fakultät Chemie der Universität Karlsruhe, Prüfungsdatum  
24.10.1986.
- /10/ Yamura, T. et al.,  
Compatibility of New Continuous Si-Ti-C-O-Fibers for Composites.  
Material Science Monograph 41, p. 199 ff, SAMPE la Baule, 1987.
- /11/ Di Carlo, J.A.,  
Creep of Chemically Vapour Deposited SiC-Fibers.  
Journal of Material Science 21 (1986) p. 217 ff.
- /12/ Kochendörfer, R.,  
Heiße tragende Strukturen aus Faserverbund-Leichtbauwerkstoffen.  
DGLR-Tagung, Berlin, Oct 5 - 7, 1987.
- /13/ Kochendörfer, R.,  
Design Aspects for Reliable Ceramic Structures.  
2nd Int. Symp. "Ceramic Materials and Composites for Engines",  
Lübeck-Travemünde, April 14 -17, 1986.
- /14/ Kochendörfer, R.,  
Compression-loaded Ceramic Turbine Rotor.  
49th AGARD Meet. Structures and Materials Panel, Spec. Meeting on "Ceramics for  
Turbine Engine Application", Cologne, Oct. 7 - 12, 1979.
- /15/ Hüther, W.; Krüger, W.,  
Keramik im Triebwerkbau.  
Jahrbuch der Wehrtechnik 1983, Folge 14, p. 158 - 169.
- /16/ Boudigues, S.; Fratacci, G.,  
Technologies concues pour l'utilisation des céramiques dans les turbo-réac-  
teurs. AGARD-Conf. Proc. No 276 "Ceramics for Turbine Engine Application", 49th  
Meeting, DFVLR Cologne, 8 - 10 Oct. 1979.
- /17/ Avran, P.; Boudigues, S.,  
Turbines Blades Ceramics Heat Exchangers-Theory and Experimental Results.  
Tokyo International Gas Turbine Congress, Tokyo 26 - 30 Oct. 1987.
- /18/ Hüther, W.; Krüger, W.,  
First Test Results of Metal-Ceramic Guide Vane.  
72nd Specialists' Meeting on "Application of Advanced Material for Turbo-  
machinery Rocket Propulsion". 3 - 5 Oct. 1988, Bath, England.
- /19/ Matsuo, I.; Nishiguchi, F.,  
The Development of Second Generation Ceramic Turbocharger.  
Automotive Ceramics: Recent Developments. SAE Paper 207, International Congress  
Detroit, Mich., Feb. 29 to March 4, 1988.
- /20/ Kobayashi, Y.; Matsuo, E.; Kato, K.,  
Hot-Gas Spin Testing of Ceramic Radial Turbine Rotor at TIT around 1250°C.  
Automotive Ceramic: Recent Developments.  
SAE Paper 207, International Congress Detroit, Mich., Feb. 29 to March 4, 1988.
- /21/ Stambler, I.,  
Urge Follow-On Funding For All Ceramic Turbine R & D.  
Gas Turbine World 17 (1987) 1, p. 30-33.
- /22/ Stinton, D.P.; Caputo, A.J.; Lowden, R.A.,  
Synthesis of Fiber-Reinforced SiC Composites by Chemical Vapour Infiltration.  
Am. Ceram. Soc. Bull., Vol 65, No. 2., 1986, p. 347 ff.

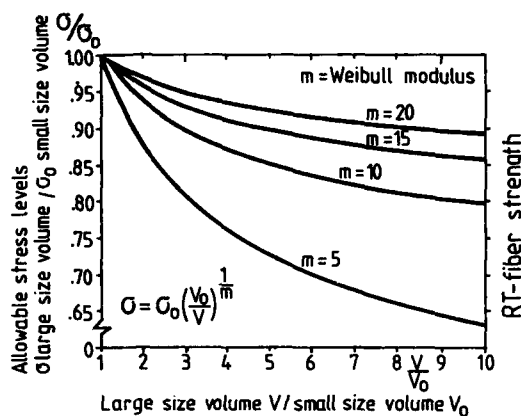


Fig. 1 Reduction of allowable stress level with increasing volume, due to failure probability.

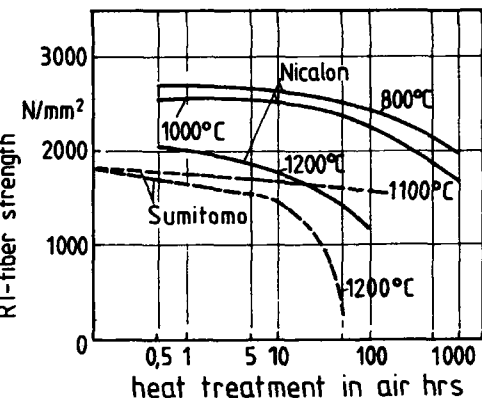


Fig. 3 RT-tensile strength of SiC-fibers and Al<sub>2</sub>O<sub>3</sub>-fiber after exposure in air.

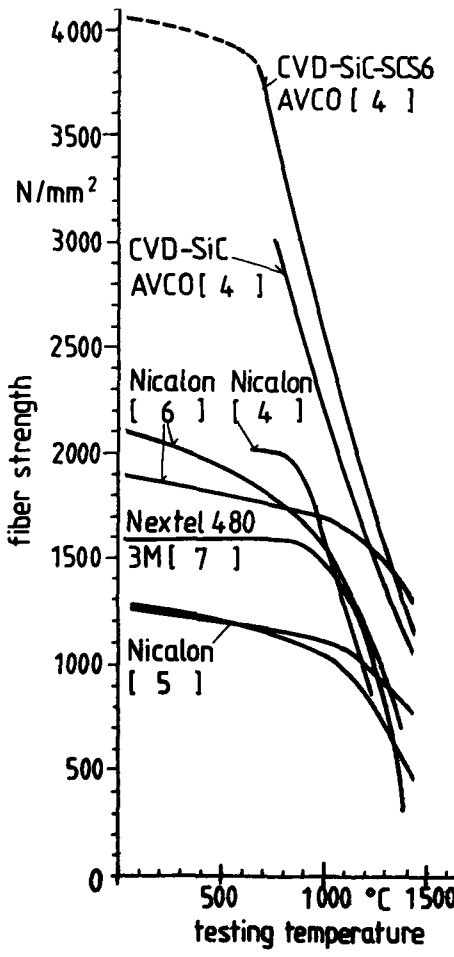
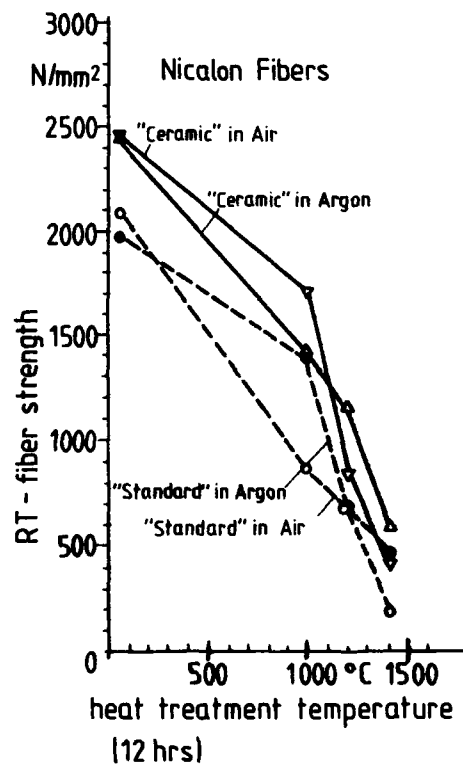


Fig. 2 Fiber strength as a function of testing temperature (short time values).

Fig. 4 RT-tensile strength of SiC-fibers after exposure in air and argon.



	SiC/SiC			C/SiC	C/C	
	SEP Cerasep M 303	Microcram Nippon Carbon	Oak Ridge Nat. Lab [2]	SEP Sepcarbinox M 111	SIGRI CC1502	Schunk CF 222
Density g/cm <sup>3</sup>	2.4	1.7 - 2.2	2.1 - 2.6	2.1	1.45	1.60 - 1.65
Fiber Content Vol %		30	30 - 42	45	45	65 - 80
Porosity %	10		< 30			5 - 8
Tensile Strength MPa	250	20		230 (RT) 410 (1500°C)	332	150 - 200
Flexural Strength MPa	300 (RT) 170 (1500°C)	37 - 50	100 - 400	500 (RT) 650 (1500°)	227	150 - 200
ILS MPa				25 (RT) 40 (1500°C)	12	8 - 12
Compression Strength MPa	850			300	160	
Young's Modulus GPa	210 (Tension)	38 (Tension)		100 (RT) 100 (1500°C)	88 (Tension) 58 (Flexure)	70 - 80
Elongation at Break %	0.8		1.0 - 2.8	0.75	1	0.2 - 0.4

Fig. 5 Data sheet values for C/C, C/SiC and SiC/SiC materials with fabric reinforcement.



Fig. 6 Compression-loaded ceramic wheel design /14/.

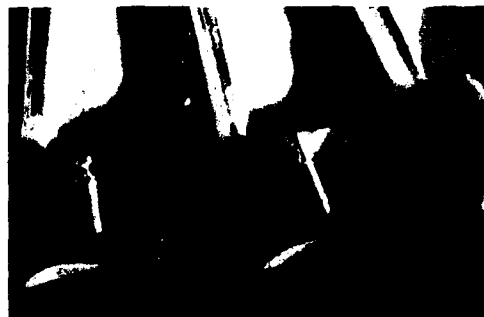


Fig. 7 A close view of a badly damaged first generation ceramic wheel, demonstrating damage tolerance.

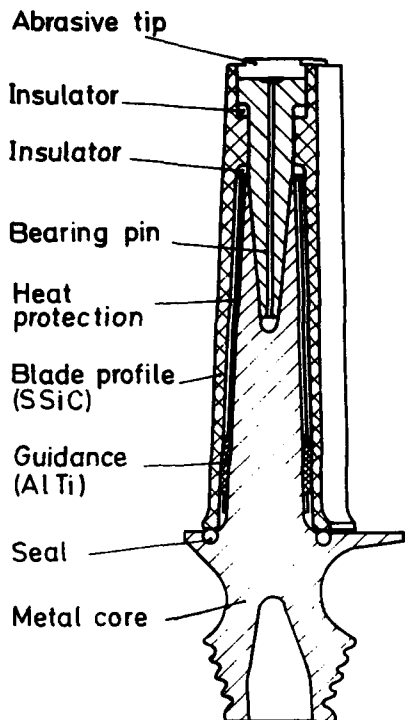


Fig. 8 Tie-rod turbine blade design with hollow ceramic airfoil.

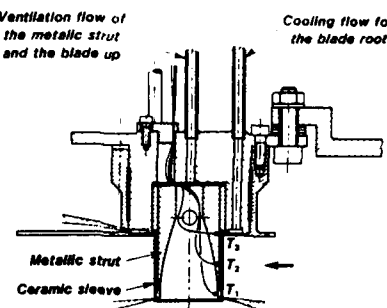


Fig. 9 Test set up for ceramic sleeve blade in static condition /17/.

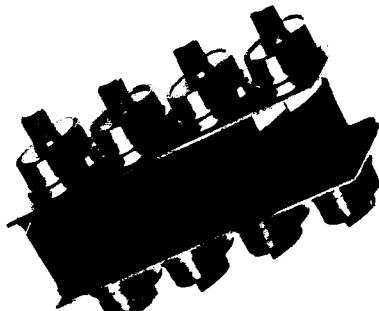


Fig. 10 Ceramic stator blades - a metal/ceramic hybrid design of MTU /18/.



Fig. 11 Rotor assembly for hot-gas spin testing of Mitsubishi/NGK ceramic silicon nitride turbine rotors /20/.

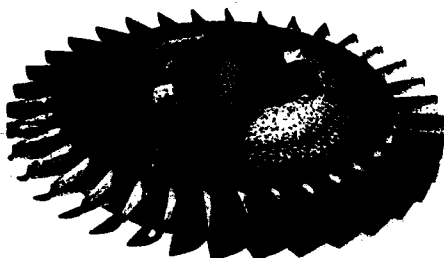


Fig. 12 SIC/SiC turbine rotor for limited life applications such as missiles.

## DISCUSSION

J. Moore, Pratt & Whitney, US. You showed a metal disk with separately attached ceramic blades. Was that rotor spun, and if it was, what were the test parameters (speed, temperature, test time, etc) and what were the results?

R. Kochendorfer, DFVLR, FRG. We did not test that rotor ourselves. The test was done by MTU and VW. I believe there are some people in the audience that can perhaps provide that information.

W. Huther, MTU, FRG. We tested inserted blades in a 166 mm tip diameter rotor in both hot and cold spin tests in several ways. About 70 blades were tested in cold spin tests of single blades at 65000 rpm with no failures. Single blades were hot spin tested at 1250°C and 40000 rpm with blade lives of 0.5 to 70 hours. A rotor with 41 blades was tested cold at 40000 rpm without failure. The rotor was also tested in an engine rig, with a total life time of 8 hours. In that case, failure occurred at 40000 rpm at 1150°C.

R. Kochendorfer, DFVLR, FRG. The main reason for using the rotor design with individually inserted blades was to apply a low cost injection molding technique for the blades. The early results, however, showed that reaction bonded silicon nitride made by injection molding was not suitable for this particular application. The tests reported here were therefore done mainly on machined sintered silicon carbide blades.

## CVD AND DIFFUSION COATINGS FOR HIGH TEMPERATURE APPLICATIONS IN TURBOMACHINERY AND ROCKET MOTORS

by  
 S.P. Field\*, J.E. Restall\*\*  
 ROYAL AEROSPACE ESTABLISHMENT  
 FARNBOROUGH HANTS, U.K.  
 and  
 C.D. Chalk, C. Hayman  
 FULMER RESEARCH LIMITED  
 Stoke Poges  
 Slough, Berks., U.K.

## SUMMARY

The paper presents a brief but critical review of recent developments in CVD metal and ceramic coatings for aerospace applications, covering in addition to standard CVD, activated CVD, diffusion CVD, pressure pulsed CVD and the more recently explored chemical vapour infiltration (CVI) processing. Fused slurry diffusion coatings are also covered. Important applications of such coatings and free-standing shapes are outlined and illustrated, particularly CVD diffusion aluminising, chromising and siliconising of turbine blades, refractory metal coatings and free-standing components of rocket motors. Future trends in materials technology will also be discussed with particular reference to the CVD coating of fibres, including modified carbon-carbon and other ceramic composites for high temperature operation in oxidising environments.

## INTRODUCTION

A number of major coating processes are now available for use in aerospace applications, many of which have received considerable development over the last thirty years as a result of impetus from the aerospace industry. Examples of the different processes include, thermal and electron beam evaporation, ion plating, sputtering, reactive sputtering, detonation gun, plasma spraying, electro-and electroless plating, slurry/fusion and chemical vapour deposition. Within some of these processes there are now important sub-divisions, and each can provide special technical and/or economic benefits when applied to particular applications.

Chemical Vapour Deposition (CVD) and fused slurry diffusion coating techniques, which respectively are covered in Sections I and II of this paper, have already gained considerable importance as a means of providing high performance metal and ceramic coatings for aerospace applications, including for example coatings for gas turbines and rocket motor components. A particular characteristic of these processes is an ability to deposit materials of high quality not achievable by other methods, and accordingly, with a growing demand for new materials with special properties, there is now significant effort directed to advancing the technology. In recent years the scale of CVD and slurry/diffusion coating has grown, and in future they are likely to become very attractive processing routes for both advanced coatings and monolithic shapes, particularly those that will be required to operate at substantially elevated temperatures.

## SECTION I - CHEMICAL VAPOUR DEPOSITION

## 1. Background

It is generally accepted that the initial stimulus for chemical vapour deposition coatings arose about the turn of the century within the lamp industry, where there was particular interest in the deposition of the high melting refractory metals, e.g. tungsten, which at that time were not readily amenable to processing into coatings by existing methods. Over the last forty years and in parallel with many of the other coating technologies, very significant advances have been made in developing CVD technology for use within the engineering, electronics, nuclear and aerospace sectors.

Although CVD is capable of depositing a very wide range of metals, non-metals and inorganic compounds, particularly binary compounds, carefully selected and controlled experimental conditions are usually necessary to ensure both optimum properties of a coating and also acceptable processing costs. Establishing these conditions by research is a first step which can then be followed by further refinement and development at pilot plant and/or production levels. With a few notable exceptions, CVD has generally been applied at small scale production levels, but there is now a very noticeable trend towards CVD coatings being produced at higher production levels, a trend which is expected to accelerate in the future as the demand grows for new coatings capable of meeting increasingly severe service requirements.

Standard chemical vapour deposition is a process whereby solid material is precipitated from the vapour phase, usually as a coating on an article or substrate, as a consequence of a thermally induced vapour phase chemical reaction. Although the standard, purely thermal CVD processes are the most widely used, there are now a number of variants of it which are quite important, including in particular, electrically assisted plasma CVD, laser assisted CVD and chemical vapour infiltration (CVI).

Thus an important requirement of standard CVD is that the substrate should be heated during coating - frequently to a substantially elevated temperature, and it is this feature which generally distinguishes CVD products from those derived from many other coating processes, in particular PVD processing where

\* Space Department.     \*\* Propulsion Department, Pyestock.

deposition occurs at or close to room temperature. Clearly if this were the only difference then CVD processes would find very limited application. However, experience has shown that there are many applications where coatings of the desired quality, all-round coverage and thickness cannot readily be achieved by other processes.

Halide reactions have played a most important role in CVD technology, and although originally most studies were made with chloride vapours, those of other halogens have been found to provide special benefits with certain systems. In combination with other vapours, halide reactions are now used in the production of a wide range of inorganic and ceramic coatings.

## 2. Types of CVD Reactions

A wide range of chemical reactions and precursor vapours are used in the preparation of CVD coatings. Examples of some of these reactions, relevant to aerospace coatings are shown in Table I.1.

Table I.1 - Examples of CVD Coating Reactions

Coating Element or Compound	Reactant Gases	Deposition Temperature (deg.C.)	Application
Boron	BCl <sub>3</sub> + H <sub>2</sub>	1200-1400	Coating for fibres; coating modifier.
Boron	B <sub>2</sub> H <sub>6</sub>	800-1000	
Aluminium	Ti <sub>1</sub> -isobutylaluminium	220- 250	IRFNA-resistant coating; aluminide diffusion coatings.
Carbon	Hydrocarbon (methane, etc.)	800-2300	CVI carbon; Pyrolytic graphite; diamond-like coatings.
Silicon	SiHCl <sub>3</sub> + H <sub>2</sub>	1000-1300	Silicide diffusion coatings; coating modifier.
Silicon	SiH <sub>4</sub>	1000-1300	
Niobium	NbCl <sub>5</sub> + H <sub>2</sub>	900-1200	Low temperature corrosion resistant coating.
Tantalum	TaCl <sub>5</sub> + H <sub>2</sub>	900-1200	Low temp. corrosion resistant coating; barrier coating
Tungsten	WF <sub>6</sub> + H <sub>2</sub>	400- 700	Erosion-resistant coating on graphite rocket nozzles
Tungsten	WC <sub>1</sub> <sub>6</sub> + H <sub>2</sub>	900-1200	Erosion resistant coating on graphite rocket nozzles.
Rhenium	ReCl <sub>6</sub> + H <sub>2</sub>	900-1100	Free-standing thruster sub-components.
Rhenium	ReCl <sub>5</sub>	1100-1300	
Iridium	IrF <sub>6</sub> + H <sub>2</sub>	600- 800	High temperature-oxidation resistant coating.
TiB <sub>2</sub>	TiCl <sub>4</sub> + BC <sub>1</sub> <sub>3</sub> + H <sub>2</sub>	900-1200	High temperature refractory coating.
SiC	SiHCl <sub>3</sub> + CH <sub>4</sub> + H <sub>2</sub>	1100-1400	High temperature oxidation resistant overlay coating; fibre composite infiltration coating.
SiC	CH <sub>3</sub> SiCl <sub>3</sub>	1100-1400	
TiC	TiCl <sub>4</sub> + CH <sub>4</sub>	900-1200	Barrier coating for carbon fibres; co-deposition coating.
MoSi <sub>2</sub>	MoCl <sub>5</sub> + SiCl <sub>4</sub> + H <sub>2</sub>	900-1200	High temperature oxidation resistant coating.
BN(hex)	BN <sub>3</sub> (X-Cl,F) + NH <sub>3</sub>	1300-1900	Possible infiltration coating for carbon fibre-based composites.
BN(hex)	B-Trichloraborazole	+1000	
BN(hex)	B <sub>2</sub> H <sub>6</sub> + NH <sub>3</sub>	800 upwards	
AlN	AlCl <sub>3</sub> + NH <sub>3</sub>	800-1200	Oxidation resistant, high thermal conductivity coating.
Si <sub>3</sub> N <sub>4</sub>	SiX <sub>4</sub> (X-Cl,F) + NH <sub>3</sub>	1300-1500	Oxidation resistant coating: CVI coating.
TiN	TiCl <sub>4</sub> + N <sub>2</sub> + H <sub>2</sub>	800-1000	Barrier coating.
B <sub>2</sub> O <sub>3</sub>	BCl <sub>3</sub> + CO <sub>2</sub> + H <sub>2</sub>	600-1200	Component of oxide ceramic coating.
Al <sub>2</sub> O <sub>3</sub>	AlCl <sub>3</sub> + CO <sub>2</sub> + H <sub>2</sub>	700-1200	Ceramic composite coating, or component of same.
SiO <sub>2</sub>	SiH <sub>4</sub> + CO <sub>2</sub> + H <sub>2</sub>	500-1200	Component of oxide ceramic coating.
SiO <sub>2</sub>	SiH <sub>4</sub> + N <sub>2</sub> O	800-1300	
TiO <sub>2</sub>	TiCl <sub>4</sub> + CO <sub>2</sub> + H <sub>2</sub>	700-1200	Component of oxide ceramic coating.

Coating conditions are generally very dependent upon the type of chemical reaction. Accordingly an outline of some of the more important types is given below.

### Hydrogen Reduction of Halides.

Metal and non-metal halides vary considerably in the ease with which they can be reduced to the element by hydrogen. Even at substantially elevated temperatures well above 1000°C, it is extremely difficult to reduce completely the more thermodynamically stable halides, including in particular the halides of the group IV metals - titanium, zirconium and hafnium. On the other hand, the halides of the group VI metals molybdenum and tungsten and those of the group VII metal rhenium, which are considerably less stable, may be readily reduced to metal, in the case of ReF<sub>6</sub> at temperatures around 250°C. Halides of the group V metals, of intermediate stability can be reduced by hydrogen to metal at temperatures above 900°C.

In the presence of additional vapours, this type of reaction may be used to deposit various inorganic and ceramic-like compounds, for example metal or non-metal borides, carbides, silicides, nitrides and oxides. In some instances, all the hydrogen required may come from the vapour of an added hydride, e.g. diborane, hydrocarbon, silane, ammonia or water, but this may be regarded as a hydrogen reduction since the free energies of formation of these hydrides and the inorganic compounds formed from them are usually relatively small. It may be noted that the deposition of many of the compounds of the

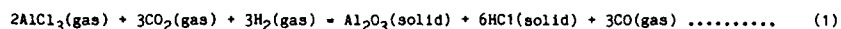
group IV metals occurs much more readily than that of the metals themselves, and this is a direct consequence of the relatively high stabilities of these particular compounds. However, the rates of deposition of these compounds are still low - microns/hour - at 1000°C. For the deposition of certain inorganic compounds it may be preferable to co-reduce two halide vapours, for example using a vapour mixture of titanium tetrachloride + boron trichloride with hydrogen to form titanium diboride.

## Thermal Dissociation of Halides

A number of the transition metals, including titanium, zirconium, niobium, tantalum, vanadium and chromium may be prepared by the high temperature thermal dissociation of their respective iodides. Also at sufficiently high temperatures, some of the less stable metal halides, e.g. rhenium pentachloride, may also be dissociated to metal. These reactions usually require higher temperatures than do the corresponding hydrogen reduction reactions. The benefit derived by the use of iodides arises from the formation on dissociation of iodine atoms which provide more favourable chemical equilibria.

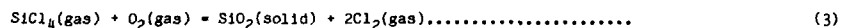
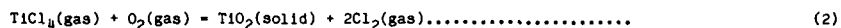
### Hydrolysis of Halides

This type of reaction has been widely used for the preparation of oxide coatings. However, because many halide vapours have a tendency to react with water vapour well below the optimum temperature of deposition, it is usual to employ a mixture of hydrogen and carbon dioxide as a more stable source of the water vapour.



### Oxidation of Halides

It is well known that oxides can be produced by the direct oxidation of halide vapours at high temperatures. The method is used widely for the preparation of titanium dioxide and silicon dioxide powders, basically according to the reactions:-



Because the precursor halide vapours can be readily obtained in a state of high purity, the method is able to produce very high quality oxide powders. It is applicable to many other oxides, and also double oxides of controlled composition.

## Chemical Vapour Transport

CVD processes based upon chemical vapour transport are widely used, particularly in the preparation of electronic materials. They are also of considerable relevance to the development of oxidation resistant diffusion coatings for turbine blades.

The chemical vapour transport method as applied to turbine blade diffusion coatings most usually involves a halide component as a gaseous carrier or 'activator'. This may be illustrated by the high temperature equilibrium as represented by the equation:-



At suitably elevated temperatures aluminium trichloride vapour will react endothermically with aluminium to produce aluminium monochloride vapour to an extent which depends to a major degree on the value of the equilibrium constant ( $K_p$ ) of the reaction. At lower temperatures this value is reduced, and hence by subsequent cooling of the equilibrium gas mixture, reversal of the reaction can be made to occur with the deposition of aluminium. Whereas material is transported from a higher to lower temperature in endothermic reactions, the reverse occurs in exothermic reactions.

Pack Metallising

By contrast, the pack aluminising of turbine blades is generally made under isothermal conditions where reversal of the equilibrium and the formation of the diffusion coating can be achieved as a result of a substantially lower chemical activity of aluminium at the turbine blade surface. It does nevertheless constitute a form of chemical vapour transport, which has considerable scope for the fabrication of all kinds of diffusion coatings on nickel, cobalt or iron based turbine alloys by halide transport equilibria, e.g. aluminising, chromising, siliconising, boronising. Although currently diffusion coatings are most usually based upon halide transport, any suitable solid/gaseous equilibria may be employed, as for example the use of the  $\text{SiO}_2/\text{Si}$  high temperature equilibrium for the formation of silicon carbide diffusion coatings on carbon-based substrates.

## Thermal Decomposition of Organo-Metallic Vapours

Volatile organo-metallic vapours are available for application in CVD coating processes. Many of these compounds can be thermally decomposed at quite low temperatures and hence are in principle attractive for preparing coatings on temperature-sensitive substrates. So far there has only been limited aerospace application of these coatings, their major use so far being within the electronics field, where coatings tend to be considerably thinner. Problems have been encountered when attempting to build up thicker coatings. For example, in the deposition of metals which form rather stable carbides it has proved difficult to obtain carbon-free deposits. For the Group IV transition metals it has not so far been possible to find suitable precursors which would allow the deposition of the metal in a reasonably pure state. Also the deposits are frequently not so well bonded to substrates as those which are produced at high temperatures, and they can also have poor cohesion. To some extent this is possibly due to lack of experience in the preparation of coatings from these compounds, together with the use of less

than optimum conditions of deposition. The method however has been used with advantage for the preparation of excellent quality, low temperature aluminium coatings of several hundred microns thickness using triisobutylaluminium or diisobutylaluminiumhydride as precursor vapours. Such coatings are pure, ductile and of low permeability to gases and vapours.

With further experience it is expected that greater use will be made of coatings derived from organo metallic compounds, particularly where the decomposition is made in the presence of other vapours to form compounds at low temperatures, for example carbides, nitrides and oxides.

### 3. CVD Process Characteristics

The main features of CVD processes may be summarised as follows:

- Substantially elevated deposition temperatures.
- Deposition time can be several hours or more.
- Coating rates from microns/hour to mm/hour related to the process chemistry.
- Excellent 'throwing-power' permits the all-round coating of components, including closed holes, fine channels, surface pores and microcracks. Difficult to coat localised areas except by masking.

### 4. CVD Coating Characteristics

CVD coatings, when applied under controlled conditions will generally display the following properties:-

- High density and void-free coatings of low permeability to gases and vapours.
- Coating thicknesses in a range microns to millimetres dependent upon the CVD coating method.
- Polyocrystalline coatings, highly orientated, frequently columnar, particularly in overlay type of coating.
- Grain size from around 0.01 to several microns, dependent upon the process and coating material.
- Adhesion of the coating can vary with deposition conditions.
- Very high purity coatings are possible.

There are many instances where because of the nature of the deposition process CVD coatings exhibit special chemical and physical properties. For example, the high degree of crystal orientation present in some coatings, e.g. pyrolytic graphite, pyrolytic boron nitride, can lead to quite useful but different thermal, electrical or mechanical properties in directions parallel and perpendicular to the direction of growth.

### 5. Aerospace Applications

There are a considerable number of different CVD materials that are either used currently or have potential application within the aerospace industry. As coatings, these materials may form part of diffusion infiltration, or overlay coating systems or may be the first step in the fabrication of free-standing components. Functionally, the coatings may for example, need to protect against corrosion or oxidation resistance up to very high temperatures, provide resistance to wear, act as diffusion or corrosion barriers, seal surface porosity in coatings or components or even provide special optical properties. Additionally, as indicated, they may offer a means for producing free-standing CVD products, including high temperature composites.

#### 5.1 Turbomachinery

The pack aluminising, chromising or siliconising of turbine blades to protect against high temperature oxidation or corrosion is very well known. As previously described, these processes make use of chemical vapour transport to produce the diffusion coatings. Essentially, the component to be coated is buried in a powder mixture of the coating metal, e.g. aluminium, a halide activator, usually a halide salt and an inert diluent, e.g. alumina, and the mixture heated for several hours at a temperature in the range 900-1100°C. This batch technique is capable of coating many hundreds of turbine blades at a time and is relatively inexpensive. However, as usually practised, the pack process does not have very high throwing power, and as a consequence cannot readily apply coatings to internal surfaces, as for example blade cooling channels, which for some advanced blades can be a limitation. CVD in which the gaseous reactants are supplied from an external source generally possesses very good throwing power, and this was demonstrated when pure aluminium coatings, deposited from triisobutyl aluminium hydride at about 2400°C, were applied to blade cooling channels. Subsequently, the coated components were converted into aluminide by heat treatment.

Although the process cost of the alkyl would have been extremely low, an alternative method, which was a novel modification<sup>(1)</sup> of the widely used pack process with substantially all the associated cost benefits, was also being explored. Briefly this comprised the introduction into the pack process of a) inert gas pressure pulsing and b) a comparatively low volatility halide activator, e.g. AlF<sub>3</sub>. Optionally, the method could be operated under reduced pressure conditions. The method was evaluated for aluminising and proved very successful for applying very good quality aluminide coatings of controlled thickness to both internal and external surfaces of blades. Subsequently, the effectiveness of the process was demonstrated in an aluminising plant capable of accommodating several hundred blades. An additional benefit deriving from the increased throwing power is the option of out-of-pack deposition, where the blades are supported above the pack rather than buried within it. In addition to avoiding possible detrimental effects on the coating due to pick up of the pack constituents, e.g. alumina, the out-of-pack processing can also provide a means of exercising better process control. Note however that for masking of blades to prevent deposition on to certain areas, account may have to be taken of the improved throwing power of the process.

The pulse metallising method has also been used with effect to aluminise, chromise and siliconise MCrAlY coatings applied by low pressure plasma spraying. Where the latter coatings are not fully dense or contain microcracks, some infilling of the porosity may also occur. Tests in the Cranfield burner rig under marine conditions have shown that pulse aluminised CoNiCrAlY(LCo22) coatings offer superior corrosion resistance at both 750 and 850°C over their fully processed plasma sprayed counterparts<sup>(2)</sup>. The method has also been used to produce chromaluminised and aluminosiliconised coatings as a 2-stage method. Oxidation and corrosion rig tests on the latter have been very encouraging. Finally, the method has also been used for aluminising low density fibrous preforms, for example nickel based felts, where the high throwing power of the method offers advantages.

In view of the benefits to be derived from aluminosiliconised coatings, studies have recently been made to produce these coatings by a novel method<sup>(3)</sup>. The components to be metallised together with the powder pack reactants are loaded into the system in the usual manner. At the outset, however, the powder pack contains all the ingredients (Al+Si+AlF<sub>3</sub>) necessary for aluminising and siliconising, although the composition needs to be carefully chosen so that a controlled thickness of aluminised coating may be achieved prior to the exhaustion of the aluminium. Siliconising of the aluminide layer proceeds when the aluminium has been reduced to a sufficiently low level. By this means aluminide layers have been siliconised to controlled depths and concentrations (fig. I,1).

In conclusion to this brief account of pressure pulse metallising, it may be of interest to mention briefly a recent innovation with regard to the halide cleaning of gas turbine components<sup>(4)</sup>, such cleaning being practised as a preliminary step before the braze repair of cracks in components. The halide cleaning studies were carried out in a pressure pulse metallising rig slightly modified to make provision for the introduction into the inert pulse gas of an external source of fluorocarbon vapour capable of removing oxide scale from cracks in the component. The pulse-assisted halide cleaning has proved effective in cleaning close to the roots of cracks (fig. I,2) and reducing active element concentrations to assist braze bonding.

### 5.2 Rocket Propulsion

Materials of interest in rocket propulsion are those which possess suitably high temperature capabilities, particularly with respect to chemical and mechanical properties. Favoured materials include the element graphite, the refractory metals niobium, tantalum, molybdenum, tungsten and rhenium, and to some extent the precious metals platinum and iridium. Compound materials are usually based upon metal oxides, nitrides and carbides.

CVD is capable of producing coatings of all of these materials. Pyrolytic graphite, produced by the thermal decomposition of hydrocarbons at very high temperatures (usually above 2000°C.) and substantially reduced pressure, may be built-up to deposits of appreciable thickness to form for example free-standing plate from which nozzles may be fabricated. Solid propellant rocket motors using nozzles of the somewhat harder pyrolytic graphite may offer superior resistance to graphite erosion as compared with conventional graphite nozzles. Pyrolytic graphite has a hexagonal layer structure with the layers orientated parallel to the deposition surface. Because these layers are only weakly bonded to each other, pyrolytic graphite coatings have a tendency to delaminate when subject to thermomechanical stresses. As a consequence, pyrolytic coatings of graphite on conventional graphite nozzles have not been particularly successful, although the delamination problem may be reduced by tailoring of the deposition conditions.

For aluminised solid propellant motors where the nozzles are required to sustain higher temperatures and generally more extreme burning conditions, graphites may not provide acceptable erosion resistance. In these circumstances tungsten (m.p.3370°C) may be a preferred material. As a lighter weight alternative to solid tungsten, CVD tungsten has been applied to graphite rocket nozzles. Good quality tungsten coatings of 2 to 3 millimetres thickness may be deposited from hydrogen/tungsten hexafluoride gas mixtures at about 600°C in a few hours<sup>(4)</sup>. Under controlled conditions, smooth, as-deposited tungsten coatings of specified thickness profile can be produced. CVD tungsten coated nozzles have performed successfully in firing tests, with minimal erosion of the tungsten.

The refractory metal rhenium has been successfully employed in the fabrication of free-standing thruster sub-components, rhenium nozzles, tubes, etc. of hydrogen and hydrazine thrusters. The CVD rhenium is deposited on to suitably-shaped mandrels of, for example, molybdenum from which it is subsequently separated by chemical dissolution of the mandrel. The benefit of using rhenium derives from the fact that it is a high melting metal (3170°C) second only to tungsten, but in contrast to tungsten it can be made with room temperature ductility. Also the metal does not react chemically with hydrogen or hydrides, which precludes the use of tantalum. Fabrication by CVD also avoids the difficulties associated with the rapid work hardening of rhenium when forming to shape by conventional metallurgical methods. The temperatures of deposition of rhenium are appreciably higher than required for tungsten, and the rates of deposition are lower. However, deposit thicknesses of 0.25mm are readily achievable. The CVD rhenium metal can be made of very good quality with suitable mechanical properties for use up to substantially elevated temperatures. High temperature burst strength data for CVD rhenium is also available<sup>(5)</sup>.

CVD platinum and iridium coatings have as yet only received limited attention for thruster applications, in part because of limitations in the current quality of the coatings. However, coatings of these metals, particularly iridium, should be capable of providing improved corrosion/oxidation resistance at substantially elevated temperatures, and hence find future application as advanced coatings.

### 6. Future Trends in CVD

There is considerable aerospace interest in materials capable of operating under oxidation/corrosion conditions at temperatures substantially higher than can currently be achieved by the use of coated superalloys or coated refractory metal alloys. Accordingly, we are now seeing research effort directed to the development of newer materials, in particular oxidation-resistant composite materials such as

oxidation resistant grades of carbon-carbon composites and also ceramic composites, and numerous publications related to these developments are already available. These developments are making use of CVD technology to a very significant degree, particularly as a means of providing matrix composite infilling with a range of materials (fig.I,3), e.g. silicon carbide, alumina, and in the enhancement of the oxidation resistance by the provision of oxidation-resistant overlay coatings. To date very little information has been disclosed on the lifetime/temperature performance of these materials under isothermal and/or thermocycling conditions, but there is little doubt that progress is steadily being made in the development of these new technologies. CVD is also assisting these technologies in other ways, for example by providing technology for the fabrication of SiC fibres and in the provision of barrier layers on fibres.

More generally, after many years, CVD now appears to be coming of age, to an extent that it is becoming annually increasingly difficult to keep track of many important studies now being made into new materials both within and without the aerospace industry. As an example of this one can cite the development of activated CVD diamond coatings which after many years research appears to be close to fruition. Recent reports indicate the practicality of fabricating free-standing CVD diamond components of quite appreciable size. Such material is likely to have a wide range of applications within the aerospace industry. Clearly there are going to be many others. Additionally, the scale of operations in CVD is continuing to grow. Very large reaction chambers up to several metres in diameter are now employed in a number of processes, as exemplified in carbon-carbon processing, and it is envisaged that these increases in scale will continue and make CVD economically attractive for the production of an even wider range of advanced materials.

## SECTION II - SLURRY DIFFUSION COATINGS FOR SATELLITE ROCKET MOTOR APPLICATIONS

### 1. Geostationary Satellite Propulsion System

The trend for future geostationary earth satellites, including the Olympus and Eurostar buses, is the use of a Unified Bipropellant Propulsion System for all of the satellite's propulsion requirements. This system offers improved propellant mass utilisation efficiency when compared to solid propellant or liquid monopropellant propulsion systems which have been used for these applications. The savings in propellant mass can be used either to increase the payload capacity or to extend the life of the satellite.

The storage propellants used for the bipropellant system are mixed oxides of nitrogen(MON) and monomethyl hydrazine(MMH). This propellant combination produces a thruster exhaust velocity between 2900 and 3100m/s compared with 2300 to 2400 m/s for solid propellants and liquid monopropellants. The gaseous reaction temperature of MON/MMH bipropellants is 2400C, thus requiring high temperature materials for the combustion chambers.

Figure II,1 shows the principal components of a typical bipropellant system and the positions of the various rocket thrusters used to control the satellite. The system is required firstly to insert the satellite into the Geostationary Orbit from the launch vehicle orbit using the Apogee Thruster and then to control both the orbital position and attitude of the satellite with the Attitude and Orbit Control Thrusters.

The Apogee Thruster raises the orbit of the satellite from an elliptical Geostationary Transfer Orbit(GTO) to the circular Geostationary Earth Orbit(GEO). The Apogee Thruster produces between 450 and 500N of thrust and is fired for a duration of between 60 and 120 minutes depending upon the mass of the satellite. The thruster is designed to limit the maximum combustion chamber temperatures to 1400C with the use of regenerative film and radiation cooling.

The second function of the system is to control the orbit of the satellite and to maintain the position against forces causing North/South and East/West Drift. These are due to gravitational forces from the sun and moon and from the earth not being a perfect sphere. The orbit control thrusters produce 10 to 20N of thrust and may be fired for 10 to 20 seconds, depending on how frequently orbit corrections are made, during which time the combustion chamber reaches the maximum operating temperature of 1400C. If the orbit is corrected on a daily basis, for a fine positional error, then up to 4000 thruster operations are required for a ten year satellite life.

The third function of the system is to apply the necessary torques to the satellite to maintain the attitude and pointing accuracy required. Attitude corrections generally use the same thrusters as those for orbit control. The disturbing torques are relatively small and only short thrust pulses, usually of less than one second duration are required.

The major component parts of a rocket thruster are shown schematically in Figure II,2. The propellants MON and MMH are fed to the synchronised flow control valves which control the thruster's operation. The propellants are atomised, mixed and distributed into the combustion chamber by the propellant injector. Combustion produces reaction temperatures of 2400C with the gaseous combustion products being expanded and accelerated through the nozzle section. The combustion chamber temperature is regulated by regenerative cooling of the injector with MMH and the heat radiated from the outside of the chamber to give maximum material temperatures of 1400C. The injector is produced from titanium alloy for good chemical compatibility with the propellants, low thermal conductivity between the combustion chamber and valves, and a low mass. Niobium alloy is used for the combustion chamber and nozzle, giving the required operating temperature capability for a reasonable material density and mass, and the niobium alloy is readily weldable to the titanium alloy injector. A protective coating is needed on the niobium alloy to prevent oxidation, and a summary of the necessary coating performance to meet the requirements of a Unified Bipropellant Propulsion System is given in Table II,1 below.

Table II.1 - Coating Performance Requirements

	THRUST (N)	FIRING TIME	MAX. TEMP. (C)	NO. CYCLES	TOTAL TIME AT TEMP. (HR)
APOGEE THRUSTER	450-500	60-120 min	1400	<10	2
ORBIT THRUSTER	10-20	10-20 sec	1400	<4000	22
ATTITUDE THRUSTER	10-20	<1 sec	A Few Hundred	<5000	14

The orbit control thrusters have the most severe operational requirement with a thruster and combustion chamber coating life of up to 22 hours and able to stand up to 4000 thermal cycles from ambient temperature to 1400C. Therefore these criteria have been adopted for determining the suitability of oxidation resistant coatings for the niobium alloy combustion chamber and nozzle. The reliability of a coating to meet these requirements is also of fundamental importance for the satellite to be able to meet its full operational design life.

## 2. Disilicide Coating Studies

### 2.1 Coating Programme

Research has been conducted into the factors and mechanisms that limit the life and durability of several disilicide based oxidation resistant coatings applied to niobium alloy, C103 (Nb10%Hf1%Ti, by weight).

Prior work in this field suggests that disilicide based coatings would constitute the most promising systems, there being many examples in the literature of these coatings being applied to refractory metals and their alloys. Indeed a fused slurry silicide coating (available from HITEMCO in the U.S.) designated R512E has already been used on the 100lb thruster in the U.S. Space Shuttle. However, this thruster operates under very different conditions to those set out in Table II.1 above, and so a specific coatings evaluation programme, designed with regard to RAE's thruster performance requirements, has been implemented to assess this and similar coating systems.

The work programme has involved 1) a critical literature survey<sup>(7)</sup>, 2) experimental studies to prepare, characterise and evaluate existing types of disilicide coating, 3) the identification and evaluation of improved coating compositions and 4) the preparation of documentation for a U.K. coating process specification<sup>(8)</sup>.

Of the coating systems studied, including proprietary CVD silicide coatings, the fused slurry silicide coatings have shown the greatest promise. The results of some studies on these coatings are described below.

### 2.2 Experimental Studies and Test Procedures

Slurry coatings, comprising mixed metal powders in an organic vehicle, were applied by dipping to C103 alloy test coupons. The coatings were then vacuum fused at 1400C. As increased knowledge of coating preparative techniques were gained it became apparent that all stages needed careful attention. Specimen edges have to be rounded and alloy surfaces have to be cleaned. Etching is one preferred method of cleaning; care has to be taken to ensure reproducible etching of specimens and adequate removal of etchant. Specimens have been fused in both a hot wall and a cold wall furnace. The latter although more costly at the outset, is probably easier to operate on a routine basis. The former requires frequent bake-outs and the use of argon soaks when the furnace is opened for loading and unloading of specimens in order to preserve cleanliness of the furnace walls, a factor which has a marked effect upon coating quality. The U.K. coatings were found to have a very similar microstructure to the U.S. coatings. Those of R512E type, containing chromium and iron as modifying elements, comprise six layers of varying composition, the latter brought about by interdiffusion of coating and substrate elements, figure II.3. Through-coating cracking is observed at fairly periodic intervals. This is caused by thermal expansion mismatch between the brittle coating and the more ductile substrate producing cracks at low temperatures. Porosity is sometimes observed within the outermost layers of the coating and this may be minimised by careful removal of the organic binder from the 'green', i.e unfused, coating prior to fusion.

Isothermal Oxidation Tests - Limited test data on the performance of the U.S. fused slurry disilicide coatings in isothermal tests at atmospheric pressure have been reported. Some of these test procedures have been replicated as far as is practical in the test programme, and they have served to demonstrate the similarity in performance between U.S. and U.K. coatings of comparable composition. Test temperatures of 1375 and 1425C were selected, these being very close to the temperatures of 2500F and 2600F used in the U.S. studies. Some coatings have been tested at 1400C in similar tests at RAE. Fused slurry coatings of several different chemistries were generally able to withstand 22 hours isothermal oxidation with moderate weight gains, as required. Failure was recognised as growth of oxide and/or consumption of the substrate.

Thermocyclic Oxidation Tests - A much more critical test of a particular coating-substrate combination was found in its response to thermocyclic oxidation. No suitable test procedure, allowing a large number of thermocycles to be accumulated rapidly, could be found in the literature and so a special test rig was constructed, allowing specimens to be automatically lowered into, and raised out of the hot zone of a vertical furnace at frequent intervals. Again the tests were carried out at atmospheric pressure. Test coupons, suspended on platinum/13%Rhodium wire, have dwell times of 30 seconds in the hot zone and 60 seconds under forced air cooling which reduces the specimen temperature to 60C. The transit

time between the two zones was 10 seconds per cycle. Tests were carried out to the same two maximum temperatures of 1375 and 1425°C as in the isothermal tests. It was found that the hot and cold temperatures and the air flow through the furnace all had a critical effect on the coating lifetime.

**Intermediate Temperature 'Pest' Oxidation tests** - A limited evaluation of coatings performance in both isothermal and thermocyclic tests at or to 750°C has been carried out. This temperature is considered high enough for significant oxidation of the coating to occur and low enough to render the coating more brittle than at higher operational temperatures. No real evidence of 'pest' type failures was found.

### 2.3 Results of Thermocyclic Oxidation Tests

Early work to assess coating performance statistically established that the R512E coating (both U.K. and U.S. prepared) on C103 alloy was not very thermal shock resistant under these test conditions with the best coatings often surviving fewer than 1000 cycles to either temperature. The surface texture of the coatings became very rough and considerable spalling with consequent weight loss occurred reducing the protective capabilities of the coating.

A coating of different chemistry, designated R512A, containing moderate proportions of chromium and titanium, has demonstrated greater thermal shock resistance in the Fulmer test programme although a wide spread of results was obtained from nominally identical specimens. A minor modification to this coating formulation however has enabled improved performance to be achieved with greater consistency. Table II.2 compares the oxidation resistance of the three types of coating described here. It shows how, for the modified R512A coating, thermocyclic performance in tests to 1425°C was very encouraging with four out of the five specimens surviving between 4000 and 7000 cycles. Only one specimen suffered a complete coating surface failure, the remainder incurring apparent local failures either at the support hole or at the bottom edge.

**Table II.2 - Summary of Thermocyclic Test Data for R512E, R512A, and Modified R512A Coatings on C103 Alloy**

Coating Type	Test Temperature (deg. C.)	Specimen Number	Fused Coating Weight (mg/cm²)	Max. Coating Lifetime (cycles)	Final Weight Change (mg/cm²)	Failure Mode
R512E	1375	31	26	900	-3.0	Hole failure, much spalling
		174	35	400	+6.0	Much spalling
		175	36	400	+6.2	" "
		176	35	625	+3.4	" "
		177	34	517	+4.0	" "
	1425	32	24	1258	-2.0	Top + bottom edge failures, spalling
		140	32	20	-16.0	Edge + hole failures
		141	32	50	+0.9	Edge + interior surface failures
		159	31	424	+2.3	Much spalling
		160	32	340	-4.2	Much spalling
		161	38	451	-6.8	Bottom edge + hole failures, spalling
R512A	1375	95	26	1670	+7.0	Bottom edge failure
		148	24	1015-1100	+5.6	Hole failure
		152	22	1000-1100	+5.1	Support wire failure (specimen lost)
		153	24	500-1318	+4.0	Hole failure
		154	24	1914-2030	+6.8	Hole failure
	1425	71	23	2200	+4.5	Bottom edge failure
		94	25	4450	+4.0	" "
		135	22	489	+4.0	All round edge failure
		136	25	470-900	+3.2	Hole failure
		155	24	150-810	+3.4	" "
		156	24	1500-2100	+5.2	Interacted with support wire (specimen lost)
		111	27	1536	+5.3	Hole failure
		146	21	1846	+7.0	" "
		147	25	1870	+9.2	" "
		149	25	2034	+8.6	Surface + bottom edge failure
R512A'		172	25	1240	+5.4	Hole failure
1425	110	27	3945	+3.4	Hole failure	
	112	25	504-1064	+4.4	" "	
	113	25	7069	+6.8	Bottom edge failure	
	128	25	4065	+5.2	General surface failure, much spalling	
	145	29	6265	+5.3	Bottom edge failure	

Transverse and longitudinal sections of the failed specimens were examined in some detail; figure II.4 is typical showing a modified R512A coating after 3945 cycles to 1425°C. It is believed that the coating functions, in part, by forming a protective oxide layer on the surface. The through-coating cracks also oxidise. In use, the innermost of the diffusion layers of the coating have broadened and

have arrested the progress of the through-coating cracks thereby preventing the ingress of oxygen towards the substrate. However, the development of extensive cracking in the coating in a direction running parallel to the substrate surface suggests that the coating is near the end of its useful life i.e. the failure points in the tests were representative of general coating wearout.

In tests to 1375°C, performance of the modified R512A coating was reduced with four out of the five specimens tested surviving between 1500 and 2000 cycles. Once again the points of failure were either the support hole or the bottom edge. When the coatings were studied in cross-section however, they were found to be in much worse condition than those thermocycled to the higher test temperature, figure II.5. The coatings were cracked and tending to fragment. Moreover, the innermost diffusion layers did not prevent the through-coating cracks reaching the substrate which consequently oxidised and became embrittled.

The high incidence of hole failures in the test programme is believed to be caused by criss-crossing of the cracks in the coating at sharply contoured edges of the substrate, figure II.6. Eventually coating segments become detached leaving the substrate with reduced protection in this region. Some hole failures may be exacerbated by interaction between the coating and the support wire used in the tests.

#### 2.4 Conclusions

Although the reduced performance of coated specimens in thermocyclic tests to 1375°C is cause for some concern, the laboratory data suggest that the modified R512fA coating on C103 alloy has the potential to meet RAE performance requirements and is an improvement over existing coating systems for this application. The broad spread of data observed for the unmodified R512A coating, with lifetimes varying by up to a factor of ten, has been observed and documented by other workers in the field<sup>(9)</sup>. The actual component temperatures to be encountered in use are to some degree unknown at present and are very dependent upon the design of a thruster and operational conditions which may vary for any particular satellite system. Overall, the results are sufficiently encouraging for a full evaluation programme for coated thrusters to be carried out in the near future, and a provisional coating process specification is available to facilitate the production of coated thruster components<sup>(8)</sup>.

Coating studies are to continue; it is hoped to broaden the scope of the test programme by the inclusion of low pressure, high temperature oxidation tests and to investigate the utility of NDE techniques in assessing the quality of as-fused coatings.

#### References

- 1) J.E. Restall and C. Hayman, "Pressure Pulsation Chemical Vapour Deposition Process for Coating Gas Turbine Blades", Proceedings of the First NATO Advanced Workshop on Coatings for Heat Engines, Eds. Robert L. Clarke, John W. Fairbanks, Dr. Ingard Kvernes, pp.347-357.
- 2) P. Hancock and J.R. Nichols, "Fundamental and Engineering Aspects of Coatings for Diesel and Gas Turbine Engineering", ibid, pp. 31-57.
- 3) J.E. Restall and C. Hayman, E.P. 0184354, App. Date 29th November, 1984.
- 4) J.E. Restall and C. Hayman, E.P. 0209307, App. Date 15th July, 1985.
- 5) P.J. Sherwood, C. Hayman and A. Bowry, "Erosion Resistant Coatings for Rocket Nozzle Applications", Chemical Vapour Deposition; 5th International Conference, 1975, p801-814, Paper 66.
- 6) A. Bowry, C. Hayman and P.J.C. Kent, "Hot Burst Strength of Vapour Deposited Rhodium", J. British Interplanetary Society, 1978, 31, p57-59.
- 7) Christine Chalk, Fulmer Research Report, "A Critical Literature Survey of Oxidation Resistant Coatings for Refractory Metals, Niobium and Tantalum and their Alloys: 1962-1985" R1078/5/October 1985.
- 8) Christine Chalk, Fulmer Research Report, "Process Specification for the Application of Fused Slurry Silicide Coatings to Niobium Alloy C103 (Provisional)", R1143/6/February 1988, Final Report, part 1.
- 9) "High Temperature Oxidation Resistant Coatings, Coatings for Protection from Oxidation of Superalloys, Refractory Metals and Graphite", NASA-CR-118647. National Academy of Sciences, Washington, 1970.

#### ACKNOWLEDGEMENT

The support of MOD (PE) for the researches undertaken by the Authors and reported here is gratefully acknowledged.



Figure I,1a Aluminium line scan of simultaneous silico-aluminising of turbine blades.



Figure I,1b Silicon line scan of simultaneous silico-aluminising of turbine blades.

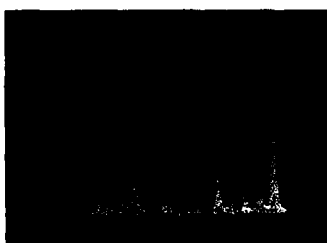


Figure I,2a Halide cleaning of cracked turbine components. Comparison scan of depleted zone and substrate (C1023) alloy (---).

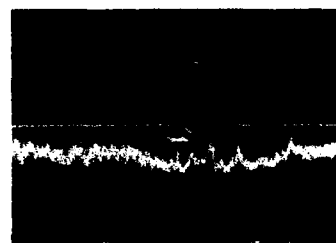


Figure I,2b Halide cleaning. Aluminium scan of depleted zone of cracked API testpiece.



Figure I,2c Halide cleaning. Aluminium scan of depleted zone of cracked API testpiece.



Figure I,2d Halide cleaning. Chromium scan of depleted zone of C1023 NGV.

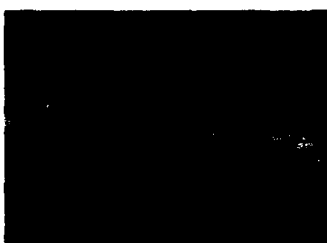


Figure I,2e Halide cleaning. Chromium scan of depleted zone of C1023 N.G.V. section.



Figure I,3 Chemical vapour infiltration. Boron nitride in-filling of compacted layers of carbon fibre cloth.  $\times 100$ .

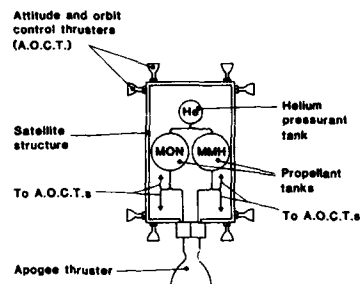


Figure II.1 Satellite Propulsion.

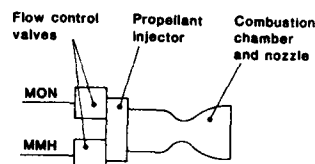
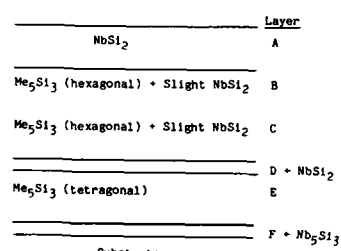


Figure II.2 A Satellite Thruster.

Figure II.3 'As-fused' R512E Coating Structure ( $\text{Me}=\text{Nb}, \text{Cr}, \text{Fe}$ ).Figure II.4 Modified R512A Coating. 3945 cycles to 1425°C. Transverse section.  $\sim \times 100$ .Figure II.5 Modified R512A Coating. 1536 cycles to 1375°C. Transverse section.  $\sim \times 100$ .Figure II.6 R512A Coating. Evidence of criss-crossing of cracks. Longitudinal section.  $\sim \times 100$ .

#### DISCUSSION

D. Colbourne, MOD, UK. Have you undertaken cyclic testing similar to that described by Dr. Chalk for your materials in turbomachinery components, and to what temperatures?

C. Hayman, Fulmer Research, UK. I wish Ted Restall were here, because he's been much more involved in this phase of the work and could provide a better answer. The evaluation of our CVD diffusion coatings, including, in particular the pulse pressure aluminate coatings, has been carried out under standard test procedures for such coatings by RAE Fyestock, Rolls Royce or Cranfield Institute of Technology. The quality of the coatings is at least equivalent to the state-of-the art coatings produced by pack cementation processing, with the additional benefits of the enhanced throwing power of the pulse pressure technique. Some test results are reported in references 1) and 2) of our paper.

R. Kochendorfer, DFVLR, FRG. What was the failure criterion in your thermal cycling tests? Was it the first crack that appeared at the surface or was it mechanical degradation due to that crack?

C. Chalk, Fulmer Research, UK. Basically, the appearance of yellow or white niobium oxide on the surface of the component was taken as a sign of failure. Weight gains and losses were also measured throughout the tests. A rapid change in weight was taken as a sign of failure. Finally, coatings were examined in cross-section. The state of the coating (signs of cracking or segmentation) and the state of the substrate (whether or not it showed signs of oxidation) were all taken into consideration.

E. Campo, Fiat Aviazione, Italy. I have two questions. First, Have you applied the coatings to the niobium alloys in your own facility or do you have an external supplier? Second, have you performed any mechanical property tests on the coated niobium alloys at the temperatures characteristic of your oxidation tests, 1400°C?

C. Chalk, Fulmer Research, UK. First, we have a facility to coat small components with fused slurry modified disilicide coatings. A 'clean' vacuum furnace capable of operation at temperatures in the region of 1400°C is required. We have also bought coatings from the United States and tested those along side our own. To the second question, we have not performed any mechanical property tests on test coupons at high temperatures, but some guide as to the effect of these disilicide coatings on the mechanical properties of niobium alloys will be obtained from thruster performance tests currently in progress.

## FUTURE ADVANCED AERO-ENGINES – THE MATERIALS CHALLENGE

by

D.R.Highton and W.J.Chrispin  
 UK Ministry of Defence (PE)  
 St. Giles Court  
 1/13 St. Giles High Street  
 London WC2N 2LD  
 UK

It should be made clear from the beginning that neither of the authors is a metallurgist or a specialist in the engineering use of materials. We are, however, responsible for ensuring that a balanced programme of aero-engine advanced engineering is pursued in the UK, and an important and growing element of this programme is that devoted to materials and processing technology. We are therefore more than a little involved in the quest for more capable materials.

The opinions expressed in this paper are those of the authors and they do not necessarily reflect official UK Government policy.

### 1.0 A Perspective of the Current Scene

From the earliest days of the gas turbine its performance potential has been constrained by the available materials. As a consequence the materials community has responded with a large number of significant developments and the following list, whilst far from exhaustive, gives some idea of their scope:-

Steady alloy refinement, particularly those having a nickel or titanium base.

Introduction of cold composites.

Development of anti-corrosion and thermal barrier coatings.

Process technology advances, in particular:-

- precision casting of turbine blades,
- uni-directional and single crystal casting.
- Iso-thermal forging.
- powder metallurgy.

However, the overall technical advances have consistently outstripped material advances due, mainly, to the evolution of advanced cooling systems and to aero-thermodynamic advances. Indeed, engineers, metallurgists and aerodynamicists have in partnership sustained a remarkable rate of development in the aero gas turbine. Many will recall a serious debate in the propulsion community some twenty five years ago on whether we had then reached a technology plateau from which it would be extremely difficult to progress further. In the event progress has continued unabated, as illustrated in Figures 1 and 2. Figure 1 shows the trend of military combat engine thrust to weight ratio (T/W) with time, and Figure 2 shows the trend in cruise specific fuel consumption for commercial engines.

In the US, the High Performance Turbine Engine Technology (HPTET) initiative (now Integrated HPTET - IHPTET) was launched in 1982 with the overall aim of doubling turbine propulsion capability by the year 2000. This implies a T/W ratio of 15-20. New material technologies will play a central role in achieving this leap in capability. In Reference 1, the USAF estimates that some 70 per cent of the increase in T/W ratio from 10 to 20 will come from taking weight out of the engine, a view confirmed in Reference 2 where AFWAL declare that the development of new materials is the key to this increase. In the UK, the Advanced Core Military Engine (ACME) programme has been pursuing advanced component technology, including materials since 1982, with a similar overall target to the US IHPTET initiative. The detailed objectives for the next phase - ACME II - are under active study, for work to be launched in 1989.

It should be noted that the progress made to date has been accompanied by a growing emphasis upon reduced operating costs, to which increased component lives have made a major contribution. In the case of military combat engines, there is in fact evidence that the increase in T/W performance has been checked by the demand for improved life and lower support costs, as shown on the figure 1 curves. In order to sustain this rate of progress and meet continuing aspirations for low operating costs, it will be necessary to seek further aerodynamic refinement, to develop even more effective cooling systems and, on the materials side, to evolve more refined alloys and processing techniques and coatings. Consider, however, Figure 3, which compares HP turbine gas temperatures of military engines with the metal temperatures capability of available blade alloys. The growing gap between these curves over the last 20 years is evidence of the increased innovation brought to the design and manufacture of ever more intricate blade cooling systems. But even with the benefit of Thermal Barrier Coatings (TBCs)

which are now being introduced progressively, it is difficult to see how the requirement for higher cycle temperatures to match the need for substantial increases in propulsion capability can be met without the emergence of radical new materials technologies.

Figure 4, though widely published before, is in our view a good illustration of the overall technical progress in military combat engines over the last twenty five years and anticipates where currently maturing technologies will take us by the turn of the century. The engine at the top is the military Spey which entered service in the Phantom in 1967. In descending order are shown the RB199, which entered service in the Tornado in 1979 followed by the XG40 demonstrator. Technology to this standard is planned to enter service about 1996 in the form of the EJ200 in the Eurofighter. Finally, an engine based upon the UK ACME (Advanced Core Military Engine) technology demonstrator programme, is illustrated in a conventional mixed turbofan configuration.

Interest in 'new' high temperature materials has probably never been greater than at the present time, with researchers embarked on a race for the new 'wonder' material which can simultaneously provide greater specific strength and temperature capability than current nickel based alloys, and at much lower cost. Such a material would enable the parasitic losses associated with current cooling systems to be reduced substantially or even eliminated, which would of itself bring substantial benefits to the gas turbine. Metal matrix composites, monolithic and reinforced ceramics and carbon in carbon are three classes of material currently receiving close attention, though these general categories cover a vast array of material and process combinations.

Whilst these materials offer great potential benefits they also present daunting engineering challenges which will have to be overcome before they will be widely exploitable in manned aircraft. Much work still needs to be done to minimise inherent weaknesses in the materials (such as brittleness, lack of oxidation resistance, lack of bond strength between reinforcing fibres and matrix), but even more from the engineering point of view in order to learn how to design to maximise the benefit from their virtues whilst minimising the effect of their weaknesses. Carbon-in-carbon is a classic example of such a material. Whilst offering the tantalising prospect of light, uncooled structures in the hottest parts of the engine, a great deal of fundamental materials and process development remains to overcome the severe drawback of its extreme affinity for oxygen. This has not proved a limitation in current applications such as heat shields and rocket nozzles, but is clearly incompatible with operating for thousands of hours on man-rated vehicles, and much work needs to be done to understand how to provide durable coatings or to inhibit the carbon matrix. In the UK, reheat components in coated carbon-in-carbon have been tested on an engine to help in understanding the problems.

On a similar theme, it is notable that notwithstanding major strides in the evolution of high strength nickel alloys for turbine discs over the last twenty years, and in the associated processing technology, the actual benefit in engineering terms has been relatively modest. This is largely due to the fatigue resistance not advancing in step with the UTS, in spite of all the attention given to process development and the control of inherent defect size.

It is the authors' view that the widespread adoption of these new materials cannot be achieved easily, cheaply or quickly. We believe that development of the aero gas turbine for manned aircraft at least, will continue to be evolutionary and that there will not be a rapid abandonment of the well established materials in favour of the new contenders. What is more likely to happen is that the new materials will be adopted in areas where their beneficial properties can be exploited without incurring undue engineering risk. For example, the application of ceramic materials to static structures such as combustor chamber linings, turbine static shrouds and gas bearing shells has been extensively demonstrated in UK advanced engineering programmes and shows great promise for early service introduction. Where favourable experience accumulates, the use of new materials will spread more widely through future engines, being introduced gradually into higher risk areas such as rotating structures. This means that in our view the long-term target of both the US and UK engine technology programmes of combat engines with a thrust to weight ratio of 20:1, will not be achieved in one step but after steady evolution. It is worth noting that T/W has progressed in steps of 40 per cent from Spey to RB199 to EJ200. Two further 40 per cent growth steps would take engine T/W to the 20:1 mark.

As has been made clear, we are concerned here mainly with engines for manned aircraft. The balance of requirements for air-breathing missiles and RPV's is somewhat different since they are not man-rated, do not require long lives and, with a few notable exceptions, do not require extremely high performance standards. Furthermore manufacturing cost is a major design driver. There is undoubtedly more scope for maturing new materials technologies rapidly in this area. Even so, the 'all-glass' or 'all-black' engines still have some way to develop before they can supplant the current engines which utilise essentially the same technologies as aircraft engines.

## 2.0 Managing the Opportunities

After fifty years of a narrowing field of candidate materials, albeit with significant perturbations, and even of manufacturing processes, the propulsion community is now confronted with an extremely wide range of options. With only limited financial and technical resources being available this creates severe resource management problems. Indeed, there would appear to be a significant risk that if premature commitments are

made to innovative materials, these 'new opportunities' might actually slow down progress.

Whatever management disciplines are imposed it is essential that at the fundamental research stage innovation should be encouraged and not stifled. However, before major financial commitments are made to a new material and/or process it is most important that the potential benefits are fully assessed from an application oriented point of view, involving both engineers and designers. This will require a multi-disciplinary approach to be adopted from an earlier stage in materials evolution than has often been the case in the past. There is also a powerful argument in favour of the major investment decisions being in the hands of the engineers who will have the ultimate responsibility for the successful validation of the new materials for the corporate design data base. Without an engineering commitment at that relatively early stage the introduction of a new material will be very much at risk. On the other hand, if engineering support cannot be won then a major investment is at that stage likely to be premature anyway.

With such a wide array of material and process development candidates (ranging from at one end of the scale refinements aimed at solving problems on existing projects to, at the other, novel materials with only long-term promise) there is also a need to clearly define corporate priorities. In some instances, where a material would potentially enjoy a wide marketability, an engine manufacturer could justifiably decide to leave suppliers to make any necessary investment. In others a sharing of financial risk between supplier and user might be necessary to ensure expeditious development. Finally, there will be key materials and process developments which engine manufacturers and/or their government customers may wish to pursue in-house with a view to enjoying the benefit of sole rights to a 'crown jewel' technology.

The balance between these three approaches will be to a large extent dictated by the resources, both financial and technical manpower, allocated by the prime engine contractors and their supporting governments to materials development. Notwithstanding the increasing emphasis being placed on materials there will always be competition with other disciplines for the advanced engineering budget and the resources will inevitably remain less than the responsible managers would believe they need.

The only satisfactory solution from an engine manufacturer's point of view would again appear to be a multi-disciplinary approach, under the leadership of a senior engineer, to the establishment of corporate priorities within the constraints of the available budget. They would need to be able to demonstrate that these priorities are compatible with those of any sponsoring government department.

### 3.0 The UK Response

This multi-disciplinary approach was formalised by Rolls-Royce Ltd in the UK some three years ago when, with the encouragement of HM Government, the company established a materials and processes strategy, managed by an R&D board under the chairmanship of a dedicated chief engineer. The 'prioritisation' process led to many long-standing activities being curtailed, and even in many cases dropped altogether, while many new 'strategies' were launched. MOD officials have been kept informed of all new strategies and have provided a certain amount of funding to support specific activities.

The scarcity of financial and technical resources dictates that the most promising materials should be identified at an early stage in the development cycle, in response to a perceived engineering need. This has been the driving theme in the formulation of the Rolls-Royce strategy. Civil market evaluation and military customer long-term aspirations, supported by cycle and design studies, have been used to identify the principal engineering requirements to which a suite of materials strategies have been matched.

Figure 5 lists those characteristics which dominate the selection of powerplants for four application areas, in a notional order of priority from the customer's point of view. New materials technologies will play a central role in achieving the increases in thrust/weight illustrated in Figure 1, both by reducing mass directly in all areas of the engine, and through the application of new high temperature materials leading to reduced cooling flows, to the benefit of higher core power and increased specific thrust. SFC improvements will be derived from higher propulsive and thermal efficiency, the necessary increases in cycle pressures and temperatures demanding improved materials if cooling penalties are not to outweigh potential benefits.

It has already been stated that in all applications, good durability is a key requirement in the continuing drive for lower through-life costs. The levels of component life and reliability now being demanded by both military and civil customers must be sustained or even improved in tandem with performance enhancements.

This objective is complicated on the military fighter and attack helicopter scene by the increasing use of rapid throttle movements required by more highly-maneuvrable aircraft, with the associated demand for increased hot end cyclic lives.

In generating their suite of materials technologies to meet these future perceived engineering needs, Rolls-Royce have focussed on 4 distinct classes of engine, namely Military Fighters, Civil turbofans, Civil Propfan/contrafan and Small Engines. Figures 6 to 9 illustrate materials identified within principal engine component areas. It will be noted that the Military Fighter engine has generated the largest share of materials requirements. This is not to say that these technologies will not find applications in Civil or Helicopter engines, but rather that the Military Fighter engine is likely to be the first application, where substantial increases in thrust/weight are needed to provide more competitive aircraft performance. Clearly, a large civil engine will benefit significantly from the availability of a high temperature material allowing SOT increases with cooling flow reductions, provided durability is not compromised. There will undoubtedly be scope for future HP spools incorporating significant amounts of new materials, developed for a military application, to be adapted to meet a civil requirement.

It is not the aim of this paper to assess the viability of the listed materials technologies. However, it is clear from Figures 6 to 9 that future progress is likely to depend on the availability of non-metallics and metal composites, and this is understandable when the potential benefits are examined. Figure 10 shows the specific strength of selected materials systems as a function of temperature. In all regimes of the engine, substantial improvements are possible if the potential of these new materials is realised. Figure 11 illustrates how the balance of materials used in the aero gas turbine may alter over the next 20 years as these new materials mature.

The key to realising the potential of these materials lies in the effective management of their development within Advanced Engineering programmes, prior to their commitment to project applications. Figure 12 sets out a model for the activities to be pursued in developing a candidate material from concept to validation, recognising that materials properties, processing requirements and design-for-purpose are intimately related and demand a multi-disciplinary approach as stated in the previous section. In broad terms, the first phase is associated with traditional laboratory-based research activity. Its aim is to determine whether the potential of the material to meet the agreed engineering requirement warrants further investment in the demonstrator-based second phase. The emphasis in Phase 1 must be to match the material to its likely application through the evaluation of generic shapes produced in representative pilot processes.

In Phase 2, full-scale components will be produced for further laboratory evaluation, full materials characterisation and assessment within demonstrator rigs and engines. In the UK, a comprehensive programme of civil, military and small engine demonstrator activity has been established (References 3 and 4), funded by MOD and DTI and managed by MOD. Elements of this programme involve, amongst other tasks, the provision of data on components featuring new materials, and it is expected that in future an increasing proportion of the substantial engine demonstrator budget will be spent on materials and related activities.

New materials require, and are beginning to receive from UK industry, a radically different approach to that given to conventional metallic materials. No longer can the manufacturing process be deemed simply as a 'tool of the trade' - it is an integral part of the overall design process required to meet the customer's unending quest for higher performance and longer life. It is important that government funding authorities and Company accountants alike recognise this and accept that substantial investment in these areas is essential if the required progress is to be made.

#### **4.0      Conclusions**

The powerplant will continue to be a critical factor in improving vehicle capability in all military and civil applications.

We appear to have reached a position where further improvements in propulsion capability depend not only on maintaining current effort in aerothermodynamic technology, but making substantial investments in new high-risk materials technology. The potential pay-offs are very high, but their achievement will demand discipline in setting clear technical goals, monitoring progress against clearly stated engineering requirements and being prepared to abandon lines of enquiry if evidence emerges that the targets will not be met.

#### **References**

1. 'Gas Turbine World', November - December 1986 Page 21.
2. J.S.Petty & R.E.Henderson, 'The Coming Revolution in Turbine Engine Technology', AGARD 1987.
3. W.J.Chrispin, 'The UK Engine Technology Demonstrator Programme'. ASME Paper 87-GT-203.
4. D.W.Hughes and W.J.Chrispin, 'Further Aspects of the UK Engine Technology Demonstrator Programme'. ASME Paper 88-GT-104.

#### **Acknowledgements**

The Authors would like to thank Rolls-Royce plc for their agreement to use the illustrations at Figures 6 to 12. The opinions expressed concerning the Rolls-Royce Materials and Process strategy are those of the Author's.

FIGURE 1 : MILITARY COMBAT ENGINES  
THRUST-TO-WEIGHT TRENDS

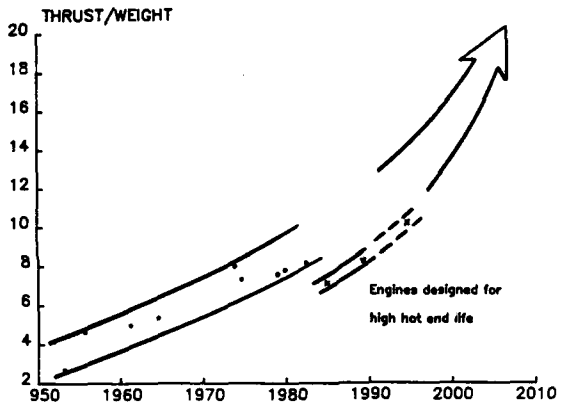


FIGURE 2 : COMMERCIAL ENGINES  
SPECIFIC FUEL CONSUMPTION TRENDS

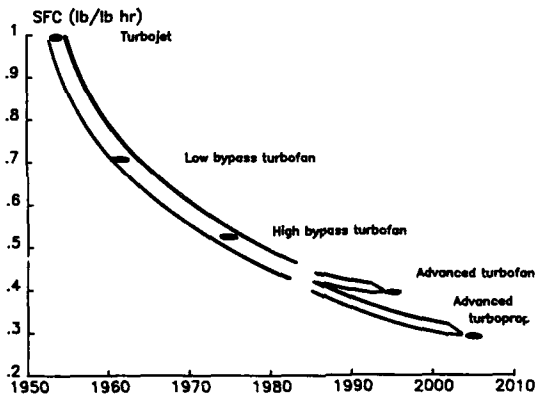


FIGURE 3 : HP TURBINE TEMPERATURES  
GAS AND METAL TEMPERATURE TRENDS

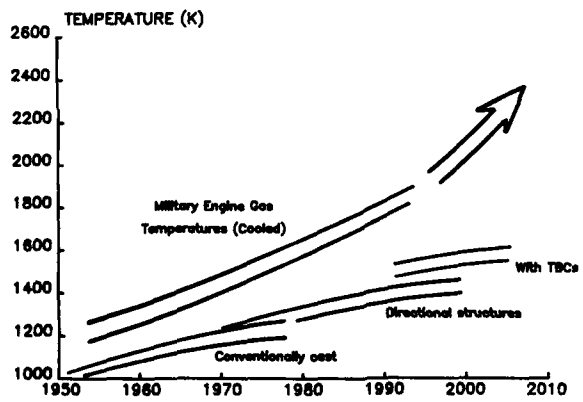


Figure 4 - The trend in fighter engines

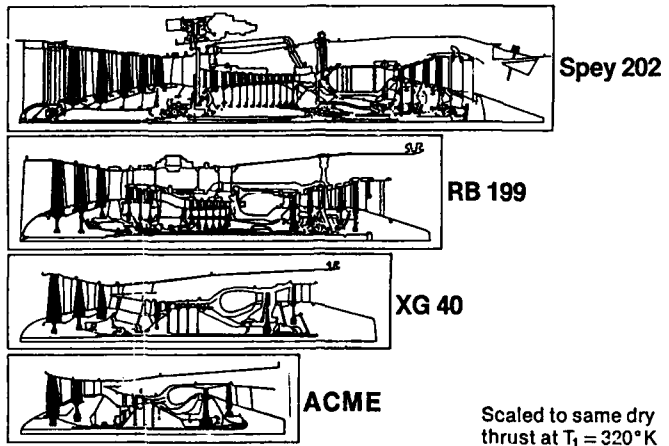


FIGURE 5 : ENGINE SELECTION CRITERIA

MILITARY FIXED WING & ATTACK HELICOPTERS

- o PERFORMANCE : THRUST- OR POWER-TO-WEIGHT
- o Durability (high cyclic usage)
- o Specific fuel consumption
- o First cost

MILITARY SUPPORT & ASW HELICOPTERS

- o RANGE : SPECIFIC FUEL CONSUMPTION
- o Durability
- o First cost
- o Power-to-weight

CIVIL HELICOPTERS

- o FIRST COST
- o Range (SFC)
- o Durability
- o Power-to-weight

LARGE CIVIL ENGINES & MILITARY TRANSPORTS

- o FUEL ECONOMY : SPECIFIC FUEL CONSUMPTION
- o Durability
- o Thrust-to-weight
- o First cost

**FIG 6 Materials and mechanical technology  
Military engines**

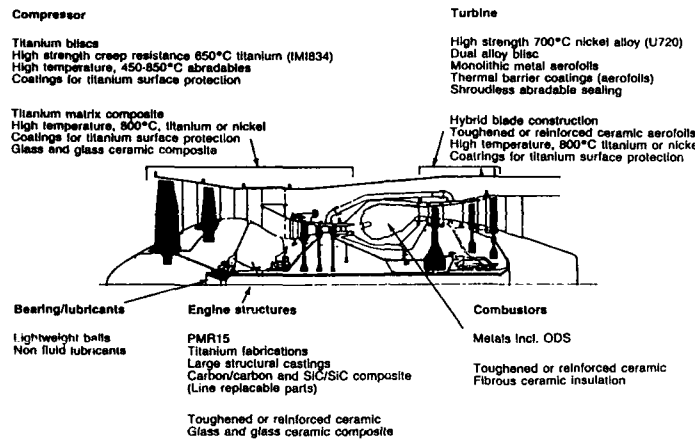


**FIG 7 Materials and process technology  
Civil turbofan engines**

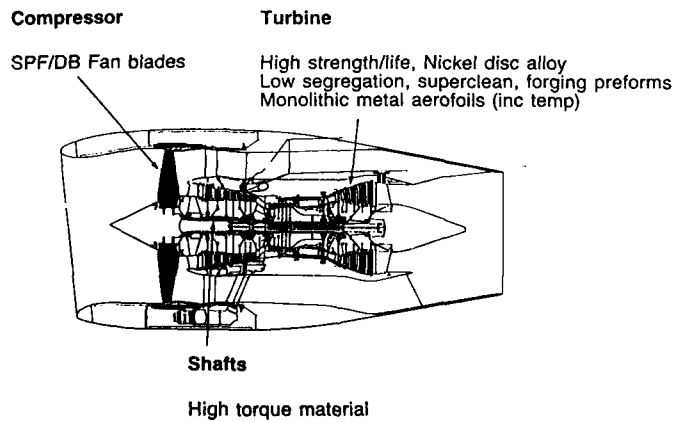


**FIG. 8 Materials and process technology  
Civil propfan/contrafan engines**

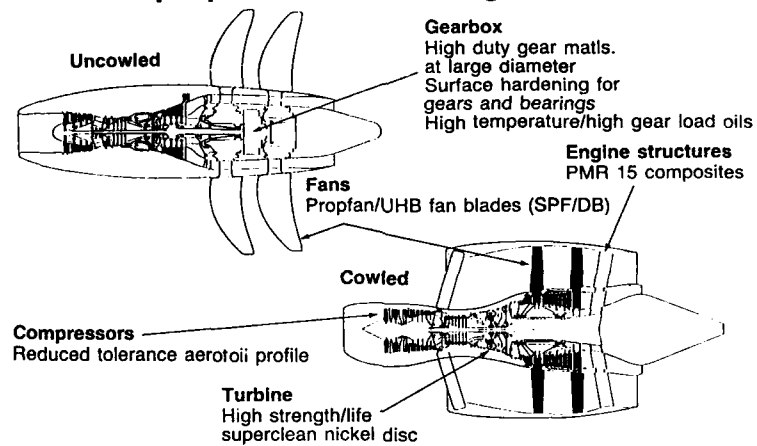


**FIG. 9 Materials and process technology  
Small engines**

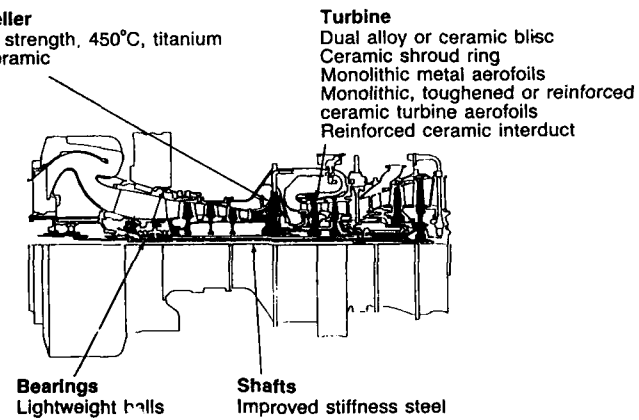


**FIG 10 Specific strengths of materials as a function of temperature**

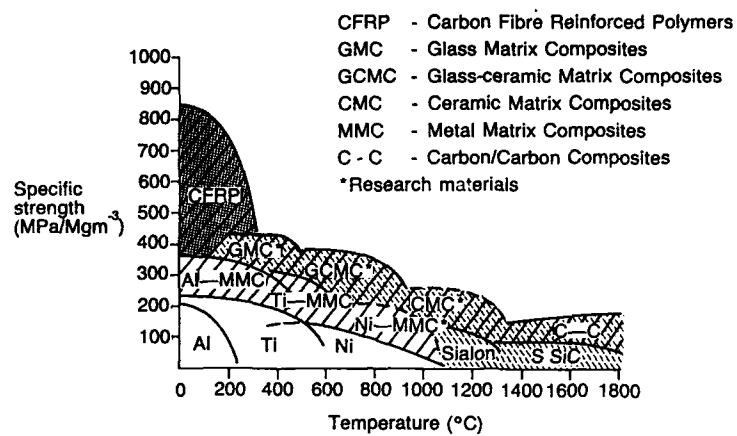


**FIG 11 Predicted Trends in Jet Engine Material Usage**

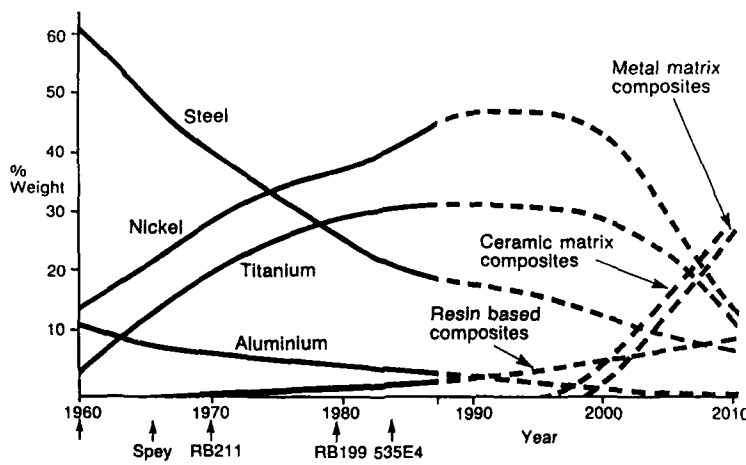


**FIG. 12 Materials and Process technology - Phases**

	ADVANCED ENGINEERING		PROJECT LAUNCH
MATERIAL	1. LABORATORY PHASE	2. ENGINEERING PHASE	3. VERIFICATION PHASE
	<ul style="list-style-type: none"> <li>• CONCEPT EVALUATION</li> <li>• MATERIAL DEVELOPMENT</li> <li>• GENERIC SHAPE EVALN.</li> </ul> <p style="text-align: center;">↓ PRELIMINARY DESIGN DATA</p>	<ul style="list-style-type: none"> <li>• COMPONENT DESIGN</li> <li>• MATERIAL CHARACTERISATION</li> <li>• COMPONENT PROVING (RIG OVERSPEED + LCF)</li> </ul> <p style="text-align: center;">↓ DESIGN DATA</p>	<ul style="list-style-type: none"> <li>• PRODUCT DESIGN</li> <li>• MATERL. VALIDATION OF PRODUCTION STD</li> </ul> <p style="text-align: center;">↓ COMPONENT VALIDATION (RIG + ENGINE)</p>
PROCESS	<ul style="list-style-type: none"> <li>• CONCEPT EVALUATION</li> <li>• PROCESS DEVELOPMENT</li> <li>• PILOT MANUFACTURE</li> </ul> <p style="text-align: center;">↓ PRELIMINARY PROCESS DEFINITION</p>	<ul style="list-style-type: none"> <li>• DEFINITION OF PROD. METHOD</li> <li>• PROD. PROCESS DEV'T.</li> <li>• MANUF. ON PROD. PROTOTYPE PLANT</li> </ul> <p style="text-align: center;">↓ INITIAL PRODUCTION PROCESS CAPABILITY DEFINITION</p>	<ul style="list-style-type: none"> <li>• PRODUCTION MANUF. ROUTE</li> <li>• PROD. PROCESS DEFINITION</li> <li>• PROCESS CAPABILITY ASSESSMENT</li> </ul> <p style="text-align: center;">↓ PRODUCTION PROCESS CAPABILITY PROVING</p>
PROGRAMME OBJECTIVES ENGINEERING MANUFACTURING	ADVANCED ENGINEERING CONCEPTS ADVANCED MANUFACTURING CONCEPTS	COMPONENT DEMONSTRATION PROTOTYPE PLANT DEMONSTRATION	PROJECT DEVELOPMENT/VALIDATION PRODUCTION PLANT DEVELOPMENT/VALIDATION

**DISCUSSION**

R. Eck, Metallwerk Plansee, Austria. Why didn't you include the refractory metals in Fig. 10? Molybdenum and tungsten alloys are already being used for short-term applications at temperatures to 3000°C.

W. Chrispin, MOD, UK. Fig. 10 was not an attempt to cover all candidate materials, but rather to show how the specific strength vs temperature envelope for the commonly used metallic alloys (aluminum, titanium and nickel) could be expanded if the potential of new metal matrix and ceramic composites were realized. Having narrowed the field of consideration down to a relatively few specific areas of investigation over the last four years, it has now opened dramatically, and it's going to be a very difficult task to single out those materials that are going to justify real investment and real commitment. The metallic envelope could certainly be increased with refractory metals, but the much greater potential of ceramic and carbon-carbon composites in high temperature applications is likely to focus effort on these systems despite the substantial problems involved in producing practical, durable components.

**NEW METALLIC MATERIALS FOR GAS TURBINES**

M.A.Hicks  
 Chief of Materials Research  
 Rolls-Royce plc  
 P.O.Box 31  
 DERBY  
 DE2 8BJ  
 UK

**Abstract**

The mix of properties required for high performance components in the gas turbine will continue to necessitate the use of metallic materials for the foreseeable future. Examples are shown in this paper which indicate how a detailed understanding of material/component behaviour and a better understanding/control of the manufacturing process are becoming increasingly important in meeting the anticipated design targets.

**Introduction**

Gas turbine development will continue to strive for higher thrust to weight ratios, better fuel efficiencies, with lower cost of ownership. These general requirements translate into the need for materials with increased strength and stiffness, reduced density, and higher temperature capability that can operate in a consistent and predictable manner for longer times.

There is a major initiative currently taking place in Europe and in the U.S. to develop the materials to meet these requirements and considerable attention is being given to the emerging, non-metallic materials such as the advanced composites which use high temperature polymers, glasses and ceramics as the matrices and silicon carbide or carbon as fibres. The traditional metallic materials are being severely challenged but significant progress continues to be made by the integration of alloy design, microstructural engineering and advanced manufacturing technology. This paper reviews some of the improvements that are being achieved with titanium alloys and nickel based superalloys which are the two families of materials most widely used in gas turbines.

**Titanium Alloys**

There has been a very rapid growth in the use of titanium alloys in the compressor section of gas turbine engines over the last thirty years as a result of their exceptionally good mechanical properties and low density (Figure 1). At present they typically account for approximately 25% of the weight of large commercial engines, finding application in discs, blades and casings. [1]

A wide series of alloys have been developed to satisfy varying component requirements ranging from the relatively high strength  $\alpha + \beta$  alloys, of which Ti-6Al-4V is the most widely used for applications up to 350°C, to the near  $\alpha$  alloys such as Ti5331s which can operate at temperatures approaching 600°C. [2,3] Table 1 shows the composition, temperature capability and approximate year of introduction for a number of the major alloys.

**TABLE 1 - COMPOSITION AND TEMPERATURE CAPABILITIES OF SOME MAJOR TITANIUM ALLOYS**

Alloy	Classification	Approx Year of Intro	Useful max temp	Chemical Composition - wt%							
				Al	Sn	Zr	Mo	Nb	V	Si	Others
Ti-6-4	$\alpha + \beta$	1954	350	6	-	-	-	-	4	-	- rem
IMI550	$\alpha + \beta$	1956	450	4	2	-	4	-	-	0.5	- rem
T16246	$\alpha + \beta$	1966	400	6	2	4	6	-	-	-	- rem
IMI679	near $\alpha$	1961	450	2.2	11	5	1	-	-	0.2	- rem
T16242	near $\alpha$	1967	450	6	2	4	2	-	-	-	- rem
IMI685	near $\alpha$	1969	520	6	-	5	0.5	-	-	0.25	- rem
T16242S	near $\alpha$	1974	520	6	2	4	2	-	-	0.1	- rem
IMI5331s	near $\alpha$	1976	580	5.5	3.5	3	0.3	1	-	0.3	- rem
IMI834	near $\alpha$	1984	600	5.8	4	3.5	0.5	0.7	-	0.35	0.09C rem

Most research in recent years has been directed towards increasing the maximum temperature capability of titanium alloys in order to extend their use as a disc material to the back end of the compressor section. It is not only tensile and creep strength that are important however, because the intended applications also call for good fatigue properties. In order to optimise this overall capability much effort has gone in to

generating a detailed understanding of the relationships between composition, processing route, microstructure and the resulting materials behaviour. As with most practical situations the final solution involves a number of compromises trading one mechanical property off against another. In general the  $\alpha + \beta$  family of alloys are associated with the highest tensile and low cycle fatigue strengths while  $\beta$  heat treated alloys display good creep properties, a high fracture toughness and the slowest rates of crack propagation. The latest high temperature titanium alloy developed at IMI, IMI834, was designed to capitalise on the benefits of both alloys types. The alloy chemistry of IMI834 has been tailored to allow heat treatment close to the  $\beta$  transus using 5-10% primary  $\alpha$  to pin the  $\beta$  boundaries so restricting grain growth.<sup>[3]</sup> The resulting grain size of the transformed  $\beta$  structure is only ~ 0.1 mm compared to typically 1 mm for the current fully  $\beta$  processed such as alloys IMI829 as shown in Figure 2. This is particularly important in terms of small fatigue crack growth because a relatively coarse grain size containing a transformed  $\beta$  microstructure of aligned  $\alpha$  platelets, can provide a rapid undeviated crack path along specific crystallographic planes as shown just to the left of the notch in Figure 3.<sup>[4,5]</sup> The tensile and fatigue strength of material taken from compressor disc forgings is typically between 10-20% higher than Ti5331s, depending on the test temperatures (Figure 4) and the creep properties of IMI834 offer a temperature advantage of approximately 30°C over Ti5331s.

Work in the US has continued to extend the near  $\alpha$  alloys and the latest development by TIMET, Ti1100, offers roughly a 55°C creep advantage over Ti6242s, the current workhorse elevated temperature titanium alloy favoured by P&W, GE and a number of other engine manufacturers. This temperature advantage has been achieved in Ti1100 without sacrificing strength or stability. The alloy does have lower toughness and higher crack growth rates than Ti-6242s.<sup>[6]</sup>

New manufacturing methods are also being developed which enable current alloys to be used more effectively. The wide chord hollow fan blade is a classic example of this. All early, high bypass ratio turbfans have solid blading made of Ti-6Al-4V, and to limit weight, long thin blades are used. However, in order to overcome vibrational problems and to help resist foreign object impact damage these blades are designed with stiffening features called 'snubbers' at mid span. This solution is associated with a 1-2% loss in specific fuel consumption due to the additional weight of the 'snubber' and aerodynamic losses caused by the disturbed air flow around it. A wide chord fan blade permits a larger air flow per unit frontal area thus increasing the engines propulsive efficiency. It is also better able to withstand foreign object damage.<sup>[1]</sup> A solid blade satisfying these design criteria would be unacceptable both in terms of its own weight and in that of the supporting disc. To overcome these problems RR has developed a 'snubberless' hollow blade which incorporates a titanium honeycomb core for stiffness. The chordal width is approximately 40% greater than previous blade designs and it has allowed the total number of blades to be reduced by about third<sup>[7]</sup>. Its construction, shown in Figure 5, involves vacuum brazing the honeycomb core between two plates of titanium which have been formed and chemically etched to generate the correct aerofoil shape. The bonded assembly is then finally established by forming to produce the finished shape. These blades are now standard on a range of Rolls-Royce engines. Further developments are exploiting the excellent formability of suitably processed titanium alloys to produce fan blades by superplastic forming and diffusion bonding. Other components can also be made cost effectively via this route.

Another growth area is the titanium casting industry.<sup>[8]</sup> Now large and quite complex parts can be produced with the required dimensional accuracy and mechanical integrity to allow casting to be considered as an alternative, cost effective manufacturing route for components previously fabricated from a number of parts and/or involving extensive machining operations.

Operating conditions in the temperature range of 600-650°C, for long periods of time, may represent a barrier for future developments in conventional titanium alloys.<sup>[9]</sup> Under these conditions the problem is not only restricted to high temperature creep because long term surface and metallurgical stability effects can also lead to a degradation in low temperature properties - in particular tensile and low cycle fatigue strength. These properties can be important under the high stress conditions experienced during take off, before the component has reached its equilibrium condition. Also there are some 'unknowns' concerning the effects of contaminants (eg. salt) on the behaviour of titanium alloys in this high temperature regime and the risk of a titanium fire will be increased following a blade rub or foreign object damage.

However, there is a very great prize to be gained if titanium could be extended to even hotter parts of the engine, initially to replace existing nickel alloys but with a longer term goal of operating up to 800°C. Research is being carried out both to develop additional strengthening mechanisms such as dispersoids or fibre reinforcement, and to establish whether titanium alumides can be exploited, either in a monolithic form or as a matrix for fibre reinforcement.

Rapid solidification processing (RSP) offers an opportunity of refining the microstructure and developing novel alloy compositions by extending the amount of alloying additions that can be retained in solid solution while still achieving a homogeneous end product. It has also been used to incorporate rare earth oxide dispersoids into the matrix.<sup>[10,11]</sup> Much more development work is needed before commercial quantities become available having the consistency of properties and behaviour demanded for gas turbine applications.

Titanium metal matrix composites (MMC's) are being developed to offer a strength and stiffness benefit over conventional alloys and at a reduced density.<sup>[11,12]</sup> Particulate, whisker and continuous fibre reinforcement are all being addressed but the technology is generally lagging behind aluminium MMC's, primarily because of reactivity problems between the matrix and reinforcement phases at the processing temperatures. Particulate or whisker reinforcement provides a smaller potential benefit than continuous fibres but is attractive in that the composite materials display isotropic properties and should lend themselves to conventional shaping operations. There may be some application for these materials if they can be produced cost effectively. High performance or stiffness critical components will necessitate the use of continuous fibre reinforcement, particularly if the properties are to be maintained to much higher temperatures.<sup>[12]</sup> Consequently this is where the majority of research is being directed. Current problems are the lack of a suitable fibre, fibre-matrix reactivity, and the associated manufacturing technology. Also more complicated stressing and design studies will have to be conducted if these materials are to be applied to use their full potential. Protective coatings have been used to protect the fibre but to date only coatings for large diameter monofilaments have shown any success, the AVCO SCS-6 fibre being the most widely used.<sup>[13]</sup> These large fibres are not ideal and severely inhibit the reinforcement of complex shapes. Typical properties achieved in a Ti-6Al-4V MMC containing a 0.35 volume fraction of SCS-6 fibre are shown in Table 2.

**TABLE 2 - TYPICAL PROPERTIES OF A 0.35VF SCS-6/TI-6-4 MMC**

Property	High Temperature Ti	Titanium MMC
RT tensile strength (L)	1080 MPa	1600 MPa
RT tensile strength (T)	1080 MPa	400 MPa
600°C tensile strength (L)	700 MPa	1200 MPa
RT tensile modulus (L)	120 GPa	250 GPa
RT tensile modulus (T)	120 GPa	180 GPa

Components made from either RSP materials or titanium MMC's will require some form of surface coating for high temperature applications.<sup>[3]</sup> The coating will have to provide protection against oxidation and corrosion but at the same time must not lead to a degradation in the basic mechanical properties of the material. Attempts to date to use coatings have met with mixed success.

Titanium aluminides have good high temperature strength and low density and good oxidation resistance to 900°C but have suffered a major drawback in terms of their unacceptable ductilities at low temperatures and the related fracture toughness and fatigue crack growth rate behaviour.<sup>[14]</sup> Much effort is being directed towards improving ductility through compositional modifications and some success has been achieved through niobium additions to Ti<sub>x</sub>Al. For example a commercially available Ti<sub>x</sub>Al based material, Ti-25Al-10Nb-3V-1Mo, shows tensile strengths some 200MPa above IMI834 at temperatures greater than 200°C (Figure 4) and between 2 and 5% ductility at room temperature. The ultimate goal may be to combine the excellent properties of Ti<sub>x</sub>Al with some form of continuous fibre reinforcement. Although titanium aluminide demonstrator components for advanced engines are being manufactured and evaluated, and there is a continuing high level of activity in the field, especially in the US, very little information has been published in recent years.

#### Nickel Base Superalloys

##### Turbine Disc Materials

The development of turbine discs for aero engines has also involved a combination of alloy design and process development technologies. Nickel based materials were first used instead of steels in the early 60's and, because of their immediate strength advantage, the forging of materials such as IN718, Waspaloy and N901 was little more than a shape making process.<sup>[15]</sup> As the operating conditions became more demanding, both in terms of temperature and stress, greater control of the manufacturing process has been introduced in order to generate improved microstructures and better mechanical properties.<sup>[16]</sup> Consequently these materials still feature in a large number of todays engines in the turbine section and in the final stages of the compressor. Alloy developments for conventionally cast-wrought products are restricted by the excessive chemical segregation and forging difficulties associated with the levels of alloying additions needed for significantly improved tensile, creep and low cycle fatigue strength. Powder processing has overcome these problems and has led to the development of Astroloy, Rene 95 and MERL 76 having proof strengths some 50% higher than the earlier superalloys (Figure 6 and Table 3). Powder processing has also eliminated the large oxide

inclusions sometimes observed in conventionally melted material but the presence of small quantities of organic or ceramic inclusions can lead to large variations in low cycle fatigue properties (Figures 7 and 8). Although sieving the powder removes the majority of defects larger than the final mesh size some high aspect ratio inclusions can occasionally penetrate the sieve and, in the worst case, these defects may act as equivalent size propagating cracks. These problems have led to a considerable amount of work in recent years aimed at producing ceramic-less powder technology which has been combined with improved powder handling and compaction techniques. In parallel "clean" ingot routes have been pursued using techniques such as electron beam cold hearth refining linked with new, controlled solidification methods to produce a homogeneous, fine grained ingot free of inclusions.[<sup>17</sup>]

TABLE 3 - COMPOSITION OF SOME MAJOR NICKEL BASE SUPERALLOYS

Alloy	Application	Chemical Composition - wt%											
		Cr	Co	Ti	Al	Mo	W	Ta	C	Zr	B	Others	Ni
Nimonic 115	blade	14.5	13.3	3.8	5.0	3.3	-	-	0.15	0.045	0.016	-	rem
In100	blade	10	15	4.7	5.5	3.0	-	-	0.18	0.06	0.014	IV	rem
MarM002	blade	9.0	10	1.5	5.5	-	10	2.5	0.15	0.05	0.015	1.5Hf	rem
PW1480	blade	10	5.0	1.5	5.0	-	4.0	12	-	-	-	-	rem
SR99	blade	8.5	5.0	2.2	5.5	-	9.5	2.8	0.02	-	-	-	rem
RR2000	blade	10	15	4.0	5.5	3.0	-	-	0.02	-	-	IV	rem
Waspaloy	disc	19.5	13.5	3.0	1.3	-	-	-	0.08	0.06	-	-	rem
Astroloy	disc	15	17	3.5	4.0	5.0	-	-	0.025	0.04	0.025	-	rem
René 95	disc	13.8	8	2.5	3.5	3.5	3.4	-	0.06	0.05	0.01	-	rem
Merl 76	disc	12.4	18.5	4.4	5.0	3.2	-	-	0.02	0.05	0.02	-	rem
U720	disc	18	14.7	5.0	2.5	3.0	1.25	-	0.04	0.03	0.035	-	rem

On the material side the emphasis has switched to a detailed understanding of the factors affecting fatigue crack nucleation and growth and the development of defect tolerant materials. Work at Rolls-Royce for example has shown that it is not always the highest strength alloys that are attractive to design engineers because these materials generally display the faster crack growth rates [<sup>5,16,18</sup>] - a fact made worse by the potentially high operating stresses offered by their tensile and low cycle fatigue properties. The major requirement is for a material having a high "usable strength". Further improvement in crack growth resistance can be realised by microstructural control brought about by careful thermo-mechanical processing. While ultrafine grain microstructures (~5μm) possess good tensile characteristics they tend to be associated with more rapid crack propagation rates and poorer creep properties. Coarse grain microstructures (50μm+) on the other hand have insufficient tensile and fatigue strength. The optimum microstructural combination has been shown to be a mixture of coarse grains surrounded by a "necklace" of small recrystallised grains as shown in Figure 9.<sup>[18]</sup> The level and distribution of retained work within the coarse grains of this necklace microstructure is also critical since the presence of highly developed planar dislocation arrays can provide easy crack initiation sites and lead to notch sensitivity.

The strict microstructural requirements placed on forgemasters by materials engineers has encouraged the development of finite element mathematical models to predict metal flow in the forging operation, and the associated microstructural development.<sup>[19]</sup> The key variables that are incorporated in the models are forging temperature, forging strain and strain rate. The models can be run through several iterations until the desired microstructure is obtained throughout the part thereby giving a higher probability of producing a "right first time" product than the more traditional approach based on a forgemaster's experience coupled with some trial and error. Such a model has been successfully employed by Rolls-Royce to produce high pressure turbine discs in U720 by isothermal forging. Hot die forging can also be modelled but requires more sophisticated constitutive equations which allow for heat losses.

The levels of cleanliness needed to give acceptable fatigue lives at the high stresses experienced in turbine discs are rapidly moving beyond current NDI capability. Therefore much greater reliance is having to be placed on engineering quality and consistency into all aspects of the manufacturing route rather than attempting to inspect out defects at the end of the operation. Use of these high strength materials has also driven the application of fracture mechanics based lifting methods which take into account the presence of crack like discontinuities from the first stress cycle.<sup>[20]</sup> However, because this is rather an inefficient way of using material, methods are being sought to take advantage of the cyclic life spent in nucleating a crack in addition to the cycles spent in the crack propagation phase. The observed scatter in cyclic life observed in

low cycle fatigue tests mainly arises from the variable behaviour in the crack nucleation and small crack growth regimes and these in turn are dependent on the nature, size, shape and distribution of the defects, the local stress field, matrix material behaviour and the local microstructure (Figure 10). All these factors need to be understood and related to a "total life" concept of component behaviour in future lifing models.<sup>[16]</sup> The next logical step beyond todays disc materials may be in the development of dual property integrally bladed discs or blisks, where an existing disc material is used for the cooler hub section where tensile and fatigue property requirements dominate, while the rim and blades are made from a cast alloy having much superior creep properties. The feasibility of this technology has already been demonstrated using a number of material combinations metallurgically bonded by hot isostatic pressing.<sup>[21]</sup> Cost effective processing together with the capability to repair blades damaged during manufacture or in service is vitally important to the economic viability of this concept. Beyond the conventional superalloys interest is being shown in nickel aluminides and nickel metal matrix composites as potential disc materials.<sup>[22,23]</sup> Both these materials have a number of technically challenging problems associated with them. In common with advanced titanium technology, the limited ductility and defect tolerance are of major concern with the intermetallics whilst the availability of suitable fibres and fibre/matrix reactivity problems, are the major problems associated with the use of metal matrix composites.

#### Turbine Blade Materials

Turbine blade materials are a classic example whereby advances in manufacturing technology have compensated for the decreasing potential for alloy development<sup>[15,19,22-26]</sup>. In todays jet engines turbine entry temperatures may approach 1400°C but it has still been possible to operate nickel alloys at these temperatures through the use of directionally solidified or single crystal alloys combined with complex cooling concepts. It would be beneficial however, to reduce the need for cooling air because it is associated with a significant efficiency penalty.

For the hottest stages of turbine blades this only appears to be possible with the application of reinforced ceramics, but improved single crystal materials would help to provide a more immediate benefit and may allow some additional stages of blading to remain uncooled.

Directional solidification provided the first major advance in temperature capability over conventionally cast, equiaxed blades, by aligning the grain boundaries parallel to the principal stress direction. Although the major motivation in this development was the removal of the crack initiation sites provided by the transverse grain boundaries the ~40% reduction in elastic modulus along the blade axis resulted in a significant reduction in plastic strain range during thermal cycling which in turn provided up to ten times improvement in thermal fatigue resistance.

In single crystal superalloys like SRR99 or PW1480, the complete absence of grain boundary strengthening elements raises the incipient melting temperature thereby allowing these materials to be solution treated at higher temperatures to provide better chemical homogeneity. A more uniform and finer Y' distribution for maximum strengthening can then be precipitated at lower temperatures<sup>[24,25]</sup>. Single crystal alloys have been in service in a number of engines since 1982<sup>[24]</sup> and second generation alloys are now well under development which give a further 10-40°C temperature advantage. Another 10-40°C improvement in metal temperature capability is being sought with third generation alloys, and the increased use of elements to enhance oxidation resistance may allow these materials to be used without protective coatings. The development of turbine blade materials and the associated increases in temperature capability are shown in Figure 11.

Even more complex cooling configurations, which would also be easier to inspect, could be provided by the use of hybrid blade technology<sup>[15]</sup>. Two alternative solutions have been examined; spar-shell and wafer constructions. Although the cooling advantages of wafer blades have been demonstrated the practical manufacturing problems involved and the cost-effectiveness are likely to prevent it ever being a production reality. The spar-shell concept shown in Figure 12 introduces the possibility of multi-piece blades with different materials being incorporated to meet the requirements of the various regions of the blade. This approach appears to have a much greater chance of success.

Corrosion resistant coatings are invariably required to protect nickel blades and vanes in corrosive and high temperature oxidation environments. Aluminide coatings, which were first introduced over twenty years ago, are still in widespread use but some components employ MCrAlX type overlay coatings which are directly deposited on the superalloy surface in order to give protection (M = Ni, Co; X = Y, Si, Ta, Hf etc). Overlay coatings are attractive in that compositional and thickness control are more flexible allowing the coating to be tailored for the particular need and consequently they are receiving much attention<sup>[26,27]</sup>. The increases in turbine entry temperature envisaged for future engines however will probably also require the use of thermal barrier coatings (TBC's) on blade aerofoils<sup>[15,28]</sup>. A zirconia coating for example could provide up to 200°C reduction in temperature at the blade surface<sup>[24]</sup>. TBC's have been successfully applied in combustion chambers and on the platforms of turbine stator vanes but the aerofoil represents a much greater challenge and will require higher temperature overlay bondcoats together with a much better understanding of the thermal-mechanical fatigue behaviour of the coating-substrate materials. Indeed most

progress in coating technology in general is likely to come in the short term by paying greater attention to, and optimising, the mechanical behaviour of coatings rather than developing new systems, on an empirical basis, specifically for corrosion resistance, as they have been in the past.

#### Summary

The development of metallic materials for gas turbines has reached a stage of maturity where improvements can only be made through an integrated approach, involving materials engineers and manufacturing technologists, to tailor material properties for specific applications via alloy composition, microstructure and process control. Better models of component behaviour are also being developed to allow these materials to be used with reliability under the increasingly demanding conditions of stress and temperature. This totally integrated approach will be even more critical for the intermetallic and composite materials which are likely to be needed to meet the design goals of future generations of engines.

#### References

1. J.F.Coplin, "Designing with Titanium", in Proceedings of Designing with Titanium Conference, Inst. of Metals, Bristol, 1986, pp 11-27.
2. D.Eylon, S.Fujishiro, P.J.Postans and F.H.Froes, "High Temperature Titanium Alloys - A Review", J. of Metals, 36, 1984, pp 55-62.
3. P.A.Blenkinsop, "High Temperature Titanium Alloys" in Materials in Aerospace, Conf. Proceedings, Royal Aeronautical Society, April 1986, pp 189-208.
4. C.W.Brown and M.A.Hicks, "A Study of Short Fatigue Crack Growth Behaviour in Titanium Alloy 685", Fatigue of Engng Mats and Structures, 5, 1983, pp 67-76.
5. M.A.Hicks and C.W.Brown, "A Comparison of Short Fatigue Crack Growth Behaviour in Engineering Alloys", in Fatigue 84, ed C.J.Beevers. EMAS, Birmingham, 1984 pp 1337-1343.
6. P.J.Bania, "Ti-1100: A New Elevated Temperature Titanium Alloy" in Proceedings of 2nd Int. SAMPE Metals and Metals Processing Conference, eds F.H.Froes and R.A.Cull, Dayton OH, 1988, pp 286-297.
7. G.A.Fitzpatrick and T.Broughton, "The Rolls-Royce Wide Chord Fan Blade" in Proceedings of TDA Int. Conf on Titanium Products and Applications, 1986, San Francisco.
8. J.K.Thorne and W.J.Barrie, "Advances in Titanium Alloy Casting Technology" in Proceedings of 2nd Int. SAMPE Metals and Metals Processing Conference, eds F.H.Froes and R.A.Cull, Dayton, OH, 1988, pp 20-27.
9. S.M.L.Sastray, T.C.Peng, P.J.Meschter and J.E.O'Neil, "Rapid Solidification Processing of Titanium Alloys", J.of Metals, 35, 1983, pp 21-28.
10. F.H.Froes and J.R.Pickens, "Powder Metallurgy of Light Metal Alloys for Demanding Applications", J. of Metals, 1, 1984, pp 14-28.
11. P.R.Smith and F.H.Froes, "Development in Titanium Metal Matrix Composites", J. of Metals, 2, 1984, pp 19-26.
12. G.A.Owens, "Reinforced Titanium for Aero Engine Applications" in Proceedings of Int. Conf on Advances in Composite Materials, ed I.C.Visconti, Milan, Italy, 1988, pp 747-761.
13. "Method of Applying a Carbon Rich Surface Layer to a Silicon Carbide Filament", US Patent No. 4,415,609, AVCO Co. November 1983.
14. H.A.Lipsitt, "Titanium Aluminides - An Overview", High Temp. Ordered Intermetallic Alloys, Vol 39, eds. C.C.Koch, C.T.Lui and N.S.Stoloff, Materials Research Society, 1985, pp 351-364.
15. G.W.Meetham, "Materials for Advanced Gas Turbines" in High Temp Alloys for Gas Turbines and Other Applications" Conf Proceedings, eds W.B.tz et al, 1986, Liege, Belgium pp 1-18.
16. R.H.Jeal, "The Specification of Gas Turbine Disc forgings", Metals and Materials, Sept 1987, pp 528-533.
17. Proceedings of the Conferences, "Electron Beam Melting and Refining - State of the Art", 1984-1987, ed R Bakish, Englewood, NJ.
18. C.W.Brown, J.E.King and M.A.Hicks, "Effects of Microstructure on Long and Short Crack Growth in Nickel Base Superalloys", Metals Science 18, 1984, pp 374-380.

19. D.Driver, "Near Net Shape Manufacture of Aero Engine Components", Metals and Materials, 1988, pp 493-497.
20. A.C.Pickard, M.A.Hicks and R.H.Jeal, "Applications of Fatigue Analyses: Aircraft Engines", in Fatigue 87, ed C.J.Beevers, EMAS Birmingham 1987.
21. G.S.Hoppin III, and W.P.Danesi, "Manufacturing Processes for Long Life Gas Turbines", J. of Metals 38, 1986, pp 20-23.
22. V.K.Sikka, "Engineering Processing and Properties of Nickel Aluminides" in Proceedings of 2nd Int SAMPE Metals and Metals Processing Conference, eds F.H.Froes and R.A.Cull, Dayton, OH, 1988, pp 62-75.
23. L.O.K.Larsson, "High Temperature Metal Matrix Composites for Gas Turbines", in Proceedings of Int. Symposium on Air Breathing Engines, National Aeronauticaical Lab, 1981, 1-54.8.
24. M.Gell, D.N.Duhl, D.K.Gupta and K.D.Sheffler, "Advanced Superalloy Airfoils", J. of Metals, 1987, pp 11-15.
25. D.A.Ford and R.P.Arthey, "Development of Single Crystal Alloys for Specific Engine Applications", in Superalloys 84, Published by Met.Soc. AIME, 1984, pp 115-124.
26. R.A.Sprague, "Material and Process Impact on Aircraft Engine Designs of the 1990's", ASME publication 82-GT-278, 1982, pp 1-10.
27. T.N.Rhys-Jones and D.F.Bettridge, "Protective Coatings for Gas Turbines", in 1st ASM Europe Tech. Conf; Materials and Processing Techniques for Structural Applications, eds T.Khan and A.Lasalmonie, Paris, France, 1987, pp 129-158.

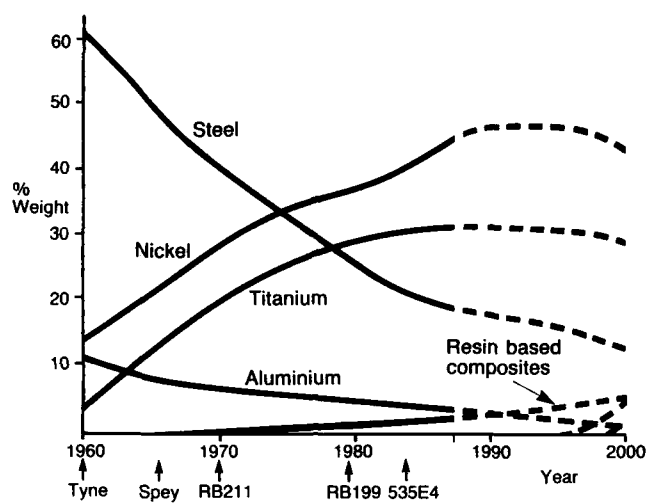


Fig.1. Trends in aero engine Materials Usage

(a) Slow cooled, fully transformed  $\beta$  microstructure  
- IMI685(b) Relatively fast cooled, transformed  $\beta$  microstructure  
- IMI685

(c) IMI834

Fig.2. Microstructures of some titanium alloys

Fig.3. Crack path in IMI685

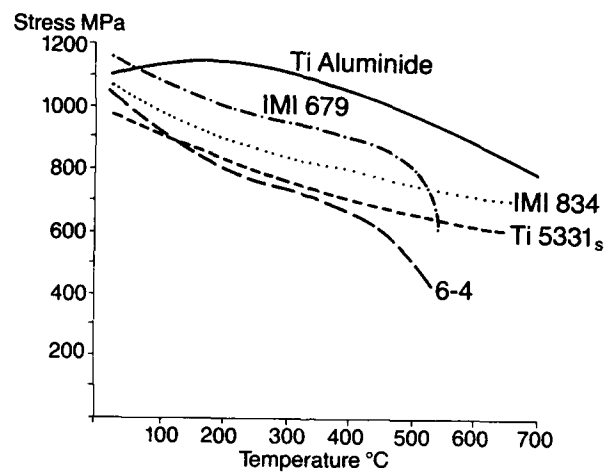


Fig.4 Typical tensile properties of some titanium alloys

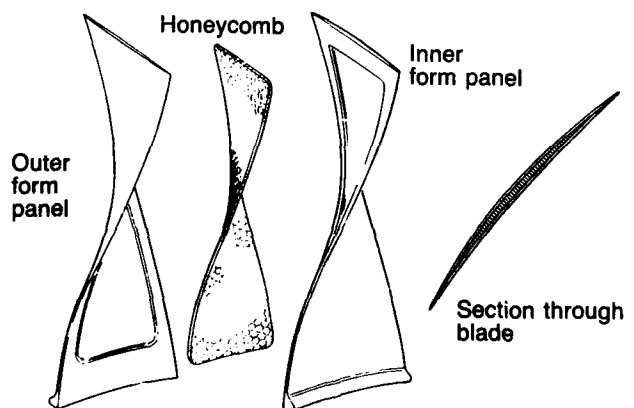


Fig.5. Wide chord fan blade construction

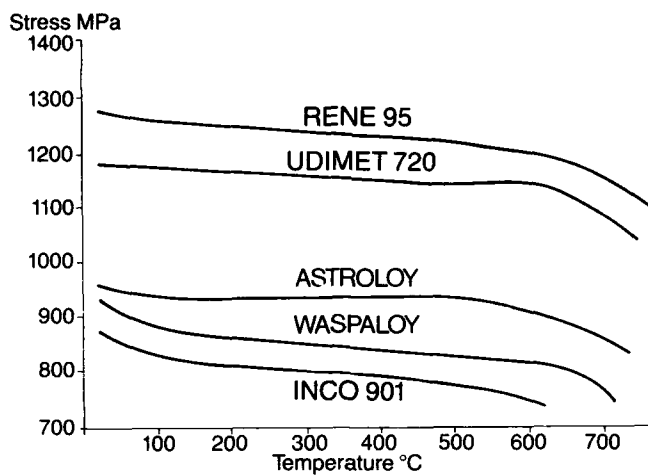


Fig.6. Typical tensile properties of some nickel based superalloys

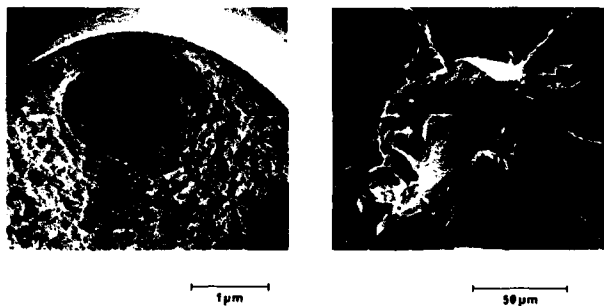


Fig.7. Low cycle fatigue failure in powder Astroloy from a subsurface defect

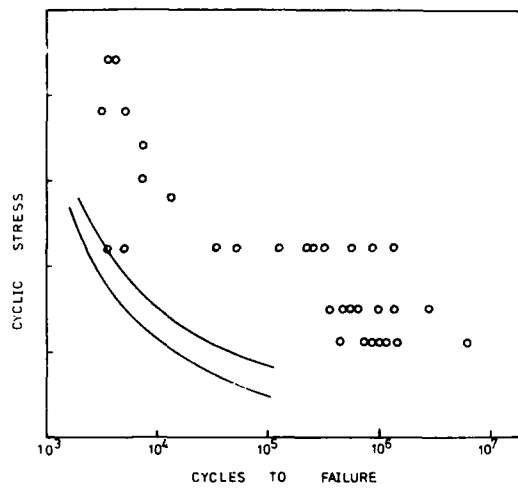


Fig.8. A comparison of LCF results between powder Astroloy (points) and Waspaloy (lines) at 600°C

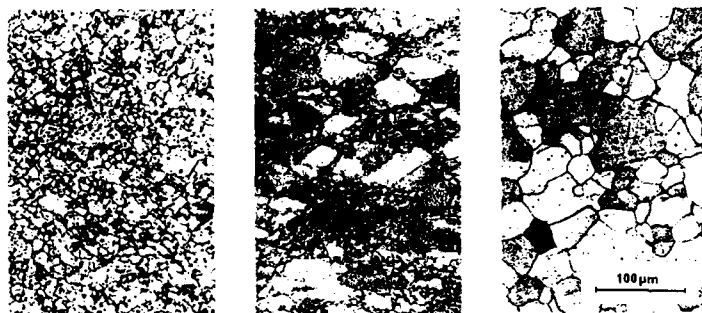


Fig.9. Microstructures in nickel based superalloys  
(a) fine grain (b) necklace (c) coarse grain

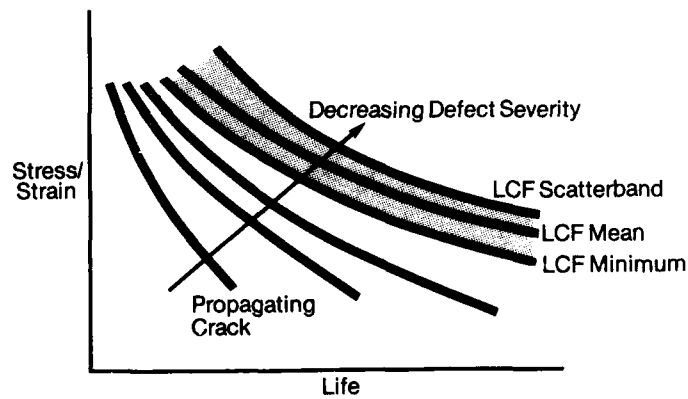


Fig.10. Cycle life curves

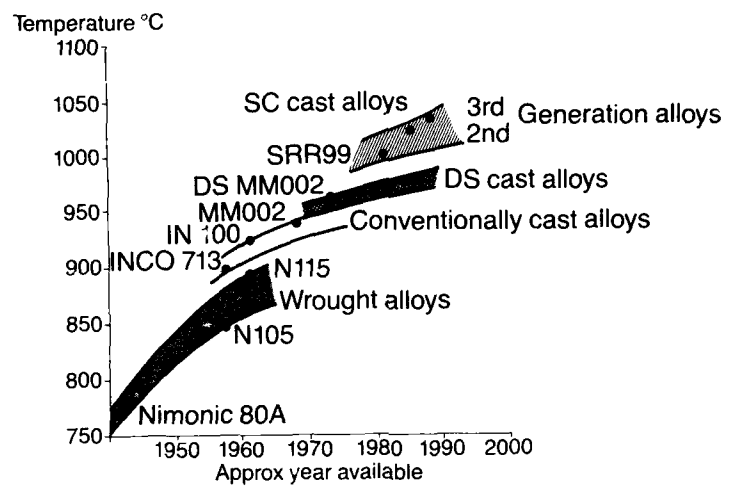


Fig.11. Temperature capability of turbine blade alloys

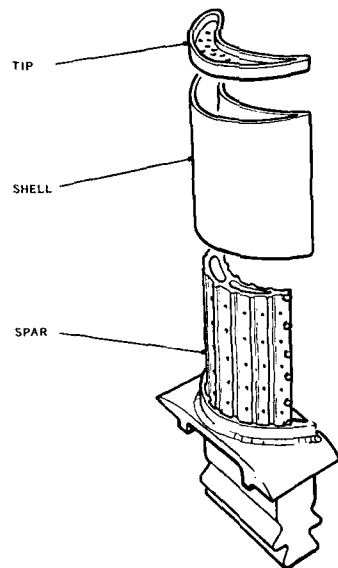


Fig.12. Spar and shell blade construction

## DISCUSSION

R. Ditz, GE, US. At the end of your paper you made the statement that in your opinion, lifting techniques for superalloys are extremely conservative. Can you elaborate on that a bit?

M. Hicks, Rolls Royce, UK. Yes, I think more about this will come out in subsequent papers during the meeting. The methods we are being increasingly forced to use in superalloys treat the material as containing a defect that behaves as a propagating crack from the very first cycle, and certainly in the worst case that is very true. But I believe it is very important to recognize those defects that can act as propagating cracks from the very first cycle and eliminate them through process control, and then through an understanding of the defect population that remains, build up a total lifting concept that introduces a crack nucleation life in addition to the traditional fatigue crack propagation life. Treating a material as containing a defect in the worst possible position, with crack propagation starting from the very first cycle is a tremendous conservatism.

Unknown SEP, France. In your paper you mention zirconia-based thermal barrier coatings for turbine blades. Could you comment on Rolls Royce's experience with zirconia thermal barrier coatings on rotating turbine blades?

M. Hicks, Rolls Royce, UK. Rolls Royce has had, like most people, a lot of experience in the use of thermal barrier coatings in combustion chambers and on platforms of nozzle guide vanes. As yet, Rolls Royce has not used thermal barrier coatings on blade airfoils, although it is doing a significant amount of work to develop that technology, as are most of the engine makers. If successful, that technology combined with the new single crystal superalloys under development would allow growth of nickel blade technology to higher and higher temperatures. So zirconia thermal barrier coatings for rotating blades is not a proven technology, but it's something that's in an advanced stage of development.

E. Campo, Fiat Aviazione, Italy. You have shown three different microstructures for Astroloy, and you stated that the necklace structure is the best. Is that true in general or is it true primarily under certain conditions? Could you elaborate, for example, on the influence of that structure on time-dependent and time-independent fatigue behavior? Could you also comment on the effect of that structure on property scatter, since it would be desirable to use a total life approach, involving both crack initiation and crack propagation in doing life predictions. I think the problem is that the initiation phase is strongly affected by large dispersions, and I should like to know if in your experience there is a difference in this regard between the three structures you showed.

M. Hicks, Rolls Royce, UK. If you look at the traditional approach, which is to go to higher and higher strength materials, then you move toward a fine grain structure. If you evaluate that material in terms of normal low cycle fatigue behavior it looks very attractive because the chances of actually getting a defect in a specimen is relatively small, with current levels of cleanliness. If you do simple laboratory testing and generate S/N type curves under either strain or load control, the material looks attractive, but it has the drawback of being relatively poor in terms of fatigue crack growth rate, both in conventional fatigue cycling with no dwell times in the loading and also in time-dependent fatigue where you add dwell times to the loading pattern. This can be due to the fine grain structure being less creep resistant or to any mechanism, including environmental interactions, that affects the grain boundaries adversely. The necklace structure gives the best all around balance of properties, both time-dependent and time-independent, and I believe that observation on Astroloy can be applied to other superalloys as well.

## Damage Tolerance Concepts For Advanced Materials and Engines

T. E. Farmer  
Pratt & Whitney  
P.O. Box 109600  
West Palm Beach, Florida 33410-9600

M. C. VanWanderham  
Pratt & Whitney  
P.O. Box 109600  
West Palm Beach, Florida 33410-9600

### **Abstract**

Planned increases in thrust to weight for future gas turbine engines require dramatically higher operating temperatures and rotor speeds. This necessitates simpler design, improved materials and sophisticated fabrication techniques. Damage Tolerance Design (DTD) has been established as the basis for gas turbine engine design and maintenance in the United States. Consideration of damage tolerance has significant influence on configurations and materials. The advanced configurations, bonded structures, composites, anisotropic alloys and less ductile materials required to meet the advanced engine goals challenge the current DTD philosophy. Fortunately, interim plans for incremental increases in performance and engine configuration to meet long-term goals afford the opportunities for developing transition technologies to meet these objectives.

### **Introduction**

Damage Tolerance Design (DTD) is the basis for structural design of military propulsion systems in the United States. The guideline for DTD is the Engine Structural Integrity Program (ENSIP) which is contained in MIL-STD-1783 (USAF) dated 30 November 1984. Damage tolerance extends the surface related fatigue (or initiation) life analyses to include assessments of life remaining after crack initiation. This concept is based on the technology of fracture mechanics. Improved safety and reliability are the result of prudent application of damage tolerance philosophy in design and development.

Damage tolerance is a more detailed durability assessment. Damage tolerance builds on the associated design analyses of strength, creep/rupture, resonance and wear by allowing improved consideration of operating margins and time or cycles to failure. To accomplish this, DTD requires knowledge of temperature, stress and material property variation through the thickness for critical (life limiting) mission points. The combination of these factors in initial characterization, design, verification and demonstration testing will provide a more reliable propulsion system. Proof of this concept lies in demonstrated inspectability of the product which is used in service to further avoid problems and allow safe extension of component life.

Verified inspection capabilities in damage tolerance are used to establish initial material quality (IMQ) and safe return to service at intervals (figure 1) established by one half of the lowest number of cycles to rupture of the largest undetected flaw per component. Inspection capabilities can be used for extension of component use beyond the historical limit of the three sigma minimum time to crack initiation. Inspectability is an integral part of the determination of component configuration, material, useable life and maintenance interval. The service interval of each module is considered equal to one half the lowest number of cycles to rupture from the largest undetected flaw for each life limiting location considered independently.

Generally, the inspection interval is being specified as one half of the retirement life for the gas turbine engine. Retirement life goals are equivalent to twenty years of service. Surface flaw propagation life has become the controlling design parameter for tactical engines for these life goals.

The application of damage tolerance design to an engine program requires additional material characterization, more analysis and increased testing of components and engines. The impacts of these efforts are presented in reference 2.

The military engine performance goals of the future will result in more demanding operating conditions for engine component durability. The enhanced understanding of component durability margin and capability afforded through damage tolerance design practices is the preferred foundation for reduced durability risk in achieving the performance goals. The goal of the Integrated High Performance Turbine Engine Technology Initiative (IHPTET) is to double the propulsion system capability by the year 2000. The tactical engine improvement goals for the year 2000 are shown in figure 2.

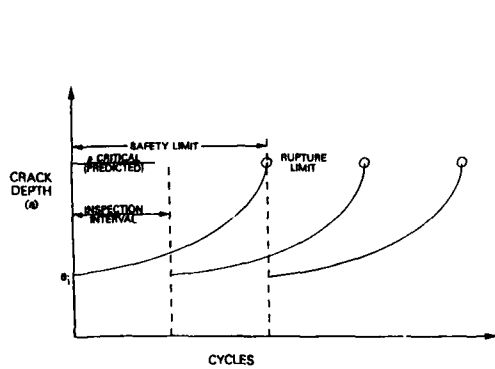


Figure 1. Propagation Life Relationships

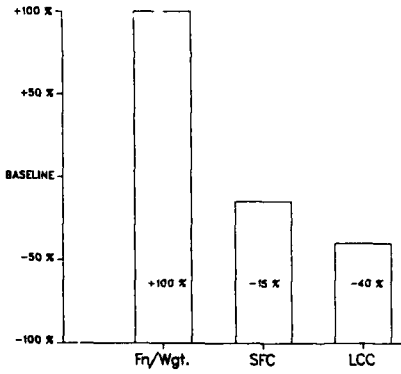


Figure 2. IHPTET Goals

To accomplish this goal, engine operating conditions will be increased. Higher operating temperatures will be sought for the associated performance benefits, as will higher speeds for the components. Higher temperature and speed to allow equivalent thrust at a reduced size (or engine weight) would result in reductions in durability margins for each component. Damage tolerance design and development philosophies provide improved understanding and control of engine durability and are, therefore, required to retain durability in propulsion systems of the future.

#### Advanced Engine

Conceptual studies of the far term engine have shown opportunities for improvements in the efficiencies of engine aero-thermodynamics and structural design. The use of 3-D computational fluid dynamic codes will allow design optimization for new 3-D aeromechanical concepts. Thermal analyses will likewise advance as these analytical procedures are employed.

The number of compressor stages will be reduced from today's standard and, thus, stage loadings will be increased substantially to produce pressure ratios equivalent to current engines. Aerodynamic efficiencies will be improved to increase the specific thrust of the advanced propulsion system. The hot section will also benefit from advanced aerodynamics and from improved thermal analyses. Advances in cooling effectiveness will reduce the cooling air requirements and enhance system performance. Propulsion system weight will be reduced by incorporation of advances in structural configurations and materials.

Damage tolerance design is the process which will reduce durability risk of advanced gas turbine configurations. Damage tolerance design is initiated with a well structured development plan; followed by thorough analysis and characterization efforts; leading to component and core engine verification tests; concluding with engine testing and the engine life management plan. The components generated by the damage tolerance design approach have improved durability, reliability and inspectability relative to the prior low cycle fatigue (LCF) based design systems. As shown in figure 3, damage tolerance design creates a simpler component with fewer stress risers or notches in the main load path. The turbine disk on the right, designed with damage tolerance, has more than twice the inspection interval and retirement life of the LCF based design on the left. One hundred eighteen holes (stress risers) were removed from the main load carrying region of the disk and replaced by surface notches of a reduced stress concentration and boltholes in a flange isolated by an integral arm. This is a significant improvement in structural design. One could arrive at this configuration by LCF analysis and experience but damage tolerance leads to this type of configuration.

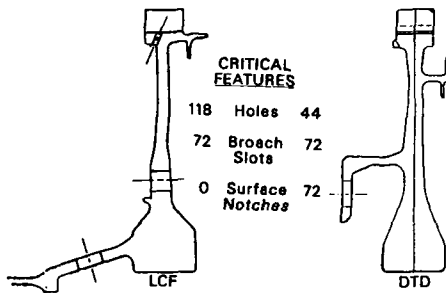


Figure 3. Effects Of Damage Tolerance On Configuration

Damage tolerance design leads to simpler configurations with lower stress gradients as a result of analysis of crack propagation life in addition to crack initiation limits. Assessment of time to rupture from an assumed flaw at the limit of the inspection process for each life limiting (critical) location increases the designer's awareness of the durability of the component. Advances in capability are best made with "eyes open" to reduce the risk of problems.

In addition to driving simplified design configurations, a damage tolerance approach has a major effect on material processing and development goals. Previously, advanced engine materials were developed to achieve maximum tensile and creep strengths, often at the expense of crack growth resistance. Now, damage tolerance is a fundamental factor in alloy and process development, and will undoubtedly figure prominently in advanced material and composite development. This approach forces early assessment of a variety of material characteristics which in the past were determined only after the fact.

Foremost among these material characteristics is fundamental resistance to crack growth, which must be quantified for life prediction (figure 4). For conventional materials, a direct assessment of damage tolerance capability can be made based on relative crack velocity vs. stress intensity behavior. Another less obvious factor in assessing a material's damage tolerance is the intrinsic initial material quality, or IMQ (figure 5), defined as a distribution of intrinsic microstructural anomalies that might lead to failure. This

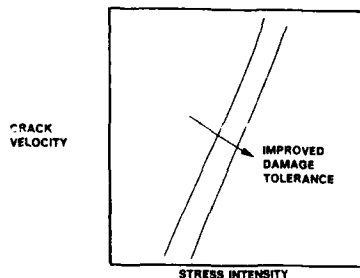


Figure 4. Resistance To Crack Growth

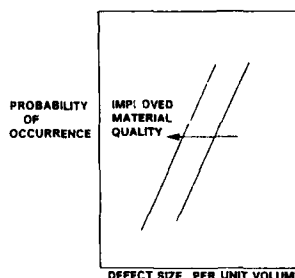


Figure 5. Initial Material Quality

concept is especially useful for quantifying the effect of defects below current NDE detection capability. Similarly, material inspectability, in the form of Probability of Detection or POD curves (figure 6) must be quantified for individual materials, since processing methods used to enhance damage tolerance may adversely affect inspectability. All of these aspects combine to yield inspection size vs. remaining life predictions for specific materials and applications, which forms the quantitative basis of a damage tolerant design and life prediction approach (figure 7).

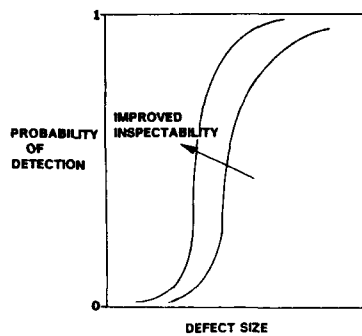


Figure 6. Material Inspectability

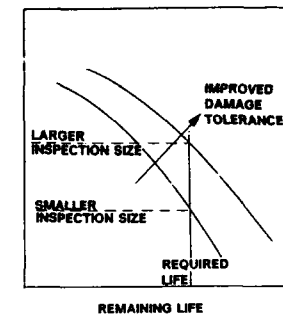


Figure 7. Assessment Of Remaining Life

Damage tolerance concepts have now been fully incorporated into gas turbine engine life prediction systems (reference 7), and provide the basis for component life predictions, assessing inspection requirements, and evaluating the effects of new materials and processing methods on component life. Advanced materials and composites will challenge specific current methods used for damage tolerance assessments, but the fundamental concepts will likely remain.

#### Compressor

The bolted compressor rotor system shown in figure 8 can not achieve the desired rim speeds and temperatures of the far term tactical engine. The bolt holes restrict the cyclic life and the nickel alloy is limited in creep to current temperatures. The drum rotor is a damage tolerant design which greatly reduces the number of notches (boltholes) and improves the life by incorporating advanced joining techniques for the nickel rotor. The weight of the rotor must be further reduced to achieve the IPTET goal of doubling the thrust to weight of the system. The rotor rim in figure 9 has 30 percent reduction in weight. This is an integrally bladed rotor which has benefitted from elimination of the mechanical attachment.

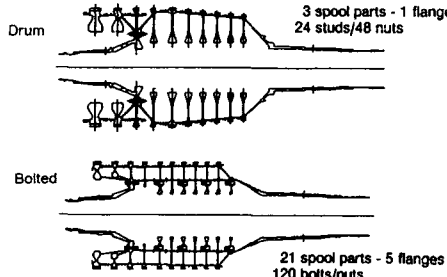


Figure 8. Compressor Rotor Comparison

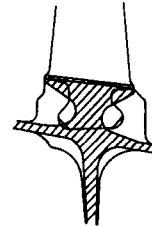


Figure 9. Compressor Rim Revision

Assessments of the welded joints of the drum rotor for damage tolerance would include material characterization, determination of probable flaw size and number, and quantification of residual stresses. The effect of this combination of factors must be addressed to establish the retirement life and inspection interval. The integrally bladed rotor has many benefits for weight and performance but the analysis of this configuration must address the inter-play of dynamic (resonance) and steady (operating) stresses. As shown in figure 10, for an operating stress of each material there is a dynamic stress that will rapidly propagate a crack. Considerations of this

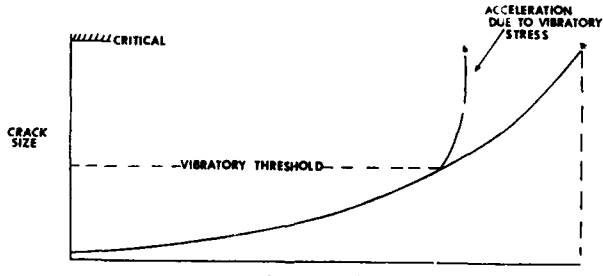


Figure 10. Vibratory Threshold Effect

damage tolerance design approach will prevent propagation of blade damage into the rotor and thus, minimize the effect of the blade damage.

Compressor rotor improvements continue with the incorporation of non-burning titanium which has 60 percent of the density of nickel. The rotor shown in figure 11 would be constructed of titanium matrix composite to allow operation at elevated temperatures. Metal matrix composites expand the rotor design envelope as shown in figure 12. The increased speed and temperature capabilities have significant benefits for improved performance. Figure 13 shows the relative rotor weights from a titanium and nickel drum rotor with mechanical attachment to the titanium matrix composite integrally bladed rotor with a reduction of over 50 percent. The titanium matrix composite rotor is projected to have the highest temperature capability.

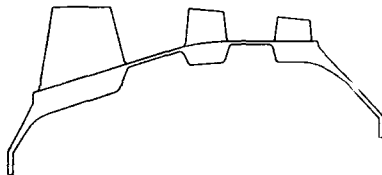


Figure 11. Advanced Compressor Rotor

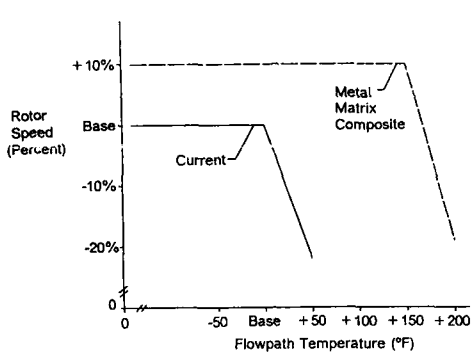


Figure 12. Compressor Rotor Design Envelope

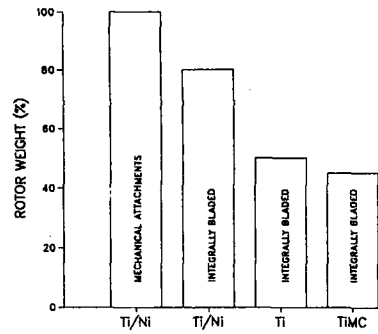


Figure 13. Rotor Weight Comparisons

#### Hot Section

The hot sections of the far term will be required to operate near-stoichiometric temperatures (3500–4500 degrees F) and maintain efficiencies of 90 percent with total cooling flows reduced to five percent. Increased turbine inlet temperature is the key to increasing specific thrust. Technology advances are required in combustor and turbine aero-thermodynamic design, cooling design, materials and coatings to minimize cooling requirements. Innovative structures are required to accept these operating conditions and reduce system weight.

Turbine attachments are a limiting design feature for current configurations. Figure 14 shows a comparison of turbine rotors with integral blades or a mechanical attachment of airfoils. Figure 15 shows a comparison of turbine rotors with integral blades versus annulus area multiplied by speed squared ( $AN^2$ ) which is a centrifugal load factor is displayed in figure 15. The plot shows a 40 to 50 percent stage weight savings for integrally bladed rotors relative to a durable mechanical attachment. Furthermore, weight savings of another 25 percent are calculated for projected ceramic matrix composite rotors in the future.

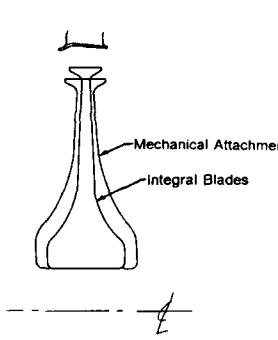


Figure 14. Turbine Rotor Trades

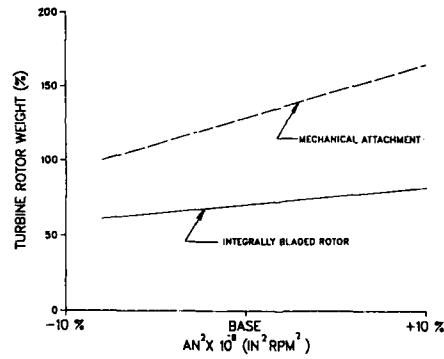


Figure 15. Turbine Rotor Weight

#### Advanced Damage Tolerance

As new material systems, fabrication techniques and configurations are introduced, life prediction and damage tolerance techniques must be developed in concert to minimize the risk of incorporation. Initially, the design system will limit the operating stress to a level below the occurrence of cyclic damage. But to achieve full potential, the damage tolerance design system must allow safe usage to the cyclic damage limit.

Damage tolerance design systems are in development for orthotropic alloys and composites. These systems consider manufacturing induced residuals and flaws; establish inspection procedures to reliably identify defects in excess of limits; and assess damage accumulation for component mission usage. Risk of incorporation of advanced configurations is reduced by compatible development and implementation of damage tolerance design systems.

Life goals for advanced propulsion systems will remain consistent with today's mission requirements for 20 years of use. Satisfaction of these life goals requires improved accuracy of damage tolerance design systems to achieve the weight goals of the programs. Conventional crack propagation life predictions have been shown to be conservative, for general applications. There is a stress level dependency associated with the conservatism. Accuracy of conventional systems improves for cases of high stress and reduced life.

Correlation factors are applied to correct the conservatism of conventional systems but improved accuracy is needed. The crack closure mechanism has been applied by W. Eber and J. C. Newman to improve the accuracy of crack growth predictions. Crack closure assesses the influence of the plastic zone at the crack tip on the crack propagation rate. This yielded material results in a plastic zone which encompasses the surface crack and effects an interaction of fracture faces. This interaction results in a reduction in the effective loading which opens and, therefore, propagates the surface defect. Figure 16 compares the accuracy of the conventional fracture mechanics system (with correlation factors) to that of a crack closure system. An A/P of 1.0 is desired as this is achieved when the actual life, A, equals the predicted life, P. Reduced component weight for a given life goal will result from this more accurate system.

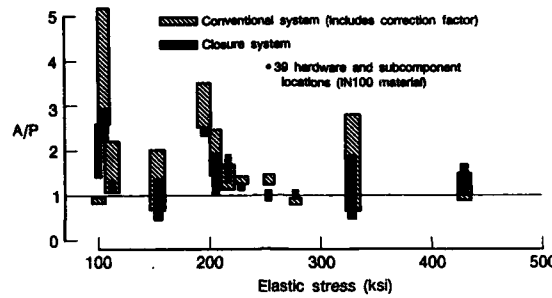


Figure 16. A/P Summary For Closure And Conventional Systems

In addition, crack growth data requirements can be reduced via an accurate crack growth analysis system. Sub-cycle damage analyses have required specimen testing over a range of stress ratios to allow accurate prediction of mission life. The crack closure analysis system has been used to reduce testing requirements by demonstrating accurate prediction of sub-cycle propagation rate based solely on simple cycle (zero to maximum stress) propagation data. This effect is shown in figure 17.

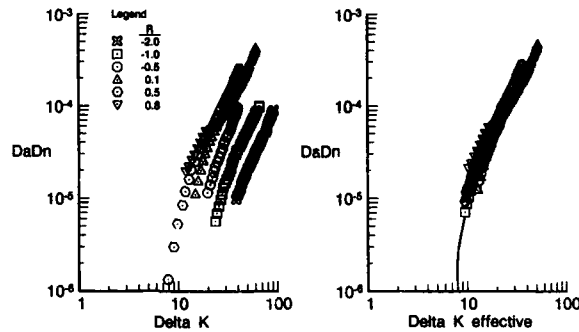


Figure 17. Closure Collapses R-Ratio Effects

Many fundamental questions (hopefully opportunities), will undoubtedly arise with advanced materials. For example, the concept of an intrinsic "initial material quality" or IMQ distribution of potential defects, may become much more important for advanced, high strength, low ductility materials, such as titanium aluminides. For these materials, initial defect tolerance may be sufficiently limiting that proof testing concepts could become a fundamental part of critical hardware acceptance and life certification. Conversely, for metal matrix composites, the IMQ concept may not be important at all, since the damage state may be a more generalized rather than local discrete phenomenon. Similarly, the simplicity of "crack velocity versus stress Intensity" as a representation of resistance to damage progression, may be generally inadequate for complex composite structures, with the possible exception of unidirectional reinforcement. It will likely have to be replaced with a more sophisticated damage description parameter, perhaps one based on fracture energy.

Finally, definition of failure may alter dramatically with new materials. For materials with relatively low damage tolerance, such as monolithic aluminides, component retirement may be determined based on exhaustion of proof test life. An additional proof test may then be considered to re-certify the component for another return-to-service interval. In addition, higher service temperatures may result in retirements based on time-at-temperature exposure limitations. For metal matrix composites, more generalized accumulation of damage may result in altogether different definitions of failure, and consequently, in the manner in which damage tolerance is assessed.

#### Summary

Damage Tolerance Design (DTD) is the standard for military engine durability analysis in the United States. The design system requires more analysis and testing than the LCF based systems employed previously. The additional assessments of the damage tolerance approach give the designer an enhanced understanding of the durability limits of the gas turbine engine component. Safe extension of engine capabilities can be accomplished with a damage tolerance design philosophy.

Damage tolerance design technologies must be enhanced to best allow the performance benefits of the advanced configurations and material systems. Fracture mechanics based design systems are in work for orthotropic materials and composites. Coordinated development of reliable life prediction systems and the new materials systems must be accomplished to reduce the risk of introduction. The improved accuracy of design systems must be achieved with advances similar to crack closure to reduce conservatism and, thereby, reduce the cost and risk of implementation of advanced configurations.

#### REFERENCES:

1. Alley, W. R., "Technology and Engine Demonstrator Programs", AIAA, Dayton, OH, 23 March 1983.
2. King, T. T., Hurchalla, J., Nethaway, D. H., "United States Air Force Engine Damage Tolerance Requirements", AIAA, Monterey, CA, 8 July 1985.
3. Cowie, W. D. and Stein, T. A., "Development Trends in Engine Durability", AIAA, Seattle, WA, 27 June 1983.
4. Farmer, T. E., "View of Future Requirements for Engine Cyclic Durability by Analysis and Testing", AGARD, Amsterdam, Netherlands, May 1984.
5. Farmer, T. E., "Impact of ENSIP on Engine Demonstrator Program", ASME, Dusseldorf, West Germany, 8 June 1986.
6. deLaneuville, R. E. and Heath, B. J., "Fracture Mechanics Life Prediction System Using Crack Closure Methodology", AIAA, San Diego, CA, 29 June 1987.
7. Cowles, B. A., "Life Prediction in High Temperature Environments: Overview of a Current Gas Turbine Engine Approach", "USDOE Workshop on Mechanics and Physics of Crack Growth: Application of Life Prediction", Keystone, CO., USA, August 4-7, 1987.

#### DISCUSSION

M. Hicks, Rolls Royce, UK. You've presented a lot of background to the method of lifting, but you haven't talked about the validation of lifting methods. Would you care to say anything about the methods Pratt & Whitney use to provide confidence that the lifting calculations carried out are indeed exact?

T. Farmer, Pratt & Whitney, US. Pratt & Whitney uses flawed, or pre-cracked specimen and component tests, carried out under loads and temperatures that best represent the engine environment, to verify its prediction techniques. Before an engine configuration is adopted now we proceed step-wise from specimen to full component tests, concentrating on the more fracture critical components, such as the rotors, with induced flaws cycled at temperature to demonstrate a correlation between the predicted and demonstrated life of the component. The use of the fracture mechanics properties, in fact, have some benefit here, since there is less scatter in the measurement of fracture mechanics properties than in low cycle fatigue. In the past, in demonstrating component capabilities in terms of crack initiation we often observed scatters of 10:1 in low cycle fatigue lives. We're now often seeing a scatter of 2:1 from minimum to typical values in fracture properties, so our evaluation can be more specific with flawed components. In our initial damage tolerance testing in the late 1970's, we ran component tests and compared them to actual tests on an intentionally flawed engine, with periodic tear-downs and inspections to track the crack growth rates of critical components.

M. Hicks, Rolls Royce, UK. Would you care to comment on the actual vs. predicted lives achieved?

T. Farmer, Pratt & Whitney, US. Initial verification testing indicated that the greatest inaccuracies occurred in bending stress fields. Improved correlations of actual vs. predicted lives have been achieved in recent testing.

P. Hancock, Cranfield Institute of Technology, UK. When considering life assessment from crack growth laws, the total life is dominated by the initial flaw size. As material processing improves, this initial defect size decreases. However, we know that the growth rate of small cracks is different from that obtained from da/dN measurements on large cracks. Can you take this into account, and how do you do it?

T. Farmer, Pratt & Whitney, US. Small defects are accommodated in our analysis in several ways. First, the effects of small to very small defects are included in our low cycle fatigue design system via specimen testing. The small defects are often noted as fatigue nucleation sites. Second, small crack studies are underway. Testing has shown, for example, the effects of microstructure and, particularly, grain size. Third, we can construct probabilistic assessments that include the probability of occurrence, propagation, and rupture of a specimen. We can, for example, cut up a lot of material and examine a lot of fracture surfaces and, with significant effort, establish an 'initial material quality' level, or IMQ, for a given material and set of processing specifications. If we've accumulated enough data we could base a life prediction on that IMQ that would characterize that component as manufactured. However, introduction to the field introduces new problems, and we must be able to account for field-induced damage as well.

R. Ditz, General Electric, US. You've raised the issue of treating handling damage, as opposed to the inherent defects that may be present in the as-manufactured part, in damage tolerant life prediction. Would you care to comment on the importance of handling damage from Pratt & Whitney's perspective and are you conducting any analytical studies to characterize such handling damage?

T. Farmer, Pratt & Whitney, US. Damage can be induced by improper manufacturing processes. For example, surface defects can be generated during the drilling of holes. Control of manufacturing processes is an important factor in component quality and component life. Inspection of critical features can be used to address this issue. Handling in the field during maintenance procedures can also generate distress. Care must be taken, for example, at mechanical attachments. The bolts and their removal can be a source of bolt hole edge distress. The use of generous edge breaks, or chamfers in design will reduce the probability of such damage.

H. Lichtfuss, MTU, FRG. You have shown us an example of an improved turbine design that avoids the use of cooling holes through the part. Does that imply that you don't need cooling at all or have you provided cooling in a more intelligent way?

T. Farmer, Pratt & Whitney, US. The turbine rotor designed for damage tolerance is cooled too, but the holes through the rotor were replaced by scallops on the rotor surface. The cover plate that goes over the disk seals the scallop and sets the orifice size to control the flow of the cooling air. The air is introduced through the front face scallop, under the blade and up through the blade's fir tree attachment. The boltholes in this design are isolated by the use of an integral arm.

MATERIAL/MANUFACTURING PROCESS INTERACTION IN ADVANCED MATERIAL TECHNOLOGIES

G W MEETHAM - CHIEF OF NON-METAL AND COMPOSITE MANUFACTURING TECHNOLOGY  
 ROLLS-ROYCE plc  
 P O BOX 31, DERBY DE2 8BJ

INTRODUCTION

Since the first flight of a gas turbine powered aircraft some forty years ago, tremendous advances in engine performance have been made in terms of thrust, thrust to weight ratio and specific fuel consumption. The performance and efficiency of gas turbine engines is a direct function of the maximum cycle temperature and, throughout the forty years in which the aero gas turbine has existed, this has provided the motivation for the continuous development of materials which are capable of operating at higher temperatures in the turbine section of the engine. Turbine entry temperatures have risen from around 700°C in the Whittle W1 engine in 1941 to around 1350°C in current advanced engines.

NICKEL SUPERALLOYS

The materials which have made the major contribution to the performance improvement are the nickel superalloys. In general terms, it is possible to divide their development into three categories (1). When nickel superalloys were initially introduced into turbine components their properties were so superior to those of their predecessors that alloy development alone was sufficient to meet the new design needs, with relatively little contribution from the component manufacturing process other than to produce the required shape. The first category is thus dominated by alloy composition and is illustrated by the nickel based disc alloys Inco 718 and Waspaloy which showed major improvement in properties in the fully recrystallised and aged condition over the earlier austenitic steels.

At a later stage in component development it was not possible to achieve the required properties by alloy development alone and the manufacturing process also became a key part of the material technology. This situation arose for example when the importance of low cycle fatigue strength of disc materials was realised and controlled thermo-mechanical processing became essential for structural control. In thermomechanical processing the material deformation conditions combined with subsequent heat treatment produce a pre-selected structure and enhance specific properties. Major factors are the dimensions of the forging stock, the design of the forging sequence, the deformation rate and the temperature at which the deformation is carried out in relation to gamma prime, carbide and other solvus temperatures. Waspaloy was one of the first superalloys to benefit from TMP with the room temperature 0.2% proof strength being increased by some 40% over that developed in the earlier turbine blade version. LCF properties have been significantly increased in Inco 901 by TMP. It has been shown that dislocations play a major role in determining component behaviour. Homogeneous dislocation distributions are satisfactory whereas heterogeneous dislocation distributions in the form of high density planar arrays can result in premature component failure. Thus in the second category, properties are dependent on both alloy composition and the manufacturing process.

The more recent developments such as directional solidification and mechanical alloying in which the process makes the major contribution to properties illustrates the third category which is process dominated. Some of the highest temperature cast blade superalloys exhibited inconsistent creep properties at intermediate temperatures and the directional solidification process was initially developed as a consequence of this problem. The elimination of grain boundaries in a direction normal to the maximum direct stress contributed a significant increase in creep strength relative to a conventional casting in the same alloy. The major improvement however was due to the fact that the crystal growth direction [100] is the direction of lowest Young's modulus. This produces major reduction in the thermal stresses arising from temperature gradients in the blade during service.

The process development chronology for major turbine section components is summarised in Fig 1.

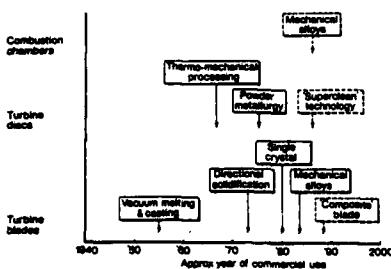


FIG 1. SUPERALLOY PROCESS DEVELOPMENT CHRONOLOGY

Analysis of the capability of nickel superalloys to meet the projected operating conditions of future engine designs indicates that new materials with significantly higher temperature capability will be needed for major turbine components. These will of necessity be non-metallic materials, in some composite form to develop the required level of defect tolerance. Although manufacturing processes are becoming increasingly significant in determining the properties of metals, as discussed, the properties of composite materials are critically dependant on the manufacturing process, which essentially creates the material. It is thus very relevant to discuss the interaction between material and manufacturing process for non-metallic systems.

#### RESIN MATRIX COMPOSITES

Resin matrix composites provide a relevant starting point for this discussion since they are established materials and their technology can usefully illustrate important aspects in the developing high temperature composite materials. In fibre reinforced plastic technology the resin may be introduced to the fibre early in the process (prepreg sheet) or late (resin injection). Both process routes have a similar objective - to replace the air in the texture of the reinforcement by resin and to fill completely the remaining space of the component shape. Chemical curing completes the fabrication process.

One result of inadequate control procedures during composite manufacture is the presence of voids in the final structure. These arise either because premature gellation takes place before pressure can be properly applied to the matrix to collapse trapped bubbles, or because the premature application of pressure to the moulding effectively expresses all the excess resin before its viscosity has increased sufficiently to withstand the pressure increase. Voidage has been shown (Fig 2) (2) to result in reduced interlaminar shear strength to cause delamination under stress and to interact with moisture absorption.

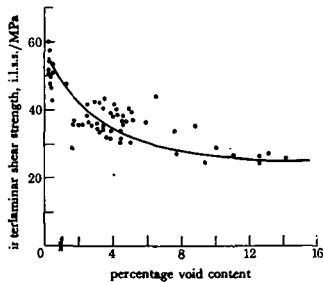
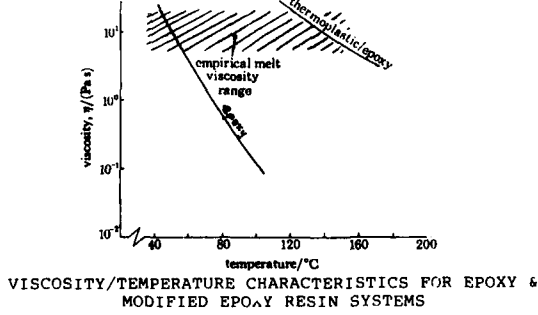


FIG 2. INFLUENCE OF VOID CONTENT ON INTERLAMINAR SHEAR STRENGTH OF TYPE III/EPOXY NOVOLAC COMPOSITE.

Knowledge of the viscosity characteristics of the resin/hardener combination is therefore an essential prerequisite to satisfactory control of the moulding cycle since virtually the only way of manipulating resin viscosity during moulding is by the application of heat. Voids are directly related to matrix characteristics.

The resin systems which were available at the time of the early CFRP developments some twenty years ago had inappropriate viscosity characteristics. The temperatures required for curing in an acceptable time were not consistent with the processing temperatures at which the viscosity was adequate to maintain pressure in the die and still provide sufficient resin mobility. A resin with the required characteristic (Fig 3) was produced by incorporating additions of a thermoplastic component to develop higher viscosity together with a flatter viscosity/temperature relationship<sup>(2)</sup>. A latent crystalline catalytic hardener was incorporated to minimise cure time.



As far as the fibre is concerned, to achieve the expected composite properties the fibre should be present in the desired orientation, in the correct volume and with the appropriate degree of surface treatment to effect the correct interfacial bond.

The importance of surface treatment was first realised in GRP. Good mechanical properties are developed if freshly drawn glass fibre is immediately resin coated, but such a material is very prone to strength degradation by attack at the fibre/matrix interface in hot/wet operating conditions. This problem is alleviated by treating the fibres with silane to promote chemical bond formation prior to composite manufacture. This does not increase mechanical properties relative to the untreated fibre material but the benefits are in minimising fibre damage during handling and in reduced property degradation in hot/wet conditions.

Untreated carbon fibre, in contrast, forms a very poor bond with the resin and consequently properties are poor. In order to achieve a good bond, the fibre surface must be activated by the introduction of oxygen atoms by, for example, electrolytic acid treatment. The degree of activation must be controlled however since too high a degree of activation can result in too strong a bond and brittle composite behaviour, as illustrated schematically in Fig 4.

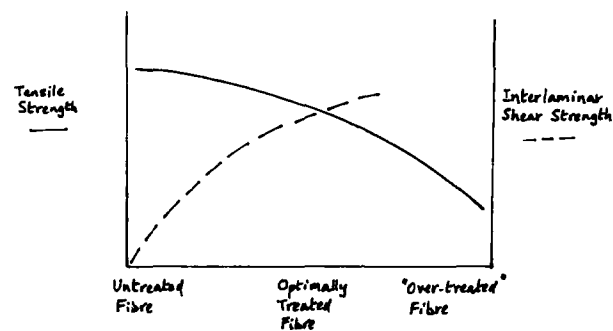


FIG 4. SCHEMATIC RELATIONSHIP BETWEEN SURFACE ACTIVATION AND STRENGTH

This illustration of the importance of interface control in CFRP is very significant because this is probably the most crucial factor in high temperature composite systems where the establishment of the required interface in the as manufactured composite may be difficult because of the necessary high temperatures in the manufacturing process and where the high service temperatures will tend to modify the interface with time.

The search for higher temperature materials is not limited to the turbine section - it applies also to the compressor section. One of the first compressor instances was when the RB162 engine was fitted to Trident IIIB aircraft as take-off booster engine. The RB162 was initially conceived as an ultralight weight lift jet and many compressor components, including casing, rotor and stator blades were made in GRP. The epoxy resin used at that time was limited to a maximum temperature around 150°C. The Trident application was equivalent to a 240 hour life at 200°C and this led to the epoxy being replaced by a polyimide resin based material. Other polyimide resins have still higher temperature potential with PMR 15 approaching 300°C. Problems such as its susceptibility to transverse microcracking on thermal cycling have to be resolved however before this potential can be realised. Thermal stresses are influenced by several factors, one of which is resin cure temperature. It has been found that curing at lower temperatures than those used in the early PMR15 development produce composites of acceptable mechanical properties together with a significantly reduced tendency to microcrack (Fig 5).

A rationalisation for the reduced microcracking has been proposed <sup>(3)</sup> in terms of the increased crosslink flexibility with low cure temperatures giving rise to reduced resin modulus and consequent reduced thermal stress.

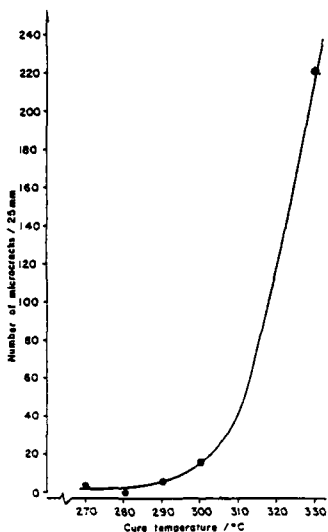


FIG 5. EFFECT OF CURE TEMPERATURE ON MICROCRACKING OF PMR15 COMPOSITE (AFTER 20 CYCLES FROM -196 TO 280°C)

#### GLASS AND GLASS/CERAMIC COMPOSITES

Interface control in CFRP was discussed earlier. It has been shown that the fibre/matrix interface in reinforced glass and glass ceramic systems has a crucial effect on properties. The interface must be strong enough to allow load transfer from matrix to fibre but not so strong as to prevent fibre pull-out. For a given material system, the creation of the required interface is critically dependant on the thermal and mechanical conditions in fabrication. Temperature and stress determine the rheological behaviour of the matrix and consequently the matrix deformation and degree of consolidation of the composite. The thermal conditions control the kinetics of the solid state reaction between the matrix and fibre to form the interface bond.

In Nicalon/pyrex composites, the required interface is developed by controlling the temperature and time of consolidation (Fig 6).

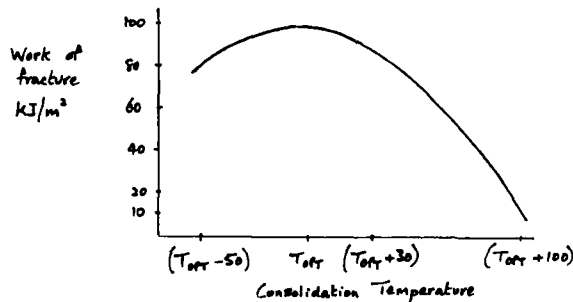


FIG 6. INFLUENCE OF CONSOLIDATION TEMPERATURE ON TOUGHNESS OF NICALON/PYREX COMPOSITE MATERIAL

Considerable reaction takes place between the fibre and matrix at the high consolidation temperatures required by the Nicalon/LAS system. A graphite interface reaction layer, probably formed by the oxidation of  $\text{SiO}_2$ , appears to be necessary for high fracture toughness ( $K_{IC} \approx 10-20 \text{ MPa m}^{1/2}$ ) and strength (MOR 700/800 MPa).<sup>15</sup> Matrices with high alkali content produce excessive reaction with the fibre and refractory metal oxides have been added to control the reaction by producing an additional carbide layer. It has been observed<sup>16</sup> that the cracks which formed during the preparation of thin slices for TEM examination always followed the interface between the two reaction layers.

#### HIGH TEMPERATURE CERAMICS

The need for defect tolerance in stressed applications will result in some form of ceramic composite. Despite the current absence of such material with the required temperature capability, certain characteristics of monolithic ceramics are of relevance.

Ceramics such as  $\text{Si}_3\text{N}_4$  and  $\text{SiC}$  contain strong covalent bonds. This is beneficial for high temperature, creep strength but is detrimental to solid state sintering since atom transport by diffusion is inhibited. In silicon nitride the sintering problem is partially resolved through the use of a liquid to catalyse material transport by a solution-reprecipitation reaction. This leads to a process subdivision which is partly dictated by liquid volume and which results in different property combinations (Fig 7).

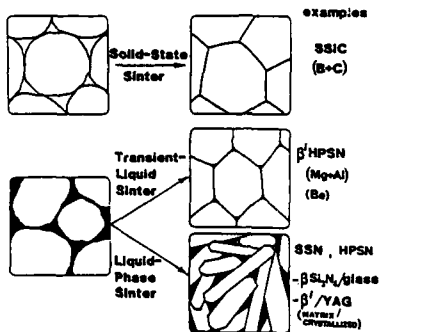


FIG 7. PROCESSING ROUTES AND MICROSTRUCTURAL TYPES OF MONOLITHIC CERAMICS

The lower liquid volumes (less than 10%) require hot pressing and tend to produce equiaxed microstructures with  $K_{IC} \approx 3-5 \text{ MPa m}^{1/2}$ . Higher liquid volumes (10-15%) can be pressureless sintered to produce fibrous microstructures with higher fracture toughness -  $K_{IC} \approx 7-9 \text{ MPa m}^{1/2}$  (8). Creep properties depend on the amount, composition and degree of crystallisation of the residual glass phase.

Fracture is initiated at pre-existing stress concentrating flaws which may be introduced during processing as inclusions or sintering porosity or may be produced during surface machining. Fig 8 shows an approximate relationship between fracture stress, flaw size and fracture toughness (9).

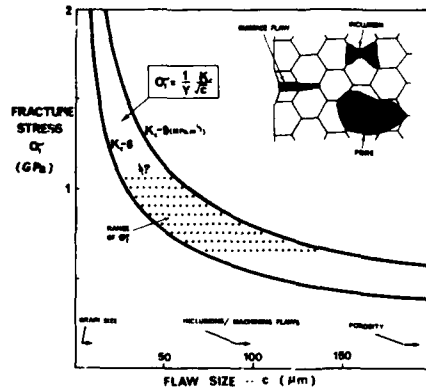


FIG 8. RELATIONSHIP BETWEEN FLAW SIZE AND FRACTURE STRESS.

The major objectives are thus to increase defect tolerance and to reduce the flaw size. Porosity has been shown to play a major role in limiting strength. This has led to studies on the effect of powder size and characteristics, since any flaws which are generated in the green body are preserved in the final fired ceramic. A small particle size favours rapid sintering and densification, but there is a tendency for powders to aggregate as their size decreases. Aggregates may vary in strength so that some are easily dispersed in subsequent process steps while others persist, even under conditions of high shear. In Al<sub>2</sub>O<sub>3</sub> this has been shown to result in variations in bend strength from 160-500 MPa and Weibull Modulus from 4-10 (10).

#### TITANIUM MATRIX COMPOSITES

Titanium matrix composites are another example of a material system which is being developed because monolithic materials are being pushed to their limit. Incorporation of silicon carbide fibres has resulted in the desired stiffness increase and weight decrease but strength properties have been generally disappointing. One of the factors that has been responsible for this is the reaction between fibre and matrix during composite fabrication. Several attempts have been made to avoid this problem, a recent one of which has been to modify the surface chemistry of the stoichiometric CVD SiC fibre (as in SCS 6 fibre) such that it is graded outwards to be first carbon-rich and then back slightly towards stoichiometry over the last 2-3μm. A reaction zone approximately 0.5μm thick has been reported (11) in as-fabricated products using SCS 6 fibre. Three point bend tests carried out on material which had been exposed at 600°C for 1000 hours after fabrication revealed separation from the matrix and separation of the filament surface from the filament, with the duplex nature of the surface being evident (Fig 9).

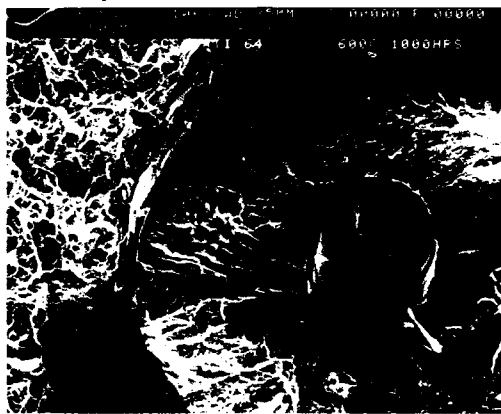


FIG 9. FRACTURE SURFACE OF TITANIUM MATRIX COMPOSITE

Room temperature tensile properties of a composite with Ti 6-4 matrix containing 35/40% unidirectional SCS 6 fibre approach rule-of-mixtures strength and stiffness in the longitudinal direction but the transverse tensile properties are less than 40% of those of Ti 6-4. The level of understanding of the factors controlling the strength of the fibre reaction zone interfacial bond must be significantly increased if transverse properties are to be improved (11).

#### SUMMARY

The importance of the processing route for high performance metallic materials has progressively increased such that the most recent nickel superalloy developments are process dominated with material composition playing an important but subsidiary role. Future engine designs will make increasing use of composite materials of various types and such materials are critically dependant on the manufacturing process, which, in essence, creates the material. Several aspects of the composite manufacturing processes are of major importance but the most crucial factor is the generation in manufacture and maintenance in service of the required interface between fibre and matrix. The necessary understanding and capability is being achieved for glass and glass ceramic composites. Titanium matrix composites have not yet reached this stage and ceramic composites with the necessary temperature capability and defect tolerance are some way from reality.

REFERENCES

1. G W Meetham The Metallurgist & Materials Technologist Sept 1982 p387
2. J W Johnson Phil.Trans R.Soc. Lond. A294 1980 487
3. D Wilson et al Proc SAMPE Conf. Anaheim USA April 1987
4. D Dawson Private Communication.
5. R F Cooper & K Chyung J.MatSci 22 1987 3148
6. R Chaim & A H Heuer Adv.Ceram. Mat 2 [2] 1987 154
7. M H Lewis Welding Institute Symposium London April 1988
8. F Lange Ceram.Bull. 62 1983 1369
9. M H Lewis & G Syers Proc. IMechE. Conf. Limerick Ireland 1982
10. N Alford et al Materials Science & Technology 2 1986 329.
11. P R Smith & F H Froes Jnl of Metals March 1984 p19.

**DISCUSSION**

R. Kochendorfer, DFVLR, FRG. You referred to interface problems quite a bit in your talk, and one might get the impression that you would always like to have a good interface. I'm not sure that's so. It's true for dynamic loading and for high composite strength, but our experience over a period of ten years with silicon carbide fiber reinforced aluminum and boron fiber reinforced aluminum has shown that we cannot combine good bonding at the interface and good fracture toughness at the same time. We can get excellent interface bonding and beautiful dynamic behavior in blades, for example, but then we get poor fracture toughness and behavior similar to that of a brittle material. We can either live with that degree of brittle behavior and provide for foreign object damage requirements some other way, or relax the degree of interface bonding. My point is that we must consider more than just the material, we must consider both materials, with some mixture of properties, and various design approaches. We should not expect to get everything from the material.

G. Meetham, Rolls Royce, UK. I think that's right. It's difficult to get both the highest strength and good fracture toughness, and in some components where we need the highest fracture toughness it may not be easy to get it. We may have to consider two types of reinforcement -- a continuous fiber reinforcement in principle will give the highest fracture toughness, but perhaps not the highest strength, and on the other hand whiskers which give not the best fracture toughness but perhaps the best strength. There may be the two types of materials.

D. Petrasek, NASA-Lewis, US. In your presentation you addressed the issue of chemical compatibility between the fiber and matrix at the interface. Are you also addressing the issue of the coefficient of thermal expansion mismatch between the fiber and matrix? That mismatch induces strains during heating and cooling cycles that can lead to the damage of both constituents. Successful development of metallic or intermetallic composites may be more limited by coefficient of thermal expansion mismatches than by fiber-matrix reactions.

G. Meetham, Rolls Royce, UK. Compatability of thermal expansion coefficients is just one of the important requirements in composite materials. Incompatibility led to thermal fatigue problems in the tungsten wire reinforced nickel-base superalloy composites developed in the United States some years ago, and the difference in coefficient of thermal expansion between fiber and resin is undoubtedly one of the factors that cause microcracking in the graphite fiber reinforced PMR-15 composites. Chemical reaction at the fiber-matrix interface can modify the initial interface behavior in a number of respects. If not understood and controlled, it can result in poor composite properties even in composite systems with compatible coefficients of thermal expansion.

**DEVELOPMENT OF STRESS AND LIFING CRITERIA  
FOR SINGLE CRYSTAL TURBINE BLADES**

by

S.Salvano, M.Stanisci and E.Campo  
Stress Department  
FIAT Aviazione  
Corso Ferrucci 112  
10138 Torino, Italy

**SUMMARY**

The stress and lifing criteria applied to turbine blades are discussed, by focusing the relevant features which make Single Crystal materials different from conventional alloys.

The discussion basis is provided by the material data and blade Finite Element analyses, collected within Fiat Aviazione activities for the application of Single Crystal alloys to advanced aircraft engines.

**INTRODUCTION**

Single Crystal (SC) superalloys have been primarily developed to enhance creep rupture life of turbine airfoils in aircraft engines. The research efforts in this new technology have been put since the awareness of the grain boundaries role in high temperature fracture phenomena [1].

The world's first structural application of SC alloys has been in 1982, followed by a rapid application growth in both commercial and military engines, with significative improvements in performance and/or durability. However the successful application of SC alloys does not mean that the related technology is mature, if maturity is understood as the capability to take full advantage from the material intrinsic properties. Progresses are expected in both process and design techniques, aided and accelerated by the modern resources in terms of process and mechanical metallurgy, structural analysis, modelling and computing capabilities.

The present paper concerns the stress criteria development for SC alloy blades, where the aim is not to cover the overall argument but mainly to focus some features in respect to which SC behaviour cannot be directly extrapolated from the experience on conventional materials. The subject is treated on the basis of some figures and analyses collected within Fiat Aviazione activities, aimed to apply SC alloys to turbine blades of advanced aircraft engines.

**ANISOTROPY**

While mechanical properties of conventional casting (CC) materials can generally be considered isotropic, provided that for a given direction a representative number of grains is tested, the mechanical properties of Single Crystals are anisotropic.

Fig.1 shows how to identify the crystallographic orientation of a blade respect to the nickel unit cell: two angles are necessary,  $\vartheta$  made between the blade axis and the Miller  $\langle 001 \rangle$  direction,  $\beta$  made between blade axis -  $\langle 001 \rangle$  and  $\langle 001 \rangle\langle 011 \rangle$  planes. Casting design must be such to keep  $\vartheta$  and  $\beta$  angles as low as possible, in any case within specified limits.

Elastic behaviour is well understood, only three constants are required to describe the elastic properties of cubic materials, they can be incorporated easily into computer codes for stress analysis. For instance the MSC/NASTRAN code enables to take into account the anisotropy by the MAT9 card.

Anisotropy of plastic deformation is complex and the present state of the art does not allow an appropriate stress analysis. Nevertheless at very high temperatures a large number of slip systems operate within the material, reducing the marked plastic anisotropy experienced at low temperature.

#### CREEP

Since the stress rupture improvement has been the driving factor in the SC development, the advantage respect to conventional alloys is well understood if reference is made to creep mechanisms.

Fig.2 shows the comparison between a CC and an SC alloy, using the Larson-Miller time-temperature parametric representation. The SC data refers to the <001> direction. The <011> direction which is well outside the allowed maximum deviation of the blade crystal alignment, has been verified as the weakest one [2]. Additional tests performed along the <011> direction at 1050°C and 1150°C have shown a reduction in creep life respectively of 3.4 and 1.5, confirming the anisotropy attenuation at high temperature.

It is necessary to derive an appropriate statistical scatter for SC blade, in order to have a reliable estimation of the blade set life at a required survival probability. A statistical analysis of 850°C creep data (fig.3) has given a Weibull modulus of 7.4, when the used specimens had angles within the current specification limits.

Cooled turbine blades involve thin walls: creep life estimation must be take into account for thickness effect.

Also in this respect, SC alloys show a superiority compared to conventional alloys, since they retain a fraction of about 75% of their thick section rupture life against about 50% of conventional castings.

#### THERMAL FATIGUE

Thermal fatigue behaviour can be predicted on the basis of isothermal low cycle fatigue (LCF) data obtained by strain control testing.

The SC alloys exhibit a better behaviour respect to CC alloys, in particular if reference is made to the <001> direction where a low Young's modulus occurs (fig.4). Anisotropy of fatigue life can be easily treated by normalizing the strain range to a stress range, as it has been experimentally demonstrated [3]. According to this finding a 20 degrees  $\delta$  angle gives place to a thermal fatigue life reduction down to a maximum of 1/5 respect to a perfectly aligned crystal. Even with the above misalignment the SC alloys keep a considerable advantage respect to conventional alloys.

#### HIGH FREQUENCY FATIGUE

To prevent blade failure by high frequency fatigue (HCF) the main design objective is the avoidance of dangerous resonances in the operating speed range. On the contrary of what happens for creep and thermal fatigue phenomena, for a fixed configuration and engine conditions, SC blades may perform worse than CC airfoils.

Since resonance frequencies are functions of the elastic constants, SC and conventional blades show quite different critical conditions as it is shown in fig.5 on the basis of a dynamic analysis performed on the fig.6 Finite Element model.

Crystallographic orientation affects the resonance frequencies. For angles ranging within the acceptance limits the material anisotropy increases the vibration characteristics scatter.

Figures 7, 8, 9 and 10 show the calculated behaviour of the blade for the first four vibration modes, where the crystallographic orientation effect is shown by the stereographic representation.

It is worth to be noted how the resonance variation is not dramatic but nevertheless it is such to require a revision of the recommended margin respect to the operating speeds. Fig.11 shows the comparison between prediction and experimental IF frequency of the blade, where the alignment effect is fully confirmed.

Another aspect which cannot be directly extrapolated from the experience on conventional castings is the centrifugal force stiffening effect. This effect has been evaluated by a Finite Element analysis and the results are reported in fig.12; it is evident how the SC blade is more sensitive to speed than the conventional blade.

#### CONCLUSIONS

SC airfoils perform better than conventional material parts with reference to creep and thermal fatigue failure modes.

Appropriate criteria require the revision of current coefficients which account for life scatters and thin wall effect.

SC airfoils behaviour is different respect to conventional material parts with reference to high cycle fatigue. An extensive use of F.E. techniques is recommended as well as the revision of the safety margins.

#### REFERENCES

- [1] F.L. VERSNYDER, M.E. SHANK:  
The development of columnar grain and single crystal high temperature material through directional solidification;  
Materials Science and Engineering 6 (1970), 213-247.
- [2] G.J.S. Higginbotham: From research to cost effective directional solidification and single crystal production - an integrated approach; Materials and Design, 8,1 (1987), 442-460.
- [3] R.L. Dreshfield: Understanding of single crystal superalloys; Metal Progress, August 1986, 43-46.

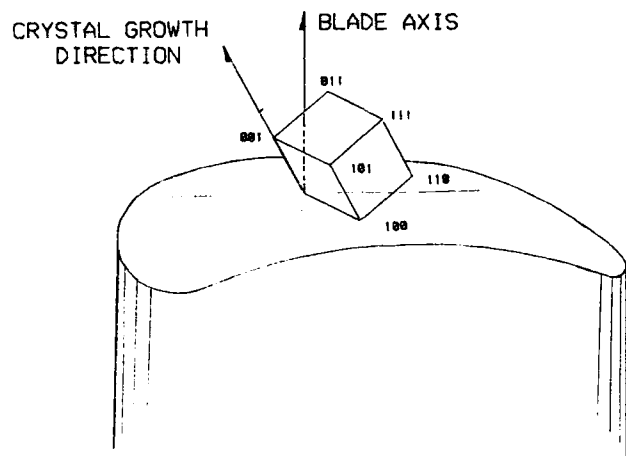


Fig. 1 - Crystallographic orientation respect to blade geometry

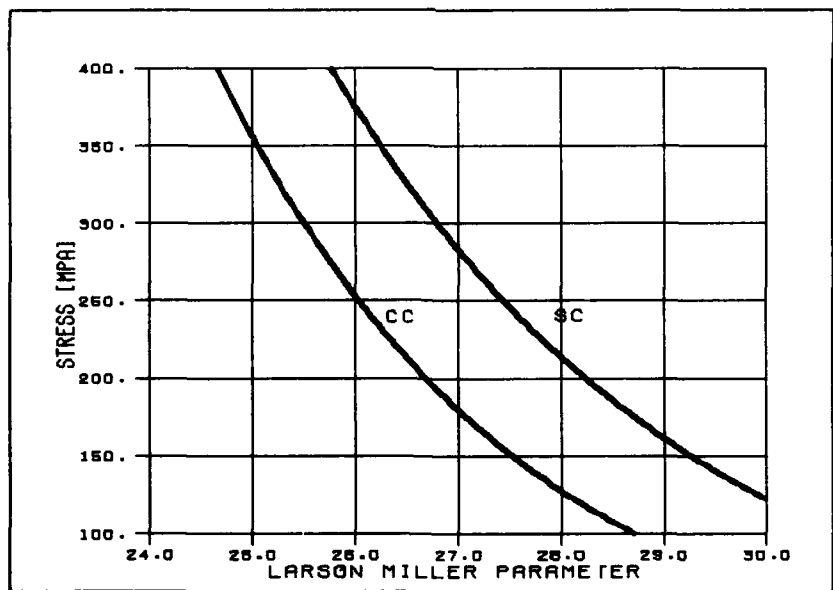


Fig. 2 - Stress-rupture data in terms of Larson-Miller parameter

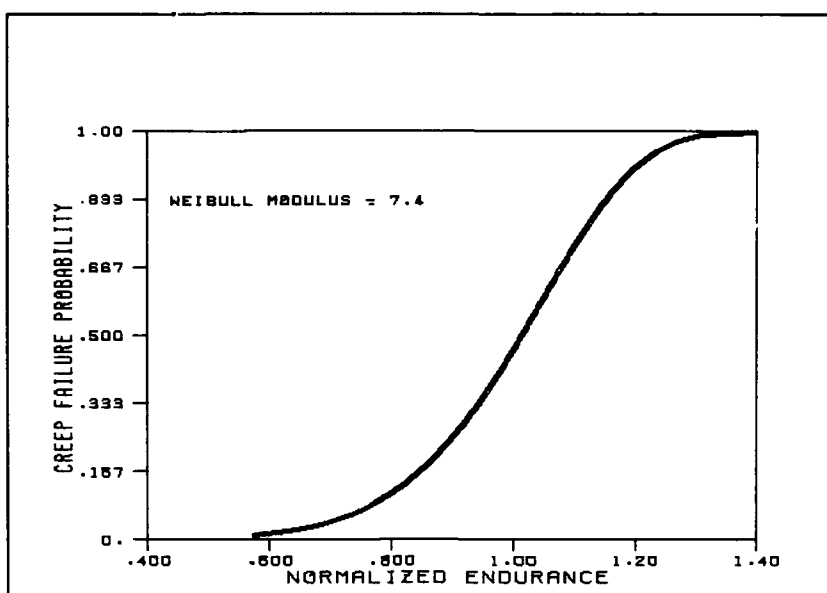


Fig. 3 - Weibull distribution of stress-rupture data

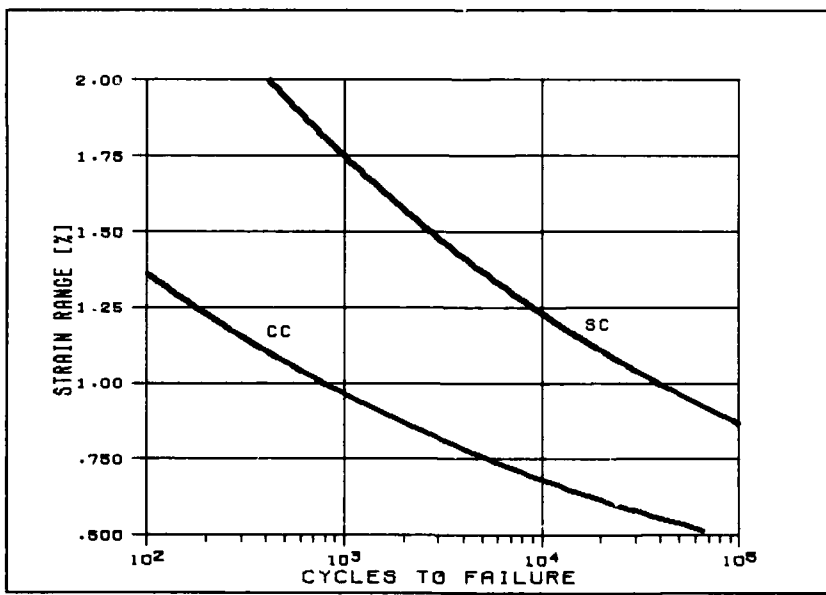


Fig. 4 - Low cycle fatigue data

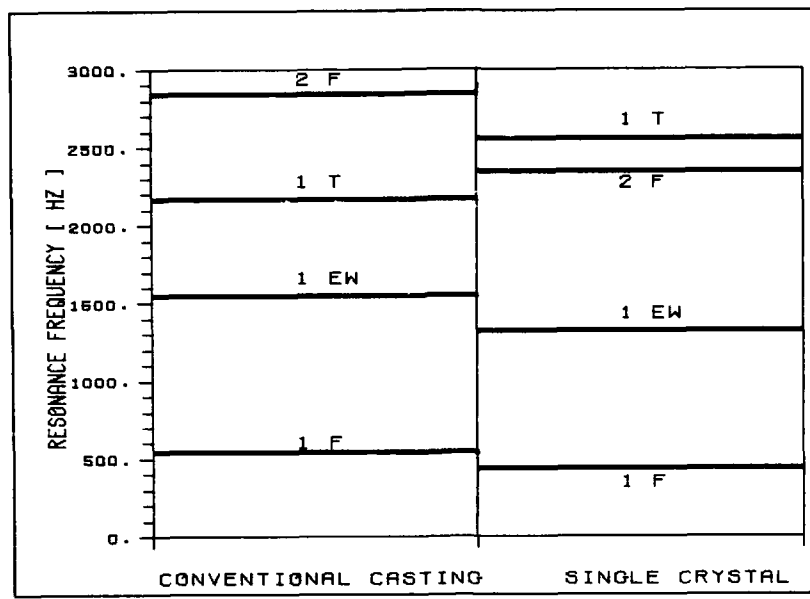


Fig. 5 - Free blade resonance spectra

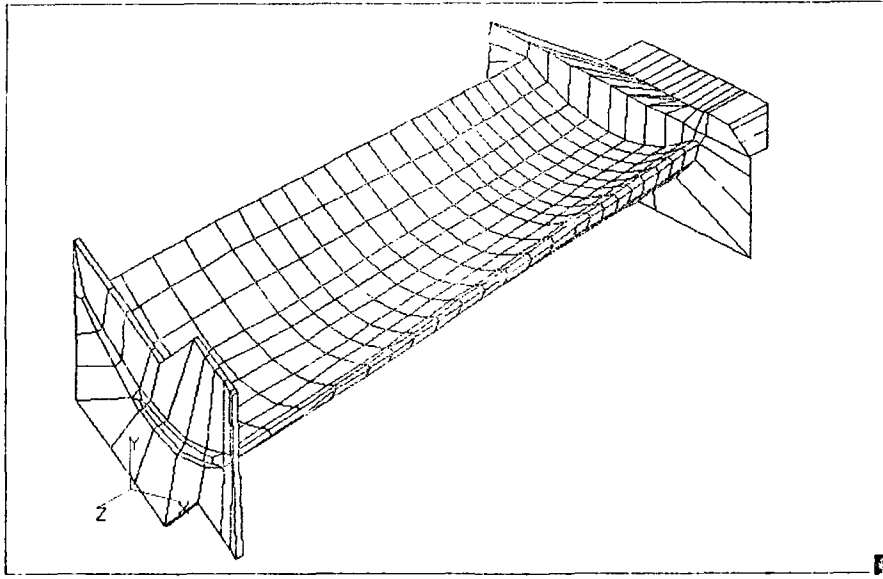
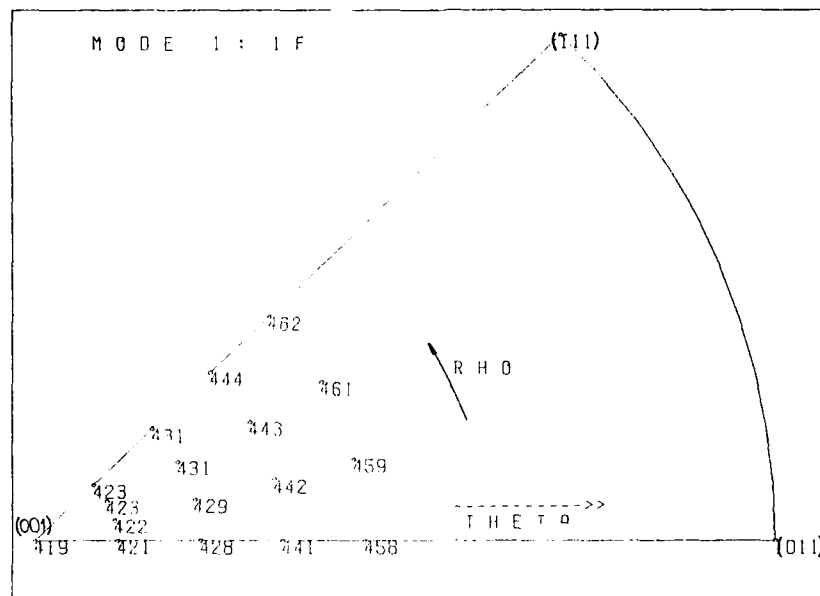
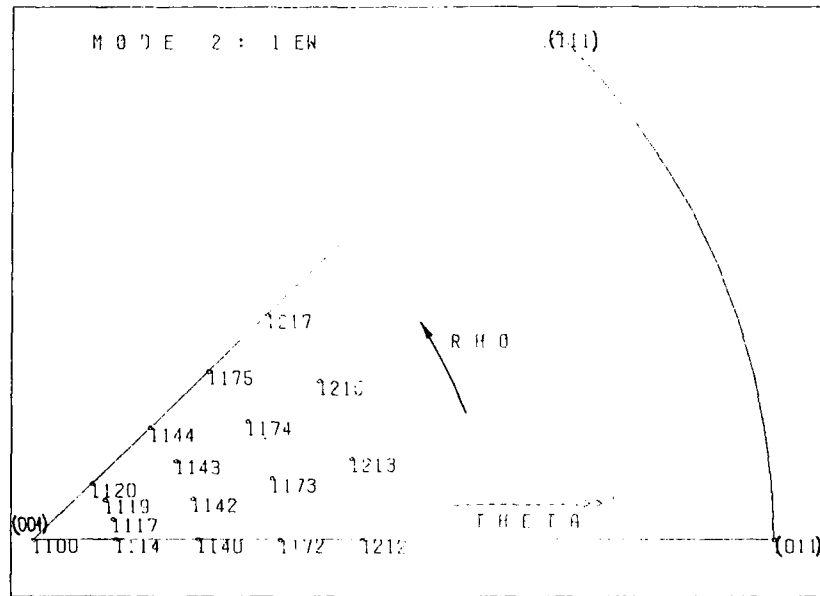
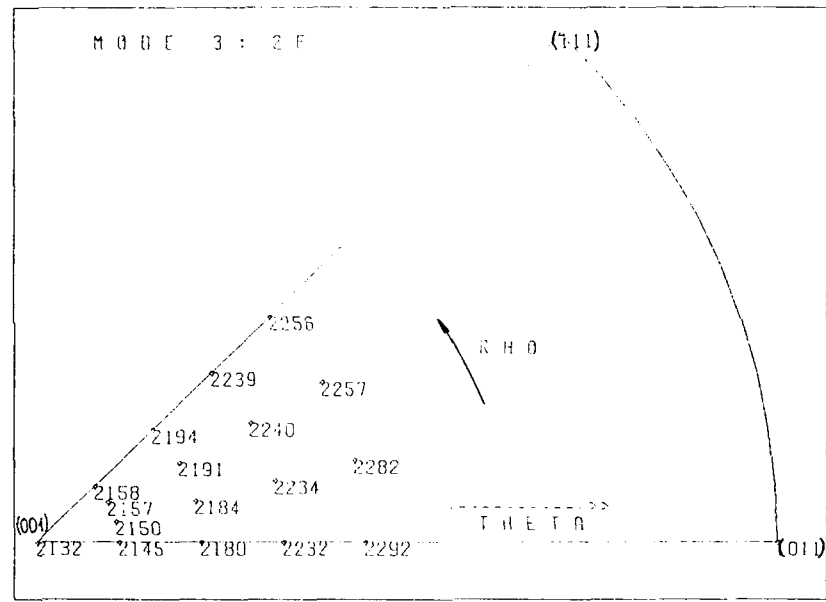
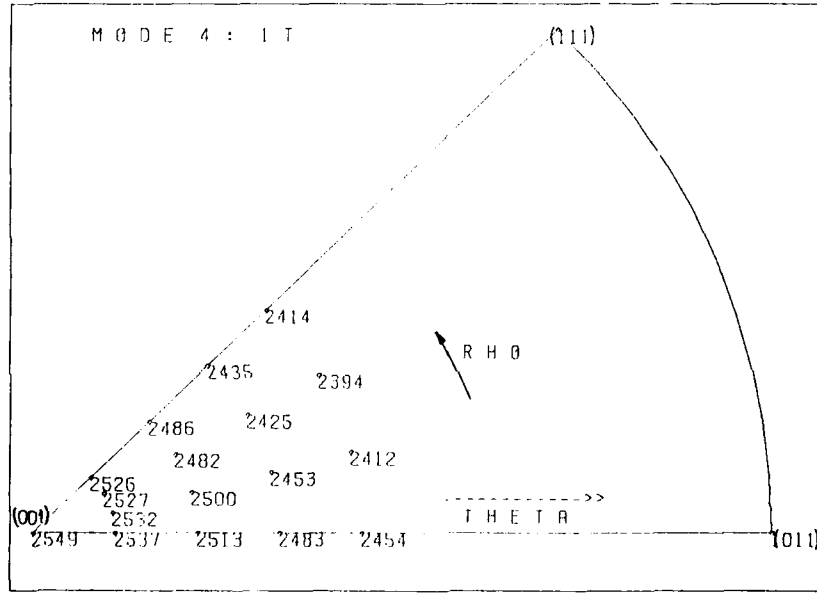


Fig. 6 - Finite Element blade model

Fig. 7 - 1F resonances vs  $\theta$  and  $\phi$  anglesFig. 8 - 1EW resonances vs  $\theta$  and  $\phi$  angles

Fig. 9 - 2 F resonances vs  $\psi$  and  $\phi$  anglesFig. 10 - 1 T resonances vs  $\psi$  and  $\phi$  angles

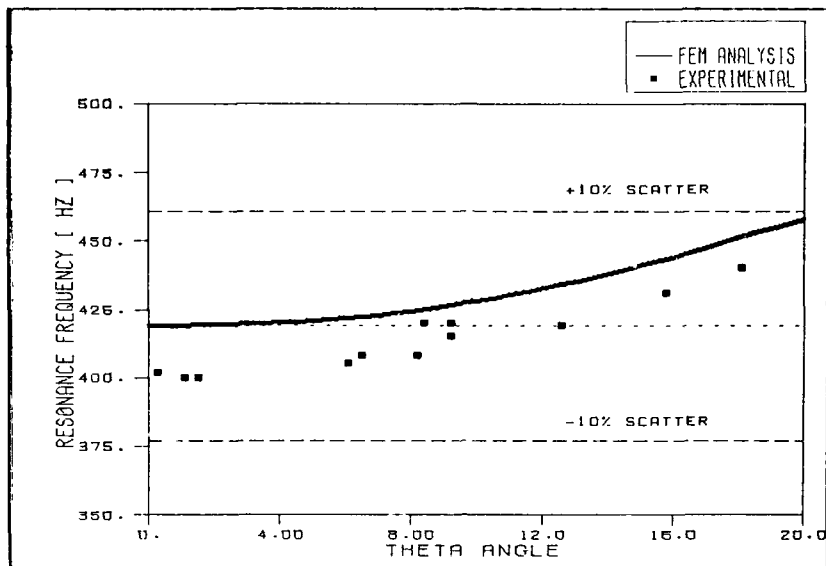


Fig. 11 - Theoretical and experimental orientation effect on 1F blade model

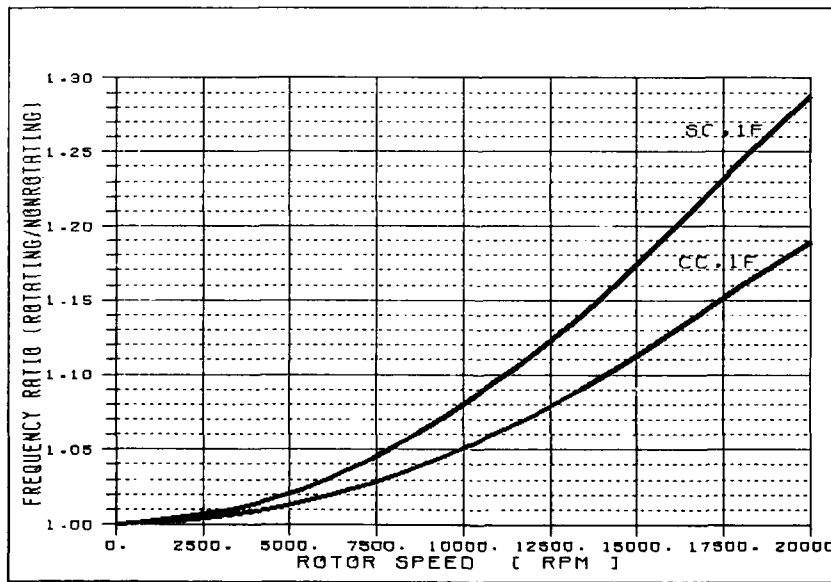


Fig. 12 - Centrifugal effect on 1F blade model

**ADVANCED MATERIALS TO COMBAT THE HIGH TEMPERATURE  
DEGRADATION PROCESSES IN TURBOMACHINERY**

by Professor P. Hancock,  
Professor of Engineering Metallurgy,  
Head of School of Industrial Science,  
Cranfield Institute of Technology,  
Cranfield, Bedford MK43 OAH, United Kingdom.

and Dr. J.F. Pestall,  
Head of Special Studies Section,  
Materials and Engineering Research Division,  
Royal Aircraft Establishment, Farnborough,  
Farnborough, Hants, GU14 0LS, United Kingdom.

**SUMMARY**

The paper begins by examining the reasons for the necessity of protective surface coatings on conventional superalloy components. Diffusion coatings, together with newer overlay coatings based on MCrAlY compositions produced by electron beam plasma vapour, are examined and their mechanisms of surface breakdown identified.

It is suggested that further developments could be made with compositions that are outside the current commercially available coatings. The limitations of the upper operating temperature of conventional coating systems suggest the need for thermal barrier coatings and the conflict between dense coatings for surface protection and porous coatings for essential mechanical stability is examined. Finally, the advantages of fibre reinforced ceramic components are considered, together with potential mechanisms of surface breakdown.

**1. INTRODUCTION**

The working environment in both gas turbines and rocket propulsion systems are extremely severe, but the requirements for the materials that are exposed to the hot gas stream in these two systems are significantly different. In rocket propulsion extremely high temperatures are experienced but the operating lifetime may be relatively short, whereas in gas turbines the operating temperature may be lower, but extended lifetimes are required.

However, the quest for increased efficiency in the gas turbine necessitates increasing gas temperatures and the requirement of minimal cost of ownership necessitates increased lifetimes of the operating components. It is this combination of increased temperature and prolonged lifetime that creates the conditions for degradation of the operating materials. This may occur by surface reactions causing progressive loss of section or by interdiffusion causing loss of strength.

In aero engines running on refined high grade distillate fuel the main degradation is caused by surface oxidation but if the engine is required to operate in a marine environment then very small amounts of sea salt ingested with the primary air can cause accelerated attack of the turbine blades and nozzle guide vanes to the extent that this attack limits the maximum operating temperature.

In this paper it is intended to review the current advanced systems used to protect hot components and, in particular, turbine blades and then to discuss possible future development of candidate materials and the problems that they will encounter due to surface attack and possible interdiffusion.

**2. CURRENT ADVANCED MATERIALS SYSTEMS FOR TURBINE BLADES**

For current aero engines where the blades operate in the region of 1000°C nickel and cobalt based superalloys are used almost exclusively. They are capable of developing higher strengths, at higher temperatures, than the iron based alloys used in the early engines of the 1940's and 50's.

To understand how the current advanced systems have developed it is profitable to look at the history of superalloy development. Obviously the first requirement is for creep strength at the operating temperature, but in these alloy systems higher strength is achieved only by reducing the chromium content. This is necessary to maintain microstructural stability and to allow increased additions of alloying elements such as aluminium, titanium and niobium which are required for optimum creep properties.

Typical results are shown in Figure 1(1) and Figure 2(2). These figures show how the level of chromium has been progressively decreased and it is chromium which provided the initial oxidation resistance by forming a protective chromia scale on the surface of the alloy. So, as the drive for increased strength has continued, the oxidation resistance of the newer alloys has decreased, as shown in Figure 1(2).

The higher strength required for modern engines means that increased alloying elements are needed and, because of difficulties in processing such highly alloyed material, this has necessitated using cast rather than wrought blades, as shown in Figure 2. Further, to avoid creep by grain boundary sliding, directionally solidified and single crystal turbine blades have been developed. This development, shown in Figure 3(3), has allowed an increase in blade temperature of less than 200°C over the past twenty years.

It is obvious that the system is now reaching an asymptote on development because the current operating temperatures are about 1050°C and the melting points of these alloys are only of the order of 1250° to 1300°C.

So the type of alloy for temperatures of the order of 1050°C is fairly predictable, but such alloys do not have sufficient chromium or aluminium to form protective surface oxides in order to offer sufficient protection against these operating temperatures. With this class of alloys, therefore, a protective surface coating must be used in order to obtain the extended lifetimes required for economical operation. The operational temperature of such coatings is therefore predictable because any significant temperature increase, using current alloys, would result in incipient melting.

### 3. SURFACE COATINGS FOR CURRENT METALLIC COMPONENTS

The properties that are required of coating systems can be briefly summarised as follows :

- . Good resistance to oxidation, corrosion and erosion
- . Surface stability, i.e. large reserve of scale forming elements
- . Good adhesion, compatibility with the base alloy in terms of expansion coefficient
- . Interfacial stability, low rate of coating/substrate diffusion
- . Ease of application
- . Low cost in relation to life cycle improvement

There are many commercial processes and compositions that meet most of these requirements for coating superalloys and these may be divided into two main groups (i) diffusion coatings (ii) overlay coatings, with a third group consisting of hybrid processes which utilise a combination of techniques to build up the final coating. These techniques and their mechanism of breakdown have been reviewed in detail recently by the authors (4), (5) and so in this paper only a brief description of the two major processes will be considered.

#### 3.1 Diffusion Coatings

Diffusion coatings can be applied by a variety of techniques including pack cementation, slurry cementation, fluidised bed techniques and metalliding. Protective coatings involving chromised, siliconised or aluminised coatings can all be produced by these techniques. The most common coating is the aluminide coating produced by pack cementation. It has been used successfully for many years to coat turbine blades. The coating is generally between 30 and 70 microns thick and performs well under simple oxidising conditions, i.e. engines operating with high grade distillate fuel in non contaminated environments, but in marine conditions serious breakdown of the coating can occur. Figure 4(5) shows an aero engine blade in marine service after only 100 hours operation which has failed due to a combination of cracking of the aluminide coating and subsequent hot corrosion of the substrate.

However, such catastrophic attack is not general for this type of coating and the stability of the diffusion coating has been recently studied in the COST 50 programme (6) and by rig testing at Cranfield (4). In these tests the behaviour of diffusion coatings was compared and, as shown in Table 1, the aluminide coatings behave very well. Tests were made at temperatures of 750, 850 and 950°C and the rate of degradation of the coatings increased in the ratio approximately 1 : 6 : 30 which means that the current operating temperatures are getting towards the limit for aluminide coatings, mainly because the protective nature of the coating is determined by an outer protective layer of NiAl (or CoAl for cobalt base alloys). As the operating temperatures increase, interdiffusion with the underlying alloy can occur and the combination of loss of aluminium due to oxidation and increase in nickel due to interdiffusion, can lead to progressive formation of γ' Ni<sub>3</sub>Al at the coating substrate interface. This γ' growth can penetrate the outer NiAl more rapidly at increasing operating temperatures and, when it does so, the protective nature of the coating is significantly diminished.

Variations such as platinum aluminising are used, where a thin layer of platinum is initially deposited by electro deposition and the blade is then pack aluminised for several hours. This treatment has been shown to give extended lives in aero engines. The reason is probably not related to enhanced corrosion resistance of the initial coating but to the ability of platinum to stabilise the NiAl phase of the coatings. Such modifications to diffusion coatings can extend the operating life but will not significantly increase the maximum operating temperatures.

One of the major limitations with this type of coating is that the available chemical compositions of the coating are limited by the nature of the process and the thicknesses of the coatings are also limited to the range of about 30 - 70 microns.

### 3.2 Overlay Coatings

Whilst the diffusion coatings have satisfied many industrial coating requirements, their performance is limited by the composition limitations that the methods of production impose. The overlay coatings do not suffer from these restrictions and perhaps the most important class of coatings for coating turbine blades is the MCrAlY alloys where the metal M is usually nickel or cobalt or a mixture of the two. Chromium can be added at levels up to 38% to impart corrosion resistance, aluminium can have levels up to 12% to give high temperature oxidation resistance and yttrium is added in the range 0.1 - 0.5% to improve oxide scale adherence.

The original development of these alloys used electron beam physical vapour deposition (EB-PVD) processes and this subject has been reviewed recently (7). A typical coating produced by EB-PVD is shown in Figure 5(5). Coating rates of up to 25 $\mu\text{m}/\text{min}$  can be achieved and coating thicknesses of between 150 and 300 $\mu\text{m}$  can be used for protection of turbine blades.

The EB-PVD process is currently being strongly challenged by a variety of plasma spraying techniques which are available in three forms - using either air, argon or low pressure plasma spraying. The standard of these coatings has improved dramatically over the past twenty years. The composition and thickness control is now satisfactory and a broad range of compositions is available. A typical example is shown in Figure 6(5) and the structure and integrity of the coating can be compared with Figure 5(5).

The advantage of the overlay coatings is that a wide range of different compositions can be achieved and the coating thickness can be considerably thicker than can be achieved by diffusion coatings.

The oxidation resistance of a full range of Ni-Cr-Al coatings produced by vapour phase alloying (8) has recently been examined. The results of the oxidation tests are shown in Figure 7(8). The results show that maximum oxidation resistance is achieved with compositions in the shaded area. The results from commercially available alloys are shown as the black points on the diagram. This suggests that there is still room for alloy improvements in this area. However, again the perceived advantage will be for longer lives at the existing operating temperatures and the possibilities of resisting working environments with higher contaminant levels rather than increased temperature applications which are determined by the melting point of the underlying blade materials.

### 4. THERMAL BARRIER COATINGS

As discussed in sections 2 and 3 of this paper the current alloy and coating systems are asymptotically reaching a maximum temperature due to the melting point of the nickel and cobalt base alloys currently used for blading material. Whilst alloy development over the last twenty years has allowed turbine entry temperatures to increase by less than 200°C, over the same period developments in blade cooling technology at Rolls Royce have allowed an additional increase in temperature over the same period of about 300°C, as shown in Figure 8(9). This is a significant advantage but it brings the added penalty that compressor air must be used for the cooling and this reduces the overall efficiency of the cycle. One way by which the degree of air cooling can be minimised is to use thermal barrier coatings.

Thermal barrier coatings with zirconia based porous outer layers and MCrAlY intermediate bond coats were introduced in the early 1970's (10) and have been successfully used for combustion chamber liners and, more recently, for stator blade platforms. This has eliminated the need for film cooling of these platforms (11).

The ceramic coatings used are porous and are characterised by high melting point coupled with low thermal conductivity. Typical values of thermal conductivity for these coatings are 1 - 3  $\text{W m}^{-1} \text{K}^{-1}$ , which compares with the thermal conductivity of an overlay coating of about 60  $\text{W m}^{-1} \text{K}^{-1}$ .

Most of the successful coatings are based on the zirconia system (12) which undergoes a phase change during heating at 1170°C from the monoclinic to tetragonal form. On cooling the monoclinic to tetragonal phase change can cause a martensitic type of change which results in a 4% increase in volume. Thermal cycling through this change then causes stresses which can destroy any coating. Additions of MgO, CaO or Y<sub>2</sub>O<sub>3</sub> are used to stabilise the tetragonal form and hence coatings based on stabilised zirconia are currently used in most commercial thermal barrier coatings. A typical example is shown in Figure 9(5). The open structure of the coating is essential both for its low thermal conductivity, but also for its mechanical stability. This is because a major problem with ceramic coatings is that their coefficient of thermal expansion is significantly different from values for the underlying metals. This has been examined in detail (13) and Figure 10 shows the stresses generated in various ceramic coatings on superalloy substrates. These results show, for example, that both silicon nitride and silicon carbide would be unsuitable ceramic coatings and that ZrO<sub>2</sub>-MgO is only able to withstand the generated thermal stresses because of its open porous structure. This structure, although essential for these thermal and structural reasons, does not provide a highly impervious coating and therefore failure of the coating can occur by reaction of the environment with the underlying bond coat.

For resistance to surface degradation a closed compact structure is required, yet for thermal insulation and mechanical stability an open porous structure is essential. It has been suggested that a novel way to develop a protective system would be to consider developing substrate alloys with coefficients of thermal expansion comparable to the proposed thermal barrier materials (14). After all, the low expansion alloys are generally based on the Ni-Fe system and it may be worth considering whether strengthening these alloys could give rise to a new generation of superalloys with compatible ceramic surface coatings.

If a suitable combination of thermal barrier and compatible substrate alloy could be achieved for successful turbine blade application, it gives the possibility of a real rise in temperature of about 300°C and therefore it is a goal well worth seeking.

##### 5. THE CHALLENGE OF FUTURE MATERIALS

The earlier sections have shown that further increase in the operating temperature will be limited by the melting points of the superalloys currently used. Refractory metals such as niobium (mp 2468°C), molybdenum (mp 2610°C) and tantalum (mp 2980°C) have been considered extensively in the past but they are all readily oxidised at their potential operating temperatures and although many attempts have been made, it has not been possible to develop reliable protective surface coatings (14).

Current thinking is therefore directed towards ceramic components and Jeal (11) has produced a schematic diagram, reproduced in Figure 11, which shows the temperature capability of the various systems under consideration.

The systems that appear to offer the possibility of real temperature increases are ceramic matrix composites including silicon carbide reinforced with silicon carbide fibre and ultimately the possibility of using carbon-carbon composites, i.e. carbon reinforced with carbon fibre. The potential of carbon-carbon composite materials has been reviewed recently by Savage (15) and Figure 12 is a slightly modified form of one of the illustrations in this paper.

It is exciting that new process technologies such as hot isostatic pressing, new fibre production routes and sophisticated coating technologies now make it possible to develop fibre reinforced ceramics. This type of development is essential for the use of structural ceramics because fibre reinforcement offers the possibility of some improvement in fracture resistance and hence an increased tolerance to defects. However, with fibre reinforcement the advantages of the reinforcing fibres are only apparent whilst the fibres do not contain significant defects. If these systems are to be used at appreciably higher temperatures than the current operating temperature, without the protection of internal cooling, then interdiffusion between the fibres and the matrix must be considered, because this could cause fibre degradation which could lead to the fracture toughness of the composite reverting to the value of the monolithic matrix.

Protection of the outer surface is also important, as irregular surface oxidation may cause defects which, although non critical in a metallic system, may reduce the fracture resistance of a ceramic component. This is an area where new work is required to determine the influence of surface attack on loss of fracture toughness.

The potential of the carbon-carbon composites is impressive but of course the problem is surface protection, as they oxidise rapidly above 400°C. According to Savage (15), the current state of the art in terms of protective coatings is to use 'silicon based ceramics SiC or  $\text{Si}_3\text{N}_4$ , as the primary oxygen barrier, coupled with internal glass forming inhibitors and sealants to seal thermal stress cracks and defects in the outer coating'. This seems to be a very complex process and slightly disturbing as the protection must be absolute. It is perhaps salutary that in Figure 11 there is a line representing the comparative behaviour of niobium. Its requirement is also one of oxidation protection and although demonstrator engines were running with niobium blades many years ago, unfortunately this problem has still not been solved.

However, this whole area of new materials offers tremendous potential but it is in its infancy. If it is to succeed it requires a great deal of effort, comparable to that which has allowed the metallic systems to reach their present level of sophistication.

##### 6. CONCLUDING REMARKS

For advanced turbine applications superalloy components must be coated with protective surface coatings. The life of such components at any temperature is governed by the operating temperature and, of more importance, the levels of contaminants in the operating environment. Further developments in coating composition are possible but they will be towards increasing life rather than increasing the operating temperature.

One technique towards increasing the operating temperatures is the use of thermal barrier coatings. The problem with these ceramic coatings is that they do have significantly different coefficients of expansion from the underlying metallic components and this can cause problems in rigid structures. It would be difficult to increase the coefficient of thermal expansion of the ceramic coatings but it should be possible to match their existing coefficients by changing the composition of the underlying metallic

materials. It may, therefore, be a fruitful line of research to develop high strength alloys with matching coefficients of thermal expansion to avoid the degradation problems associated with the current systems.

Finally, the fibre reinforced ceramic systems do offer great promise but, if they are to be used at very high temperatures then they will also have problems related to the thermal degradation of the structure. If these systems are to achieve their obvious potential they must be 'application pulled' and pulled hard!

#### REFERENCES

1. H.W. Grunling, Proc. Int. Conf. on the Behaviour of High Temperature Alloys in Aggressive Environments, Petten, Metals Society, London 1979, pp 137-162.
2. S.W.K. Shaw, Proc. 3rd US/UK Conf. on Gas Turbine Materials in a Marine Environment, Bath, 1976, Session (IV), Paper 1.
3. T.D. Alexander and P. Driver, Proc. 1st Int. Conf. on Materials in Aerospace April 1986, Royal Aero. Soc., London, 1986, pp 168-188.
4. J.R. Nicholls and P. Hancock, Industrial Corrosion Vol. 5, No. 4, July 1987.
5. J.F. Pestall, J. Naval Eng., Vol. 30, No. 3, Dec. 1987, p 559 - 585.
6. M. Malik, R. Morbioli and P. Huber, in Proceedings of 'High Temperature Alloys for Gas Turbines', 1982. (P. Brunetaud et al, editors). D. Reidel Publishing Co., Holland, p 53-86.
7. D.H. Roone, Mater. Sci. Eng., 88, 1987, 349.
8. Work by I.H. Hussain, J.R. Nicholls and P. Hancock, quoted by P. Hancock in Ceramic Coatings for Heat Engines, Proc. Materials Research Soc., Strasbourg, 1985. Les Editions de Physique, Paris 1985, p 163-179.
9. S. Ryworth, Rolls Royce Mag., 29, 1986 p 21.
10. R.C. Tucker, T.A. Taylor and M.H. Weatherly. Proc. 3rd US/UK Conference on Gas Turbine Materials in a Marine Environment, Bath, UK, 1976. Session VII, Paper 2.
11. R.H. Jeal, Metals and Materials, Vol. 4, No. 9. 1988. p 539-542.
12. J.F. Pestall, K.T. Scott. Proc. MRS Conference, Strasbourg, Nov. 1985, p 93-100.
13. P. Hancock, MRS Conference, Strasbourg, Nov. 1985, p 163-179.
14. P. Hancock, Materials Science and Engineering 88, 1987, p 303-311.
15. G. Savage, Metals and Materials, Vol. 4, No. 9, 1988 p 544-548.

**Table 1 - Ranking Order of Coatings Included in the COST 50 Programme  
(Burner Rig Test and Aerofoil Components) and Cranfield Burner  
Rig Tests (from Reference 4)**

<b>COST 50 Programme</b>		<b>Cranfield Burner Rig Tests</b>	
<b>Aerofoil Component</b>	<b>Burner Rig Tests</b>	<b>500h @ 750°C</b>	<b>500h @ 850°C</b>
<b>'A' 950°C max 3000h</b>			
<b>Best</b>			
Pt aluminides (RT22,LDC2)	Ti/Si Slurry (Elcoat 360)	S.I.P. NiCrTiAl - Pt Aluminide	Pt Aluminide (JML1) - Conventional Aluminide
-	-	-	-
Aluminide (PWAT3)	Pt aluminide (LDC2)	Plasma sprayed CoNiCrAlY(LCO22) + pulse Al	Plasma sprayed CoNiCrAlY(LCO22)
-	-	-	-
+ pulse Al	-	-	-
Pack chromised +	Pt chromised	Conventional Aluminide	(2) -----
Pack aluminide	-	-	S.I.P. NiCrTiAl -
Chromised	Plasma sprayed CoNiCrAlY(LCO22)	(2) -----	Plasma sprayed CoCrAlY -
-	-	-	-
Chrome aluminised (HI 15)	FR-PVD CoCrAlY (ATD6)	FR-PVD CoCrAlY (ATD6)	FR-PVD CoCrAlY (ATD6)
(1) ----- CoCrAlY (20-24Cr,10Al)	Chromised	-	-
NiCrAlY (20-24Cr,10Al)	Chrome aluminised	Chromised	Chromised
-	-	-	-
<b>Worst</b>	Pack aluminised (MPS 320)		Chrome aluminised

Blade type 'A' - first stage turbine blade of solid configuration, with narrow cooling holes, max. metal temp. 950°C, operating on short routes.

- (1) Corrosion rate of uncoated alloy
- (2) Coating penetrated

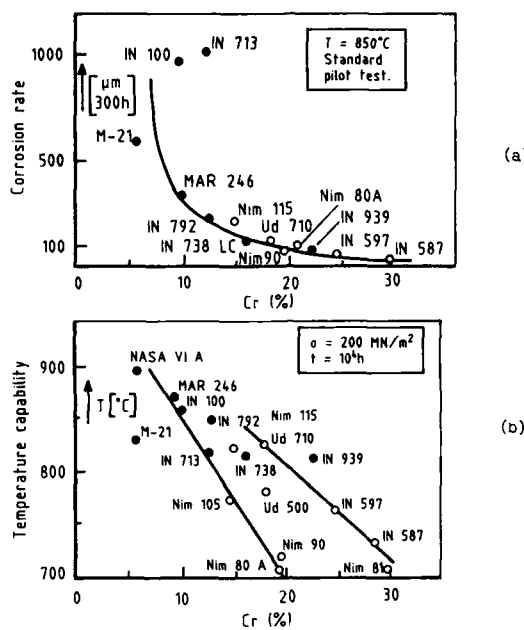


Figure 1 - Influence of chromium content on a) oxidation resistance and b) creep rupture strength of current superalloys

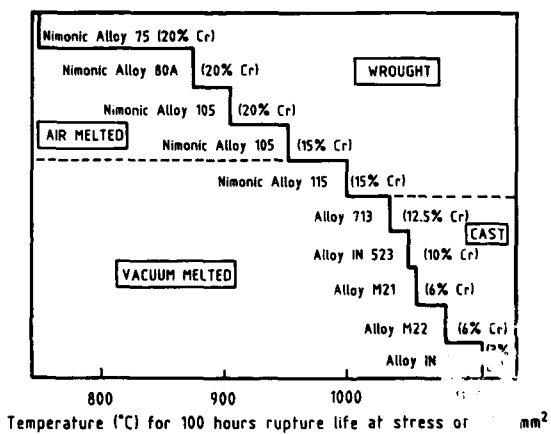


Figure 2 - Stress rupture temperature capability v. chromium content of blading alloys (2)

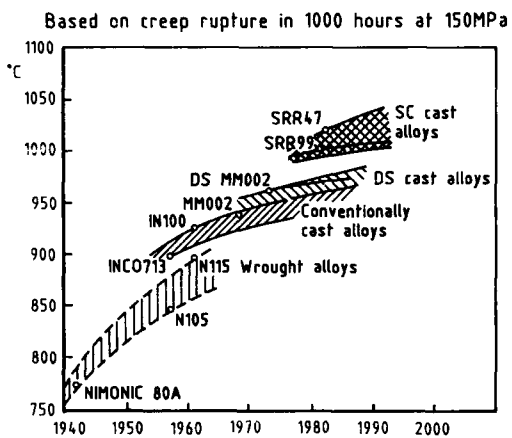


Figure 3 - Development of turbine blade material (3)



Figure 4 - Aluminised blade after engine test (5)



Figure 5 - Micro sections through EB-PVD coated blade (5)  
 1. blade alloy  
 2. coating 100 microns thick  
 3. Nickel plate  
 4. plastic mount

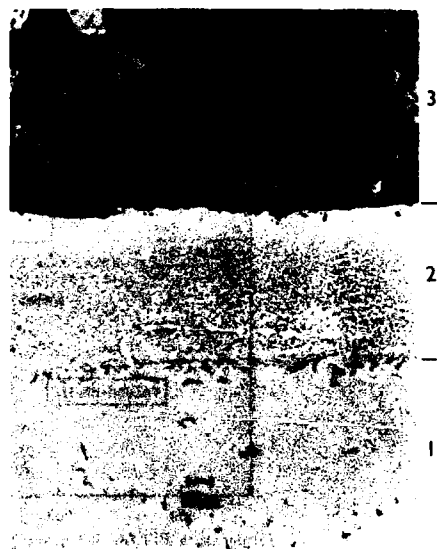


Figure 6 - Microstructure of fully processed plasma sprayed overlay coated blade (5)  
 1. blade alloy  
 2. coating  
 3. plastic mount

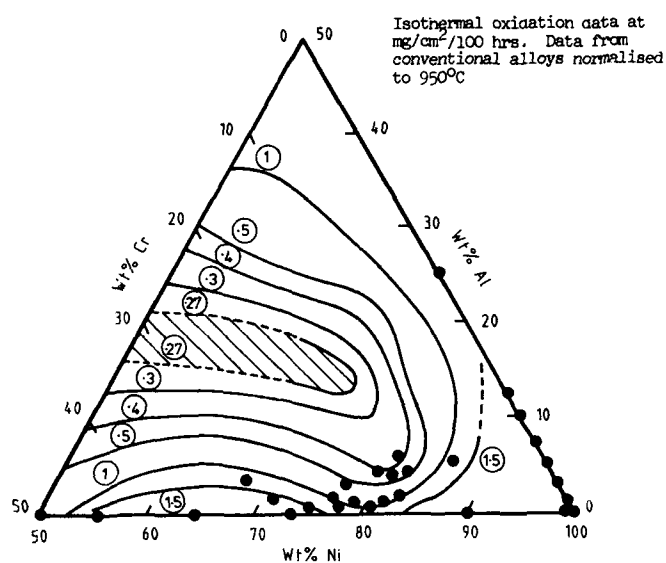


Figure 7 - Ternary diagram illustrating the oxidation behaviour of Ni-Cu-Al coatings compared with available material presented as individual points (8)

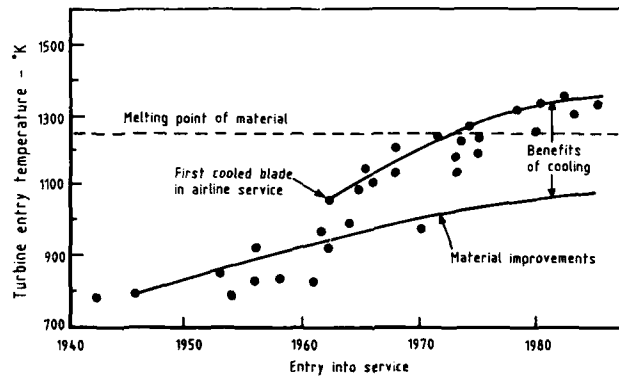


Figure 8 - Increase in operating temperature of Rolls Royce turbines showing the contribution of blade cooling (9)



Figure 9 - Plasma sprayed thermal barrier coating (4)

- A. Partially stabilised zirconia coating
- B. MCrAlY bond coat
- C. Metal substrate

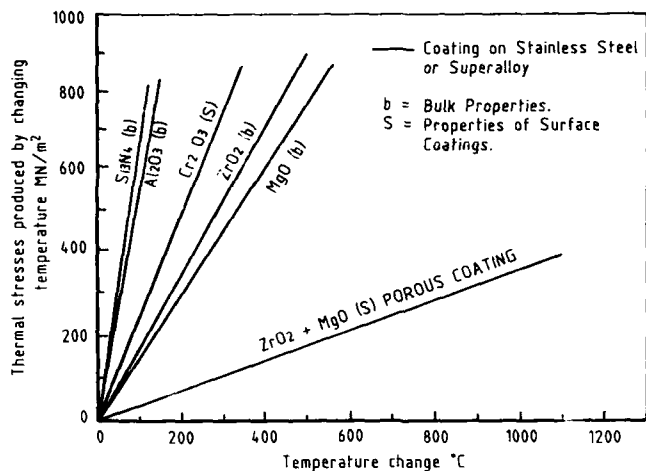


Figure 10 - Thermal stresses generated in ceramic coatings on superalloy substrates by various temperature changes

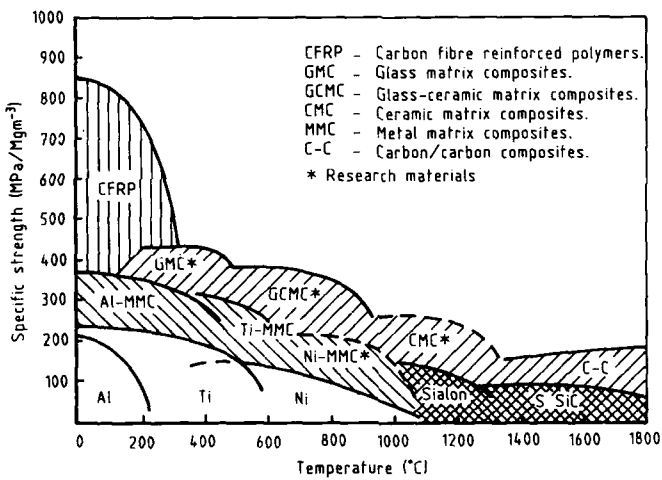


Figure 11 - Specific strength of structural materials after Jeal. (11)

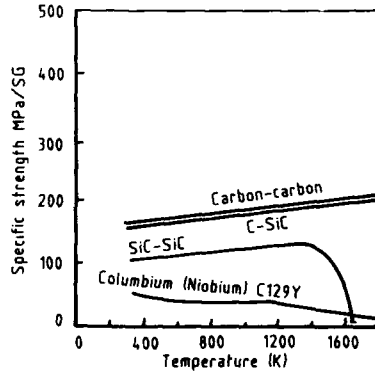


Figure 12 - Specific strength of fibre reinforced coatings (15)

**DISCUSSION**

E. Thompson, United Technologies Research Center, US. In your presentation you mentioned the importance of ion diffusion through the oxide film formed on the aluminides. Isn't spalling of the oxide the most important problem associated with this type of protective film in many applications?

P. Hancock, Cranfield Institute of Technology, UK. Yes, I agree that spalling is life limiting in many industrial applications where thermal cycling occurs as a normal condition. My point concerning diffusion through the film is that if diffusion is too rapid, then the film wouldn't be considered for use at all.

R. Kochendorfer, DFVLR, FRG. I would like to comment about your point concerning thermal barrier coatings. There is work underway at DFVLR-Cologne pursuing exactly the approach you mentioned for their improvement, the matching of the thermal expansion of the metal to that of the ceramic.

**THE DEMONSTRATION OF MONOLITHIC AND COMPOSITE CERAMICS  
IN AIRCRAFT GAS TURBINE COMBUSTORS**

by

Frank G. Davis  
Garrett Engine Division  
Allied-Signal Aerospace Company  
Phoenix, Arizona U.S.A.

and

Dale A. Hudson  
Aero Propulsion Laboratory  
U.S. Air Force Wright Aeronautical Laboratories  
Wright-Patterson Air Force Base, Ohio U.S.A.

**SUMMARY**

Since the mid seventies, the Air Force Wright Aeronautical Laboratories Aero Propulsion Laboratory has been on a course to evaluate and demonstrate the application of advanced non-metallic materials in experimental gas turbine engines. Potential increases of several hundred degrees or more in operating temperature represents a quantum leap in engine capability. Under two contracts since the late seventies, Garrett Engine Division, Allied-Signal Aerospace Company has been developing non-metallic gas turbine combustor technology. As part of the programs, combustion rig tests have been successfully performed at near-stoichiometric conditions on two ceramic combustor configurations. These combustors were annular, through-flow designs similar to the metallic burners used in present-day military propulsion gas turbines. The first configuration used monolithic ceramic segments as a portion of the inner and outer combustor liners. The segments were supported by an external metal structure. These segments were fabricated from silicon carbide material. In the most recent program ceramic composite rings were used to form the inner and outer liners. The rings were composed of silicon carbide fibers and a silicon carbide matrix. The ceramic composite rings required no external support structure. Testing consisted of both steady-state and transient operations. During transient testing, the combustors were subjected to rapid thermal cycling. Testing of silicon carbide and silicon nitride ceramic materials has just begun.

**INTRODUCTION**

Advanced materials have always played a key role in the design and capability of military systems. Until recent years metals have been the only class of structurally useful high temperature materials. Since the mid seventies high purity ceramics development has produced numerous new high temperature materials which offer great potential for increasing gas turbine performance. The increased performance requirements of future military aircraft require that substantial improvements be made in their propulsion systems. The desire for faster acceleration and rates of climb dictates that engine thrust-to-weight ratios (T/W) be increased dramatically. Research activities are currently in progress with the goal of doubling T/W over the next 20 years as shown in Figure 1. Reduction of vehicle weight contributes 60% of the potential gains from advanced non-metallics. The remaining 40% of the potential gain comes from higher power available from higher temperature operation. Advanced non-metallic materials are a major thrust of the Air Force's effort to double propulsion thrust to weight.

Studies have shown that to increase T/W requires that higher cycle pressures and temperatures be used while the weight of the individual engine components be reduced. With respect to the combustor, the requirement for increased cycle pressures and temperatures causes a two fold problem. First, increasing the compressor pressure ratio also increases the temperature of the air exiting the compressor and entering the combustor. By increasing the compressor air temperature, its ability to cool the combustion liner walls is reduced. Increased pressure also produces a more luminous flame that transfers more heat to the liner walls resulting in an increased demand for cooling. Second, as the turbine inlet temperature is increased to near-stoichiometric conditions, more of the air entering the combustor is required for the reaction process and less is available for liner cooling. This tendency is shown schematically in Figure 2.

The obvious conclusion reached from the above information is that as cycle pressures and temperatures increase, there will come a point when there is insufficient air available for cooling conventional metallic combustion liners. Thermal barrier coatings and advanced cooling techniques will permit the use of metallic combustors for a time, but during the next decade uncooled, nonmetallic combustors will be required for advanced military engines if T/W goals are to be attained.

In anticipation of this requirement, research and development activities have been initiated by the gas turbine industry under both company and Government funding. These programs have involved both material characterization and component evaluation of a wide

range of nonmetallic materials. Material strength versus temperature maps, such as Figure 3., help identify candidate materials which may have the greatest usefulness and payoff. At the Garrett Engine Division(GED), this activity has focused on the use of ceramics. Initial work was limited to monolithic ceramics, but recently ceramic composites have also been evaluated. This paper will describe these ceramic combustor test programs.

#### MONOLITHIC CERAMIC COMBUSTORS

GED's research on the use of ceramic combustors for advanced military engine applications began in 1978 when it was awarded the Air Force funded Advanced Material Segmented Combustor (AMSC) Program (F33615-78-C-2045). This program ran through March, 1983 and a detailed report of the activities of this program were published in a final report. The Segmented Ceramic Combustor Demonstration (SCCD) Program (F33615-83-C-2354) was a follow-on to the AMSC Program and was awarded to GED in February of 1984 and is still ongoing.

#### AMSC Program

The objective of this program was to demonstrate the potential of monolithic ceramics to effectively function in a combustor operating at near-stoichiometric conditions. Material selection to achieve the program objectives required an extensive evaluation of the available ceramic materials. This review included a thorough literature review to identify candidate materials followed by material characterization tests of the candidates at GED to determine their suitability as combustor materials. Silicon carbide (SiC) and silicon nitride ( $Si_3N_4$ ) were selected as the candidate materials and a number of fabrication techniques were considered. Hot pressed materials were eliminated from consideration due to their strength degradation at elevated temperatures. Sintered  $Si_3N_4$  was not readily available at the time of the program and was also eliminated. Other materials considered were sintered alpha SiC (SASC), reaction bonded  $Si_3N_4$  (RBSN) and recrystallized SiC. Of these three, SASC, produced by Carborundum, was selected because it had the best strength at elevated temperatures and was the easiest to fabricate. Figure 4. shows the results of the testing to evaluate strength versus temperature for the candidate materials.

The materials considered during the AMSC program were not mature but rather new emerging ceramics that were continuously being improved. Little design information was available at the temperatures that would be encountered during combustion testing. Therefore, GED performed considerable in-house evaluation of the candidate materials to ensure that the one selected would survive the combustor environment.

#### Aerothermodynamic Design

It was well known that high thermal gradients lead to ceramic failures. The major aerothermodynamic design effort was aimed at achieving a uniform near-wall gas temperature while maintaining a high combustion efficiency at the near-stoichiometric operating conditions. The final combustor aerothermodynamic design was achieved after several iterations of GED's three-dimensional combustor performance model and the application of other computer design codes and empirical correlations. A cross section of the combustor is shown schematically in Figure 5.

The dome and primary zone of the combustor were metallic and were film cooled. To achieve the desired high combustion efficiency required that reaction air be introduced through orifices in the inner and outer liner walls as well as through the dome. If these orifices had been placed in the ceramic liners, the high thermal gradient caused by the relatively cold air flowing through the orifices could have resulted in a ceramic failure. Therefore, the primary zones of the inner and outer liners were fabricated from metal and contained the necessary orifices. High film cooling rates were used to ensure the durability of the metal liners. The down stream portion of the combustor (normally referred to as the "dilution zone") was ceramic. Dilution orifices were not required in this region due to the near-stoichiometric operation of the combustor; almost all of the air was required for combustion.

To ensure an even distribution of fuel into the combustor, large diameter airblast fuel nozzles were used with a one-to-one spacing ratio. Prototypes of candidate nozzle designs were tested on flow-stands and the results incorporated into combustor design evaluation. The nozzle that produced the best combination of low near-wall temperature gradients and high combustion efficiency was chosen for rig testing.

#### Mechanical Design

To minimize the effects of thermal and mechanical stresses, the ceramic components were designed as segments. Figure 6. is a picture of a segment used in the inner liner. The outer liner had two rows of 12 segments and the inner liner had two rows of six segments. The segments were attached to metal support structures by tabs. The support structures provided the proper axial alignments, provided for thermal growth differentials between metal and ceramic components, and maintained a slight preload between the ceramic segments to minimize air leakage.

To accommodate this mechanical design activity, existing GED design codes were updated to incorporate ceramic material properties. These revised codes were then used to evaluate potential tab configurations and to determine acceptable preload levels.

Estimated stress levels within the segments were determined using the projected near-wall hot gas profile supplied from the aerothermodynamic analysis. The thermal model first estimated the temperature levels within the segments and these data were used as input to the stress model which calculated estimated stress levels. A sample output from this analysis is shown in Figure 7. This procedure was iterated to produce ceramic segment configurations with acceptable stress levels.

#### Combustion Rig Testing

The combustor was tested in a full annular configuration in a test rig that had been modified to accommodate high discharge temperatures. Gaseous emissions were measured at the discharge of the combustor with an eight point rotating rake that sampled in ten-degree increments. At high combustor outlet temperatures ( $T_4 > 3000^{\circ}\text{F}/1650^{\circ}\text{C}$ ) the temperatures and combustion efficiencies were calculated from the emissions data.

Testing consisted of both steady state and transient (cyclic) conditions and was performed at inlet pressures up to ten atmospheres. Maximum combustor outlet temperatures were in excess of  $3500^{\circ}\text{F}/1927^{\circ}\text{C}$ . The inner liner ceramic segments survived more than 12 hours of operation with more than five hours of that time at discharge temperatures exceeding  $3000^{\circ}\text{F}$ . In addition, the inner segments were subjected to ten light-offs, three rapid shutdowns and 21 six-minute cycles of approximately  $2000^{\circ}\text{F}/1111^{\circ}\text{C}$  delta T.

The outer liner ceramic segments survived three hours of steady-state operation at temperatures in excess of  $3000^{\circ}\text{F}$ . However, during a run with temperatures in excess of  $3500^{\circ}\text{F}$ , a facility problem occurred necessitating an emergency shutdown. Inspection of the burner revealed that eight of the outer segments had been damaged; four of the segments had been broken into two or more parts. In spite of the failures, the integrity of the combustor was maintained as shown in Figure 8. None of the inner segments were damaged during this or subsequent testing. Inspection of the failed segments indicated they had failed during the emergency shutdown.

The damaged segments were replaced and the test repeated. After approximately 40 minutes of operation at temperatures in excess of  $3500^{\circ}\text{F}$ , the fuel pump shaft sheared off resulting in a nearly instantaneous fuel shut-off. The core temperature of the combustor dropped to lightoff temperature in less than a second. Inspection of the combustor revealed four outer segments were broken but still intact and serviceable. It was decided to continue testing with the broken segments and three six-minute cycles of approximately  $2000^{\circ}\text{F}$  delta T were run. Inspection following the cyclic testing revealed a total of nine broken segments. As before, all segments were intact. Examination of the broken segments indicated that the failures were caused by contact stresses resulting from excessive axial loads.

#### Conclusions

Conclusions reached from the AMSC program were that the GED design approach offered a viable method of operating a combustor at near-stoichiometric conditions. The performance of the inner liner ceramic segments demonstrated the potential for this type of combustor configuration. The question raised by the testing was why the outer segments were subjected to higher contact stress levels than the inner segments.

#### SCCD Program

The goals of the SCCD Program are to build on the success of the AMSC Program. The SCCD began in early 1984 and is still in progress. The program objectives are three-fold:

- 0 Determine the cause for the failure of the AMSC outer segments
- 0 Demonstrate a combustor with inner and outer liners totally ceramic
- 0 Test at higher operating temperatures and faster cycle rates

#### Material Selection

During the six years that elapsed since the beginning of the AMSC Program, significant advances have been made in monolithic ceramics. At the beginning of the SCCD Program an extensive evaluation of potential ceramic vendors and the characteristics of their materials was made. Two material were selected for combustor test evaluation during the SCCD Program. These are:

- 0 SASC produced by Carborundum
- 0 Sintered  $\text{Si}_3\text{N}_4$  produced by Kyocera

Both of these materials were found to have the strength required at the SCCD operating temperatures. A plot of strength versus temperature for both materials is shown in Figure 9.

#### Aerothermodynamic Design

An objective of the program is to demonstrate a combustor whose inner and outer liners are entirely ceramic. Two aerothermodynamic designs were considered and evaluated analytically. The first had all of the air entering the combustor through the dome

(swirlers and airblast fuel nozzles). The second was similar to the AMSC design in that it had air injected through primary orifices located in the inner and outer liners in addition to dome injection. The latter configuration was chosen due to the superior combustion efficiency (approximately five percent higher) predicted by the combustion design code at the near-stoichiometric operating conditions. Refined versions of the codes used in the AMSC Program were used to establish the final SCCD aerothermodynamic design. As before, maintaining low near-wall thermal gradients was a major design criterion.

#### Mechanical Design

Two major mechanical design activities were undertaken as part of the SCCD Program: evaluation of the failed AMSC outer segments and the mechanical design of the SCCD combustor.

An extensive analysis of the AMSC design revealed that the loads, both mechanical and thermal, were higher by a factor of five for the outer segments than for the inner. This was caused by the nonlinear characteristics of the axial retention springs used to position the segments. The original analysis made during the AMSC Program assumed that these springs behaved linearly, but closer examination, including a test of the spring's deflection versus load characteristics, revealed they behaved exponentially. Because of the nature of the AMSC design, this tended to unload the inner segments and place excessive load on the outer segments. It is believed that this increased load on the outer segments lead to the contact stress failures.

The SCCD combustor mechanical design incorporated the information learned from the previous failure analysis. The segment retention method was redesigned to facilitate assembly and to ensure a uniform load on both inner and outer ceramic segments throughout the combustor operating range.

A cross section of the SCCD combustor is shown schematically in Figure 10. The inner and outer liners consist of three rows of ceramic segments extending from the combustor dome to the exit. Between the first and second row of segments of both inner and outer liners are narrow metallic rings that contain the primary orifices. These rings are segmented and the hot gas side of the segments coated with a thick layer of ceramic thermal barrier coating (TBC). These orifice rings were necessary to prevent the exposure of the ceramic segments to the high thermal gradients associated with orifice flow. These gradients would result in failure of the ceramic segments, but actually help to improve the durability of the narrow metallic rings. A photograph of an orifice ring segment is shown in Figure 11.

Thermal and stress analyses similar to that described for the AMSC combustor design were performed for the SCCD configuration using updated mechanical design codes. The final configuration was designed to operate at the elevated temperatures without excessive contact stress and therefore survive intact without ceramic failure.

#### SCCD Program Status

The first rig testing under the SCCD Program entailed operating the AMSC configuration combustor at higher cycle rates. The combustor used the AMSC ceramic segments on the inner liner and metal rings on the outer. These rings, while not satisfactory for high temperature steady-state operation, were adequate for the transient testing. Testing began at the six-minute cycle rate tested during the AMSC Program and decreased in the following increments:

0	3 minutes
0	1 minute
0	30 seconds
0	10 seconds

As before, the combustor was cycled over a 2000°F delta T range. From low temperature to high and back to low constituted one cycle. Following the completion of the ten-second cycle testing, the rig was shut down and inspected. No broken ceramic segments were observed. The rig was then run at the ten-second cycle condition continuously for two hours, accumulating over 700 cycles. During the testing, there was no loss of performance. However, upon inspection of the combustor, one of the segments was broken. The break was similar to that observed with the outer segments in that it appeared to be caused by contact stress and the broken portions of the segment remained intact.

The SCCD program testing of the final combustor configuration has begun with both carbide and nitride materials. The silicon carbide segments were tested first over the test plan described above. Early results are consistent with those found under the AMSC program. Some segments have been cracked due to surface damage inflicted by contact stresses and are shown in Figure 12. Damage patterns indicate an improvement in design practice with further improvement in design and manufacturing standards needed. The silicon nitride segments are in test and are holding up well. No further data are available at this time.

#### CERAMIC COMPOSITE COMBUSTOR

The AMSC and SCCD Programs have demonstrated the feasibility of using ceramics for near-stoichiometric combustor operation. They have also identified some problem areas,

specifically, the lack of adequate toughness of monolithic ceramics. Even though broken ceramic segments were retained intact and continued to operate successfully at high temperatures and high cycle rates, the monolithic ceramics cannot at this time be considered viable for man-rated applications. What is needed is a material with the same demonstrated temperature capability as monolithics with a low sensitivity to contact stress and increased toughness. Ceramic composites may meet this requirement.

In August, 1985, GED was awarded the Ceramic Composite Combustor Screening (CCCS) add-on to the SCCD Program. The objective of the add-on was to evaluate composite ceramics as an alternative to monolithics for combustor applications. This evaluation was to take place in the AMSC test rig utilizing as much of the AMSC combustor hardware as possible. Testing was to be accomplished at the same conditions as the AMSC combustor.

#### Material Selection

SEP of France was selected to supply the ceramic composite based on their experience with this relatively new material. SEP engineers worked with the GED Materials Engineering staff in designing the architecture for the ceramic. A SiC/SiC composite was selected as having the most desirable properties for the CCCS application. This material is fabricated from plain weave cloth made from Nicalon SiC fibers. The matrix is chemical vapor infiltrated SiC. Test specimens were fabricated from this material and a series of tests were performed at GED to determine the following properties:

- 0 Tensile strength
- 0 Flexure behavior
- 0 Interlaminar shear strength
- 0 Interlaminar tensile strength
- 0 Fracture toughness

Figure 13. shows a comparison of the relative toughness of the SEP composite versus the monolithic. As can be seen in the figure, the fibers restrict the propagation of cracks through the matrix thereby preventing a complete part failure.

#### Aerothermodynamic Design

The operating requirements of the CCCS combustor did not change from the AMSC design. Therefore, no additional analysis was required.

#### Mechanical Design

The objectives of the CCCS add-on were to use as much of the existing AMSC hardware as possible and run at the same AMSC conditions to facilitate a direct comparison between the monolithic and composite ceramics. Figure 14. shows a schematic cross section of the CCCS combustor. As a result of the increased toughness of the composite, it was no longer necessary to design the ceramics in segments. For the CCCS configuration, a single outer ring replaced 24 segments and a single inner ring replaced 12 segments. By eliminating the segmented design, the metallic support structures were no longer required, dramatically reducing the overall weight of the combustion system. The rings were supported in the combustor by the improved design retention springs to produce minimal and uniform loading.

Two sets of rings were fabricated, one without orifices and one with four 0.25-inch diameter orifices machined 90-degrees apart in both the inner and outer liners. A picture of these two sets of rings is shown in Figure 15. The rings without orifices is the more conservative design and more closely approximates the AMSC configuration. The rings with orifices were fabricated to determine if the ceramic composite would be tolerant to the thermal gradients generated by orifice flow. A successful test of the later configuration would allow for full ceramic liners to be fabricated from ceramic composites without the need for metallic orifice rings like those used in the SCCD design.

#### Combustion Rig Testing

The CCCS program completed its testing in May 1987. The two sets of ceramic composite rings were tested at two combustor outlet temperatures:  $T_4 > 3000^{\circ}\text{F}$  and  $T_4 > 3500^{\circ}\text{F}$ . Testing began with the rings without orifices. The first test was one hour steady state at  $T_4 > 3000^{\circ}\text{F}$ , followed by a tailpipe inspection. No damage was found on either the inner or outer rings. The second test was at  $T_4 > 3500^{\circ}\text{F}$  and resulted in interlaminar cracking of the inner ring and some hot surface cracks. The outer ring sustained 13 axial cracks, ten of which were through both the radial and axial widths. A picture of the outer ring is shown in the photograph of Figure 16. All material was retained and no secondary damage occurred.

The rings with orifices were tested next, again beginning at  $T_4 > 3000^{\circ}\text{F}$  steady state. After one hour tailpipe observations noted interlaminar cracking on the inner rings. The outer ring sustained six axial cracks, four of which penetrated both axial and radial thickness. No material was lost and no cracks were associated with the orifices. Based on previous experiments, the ceramics hold their positional integrity even though cracked. Therefore, the "on" was made to continue testing. After one hour of hotter steady state testing, the tailpipe inspection found three more axial cracks on the inner ring which had propagated radially to the interlaminar crack. Two small cracks on the outer

rings had propagated through the width and thickness. Again no cracks were associated with the orifices.

After the steady-state testing, the rings with the orifices were continued into cyclic testing, undergoing increments having three-minute, one-minute, 30-second, and ten-second cycles. Endurance testing followed the incremental sequence and was composed of one hour of one-minute cycles. A tailpipe inspection was conducted at the end of each cyclic increment. After the three-minute increment, the inner ring section which had previously delaminated broke off. The damaged inner ring is shown in Figure 17. There was no visible damage to the outer ring. Through the one-minute, 30-second and ten-second increments there was no further visible damage. The endurance test produced additional delamination of the inner ring.

The ceramic composite rings without orifices underwent a total of two hours test of time and the rings with orifices underwent about four hours of testing. Early analysis had anticipated outer ring cracking and the test results matched well with anticipated results. Both inner and outer ring fracture modes were consistent through the testing. The tests are considered highly successful, especially since both sets of rings maintained their integrity throughout the testing and there was no cracking induced by the orifices. The interlaminar cracking that occurred appears to be due to the leading and trailing edge lip design. The thermal stresses in the lip appear to have produced a bending moment in the material.

#### CONCLUSIONS

The AMSC and SCCD programs have demonstrated the excellent temperature capability of ceramic materials and their potential for gas turbine applications. Obviously a great deal of work remains in this relatively infantile industry of structural high-temperature ceramics. Design integration of non-metallics with a highly flexible metal engine remains the challenge to overcome. Both design and materials improvements are required before these non-metallics can go into operational vehicles. Early applications will have to be limited life, non-man-rated vehicles. The newer ceramic composite materials will also greatly help extend applications as their strength and toughness improve. Overall the future of ceramics and ceramic composites in military and civilian gas turbines is very large and very bright.

**THE ATEGG/JTDE GOAL IS TO DOUBLE  
T/W BY YEAR 2000**

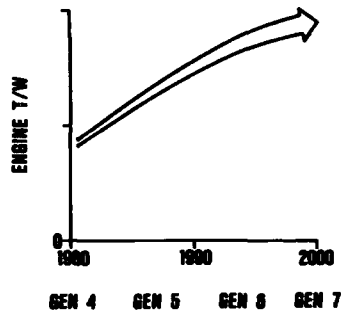


Figure 1. ATEGG/JTDE Goal

**TO MEET THE T/W GOAL REQUIRES  
HIGH CYCLE TEMPERATURES**

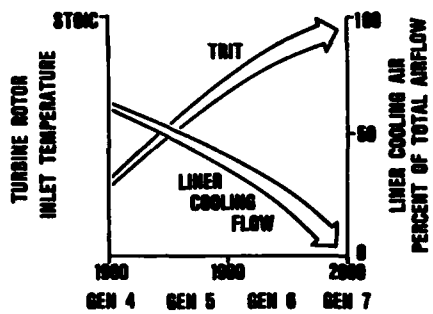


Figure 2. Liner Cooling Requirements

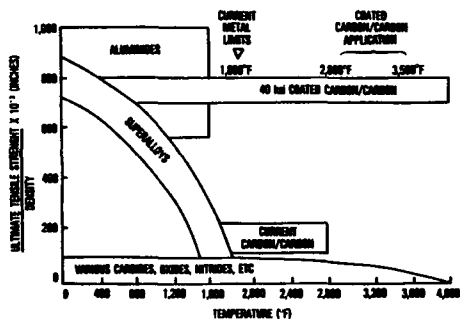


Figure 3. Material Strength Map

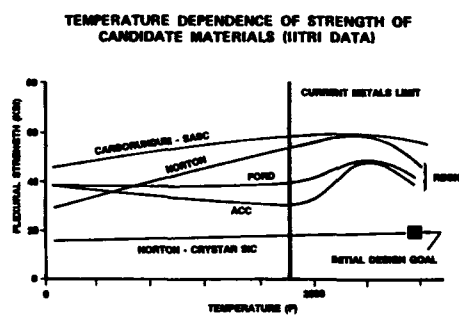


Figure 4. Strength for Candidate Material

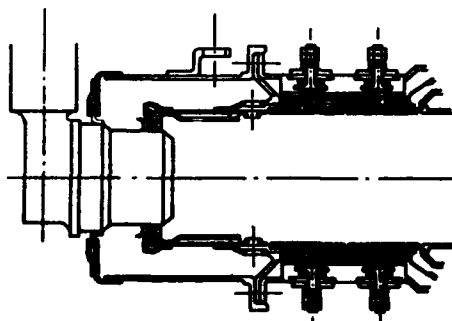


Figure 5. AMSC Ceramic Liner

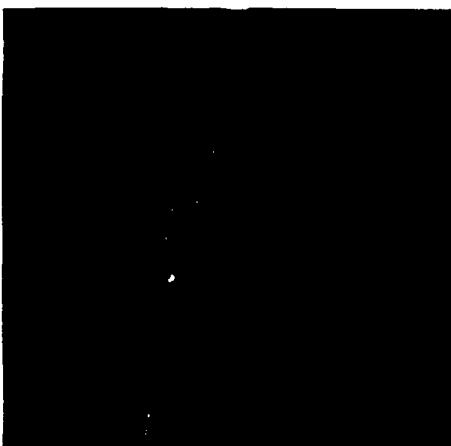


Figure 6. AMSC Silicon Carbide Segments

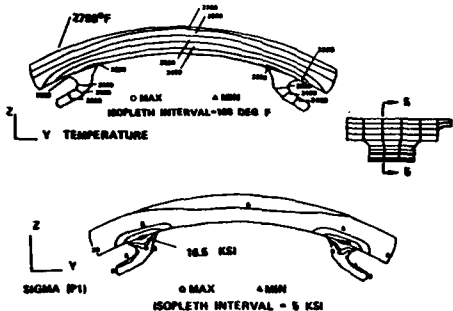


Figure 7. Ceramic Segment Stress Model



Figure 8. Cracked AMSC Segment

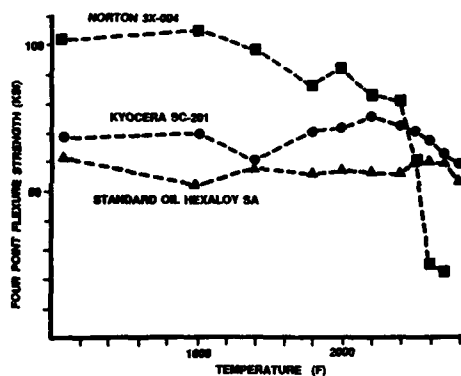


Figure 9. Flexure Strength vs Temperature

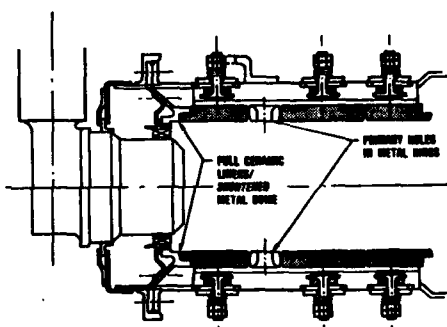


Figure 10. SCCD Combustor Concept



Figure 11. SCCD Orifice Rings

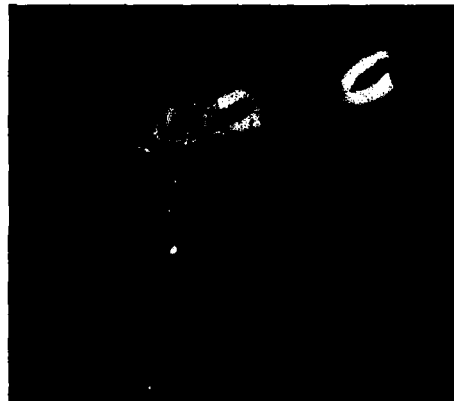


Figure 12. SCCD Silicon Carbide Segment

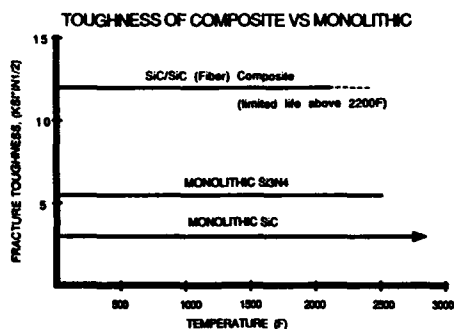


Figure 13. Fracture Toughness

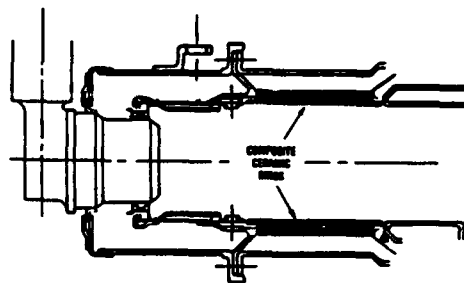


Figure 14. Ceramic Composite Concept

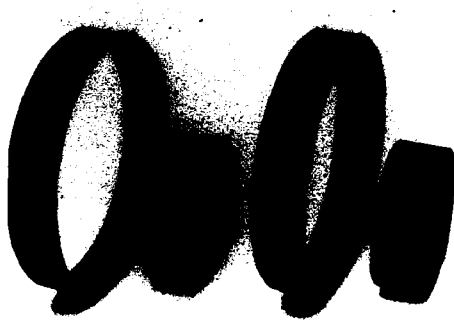


Figure 15. SiC Composite Rings



Figure 16. Composite Outer Ring



Figure 17. Composite Inner Ring

**DISCUSSION**

R. Kochendorfer, DFVLR, FRG. First, I would like to congratulate you that you modified your design when changing your material. Did you test your combustor at pressure?

D. Hudson, US Air Force, US. Yes, the testing was conducted at roughly ten atmospheres.

## COMPOSITE MATERIAL SYSTEMS FOR HIGH TEMPERATURE APPLICATIONS

Earl R. Thompson  
Assistant Director of Research for Materials Technology  
United Technologies Research Center  
East Hartford, Connecticut 06108 US

### SUMMARY

One approach to the demands of high temperature, structural applications, being actively pursued at our research center, is through the development of composite materials. For applications up to approximately 1200°C, the materials research is primarily centered upon the fiber reinforcement of glass and glass-ceramic matrices. For applications above 1200°C, the development of coating systems for the protection of high-strength carbon-carbon composites is the prime focus.

In terms of fabrication, the glass and glass-ceramic matrix composites reinforced by carbon and silicon carbide fiber yarns can be understood by considering the thermoplastic nature of the matrix constituent. Continuous, as well as chopped, fibers have been successfully used to reinforce these brittle matrices. When optimally fabricated, the resultant composites have displayed a combination of high apparent toughness and high strength at room and elevated temperature.

Carbon-carbon composites have extremely high temperature (> 2000°C) capability and excellent strength retention in inert environments. The major application limiting property of these composites is the lack of coatings which will provide the required long life, high-temperature oxidation resistance. Multilayer coating approaches which depend upon silicon nitride as the primary oxidation resistant barrier have been developed at our research center. The background leading to this choice and a consideration of our experience with this coating are considered.

### INTRODUCTION

The creation of many, advanced aerospace systems is functionally dependent upon structural materials with improved temperature capabilities. Furthermore, the very nature of air- and spacecraft places a premium on lightweight structures. One is therefore led to the belief that composites materials, which offer the promise of improved structural properties coupled with low density, i.e. materials with high specific strength and elasticity, will become the primary aerospace construction materials of the future. This belief should be tempered by the understanding of the difficulties associated with the development and applications of materials which must function under conditions of complex thermal and mechanical loadings. It is obvious that application engineers will always favor isotropic, monolithic materials which also possess a margin for error that is provided by ductility. Therefore, advanced composite materials will continue to face considerable resistance in finding

application despite their apparent advantages. Such materials should be introduced in components that may not provide the largest payoff but which allow confidence and experience to be built without jeopardizing an entire system.

In Figure 1 is shown a group of materials which are being developed to address structural demands over a wide temperature range. Represented in this figure are currently demonstrated temperature capabilities of metal alloys and composite materials and goals for metal alloys, intermetallics, and composite materials that might be achieved by the end of the next decade. Absent from this figure are the monolithic structural ceramics. Such materials will undoubtedly find certain applications, but it is the author's opinion that ceramic composites offer the greater promise for wider structural applications.

This paper will focus on the development of two composite systems which have been the subjects of concerted research programs at our research center. The first system is prepared from fiber, usually carbon or silicon carbide yarn, and glass or glass-ceramic constituents; such systems have been trademarked COMPGLAS® by United Technologies. The second composite system is coated carbon-carbon. As may be noted by reference to Figure 1, these materials are representative of systems with an extraordinarily high temperature potential. Furthermore, the densities of these materials, which are approximately equal or less than that of aluminum alloys, are especially attractive.

#### DISCUSSION OF COMPOSITE SYSTEMS

##### COMPGLAS®

Research on the family of fiber-reinforced ceramics which has become known as COMPGLAS® was initiated almost 15 years ago at our center. This investigation was prompted by the growing activity in the development of structurally performant ceramic materials, our experience in the creation of fiber reinforced polymer and metal matrix composites, observations we had made on the fracture behavior of fine tungsten wire reinforced silica composites, and the initial reports of strengthening that had been obtained in boron monofilament reinforced<sup>1</sup> and carbon yarn reinforced glass<sup>2</sup>. One key to the successful developments that have occurred with this class of composites is that they have been a direct extension of our experience with resin and metal matrix composites. In each of these cases, a higher elastic modulus fiber has been utilized to reinforce a lower elastic modulus matrix. One could therefore anticipate a modulus enhancement of the matrix phase and fiber strengthening. It has also been observed that systems can be created with a measure of reliability (toughness); this is a result of the nature of the interfacial bond between fiber and matrix.

Although our initial experiments in fiber reinforced glass and glass-ceramics utilized monofilament reinforcements, this emphasis was abandoned early and attention was shifted to fibrous yarn reinforcements, especially carbon. With the advent of the silicon carbide type yarn, Nicalon, produced by Nippon Carbon, research was principally directed toward a system containing this fiber in a glass-ceramic matrix which could be produced in a glassy form and later transformed to a crystalline matrix with a small fraction of residual glass. The focus on a silicon carbide yarn-type reinforcement was prompted by the desire to produce a composite system that would be oxidatively stable at elevated temperature.

### Fabrication

Preparation of a glass-powder infiltrated yarn prepreg and the fabrication of a composite has been accomplished as depicted in Figure 2. This process and the subsequent hot consolidation have been previously described<sup>3</sup> and only the essential elements are repeated here. The fibrous yarn devoid of any organic finish is passed through an agitated aqueous solution containing a powdered glass and an organic binder. The infiltrated yarn is filament wound, cut, stacked in the requisite array, and fired to remove the organic binder. Consolidation of the composite material is carried out in a vacuum hot press at a sufficiently high temperature to make the glass behave as a viscous liquid. Full infiltration of the fibrous yarn is usually accomplished with a small amount of residual porosity, ~1 percent. Microstructure typical of a cross-plied composite is shown in Figure 3. Although the displayed microstructure is for a system of approximately 50 volume percent silicon carbide fibers in a lithium aluminosilicate (LAS) glass ceramic, the structure of a carbon fiber reinforced system would appear identical except for the size and shape of the fibers in cross-section.

### Physical and Mechanical Properties

Thermal expansion properties. The glass and glass-ceramic matrices for these composites can be chosen such that their thermal expansion characteristics are similar to the fibers used for their reinforcement. These properties are, of course, anisotropic as are the composite mechanical properties. Because of the extremely low coefficient of expansion of carbon fibers along their length and the low expansion of the silicon carbide yarn, resulting composites have demonstrated low thermal expansion and have also shown excellent resistance to thermal shock. In certain systems, quenching into water from 1100 to 1200°C has caused no strength reduction.<sup>4,5</sup> Because of the opportunity to tailor these expansion properties, one area of potential composites application is for structures which require low thermal expansion coupled with high specific modulus and strength. An example of the thermal expansion response of a unidirectionally carbon reinforced borosilicate glass is shown in Figure 4.

Carbon fiber reinforced composites. There are a wide variety of available carbon fibers with elastic moduli ranging from 28 to 690 GPa. Those of interest for reinforcing glass and glass-ceramic matrices would possess an elastic modulus in excess of that of the matrix phase, i.e.  $E > 70$  GPa. Through the use of the very high stiffness pitch (P-100) fibers (modulus, 654 GPa), a unidirectionally reinforced composite with an elastic modulus in excess of 330 GPa has been produced. The tensile stress-strain curve for such a composite is displayed in Figure 5. These data are from a study performed for NASA.<sup>6</sup>

In Table I are listed tensile properties of continuous and discontinuous carbon fiber reinforced borosilicate glass matrix composites.

The tensile stress-strain curves for the unidirectional and cross-plied carbon reinforced composites reported in Table I are shown in Figure 6. The response of the unidirectional material is approximately linear to the point of fracture. A small decrease in the stiffness of the composite is observed beyond a strain of 0.1%; this is attributed to matrix microcracking. The fracture surface of this material reveals extensive fiber pullout. This suggests the composite lacks a high degree of notch sensitivity. This may be the most important difference between fiber reinforced glass or glass-ceramics and unreinforced ceramics. Measurements of the toughness of carbon reinforced glass, silicon carbide yarn reinforced glass-ceramic and carbon reinforced

TABLE I

Room Temperature Properties of Continuous and Discontinuous  
Carbon Fiber Reinforced Borosilicate Glass<sup>7</sup>

<u>Unidirectional</u>	<u>0/90 Cross Ply*</u>	<u>Discontinuous**</u>	
$E_0 = 168 \text{ GPa}$	$E_t = 16.8 \text{ GPa}$	$E_0 = 72 \text{ GPa}$	$E = 48 \text{ GPa}$
$\text{UTS}_0 = 580 \text{ MPa}$	$\text{UTS}_t = 29 \text{ MPa}$	$\text{UTS}_0 = 246 \text{ MPa}$	$\text{UTS} = 150 \text{ MPa}$
$\epsilon_{lf_0} = 0.36\%$	$\epsilon_{lf_t} = 0.45\%$	$\epsilon_{lf_0} = 0.32\%$	$\epsilon_{lf} = 0.6\%$
$\text{CTE}_0 = -0.1 \text{ ppm}/^\circ\text{C}$	$\text{CTE}_t = 4.6 \text{ ppm}/^\circ\text{C}$		

\*Thornel 300 carbon fiber with scrim    \*\*HM carbon fiber  
Vol percent fiber = 54%; 30%    Density = 2.0 gm/cm<sup>3</sup>; 2.1 gm/cc\*\*

epoxy have shown that they display comparable resistance to crack growth from a prenotch in three-point bend specimens.

Flexural testing of Th-300 carbon fiber reinforced borosilicate glass composites has also been accomplished as a function of temperature. The results of this testing are shown in Figure 7. The specimens were held at temperature in air for a period of 30 minutes prior to the test. The carbon fibers in the specimen surface are degraded by oxidation at temperatures above 500°C. Above 600°C strength loss is associated with matrix softening as well as fiber oxidation.

An analogy has been made between thermoplastic resin and glass reinforced by carbon fibers because of the similarity of their fabrication and mechanical performance.<sup>7</sup> The glass matrix composites are useful to higher temperatures and are less susceptible to environmental degradation.

Silicon carbide yarn reinforced composites. The interest in identifying systems, which were less sensitive to the problems of oxidation at temperatures above 500°C as experienced by the carbon fiber reinforced glass composites and which possessed a more refractory matrix, inspired research that has been directed toward silicon carbide (Nicalon) yarn reinforced glass-ceramic matrix composites. Basic research on these systems has been funded at our research center by the Office of Naval Research and applications research by the Naval Air Development Center.

Initial experiments with silicon carbide yarn reinforced borosilicate and high silica glasses demonstrated that high strength composites with useful toughness could be produced.<sup>8</sup> Although the high silica glasses are substantially more refractory than a borosilicate glass, their highly viscous character at high temperature causes them to be difficult to fabricate. Certain glasses possess relatively lower viscosities and also possess a glass-ceramic character which allows them to be devitrified to achieve high temperature strength. Our work has centered primarily on a series of lithium aluminosilicate (LAS) glass ceramics as matrices.<sup>5</sup> Other, more refractory, glass-ceramics including those based on magnesium aluminosilicate, barium magnesium aluminosilicate and calcium aluminosilicate are also under study here as well as other research laboratories. These offer the potential of increasing the matrix use temperature by approximately 200°C.

After hot pressing of the SIC/LAS composites, the matrix is primarily in a glassy form which crystallizes upon heat treatment leaving a small amount of glass phase at grain boundaries. Because of the nature of the silicon carbide yarn, the reaction between the matrix and fiber creates an interface which is thin and rich in

carbon.<sup>9</sup> The formation of this interfacial layer is responsible for the excellent crack growth resistance of this brittle matrix composite. Compositions have also been investigated which prevent this reaction, cause strong bonding of the matrix and fiber, and which result in composites that behave in a completely brittle fashion.

The flexural strengths of three SiC/LAS composite systems are shown as a function of temperature in Figure 8.<sup>5</sup> These measurements were made upon unidirectionally reinforced composites by three-point flexural tests in an inert environment. The systems are shown to be very strong and, in the case of the LAS-III matrix material, to maintain its flexural strength to a temperature approaching 1200°C. Changing of the testing atmosphere to air has a detrimental effect on the LAS-III system in the intermediate temperature range as shown in Figure 9. This effect is due, at least in part, to oxidation of the interfacial zone permitted as the matrix begins to microcrack. This environmental interaction and its consequences are areas of continued research.

Despite the environmental sensitivity noted above, the SiC yarn reinforced glass-ceramic composites have demonstrated sufficiently attractive properties to be considered as viable candidates for certain high temperature structural applications. For example, tensile testing of SiC/LAS-III composites in argon at temperatures to 1300°C has demonstrated that Nicalon remains an effective reinforcement. A unidirectional strength on the order of 860 MPa at 1300°C has been observed. Nonetheless, research directed toward creating an improved fiber - one that has higher strength and stiffness and a greater tolerance to high temperature exposure - should be encouraged.

#### COATED CARBON-CARBON COMPOSITES

Carbon-carbon materials are a class of composites consisting of a fibrous carbon reinforcing material within a carbon matrix. By choosing a high strength and high modulus fiber, a material constructed with various fibrous orientations can be created and exhibit high strength and stiffness at temperatures in excess of 1900°C. The matrix phase is produced by two basic methods. The first technique is a pressure infiltration of the preformed carbon fiber array by an organic which is pyrolyzed to yield a carbonaceous char. The second approach is by the chemical vapor infiltration of the array by the deposition of carbon from a hydrocarbon such as methane. In addition to the attractive structural properties offered by these materials, they exhibit low coefficients of expansion (in the range of 1 to 2 ppm/°C), which minimize thermally induced stresses, and high thermal and chemical stability in inert atmospheres. Carbon-carbon composites require surface protection when used in oxidizing environments at temperatures above about 400°C.<sup>10</sup> Recent developments in the field of ceramic, oxidation-protection coatings for carbon-carbon composites is considered in this section.<sup>11</sup> Funding of research for the development of high temperature coatings for carbon-carbon has been provided to our research center by DARPA through the Naval Air Development Center.

The many issues which need to be addressed in order to develop a successful oxidation protection system for carbon-carbon materials at high temperatures are indicated in Figure 10. Although all issues prove difficult, the aspect of thermo-mechanical compatibility is especially troublesome. This results from the fact that the extremely low thermal expansion coefficient of the substrate causes candidate ceramic coatings which are deposited at elevated temperature to be in residual tension. In most instances, the ceramic coatings are, in fact, microcracked. Since the oxidation threshold for carbon-carbon oxidation is on the order of 370°C (see

Figure 11) which can be improved to approximately 600°C by the addition of certain oxidation inhibitors, a sealant technology is required to address the oxidation occurring as a consequence of the coating cracks. Glasses based on boron oxide have proven most useful for sealing these cracks. As the oxidation exposure temperature approaches the coating deposition temperature, these microcracks are mechanically closed and are filled by products of oxidation of the protective coating system. Exposures above the deposition temperature place the coating under residual compression - a stress state tolerated more easily by a brittle coating.

At very high temperatures, the issues of thermochemical compatibility of coating and substrate, the diffusion rates of oxygen and carbon through the coating, and the volatility of the coating assume greater importance. Our experience, and those of others who have worked with us in addressing the problem of creating a coating system for carbon-carbon which is protective over a wide range of temperature, has indicated that the solution is best provided by a multilayer coating.

Because the silicon-based ceramics, silicon carbide and silicon nitride, possess low coefficients of thermal expansion, 5.5 and 4.0 ppm/°C, respectively, and exhibit low rates of oxidation up to 1760°C, they have been prime candidates for ceramic protective coatings of carbon-carbon composites. Although both types of coatings are microcracked on high strength carbon-carbon substrates, microcracking is reduced by the closer match in expansion of the silicon nitride coating. Our experience also suggests that the oxidation performance of chemically vapor deposited silicon nitride is at least as good as that of chemically vapor deposited silicon carbide. The gas pressures that are created within the Si-SiC-SiO<sub>2</sub> and the Si-Si<sub>3</sub>N<sub>4</sub>-SiO<sub>2</sub> systems as a function of temperature are shown in Figure 12.<sup>11</sup> These thermodynamic analyses indicate that in both systems silica films may be stable until approximately 1800°C after which the gas pressure exceeds one atmosphere.

The appearance of a silicon nitride coating on a carbon-carbon composite after a two hour exposure in flowing air at 1760°C may be seen in Figure 13. Stable growth of a silica protective film has occurred. Microcracks which were apparently sealed at the high temperature may also be clearly seen in this figure.

The specific weight change experienced by 2-D carbon-carbon, coated by chemically vapor deposited silicon nitride, is shown as a function of temperature of the isothermal exposure in Figure 14. These data show that the silicon nitride is intrinsically protective above 1250°C. As discussed earlier, below this temperature the system may experience large losses in weight due to oxidation of the substrate through the paths provided by the microcracks. In this intermediate range of temperature, a boria-based glass sealant developed by GA Technologies has been used successfully to stem the substrate oxidation at the microcrack sites. Further work is required to optimize such a sealed system for application over a wide range of temperature to >1550°C.

#### CONCLUDING REMARKS

Fiber reinforced glass and glass-ceramics are representative of a class of high temperature, low density composites which have exhibited structurally useful properties to temperatures above 1100°C. It may be realistically expected that these systems will be developed to achieve use temperatures of 1300°C. Ceramic matrices which are devoid of glassy phase and improved reinforcing fibers may be necessary to achieve still higher temperatures of application.

Substantial progress has been made toward creating carbon-carbon composites which can be reliably applied in air in load bearing structures at very high temperatures (up to 1760°C). A central problem to the application of carbon-carbon composites remains oxidation protection at intermediate temperatures. Substrate inhibition, glass-sealant technology and multilayer coatings will most likely be required to create complete protection of carbon-carbon composites over a wide range of temperature.

#### REFERENCES

1. A. C. Seifert, Fiber Reinforced Ceramic Composites and Method of Producing Same, U.S. Patent 3,575,789, April 20, 1971; and Fiber Reinforced Ceramics, U.S. Patent 3,607,608, Sept. 21, 1971.
2. R. A. Sambell, A. Briggs, D. C. Phillips, and D. H. Bowen, "Carbon-Fiber Composites With Ceramic and Glass Matrices Fibers," *J. of Mater Sci.*, 7 676-681 (1972); D. C. Phillips, "The Fracture Energy of Carbon Fiber Reinforced Glass," *ibid*, 7 1175-1191 (1972); D. C. Phillips, R. A. Sambell, and D. H. Bowen, "The Mechanical Properties of Carbon Fiber Reinforced Pyrex," *ibid*, 7 1454-1464 (1972); S. R. Levitt, "High Strength Graphite Fibre-Lithium Aluminosilicate Composites," *ibid*, 8 793-806 (1973).
3. J. F. Bacon, K. M. Prewo and R. D. Veltri, "Glass Matrix Composites - II. Alumina Reinforced Glass," Proc. Second Int'l Conf. on Composite Materials, Toronto, Canada, edited by B. Noton, AIIME, New York, NY, 753-769 (1978).
4. J. Crivelli-Visconti and G. A. Cooper, "Mechanical Properties of a New Carbon Fiber Material," *Nature*, 221 754-755 (1969).
5. K. M. Prewo, J. J. Brennan and G. K. Layden, "Fiber Reinforced Glasses and Glass-Ceramics for High Performance Applications," *Ceramic Bulletin*, 65 305-313 and 322 (1986).
6. K. M. Prewo and E. R. Thompson, "Research on Graphite Reinforced Glass Matrix Composites," NASA Contract Report 165711 (May 1981).
7. K. M. Prewo and E. J. Minford, "Graphite Fiber Reinforced Thermoplastic Matrix Composites for Use at 1000°F," *SAMPE Jl.* 21-2 26-33 (1985).
8. K. M. Prewo and J. J. Brennan, "High Strength Silicon Carbide Yarn Reinforced Glass Matrix Composites," *J. Mat. Sci.*, 17 1201-1206 (1982).
9. J. J. Brennan, "Interfacial Characterization of Glass and Glass-Ceramic Matrix/Nicalon SiC Fiber Composites," Tailoring Multiphase and Composite Ceramics, edited by R. E. Tressler, G. L. Messing, C. G. Pantano and R. E. Newnham, Materials Science Research 20, Plenum Press, New York, 549-560 (1986).
10. John D. Buckley, "Carbon-Carbon, An Overview," *Ceramic Bulletin*, 67 364-368 (1988).
11. James R. Strife and James E. Sheehan, "Ceramic Coatings for Carbon-Carbon Composites," *Ceramic Bulletin*, 67 369-374 (1988).

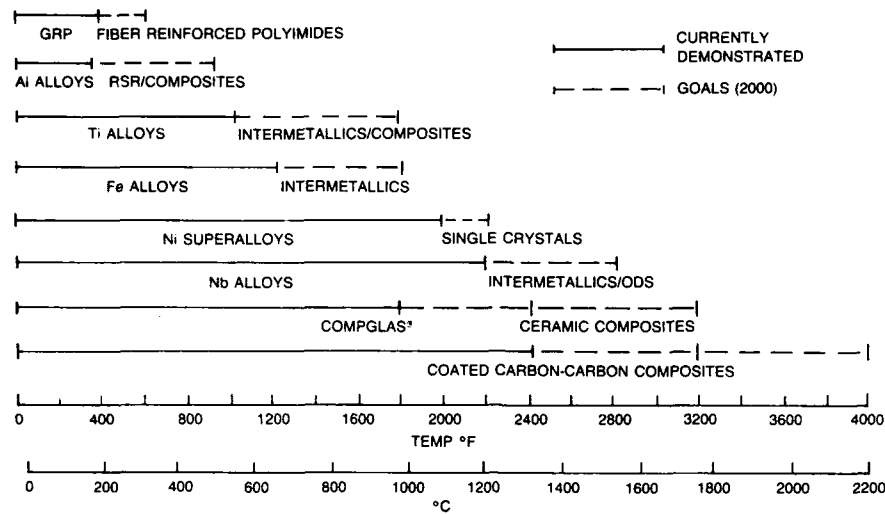


Figure 1. Temperature limits of structural materials

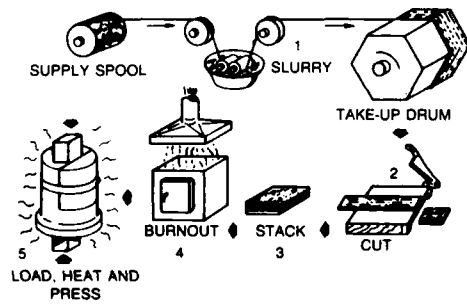


Figure 2. Steps in tape lay-up processing of glass matrix composites.



Figure 3. Microstructure of 0/90 SIC/LAS-1

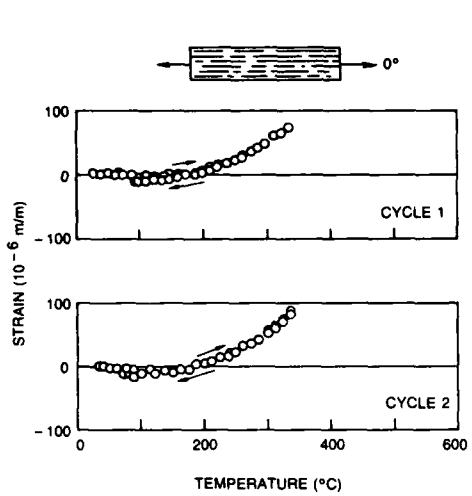


Figure 4. The axial ( $0^\circ$ ) thermal strain vs temperature for a unidirectional 54 v/o Th-300 fiber reinforced borosilicate glass matrix composite

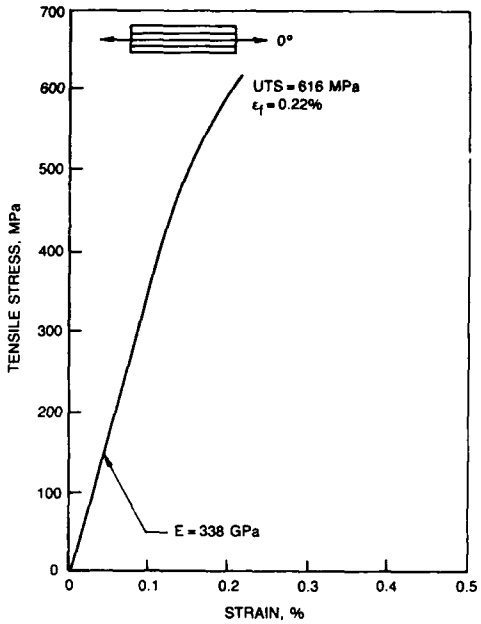


Figure 5. Tensile stress-strain curve for unidirectional 54 v/o P-100 reinforced borosilicate glass matrix composite

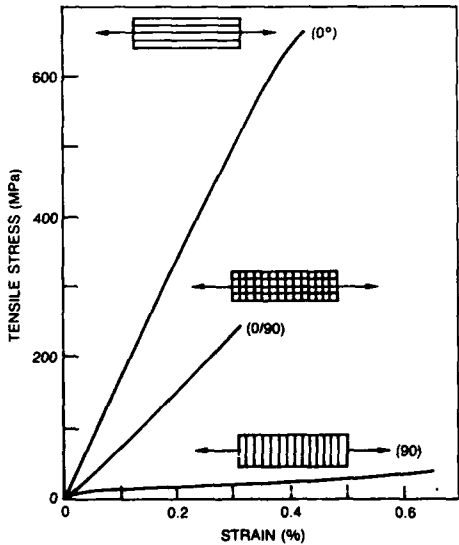


Figure 6. Tensile stress-strain curves for unidirectional and cross-ply 54 v/o Th-300 reinforced borosilicate glass matrix composites.

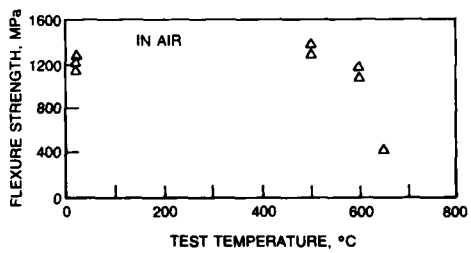


Figure 7. Th-300 unidirectional fiber reinforced composite flexural strength for tests performed at temperature in air with a 30 minute hold at temperature prior to test

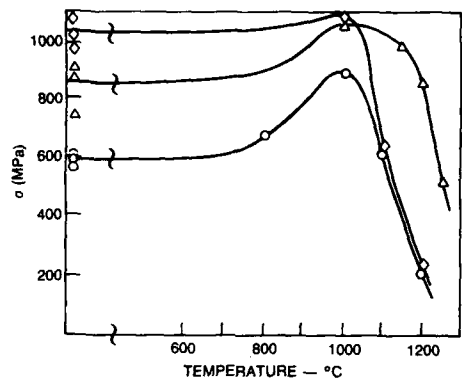


Figure 8. Three-point flexural strength in argon vs temperature for unidirectional LAS matrix/SiC yarn composites; (○) LAS-I matrix, (◊) LAS-II matrix, and (△) LAS-III matrix

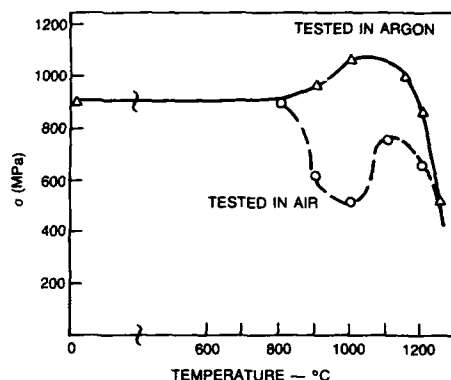


Figure 9. Three-point flexural strength in argon and air vs temperature unidirectional LAS-III matrix/SiC yarn composites

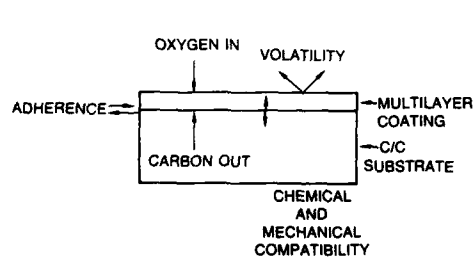


Figure 10. Critical factors for oxidation-protection system of carbon/carbon composites

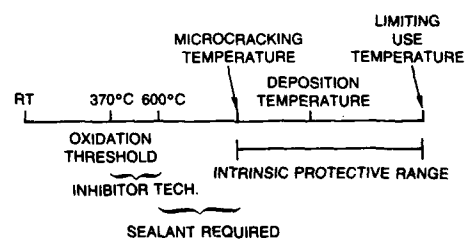


Figure 11. General oxidation behavior of coated high performance carbon/carbon composites

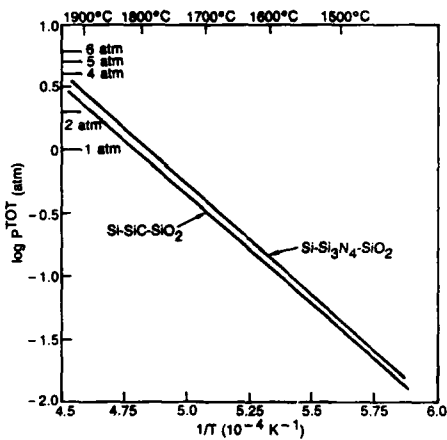


Figure 12. Total gas pressures in Si-SiC-SiO<sub>2</sub> and Si-Si<sub>3</sub>N<sub>4</sub>-SiO<sub>2</sub> systems.

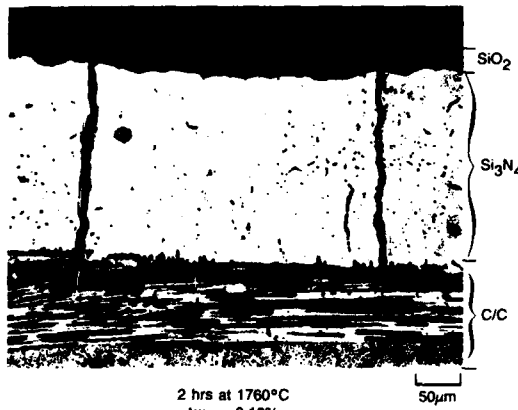


Figure 13. SiO<sub>2</sub> scale stability on CVD Si<sub>3</sub>N<sub>4</sub> flowing air environment

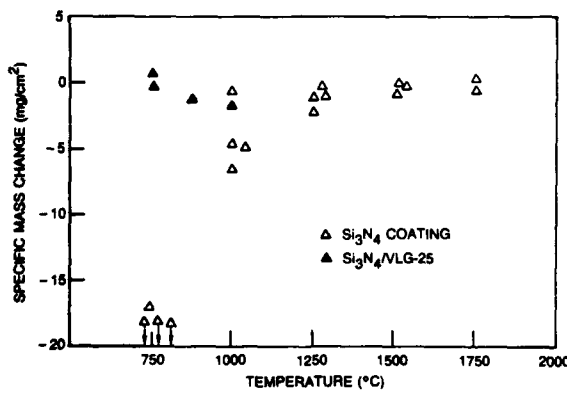


Figure 14. Isothermal oxidation behavior of Si<sub>3</sub>N<sub>4</sub>-coated 2-D carbon/carbon composite — 5 h in flowing air

## DISCUSSION

U. Neumann, Sigri, FRG. Did your company develop a nondestructive testing technique for the measurement of the thickness of coatings on carbon-carbon composites?

E. Thompson, United Technologies Research Center, US. No, we have not. We have, however, used nondestructive tests to look for flaws in the coatings. So far we've approximated the thickness of the coatings based on our experience and knowledge of the CVD process. The CVD coating process is relatively slow, on the order of 25 micrometers/hr, so it takes a number of hours to form a coating of the desired thickness.

R. Kochendorfer, DFVLR, FRG. I have two questions regarding the first part of your presentation. The first is, what is the failure mechanism responsible for the knee in the stress-strain curve for your unidirectionally reinforced silicon carbide fiber-glass composites under tensile loading? Is it related to the fiber-matrix bonding condition? Is there a relation between the strength level at which the knee occurs and the fracture toughness of the composite?

E. Thompson, United Technologies Research Center, US. The knee in the stress-strain curve for unidirectionally reinforced silicon carbide-lithium aluminosilicate composites occurs as a result of the onset of matrix microcracking. The composite strain at which it occurs should be a function of specimen fabrication history and the difference between the thermal expansion of the fibrous reinforcement and the matrix material. If fabricated improperly, a strong chemical bond can be established between the matrix and fiber and then failure occurs catastrophically -- ie. cracks initiated in the matrix propagate through the fibrous reinforcement without diversion. There is, therefore, a relation between the ultimate tensile strength, the value at the knee in the curve, and the toughness of the composite.

R. Kochendorfer, DFVLR, FRG. That is basically my point. I am concerned about the possibility of having high strength and high fracture toughness simultaneously. I think that if we want to have high fracture toughness then we have to have weak bonding, and then if we take the strength level at the knee in the curve as the design limit load we cannot have the highest strengths possible in these composites.

E. Thompson, United Technologies Research Laboratories, US. That's right, but polymer matrices in polymer composites also microcrack, and we use them above the point of first microcracking. If we have an interface that can withstand the environment, then we can use the composite above the point of first matrix microcracking. The most important question, therefore, is what is the stability of the interface. I would expect that these systems will in fact be usable in service with some matrix microcracking in areas of localized stress concentration.

R. Kochendorfer, DFVLR, FRG. My second question is, what have you found with regard to fiber degradation in the long-term exposure of silicon carbide fiber reinforced glass composites and what are the influences of temperature and oxidation?

E. Thompson, United Technologies Research Center, US. We've carried out creep experiments on Nicalon fiber reinforced glass-ceramic composite systems. As I recall, at temperatures on the order of 1100°C for times of several hundreds of hours, we have not experienced notable strength reductions in the fibrous reinforcement as a result of the exposure. Even at 1300°C for short time exposures, the fibers, when encased by the matrix, retain a high strength level. I would not expect that to be the case for long time exposures at that temperature, however. As I mentioned in my presentation, the oxidation problem is primarily associated with the interfacial reactions occurring when the interface is exposed as a result of matrix microcracking during loading. At loads less than that which causes microcracking, the system is generally resistant to oxidation.

P. Hancock, Cranfield Institute of Technology, UK. I have two questions concerning the second part of your presentation, related to the protection of carbon-carbon composites. First, in view of the low fracture toughness values of the coated materials, do you find that, after initial microcracking, a few of the cracks continue to propagate through to the underlying material or do other secondary cracks develop on further thermal cycling? Second, have you done any creep testing on these protected carbon-carbon composites yet?

E. Thompson, United Technologies Research Center, US. The microcracks which are formed within the coating as a result of the differential thermal expansion between coating and substrate extend through the silicon nitride to

essentially the carbon-carbon substrate. I expect some secondary microcracking does occur as a result of thermal cycling. This secondary microcracking should saturate after some equilibrium coating segment size is achieved. With regard to your second question, I am not aware of creep data on systems of this type. This is due, at least in part, to the lack of the testing equipment required to carry out such measurements at temperatures above 1600°C.

**UTILISATION DES COMPOSITES HAUTES TEMPERATURES  
DANS LES TURBOREACTEURS**

par  
R.MESTRE  
S.N.E.C.M.A.  
Centre de Villaroche  
MOISSY-CRAMAYEL  
77550  
France

**Résumé :**

Le développement de turboréacteurs militaires modernes présentant des rapports Poussée/Masse élevés conduit à l'emploi de matériaux composites dans les parties chaudes de ces machines.

Dans ce contexte, la SNECMA développe des applications de matériaux céramiques composites au niveau des turbines, du système de Post-Combustion et des tuyères, zones du moteur où les températures de gaz dépassent 2000 K en longue durée.

Les matériaux CERASEP (SiC-SiC) et SEPCARB (C-SiC) produits par la SEP ont été retenus pour la réalisation de volets de tuyère et d'éléments de structure. Des essais partiels ont été réalisés sur des pièces prototypes afin de valider les procédés de fabrication et les critères de conception. Des pièces de technologie moteur ont été réalisées et ont subi des essais d'endurance sur moteur dans des conditions représentatives d'une utilisation opérationnelle.

Le développement de fibres SiC résistant à plus haute température permettra d'étendre le champ d'application de ces matériaux.

**Introduction**

Les principales exigences concernant le développement d'avions multirôles portent sur :

- les exigences opérationnelles (missions)
- la discréption (Radar, Infra-rouge)
- le taux de disponibilité,
- le coût global de possession.

En conséquence, les turboréacteurs de la prochaine génération devront présenter :

- un rapport poussée sur masse élevé,
- des performances améliorées,
- une fiabilité accrue,
- un coût de possession réduit.

L'évolution du rapport poussée sur masse et celle de la température d'entrée turbine des turboréacteurs militaires traduisent l'impact de ces deux premières exigences (planche 1). Le développement d'un moteur de masse minimale nécessite une action conjuguée dans les domaines suivants :

- Aérodynamique et cycle Thermodynamique.
- Rendement des composants.
- Technologie et optimisation mécanique.
- Matériaux basse densité (métalliques-composites).

La résistance spécifique élevée de certains matériaux composites (Résistance/Densité) leur permet de concurrencer sur le plan de la masse les alliages traditionnels. On constate ainsi une généralisation de l'emploi de matériaux composites à matrice organique renforcés par fibres de Verre, Carbone ou Kevlar dans les parties froides des Turbo-soufflantes civiles (Nacelle-capots - Redresseurs secondaires...).

La température a longtemps constitué un frein majeur à l'utilisation de matériaux composites sur turboréacteur militaire. Le développement de nouvelles résines organiques (Type PMR15) a permis d'étendre leur domaine d'application dans les parties "froides" des moteurs militaires. Par ailleurs, l'émergence de composites thermo-structuraux ouvre l'accès aux parties les plus chaudes des turboréacteurs.

Ce document présente le programme d'application des composites Hautes Températures engagé par la SNECMA en coopération avec la Société Européenne de Propulsion (S.E.P) en 1982 avec le soutien des Services Officiels Français.

#### Matériaux composites pour Turboréacteurs militaires

Un simple regard sur la coupe moteur présentée planche 2 permet de constater que la température des gaz atteint très rapidement 300°C qui constitue la température limite d'utilisation des matériaux composites organiques. La température des gaz continue de s'accroître pour atteindre 1800 - 2000°C au niveau de la chambre de combustion et du système de Post combustion.

Parmi les fibres aujourd'hui disponibles sur le marché, les fibres de Carbone, de Carbure de Silicium (SiC) et d'alumine conservent des propriétés mécaniques intéressantes à haute température :

- La fibre de Carbone conserve des propriétés mécaniques intactes au delà de 2000°C en atmosphère neutre. Malheureusement, cette remarquable stabilité ne peut être exploitée pleinement du fait de l'extrême sensibilité de cette fibre à l'oxydation dès que l'on dépasse une température de 350°C sous air.
- Les fibres de SiC actuelles peuvent être employées en longue durée jusqu'à 1200°C (limitation due à la présence de Silice ou d'oxygène dans leur composition). A terme, la prochaine génération de fibres de SiC devrait porter cette limite vers 1600°C.
- Les fibres d'alumine (fibres longues) peuvent être employées jusqu'à 1200°C. Leur plus grande fragilité rend leur mise en oeuvre plus délicate.

Il résulte de cette brève analyse que la fibre SiC apparaît, aujourd'hui, comme le meilleur candidat pour les applications à haute température.

De nombreux matériaux peuvent être envisagés pour constituer la matrice de matériaux composites pour haute température (Carbone-Métal-Verre-Céramique). Chaque classe de matériaux possède des atouts ou des handicaps spécifiques; sans prétendre être exhaustif, on peut dresser un panorama des voies envisageables et des perspectives d'emploi :

- Matrice Carbone : le Carbone-Carbone grâce à la stabilité de la fibre à très haute température dispose de perspectives d'utilisation prometteuses. La mise au point de traitements anti-oxydation compatibles avec la durée de vie requise pour un turboréacteur pourrait permettre, à terme, d'envisager son emploi aux très hautes températures.
- Matrice Métallique : de nombreux travaux sont actuellement en cours pour améliorer les caractéristiques mécaniques et la tenue en température de divers alliages (Aluminium-Titane-Nickel) en les renforçant par des particules, Wisker ou fibres en céramique.
- Matrice Verre : Des matériaux du type SiC/Verre ont démontré une bonne tenue mécanique jusqu'à 700°C. Des perspectives d'emploi jusqu'à 1000°C existent, mais de tels matériaux ne sont encore qu'au stade du laboratoire. La composition du verre et la nature des interfaces devront être optimisées afin d'obtenir un bon compromis caractéristiques mécaniques/comportement en environnement moteur.
- Matrice Céramique : le choix des matériaux céramiques (SiC-Alumine-Silice-Zircone...) et des procédés (Voie liquide-Sol gel-Infiltration phase vapeur...) est très vaste. De nombreuses combinaisons de matériaux peuvent être réalisées (C-SiC, SiC-Silice, Alumine-Alumine, SiC-SiC,...).

Les céramiques renforcées sont beaucoup moins fragiles que les céramiques massives, ce qui atténue les problèmes d'intégration (formes-liens) et permet la réalisation de pièces structurales de haute fiabilité. On peut espérer atteindre des températures de 1600°C avec du SiC-SiC (planche 3).

De cet examen (non exhaustif) on retiendra la diversité des matériaux composites candidats à l'application aux parties chaudes des turboréacteurs. Les choix de matériaux opérés lors de l'engagement du programme d'application n'ont pas seulement pris en compte les caractéristiques thermo-mécaniques, mais aussi le niveau de connaissance du matériau et le degré de maturité des procédés.

La SEP, grâce à son savoir faire industriel acquis pour des applications spatiales, a proposé des matériaux composites thermo-structuraux répondant à ces deux derniers critères. En effet, la SEP a développé et mis au point des matériaux Carbone-Carbone pour application sur moteur fusée dans le courant des années 70. Cette expérience a ensuite été transposée pour l'élaboration de céramiques renforcées à matrice SiC.

#### Programme de Démonstration

Les objectifs principaux de ce programme sont les suivants :

- Sélection et évaluation des matériaux.
- Validation des critères de conception.
- Optimisation des procédés (qualité-coûts).
- Vérification des gains de masse objectifs.

L'organigramme général de ce programme figure planche 4. Les étapes clés de ce programme ont été les suivantes :

- |                                      |       |
|--------------------------------------|-------|
| - Evaluation matériel                | 83-87 |
| - Essais de pièces prototypes        | 84    |
| - Essais partiels de qualification   | 86-87 |
| - Essais sur moteur de démonstration | 87-88 |

Des programmes portant sur la caractérisation approfondie des matériaux et le Contrôle Non Destructif des pièces sont menés en parallèle. L'expérimentation de ces pièces sur moteur en conditions d'altitude simulée, puis sur avion, constituera l'aboutissement de ce programme de démonstration.

Des composants de tuyère et du système de réchauffe ont été retenus (planche 5) pour diverses raisons :

- sévérité de l'environnement thermique,
- gains de masse substantiels,
- impact sur le centrage des masses de l'avion,
- ventilation réduite ou durée de vie accrue,
- risques raisonnables compte tenu de la connaissance initiale des matériaux.

Le moteur SNECMA M53-P2 qui équipe le MIRAGE 2000 (AMD) a été choisi comme véhicule de démonstration (planche 6). La température des gaz dépasse 2000°K (1727°C) au Plein gaz avec Post-Combustion (PGPC).

Quatre types de composants ont été sélectionnés :

- Cône d'échappement.
- Anneau de réchauffe.
- Volet chaud de tuyère.
- Volet froid de tuyère.

#### Sélection/Evaluation des matériaux

Sans revenir en détail sur les raisons techniques du choix, les matériaux composites à Matrice Céramique ont été retenus pour ce programme pour les raisons suivantes :

- faible densité,
- résistance mécanique élevée,
- bonne ténacité,
- tenue à haute température,
- résistance aux chocs thermiques,
- savoir-faire industriel SEP.

Deux matériaux composites à Matrice Céramique produits par la SEP ont été sélectionnés :

- SiC-SiC (CERASEP TM)
- C - SiC (SEPCARB-INOX TM)

Ces matériaux sont élaborés à partir de préformes en tissus de Carbone ou de SiC; la matrice est obtenue par Infiltration par voie gazeuse de SiC (Chemical Vapor Infiltration). Ce procédé permet d'obtenir un matériau d'une grande pureté et assure une excellente reproductibilité.

L'emploi du C-SiC a été limité à une température de 600°C dans le cadre de ce programme. La matrice SiC assure la protection anti-oxydation des fibres de carbone. Différents traitements de finition ont été appliqués aux pièces pour améliorer encore l'efficacité de cette protection.

Les matériaux Carbone-Carbone n'ont pas été retenus pour le programme complet de démonstration compte tenu de la grande sensibilité de la matrice à l'oxydation. Cependant, des volets froids ont été fabriqués par la SEP et essayés sur moteur en vue d'obtenir une première expérience sur ce type de matériau dans l'environnement d'un turboréacteur.

Un programme de caractérisation approfondie a été mené sur les deux matériaux retenus C-SiC et SiC-SiC :

- Analyse de la structure.
- Résistance à haute température.
- Cyclage thermique.
- Fatigue Vibratoire et Oligocyclique.
- Vieillissement oxydant.
- Erosion.

Ces essais ont permis d'affiner la composition des deux matériaux testés et de disposer d'une base de données pour le dimensionnement des pièces prototypes.

#### Développement/Essais de composants

##### Volets Froids (planche 7)

Le matériau C-SiC a été retenu compte tenu de la température limitée atteinte en extrémité de volet (550°C).

Le volet se présente sous la forme d'une plaque auto-raidie. Cette conception conduit à un gain de masse de 25% par rapport à un volet en alliage de Nickel.

Un essai de fatigue vibratoire a été réalisé dans une configuration de montage type moteur. La résistance ultime d'un volet métallique avait été évaluée au préalable. Le volet composite a résisté à des charges deux fois supérieures à celles appliquées au volet métallique. A l'issue de cet essai, le volet composite ne présentait aucun indice d'endommagement.

Un essai de rupture sous effort de pression a été réalisé. La charge de rupture mesurée est cohérente avec les estimations effectuées à partir d'essais sur éprouvettes mécaniques.

##### Volets Chauds (planche 8)

Compte tenu du niveau de température plus élevé que rencontrent ces volets, le matériau SiC-SiC a été retenu. Le gain de masse par rapport au volet métallique atteint 60% (Alliage base Cobalt).

Un essai de fatigue oligocyclique sous charges nominales a été réalisé avec succès. L'instrumentation en jauge de contrainte a confirmé les niveaux de sollicitations prévus par calcul par Éléments Finis.

##### Cône d'échappement

Le matériau SiC-SiC a été retenu, ce qui conduit à un gain de masse de 30% par rapport à un cône en alliage base Cobalt.

Un essai de fatigue vibratoire (charges maximales) a été réalisé dans des conditions représentatives du montage moteur; aucun endommagement par fatigue n'a été constaté. Par ailleurs un essai de mise en pression a été réalisé (essai d'épreuve). La pression d'écatement est conforme à celle estimée à partir des essais sur éprouvettes. Cet essai confirme la marge de sécurité très importante vis à vis de la tenue en pression, la géométrie du cône découlant du respect des critères vibratoires.

Deux cônes ont été testés en cyclage thermique au banc partiel (planche 9). Chaque pièce a supporté, sans dommage, 360 cycles à une température maximale de gaz de 1000°C.

##### Anneau accroche flamme

L'emploi du SiC-SiC conduit à un gain de masse de 50% par rapport à un alliage base Cobalt. Des essais de vieillissement thermique ont été réalisés sur secteurs d'anneau. Deux tranches de 50 cycles à température maximale de 800°C ont été réalisées. Entre chaque tranche, les secteurs ont été vieillis 500 heures à des températures comprises entre 900 et 1050°C. Sur les trois configurations testées on ne déplore qu'une rupture liée à un montage défectueux.

A l'issue de ces essais, un anneau a été testé en cyclage thermique derrière une chambre de combustion (planche 10). Deux tranches d'endurance ont été réalisées sans endommagement de la pièce :

- 360 cycles à 1000°C
- 360 cycles à 1150°C

#### Essais sur moteur de démonstration

A la suite des essais de qualification, trois composants ont été retenus pour essais sur moteur :

- Cône d'échappement.
- Volets froids de tuyère.
- Volets chauds de tuyère.

Plus de 200 heures de fonctionnement en endurance accélérée ont été réalisées dont une fraction importante dans des conditions maximales de température (PGPC). La sévérité et la durée de cet essai sont représentatives des conditions d'utilisation sur moteurs futurs.

Les pièces ont été instrumentées en thermocouples, peintures thermosensibles et jauge de contraintes de façon à mieux évaluer leur comportement dans l'environnement du moteur.

Aucune anomalie n'a été décelée en cours d'essais; on peut constater le bon état général des pièces sur la planche 11. Des contrôles non destructifs sont en cours.

Ces pièces seront à nouveau montées sur moteur pour subir une caractérisation complémentaire dans des conditions d'altitude simulée.

Un essai en vol sur MIRAGE 2000 (planche 12) est planifié en 1989 afin de vérifier leur comportement en utilisation opérationnelle.

Le programme d'essai déjà réalisé permet de tirer certaines conclusions préliminaires :

- Les objectifs de masse ont été atteints.
- Les composants en C-SiC et SiC-SiC ont démontré leur capacité à fonctionner en longue durée à haute température.
- Les principes de liaison des pièces céramiques aux structures métalliques ont été validés.
- Les matériaux C-SiC et SiC-SiC sont désormais applicables sur moteurs en développement.

#### Conclusions et Perspectives

Le programme de développement de pièces en matériaux composites à Matrice Céramique a abouti à l'expérimentation couronnée de succès, de composants de turboréacteurs en longue durée sur moteur.

Les matériaux mis au point à cet effet (C-SiC et SiC-SiC) seront utilisés pour la réalisation de composants dans le cadre de moteurs en cours de développement.

Le champ d'utilisation de ces matériaux est très vaste et n'a pas été entièrement couvert. L'application de ces nouveaux matériaux à des composants plus sollicités - plus critiques - plus chauds (aubes de turbine - disques - carters) implique une poursuite des travaux suivant plusieurs axes :

- Développement de fibres haute résistance/haute température.
- Amélioration des protections anti-oxydation.
- Actions sur les coûts par l'optimisation des procédés.
- Analyse des mécanismes d'endommagement des matériaux.

Ces travaux permettront de développer de nouveaux composants en céramique composite légers et fiables ce qui contribuera à l'amélioration des rapports Poussée/masse des turboréacteurs de la prochaine génération.

### Trends in Military Engine Applications

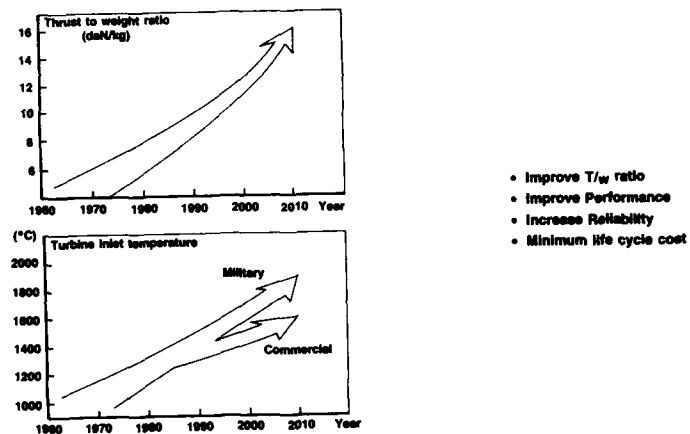
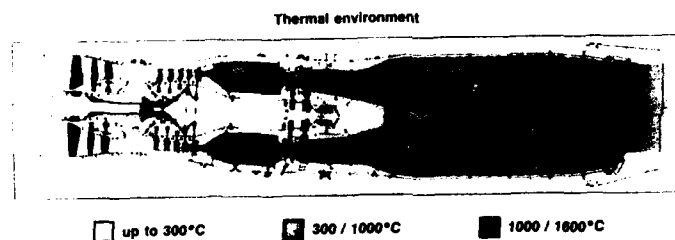


FIGURE 1

### Application of composite materials for turbojets



- Resin matrix composite for cold section components (up to 300°C)
- Glass matrix composite with silicone carbide SiC fiber (up to 1000°C)
- SiC - SiC ceramic composite with perspective of 1600°C temperature
- Carbone - carbone ceramic composite for perspective of 2000°C temperature

High temperature composite is a major challenge  
for mass reduction in hot section

FIGURE 2

### Material development overview

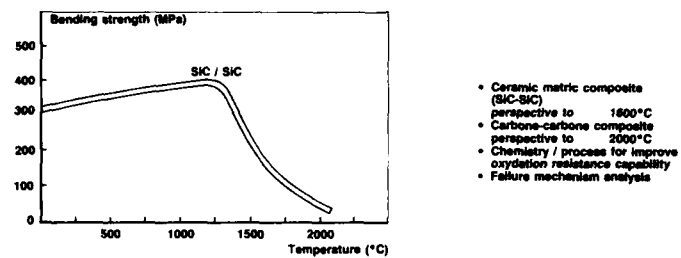


FIGURE 3

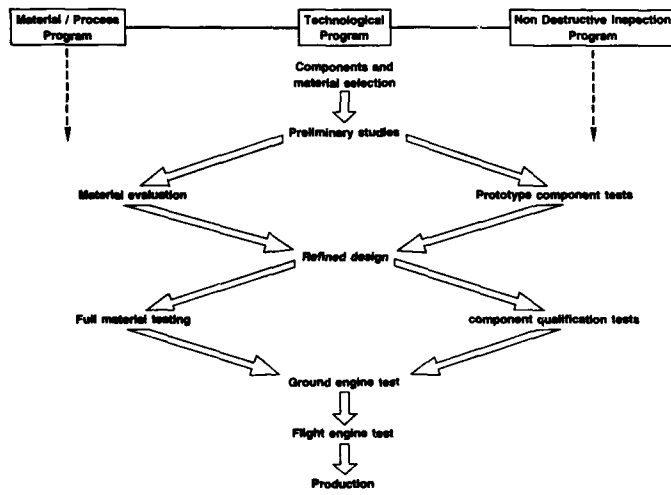
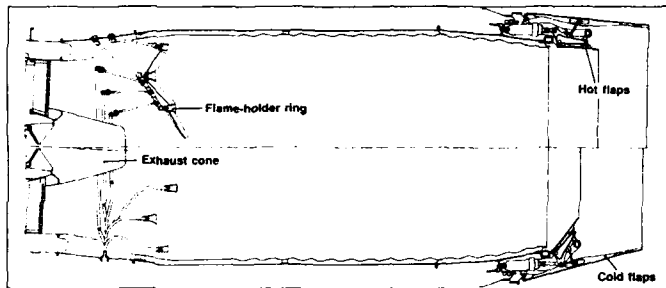


FIGURE 4

#### Components selection

Reheat and nozzle components were selected

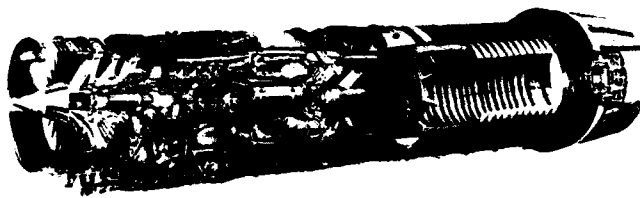


- High temperature environment
- Substantial weight savings
- Great impact on the center of gravity of the aircraft
- Cooling reduction or life improvement
- Reasonable risk according to the initial material knowledge

FIGURE 5

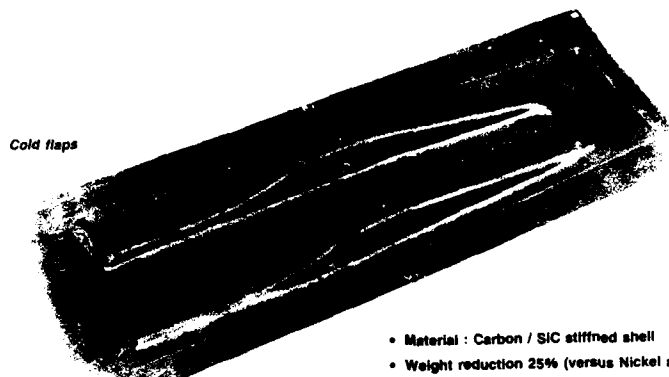
#### Engine demonstrator

SNECMA M53-P2



- Mirage 2000 powerplant (A.M.D.)
- Selected by 7 countries
- Net thrust 9 700 kgg (ground conditions)
- Reheat temperature beyond 2000°K

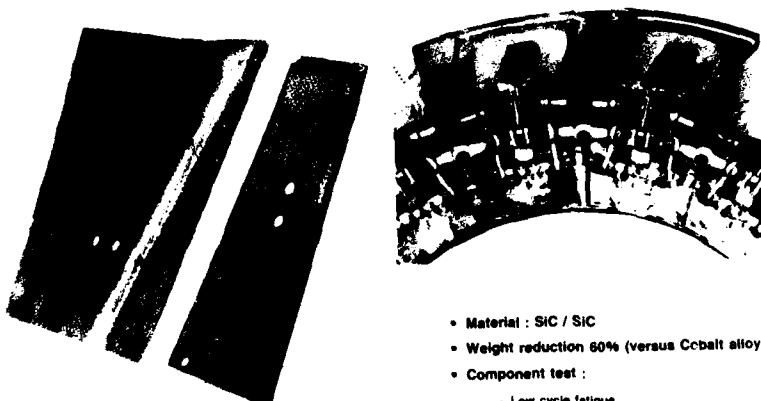
FIGURE 6

**Component tests**

- Material : Carbon / SiC stiffened shell
- Weight reduction 25% (versus Nickel alloy)
- Component test :
  - High cycle fatigue
  - Pressure loading

**FIGURE 7****Component tests**

Hot flaps



- Material : SiC / SiC
- Weight reduction 60% (versus Cobalt alloy)
- Component test :
  - Low cycle fatigue

**FIGURE 8**

**Component tests**

Exhaust cone



- Material : SIC / SIC
- Weight reduction 30% (versus Cobalt alloy)
- Component test :
  - Pressure proof
  - Full scale rig test
  - High cycle fatigue

FIGURE 9**Component tests**

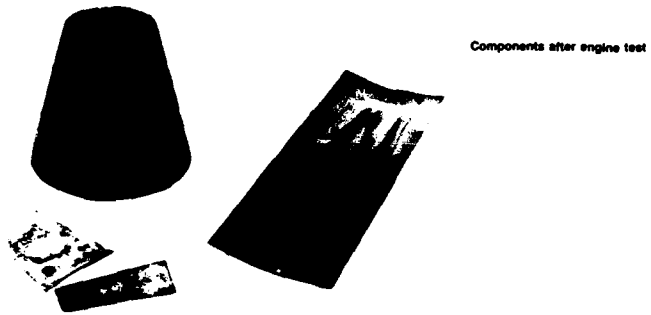
Flame-holder ring



- Material : SIC / SIC
- Weight reduction 50% (versus Cobalt alloy)
- Component test :
  - Oxidation test (sectors)
  - Full scale rig test
  - Attachement lugs resistance

FIGURE 10

Preliminary conclusions



Components after engine test

- Weight target reached
- Long term / high temperature exposure ability
- Materials available for production engine design

FIGURE 11

Next step



Mirage 2000 (A.M.D)  
Flight test scheduled in 1989

FIGURE 12

## INITIAL RESULTS OF TESTS ON METAL-CERAMIC GUIDE VANES

by

W. Hüther

and

W. Krüger

MTU MOTOREN- UND TURBINEN-UNION MÜNCHEN GMBH  
 Dachauer Str. 665  
 8000 München 50  
 West Germany

## SUMMARY

Metal-ceramic guide vanes consist of an outer ceramic shell and an inner metallic core, which is cooled. The hot gas contacts only the uncooled ceramic shell, so that the total amount of cooling air is reduced to a low value compared with conventional guide vanes. A linear arrangement of four guide vanes in a size which would be suitable for the RB 199 was built and tested with hot gas at atmospheric pressure. It could be shown that material temperature of the ceramic shell higher than 1870 K (2900 F) are possible, under static as well as cyclic loading.

## 1 DESIGN CONCEPT

Ceramic materials can withstand very high temperature up to around 1900 K (3000 F) without cooling. The realization of ceramic guide vanes for gas turbines therefore is an attractive target. The problems of ceramic materials are brittleness and large scatter of strength. Until now, these properties have prevented the application of ceramics for highly stressed gas turbine components.

The successful use of ceramics in the hot section of gas turbines should be possible, when the stress level is low. Besides the unavoidable thermal stresses, the external loads on a ceramic part should be as small as possible. This consideration leads to the concept of a metal-ceramic guide vane. Such a vane consists of an outer ceramic shell and a metal structure within (fig. 1.). Only the ceramic shell is in contact with the gas and needs no cooling. The metal structure is cooled. It mainly consists of a metallic core which is surrounded by sheet metal. The cooling air passes through the gap between the metallic core and the sheet metal. Direct heat flow from the ceramic shell to the metallic structure is avoided by heat-insulating elements.

The realization of this design needs a certain minimum size of the guide vane. Therefore a guide vane in the size corresponding to the RB 199 was chosen for the further investigations.

A plane cascade consisting of four metal-ceramic blades and a rig for tests under atmospheric pressure was constructed. Fig. 2 shows the plane cascade.

Silicon carbide offers the highest temperature potential of the ceramic candidate materials. Therefore the ceramic shells were manufactured from sintered  $\alpha$ -silicon carbide by cold isostatic pressing and green machining.

Fig. 3 shows the mould, consisting of a core with the shape of the inner contour of the vane and a press-bag. In fig. 4 the green body before and after machining can be seen.

For the insulation between ceramic shell and metallic core aluminium-titanate and alternatively partially stabilized zirconia were chosen. The metal parts were spark machined from IN 100.

For testing the blades under atmospheric pressure, a rig was built up. It consists of a combustor and a heat exchanger. Because of the high temperature needed for the test of the vanes, it was necessary to use silicon carbide for both combustor and heat exchanger.

## TEST AND RESULTS

The application of the results of atmospheric tests to real turbine conditions is very difficult. Uncertainties arise from different Mach- and Reynolds-numbers. Nevertheless hot gas temperature was varied from 1375 K to 1675 K and the temperatures

of the cooling air at entry and exit of the metallic core and the temperatures of leading and trailing edge of the metallic core were measured.

With the results of these measurements a calculation was performed, to obtain a first estimation of the mass flow of cooling air necessary under real turbine conditions. Based on the conditions of the RB 199, the estimate showed that about 2 % of the whole mass flow of the compressor would be necessary for a nozzle with 34 vanes.

In the next step the metal ceramic blades were tested under static and cyclic conditions.

**First test (static):**

Hot gas temperature	1800 K
Time	200 h
<b>Subsequent:</b>	
Hot gas temperature	1900 K
Time	100 h
<b>Second test (cyclic):</b>	
Hot gas temperature	800 K / 1900 K
Heating rate (average)	90 K / min.
Time at 1900 K	3 min.
Cooling rate (average)	75 K / min.
Number of cycles	100
Total time in hot gas	25 h

After the test, the ceramic shell and the metal core of the vanes shows no damage (fig. 5). Only the insulators were broken in several parts. The design of the vanes assures that this effect has no influence on the function of the cascade. The metallic parts, which fix the vanes in the rig, were damaged by hot gas corrosion. This is a matter of the test rig and not a problem of the cascade itself. An attempt to increase the temperature above 1900 K, was not successful. Temperatures in the range of 1970 K caused fracture in the ceramic shells.

**FUTURE ASPECTS**

Because of the promising results, a metal ceramic vane which fits to one of MTU's rig turbines was designed. Fig. 6 shows this vane. The design is very similar to that used in this work, except that the size of the ceramic platforms was minimized to reduce stresses in the ceramic shells. Therefore a part of the platform is still metal. This part needs additional impingement cooling and will be coated with zirconia as a thermal barrier.

In the mean time, the strength of the silicon carbide material could be improved remarkably. Therefore it is hoped that the temperature limit of an uncooled ceramic shell may be increased to 1950 K. Without cooling the ceramic shell, higher temperatures do not seem to be possible, because of the oxidation of the ceramic material.

For higher temperatures, cooling concepts for the ceramic shell are necessary. Cooling may be achieved by the radiation of the ceramic shell to the metallic core or by other methods.

Even when cooling of the shell is necessary, metal ceramic guide vanes will result in a substantial reduction in the amount of cooling air required as compared with conventional vanes.

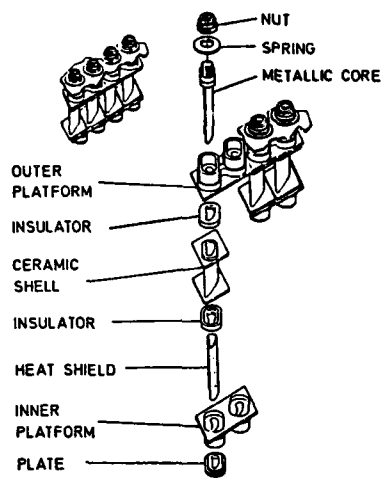


Fig. 1: Principle of metal-ceramic-vanes

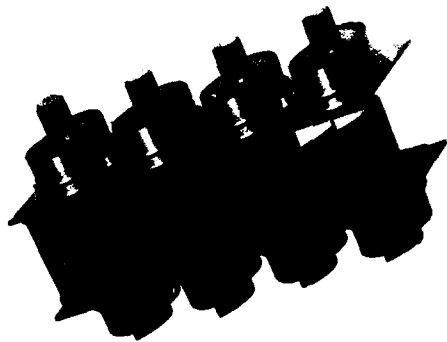


Fig. 2: Plane cascade, consisting of four metal ceramic blades

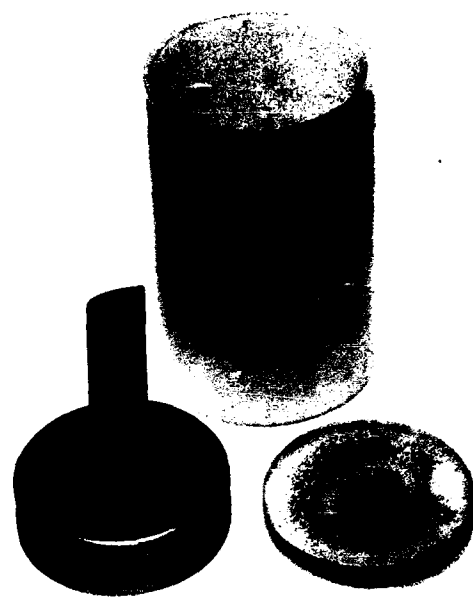


Fig. 3: Mould for cold isostatic pressing ceramic shells

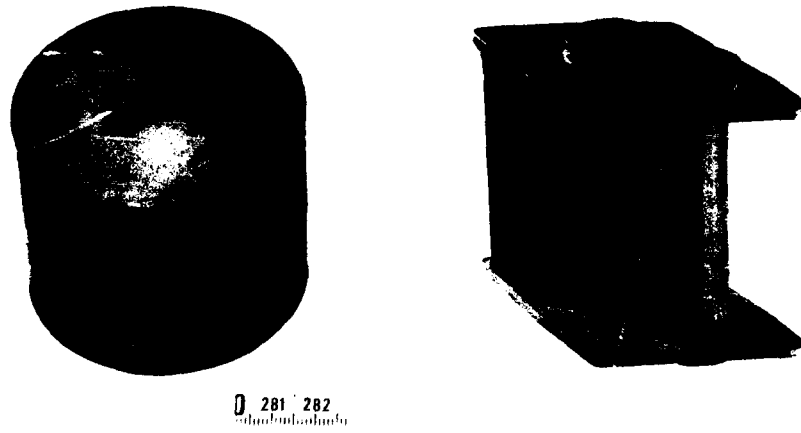


Fig. 4: Green body before and after machining

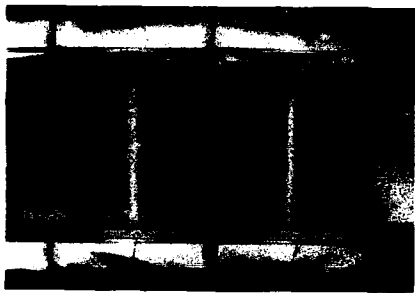


Fig. 5: Metal-ceramic vanes after hot gas test at 1900 K

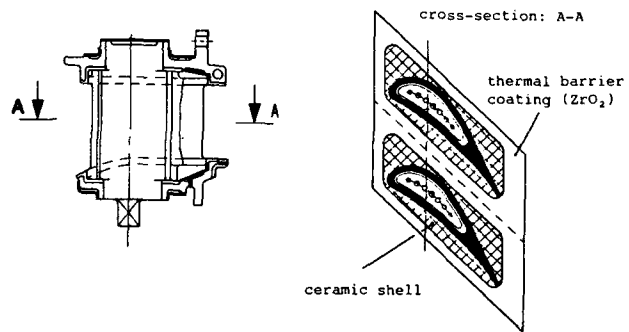


Fig. 6: Metal-ceramic vane, suitable for the rig-engine VT3

## INTERACTION OF COATINGS WITH BASE METALS AT HIGH TEMPERATURE

by

H.W.Grünling, K.Schneider, L.Singheiser  
Materials Technology Laboratory  
ASEA Brown Boveri A.G.  
Kallstädter Strasse 1  
Postfach 351  
6800 Mannheim  
Federal Republic of Germany

### 0. Summary

The interaction of aluminide, CoCrAlY- and NiCrAlY-based coatings on the nickel-based alloy IN 738 LC was investigated in the temperature range 850°C to 1000°C. Due to intensive interdiffusion behaviour of CoCrAlY-coatings with Ni-based alloys the coating composition changes to CoNiCrAlY at high temperature. The degradation of the coating occurs primarily by Al-diffusion into the alloy. NiCrAlY-coatings show less interdiffusion with Ni-based alloys. Coating degradation occurs by oxidation. A similar behaviour was observed for aluminide coatings. Interdiffusion effects between coatings and alloys increase N<sub>Y</sub>-numbers in the interdiffusion zone resulting in the precipitation of brittle phases.

### 1. Introduction

With increasing gas inlet temperatures in industrial gas turbines and aero engines, the progressive design and efficiency increase had to be partially compensated by the development of sophisticated cooling systems due to a less progressive development rate for structural alloys /1/. Alloy development is still strongly focused to increase creep strength by development of high γ' containing alloys, oxide dispersion strengthening, and improving of casting technologies /2/. The corresponding development of coatings was focused on oxidation and hot corrosion improvement /3/.

The development of MCrAlY-type coatings based on Ni and Co during the last 20 years was not essentially dependent on alloy development. These types of coatings offered the possibility to tailor coating systems independent of alloy development without any influence from structural alloys. Oxidation and hot corrosion specialists had the opportunity to optimize coating compositions with respect to oxidation and hot corrosion resistance and to optimize deposition techniques such as EB-PVD or vacuum plasma spraying to maintain the required high temperature corrosion resistance. Interdiffusion effects due to differences in composition of the coating and the substrate influence coating composition and the resulting protective properties of MCrAlY-coating after times which are beyond commonly used laboratory investigations.

This paper describes the interdiffusion behaviour of simple aluminides and Pt-modified aluminides on IN 738 LC as well as the interdiffusion behaviour of CoCrAlY- and NiCrAlY-type coatings on the same structural alloy.

## 2. Chemical interaction of Co-based coatings with nickel-based alloys

Chemical interaction between a Si-modified Co<sub>29</sub>Cr<sub>6</sub>Al<sub>0.9</sub>Y-coating and the nickel-based alloy IN 738 LC was investigated at 1000°C and 850°C up to 5000 hours. The vacuum plasma sprayed CoCrAlY-coating consists of a CoCr-matrix with ~ 3 wt-% Al in solid solution and fine globular precipitations of  $\beta$ -CoAl. During high temperature exposure at 1000°C in air dissolution of  $\beta$ -CoAl and change of Al-solubility occurs due to oxidation and interdiffusion effects. Dissolution of  $\beta$ -CoAl at the coating/alloy interface results in subsequent precipitation of mixed  $\beta$ -(Ni, Co)Al in the interdiffusion zone (Fig. 1). After 5000 hours a 200  $\mu\text{m}$  thick CoCrAlY-coating is nearly free of  $\beta$ -CoAl (Fig. 1). The thicker coating shows  $\beta$ -CoAl-depleted zones at the surface due to  $\text{Al}_2\text{O}_3$ -scale formation and at the coating/substrate interface due to interdiffusion effects. Line scan analysis of important alloying elements in the coating and alloy are shown in Fig. 2. The concentration profile for Al indicates rapid inward diffusion of Al into the alloy. The Al-concentration in the  $\beta$ -CoAl-depleted zone at the surface has been measured to be ~ 3 wt-% in solid solution. In the  $\beta$ -CoAl-containing matrix the concentration gradient of Al is directed toward the structural alloy. In the  $\beta$ -CoAl-depleted zone adjacent to the alloy the Al-concentration is comparable with the Al-content at the surface of the coating. In the interdiffusion zone the Al-concentration rapidly increases, due to the formation of (Ni, Co)Al in the diffusion zone. Co-diffusion out of the coating is also observed. Due to (Ni, Co)Al formation the Co-concentration decrease in the interdiffusion zone is relatively small. A sharp decrease of Co occurs outside the interdiffusion zone adjacent to the unaffected alloy. Rapid diffusion of Ni from the alloy into the coating is also observed changing the type of the coating from CoCrAlY- to CoNiCoCrAlY-type. Ti shows high diffusivity from the bulk alloy into the coating and may affect Al-solubilities, oxidation behaviour and oxide adherence.

Careful analysis of  $\beta$ -CoAl depletion as a function of time shows that the oxidation induced  $\beta$ -CoAl depletion growth rate follows a parabolic rate law (Fig. 3). This growth rate is associated with the growth of the  $\text{Al}_2\text{O}_3$ -scale which is parabolic if oxide spalling or crack formation in the scale does not occur. During isothermal oxidation experiments the  $\text{Al}_2\text{O}_3$ -scale shows parabolic growth behaviour (Fig. 4).

The growth of the  $\beta$ -CoAl - depleted zone at the coating/alloy interface follows a linear rate law (Fig. 3). The same behaviour was found for the growth of the  $\beta$ -(Ni, Co)Al enriched interdiffusion zone. At 1000°C the growth rate of the  $\beta$ -CoAl-depleted zone is smaller compared with the growth rate of the  $\beta$ -(Ni, Co)Al containing interdiffusion zone. The matrix of the interdiffusion zone consists of a NiCoCr solid solution and precipitations of Ta-, Ti- and Mo-rich MC-type carbides.

The linear rate laws for  $\beta$ -CoAl-depletion and  $\beta$ -(Ni, Co)Al precipitation can be well understood by some qualitative thermodynamic considerations. The thermodynamic activity in the Ni-Al-system is lower at the same Al-content compared with the Co-Al and Cr-Al-system /6/. Fig. 5 gives an example of thermodynamic activities for Al and Ni at 1000°C /6/. According to GIBB's rule the activities in the Ni-Al system are constant if two phases are present in a binary mixture. Activity changes occur only if one phase is present. With increasing temperatures the extreme deviations of acti-

vity from ideal solid solution behaviour become smaller. A similar activity vs composition behaviour is found for Co-Al and Cr-Al ///. In these systems the Al-activity is higher at the same Al-content compared with the Ni-Al-system. The activity of Al in a CoCrAlY-coated nickel-based alloy can be qualitatively described as shown in Fig. 6. After short annealing time the Al-activity in the CoCrAlY-coating is higher compared with the Ni-based alloy which has a low Al-activity because only  $\gamma'$  is present in equilibrium with Al in solid solution. Incorporation of Co into Ni-aluminides increases the entropy of mixed aluminides and results in higher stability. The formation of  $\beta$ -(Ni, Co)Al during high temperature exposure keeps the Al-activity at very low levels. This results in a high Al-gradient which remains nearly constant unless remarkable dissolution of  $\beta$ -CoAl occurs. If the diffusion coefficients of Al and Co are independant of the coating and alloy composition from Fick's first law  $j_{\text{Al}} = - D_{\text{Al}} \frac{da_{\text{Al}}}{dx}$  a constant flux of Al across the coating alloy boundary results. Extended  $\beta$ -CoAl depletion in the coating after long times requires a transition from linear to parabolic growth behaviour of  $\beta$ -CoAl depleted zones and  $\beta$ -(Ni, Co)Al enriched interdiffusion zones. A quantitative treatment of interdiffusion, phase formation and phase composition is impossible due to the lack of thermodynamic data for ternary aluminides, the influence of further alloying additions on thermodynamic activities and diffusivities. After complete dissolution of  $\beta$ -CoAl in the CoCrAlY-coating further high temperature exposure results in dissolution of  $\beta$ -(Ni, Co)Al due to diffusion of Al into the bulk alloy (Fig. 7) with subsequent void formation in the interdiffusion zone. Kirkendall void formation can be mainly attributed to the high flux of Al from the interdiffusion zone into the bulk alloy.

At  $850^{\circ}\text{C}$  interdiffusion of CoCrAlY-coatings results also in the formation of  $\beta$ -(Ni, Co)Al (Fig. 8). The  $\beta$ -(Ni, Co)Al layer growth rate is smaller compared with the  $\beta$ -CoAl dissolution (Fig. 9). This can be attributed to the higher volume fraction of  $\beta$ -(Ni, Co)Al in the interdiffusion zone compared with higher temperature. The shape of  $\beta$ -(Ni, Co)Al is more globular at lower temperatures and more needle-shaped at elevated temperatures due to limited diffusion rates. Co-diffusion seems to be limiting for the extent of aluminide precipitates into the bulk alloy. Diffusivity measurements have been performed for some coating elements (Fig. 10). Si-diffusion out of the coating is much faster compared with Co-diffusion. There is no significant difference in Co and Si diffusivities between the alloy IN 738 LC and the ODS alloy MA 6000. This can be explained by the composition of the alloys which are very similar except the Co-content. The activation energy obtained for Si-diffusion is somewhat lower compared with literature data for Si-diffusion in nickel.

### 3. Interdiffusion of Ni-based coatings with Ni-based alloys

Nickel-based coatings have a better chemical compatibility with nickel-based alloys. Fig. 11 shows a metallographic cross section of IN 738 LC coated with a Si-modified Ni<sub>25</sub>Cr<sub>5</sub>Al<sub>10.5</sub>Y coating after 5000 hours at  $1000^{\circ}\text{C}$ . The microstructure of the coating is very uniform. The interdiffusion zone is enriched with some Ti- and Nb-containing silicides and Ta-, Ti-rich MC-type carbides. Silicide formation occurs only within a small interdiffusion zone, where the Si-content is high enough. At lower Si-levels a continuous decrease of Si occurs without any phase formation (Fig. 12). Diffu-

sion of Al into the substrate is relatively slow compared with CoCrAlY-coated IN 738 LC. The small amount of  $\beta$ -NiAl originally present in the coating has been dissolved due to oxide formation at the coating/oxide interface resulting in small Al-activity differences between the coating and the substrate. Ti diffusion into the coating is comparable with Ti diffusion in CoCrAlY-coatings. At 850°C the coating composition after long time exposure consists of a NiCrAl-matrix with fine globular precipitation of  $\alpha$ -Cr (Fig. 13). Oxidation and interdiffusion with the bulk alloy results in  $\alpha$ -Cr dissolution at the coating surface and the coating/alloy interface.  $\alpha$ -Cr dissolution follows a parabolic rate law, indicating rate limiting diffusion processes (Fig. 14). Oxidation at the coating surface lowers the Al-content and increases Cr-solubilities. At the coating/substrate interface Al diffusion into the alloy and Co diffusion into the coating are responsible for increased Cr solubilities in the coating. EDX line scans of important elements in the coating and alloy confirm the low interdiffusion behaviour between NiCrAlY-coatings and IN 738 LC (Fig. 15).

#### 4. Interaction of aluminide coatings with nickel-based alloys

Chemical interaction of aluminide coatings with nickel-based superalloys is strongly dependent on the coating deposition process (high or low activity process) and the alloy composition. High activity processes with rate limiting Al diffusion in the aluminide result in coatings with high amounts of precipitates in the coating and a more uniform distribution of alloying elements.

Due to the limited solubility of Cr in NiAl Cr-rich precipitates are uniformly distributed in the NiAl-phase /8/ in high activity aluminide coatings. Low activity coating deposition techniques produce very homogenous NiAl coatings. The coating composition is less dependent on the alloy composition compared with high activity processes. The limited solubility of NiAl for Cr and some other alloying elements produces interdiffusion zones with high Cr- and refractory element concentrations. The microstructure of the interdiffusion zone depends primarily on the Cr-content of the alloy /9/. High Cr-contents (~ 20 wt-%) produce thick coherent Cr-rich zones between the aluminide coating and the bulk alloy. Due to limited Al and Ni-solubilities and lower diffusivities the NiAl-coatings on high Cr containing alloys are thinner compared with alloys which have lower Cr contents /8, 9, 10/.

In Fig. 16 and 17 the microstructure and composition of aluminide coatings on IN 738 LC and MA 6000 after the coating process is shown. The aluminide coatings have been deposited by CVD-techniques /10/ using  $AlCl_3/H_2$  gas mixtures at 1100°C. The deposition time was 20 hours. Due to the low  $AlCl_3$ -pressure in the gas phase an aluminide coating with low Al-content and uniform composition was produced by outward diffusion of Ni from the bulk alloy. The interdiffusion zone of both alloys shows a lamellar structure and consists of NiAl, Cr-rich phases and precipitations rich in Ta, Nb and Ti. The interdiffusion zone of the alumized IN 738 LC is more regular compared with aluminized MA 6000. After short time annealing at 1000°C the interdiffusion zone becomes more irregular (Fig. 18). Coalescence and rearrangement of Al- and Cr-rich phases occurs in the outer part of the interdiffusion zone. In the inner part of the interdiffusion zone the Cr-rich phases become more needle shaped. After 6000 hours exposure at 1000°C the aluminide

coating consists of an outer NiAl-phase with some grains of Ni<sub>3</sub>Al-type composition with low Cr-contents, M<sub>23</sub>C-type carbides and high Cr-containing precipitates in an Ni<sub>3</sub>Al-type matrix (Fig. 19). The degradation of the NiAl-phase occurs primarily by diffusion of Al into the bulk alloy and rearrangement of the NiAl-phase at the coating surface.

At higher temperatures rapid dissolution of Cr-rich precipitates occurs due to increased solubilities and diffusivities (Fig. 20). Degradation of the NiAl-phase occurs by rapid oxidation as well as by rapid diffusion of Al into the bulk alloy.

Rapid coalescence of Cr-rich phases with low Al-content are observed in the metallographic cross section. Long time exposure results in complete degradation of the NiAl-phase (Fig. 21). The original NiAl-coating consists of Ni<sub>3</sub>Al with a very homogenous composition. The original interface between the NiAl-phase and the interdiffusion zone still remains indicating that Cr diffusion into the alloy occurs. A similar interdiffusion behaviour was found for MA 6000 (Fig. 22) at 1100°C. In the outer part of the interdiffusion zone void formation occurs which may be attributed to lower condensation energies of vacancies compared with dispersoid-free alloys.

Void formation was also observed at 1000°C after long time exposure (Fig. 23). In the interdiffusion zone rearrangement of aluminide and Cr-rich phases occurs. X-ray maps of Ti and Al (Fig. 23) as well as EDX line scans (Fig. 24) indicate high γ' enrichment in the interdiffusion zone due to Al diffusion into the alloy and Ti diffusion out of the alloy into the interdiffusion zone. Precipitation of phases with different composition changes the homogeneous distribution of dispersoids in the alloy (Fig. 23). Y<sub>2</sub>O<sub>3</sub> is enriched at phase boundaries of precipitations in the interdiffusion zone. The exact mechanism of Y<sub>2</sub>O<sub>3</sub> displacement is unknown. We assume that a gradient in surface tension around a Y<sub>2</sub>O<sub>3</sub>-particle may be responsible for dispersoid displacement.

Pt-modified aluminides on IN 738 LC exhibit similar structural stability compared with simple aluminides. Fig. 25 and 26 show metallographic cross sections of RT22 coated IN 738 LC after the normal heat treatment and after 5000 hours operation at 950°C surface temperature on a first stage vane. Incorporation of Pt in NiAl and the formation of PtAl<sub>2</sub> phases indicate the high thermodynamic stability of Pt-modified aluminides. After 5180 hours of operation PtAl<sub>2</sub> phases are still present in the near surface region of the coating. The thickness of the aluminide coating was increased from about 80 μm to 100 μm.

Transformation of NiAl into Ni<sub>3</sub>Al during aluminide degradation depends on oxidation and Al-diffusion rates. Degradation of the aluminide phase starts with uniform decrease of the Al-content in the Ni-rich NiAl-phase, due to higher diffusivity rates in β-NiAl compared with Ni<sub>3</sub>Al or Al in solid solution /11/. The interdiffusion coefficient in Ni-rich NiAl at 1000°C is  $6.2 \cdot 10^{-10} \text{ cm}^2/\text{s}$ , in Ni<sub>3</sub>Al  $6.3 \cdot 10^{-11} \text{ cm}^2/\text{s}$  and in the γ-phase  $4.9 \cdot 10^{-11} \text{ cm}^2/\text{s}$  /12/. Transformation of β-NiAl into Ni<sub>3</sub>Al occurs if the stability limit at the lowest Al-content in the NiAl-phase is obtained.

## 5. Influence of long-time interdiffusion effects on chemical and mechanical properties of coated superalloys

Interdiffusion effects between coatings and structural alloys may affect the coating composition and solubilities of important alloying elements. Nickel based coatings and aluminide coatings are less affected by interdiffusion effects at elevated temperatures. Life time determining is primarily diffusion of Al out of the coating into the bulk alloy at very high temperatures. The oxidation and hot corrosion behaviour of these types of coatings is mainly influenced by Ti-diffusion into the coating. High Ti-contents promote  $\text{Al}_2\text{O}_3$ -scale growth and spalling of oxides. This behaviour can be expected for alloys with high  $\gamma'$  contents, which contain 4 to 6 wt-% Ti. The decrease of Ti-contents in the superalloy influences  $\gamma'$  contents in the near coating region of the alloys.

High diffusivities of Al and Si from coatings into alloys increase N<sub>i</sub>-numbers and reduce their ductility. Increased Si-contents may also reduce solidus temperatures of alloys. At intermediate temperatures an increase of Al- and Cr-content in the interdiffusion zone promotes  $\sigma$ -phase formation and subsequent embrittlement of the alloy.

Due to the low Cr-content in low activity aluminide coatings degradation of the coating by Al-diffusion into the alloy and subsequent Ni<sub>3</sub>Al-formation results in increased oxidation rates of the Ni<sub>3</sub>Al-phase. Al diffusion out of the aluminide phase is not accompanied by a counter current Cr-diffusion to the coating surface. The critical concentration for  $\text{Al}_2\text{O}_3$ -scale formation strongly depends on the Cr-content of the coating. Increase of Cr-content lowers the critical Al-concentration.

CoCrAlY-type coatings on nickel based alloys exhibit the highest changes in composition and microstructure during high temperature operation due to intimate interdiffusion of Ni and Co. The effects of interdiffusion of some important coating and alloy elements are summarized in Fig. 27.

Mechanical properties of a coated high temperature component such as creep behaviour are not affected by interdiffusion if the structural alloy is very thick compared with the coating and interdiffusion zone. But for filigree structures such as cooled vanes or blades with high cooling efficiency and thin wall sections, interdiffusion effects may affect the mechanical properties of the component due to long range penetration depths of some alloying elements. Fig. 28 and 29 give an example of superimposed temperature gradients on the concentration profile of a diffusing species. The calculations have been performed using finite difference techniques. Literature data for Al diffusion in Ni have been used to calculate the Al-concentration profile under isothermal and non-isothermal conditions with different superimposed temperature gradients after 30.000 hours. At a coating/alloy interface temperature of 1200K superimposed temperature gradients result in lower penetration depths compared with isothermal conditions. A temperature gradient of 100 K/mm reduces the amount of Al which diffuses into the alloy by about 15 %. At higher temperature (1400 K at the coating/alloy interface) the reduction of Al diffusion is about 50 % at the same temperature gradient of 100 K/mm compared with isothermal conditions. The results of these calculations show that penetration depths are remarkably reduced by temperature gradients compared with isothermal conditions.

**Literature**

- /1/ R.F. Singer, Conf. Proc. "PM Aerospace Materials 84", Bern, (1984)
- /2/ G.W. Meetham, Mat. Sci. Technol., 1, 290, 1986
- /3/ T.R. Vargas, W.E. Ulion, T.A. Goebel  
Thin Solid Films, 73 (1980), 407
- /4/ J.M. N'Gandu Muamba, R. Streiff, D.H. Boone,  
Mat. Sci. Eng. 88 (1987), 111
- /5/ M.R. Jackson, T.R. Raiden, Met Trans Vol 8A,  
(1977) 1967
- /6/ A. Steiner, K.L. Komarek, Trans TMS-A/ME,  
Vol. 230 (1964) 786
- /7/ W. Johnson, K. Komarek, E. Miller, Trans TMS-AIME,  
Vol 242 (1968), 1685
- /8/ R. Pichoir in "Materials and Coatings to Resist  
High Temperature Corrosion" ed. by D.R. Holmes,  
A. Rahmel (1978), 271
- /9/ E. Fitzer, H.J. Mäurer in "Materials and Coatings to  
Resist High Temperature Corrosion" ed. by Dr. Holmes,  
A. Rahmel (1978), 253
- /10/ L. Singheiser, G. Wahl, A. Reich, Proc. of. 4th Europe  
Conf. on CVD, ed. by J. Bloem, G. Verspui and L.R. Wolff  
(1983), Eindhoven, 122
- /11/ G.F. Hancock, B.R. McDonnell phys. stat. sol (A) 4,  
(1971), 143
- /12/ M.M.P. Janssen, G.D. Rieck, Trans TMS AIME Vol 239  
(1967), 1372

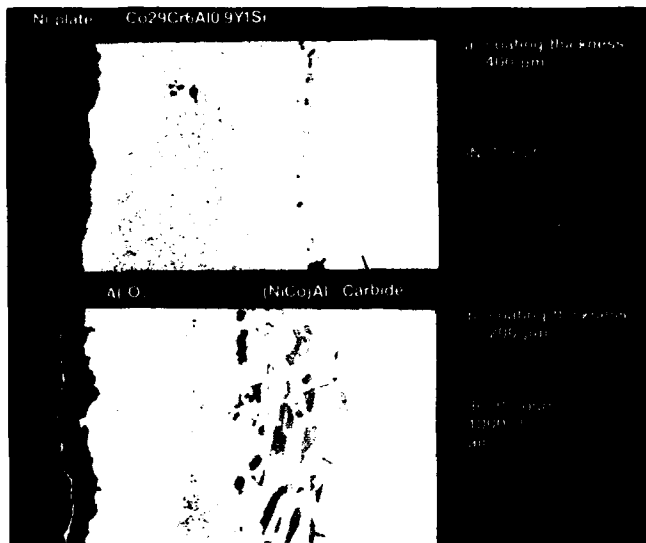


FIG. 1: METALLOGRAPHIC CROSS SECTION OF SI-MODIFIED  
COCRALY COATED IN 738 LC AFTER 5000 HOURS  
OXIDATION IN AIR

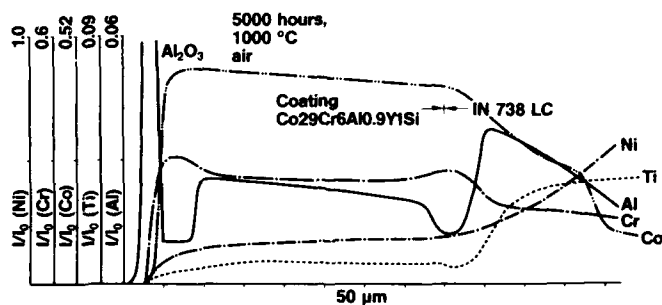


FIG. 2: EDX-DISTANCE PROFILES FOR NI, TI, AL, CR AND CO FROM  
METALLOGRAPHIC CROSS SECTION OF FIG. 1A

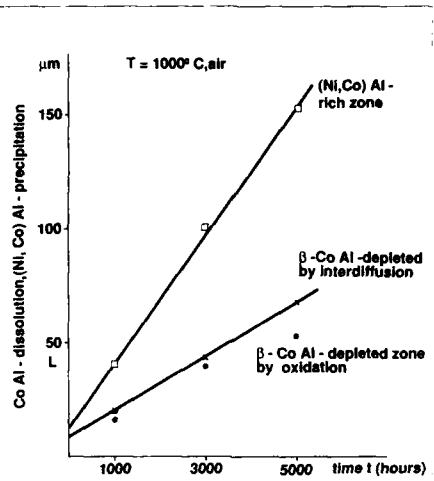


FIG. 3:  $\beta$ -COAL DEPLETION AND  $\beta$ -(Ni, Co) AL PRECIPITATION AT 1000°C IN A Si-MODIFIED COCRALY-COATING

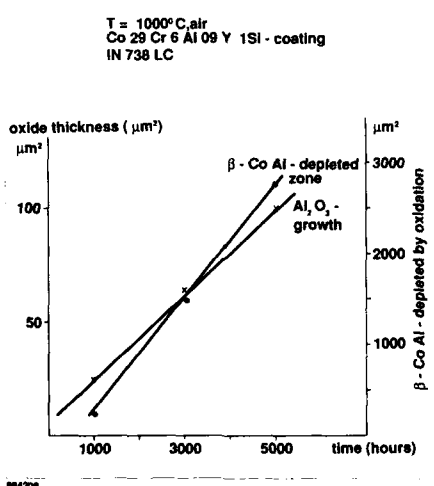


FIG. 4: PARABOLIC PLOT OF  $\text{Al}_2\text{O}_3$ -SCALE GROWTH RATE AND  $\beta$ -COAL DEPLETION AT 1000°C (Si-MODIFIED COCRALY)

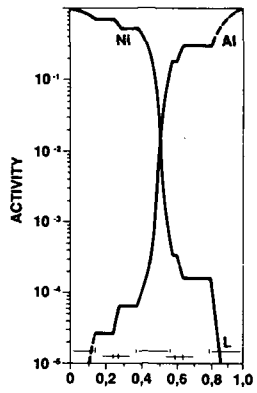


FIG. 5: THERMODYNAMIC ACTIVITIES OF AL AND NI IN THE NI-AL-BINARY SYSTEM (1000°C)

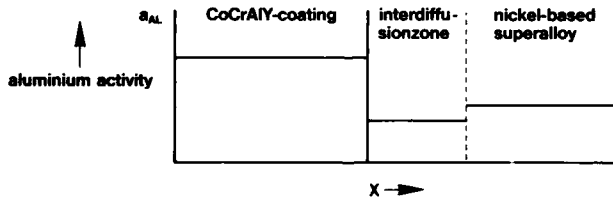


FIG. 6: SCHEMATIC REPRESENTATION OF AL-ACTIVITY IN A COCrAlY-COATING, INTERDIFFUSION ZONE AND NICKEL BASED ALLOY

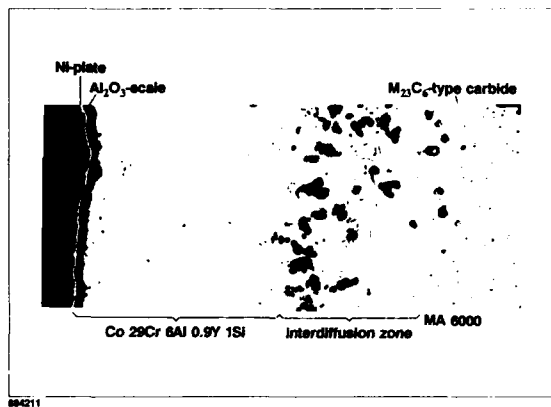


FIG. 7: KIRKENDALL POROSITY FORMATION IN CoCrAlY-COATED MA 6000  
(5000 HOURS, 1000°C, AIR)



FIG. 8: Si-MODIFIED CoCrAlY-COATING AFTER 5000 HOURS AT  
850°C IN AIR

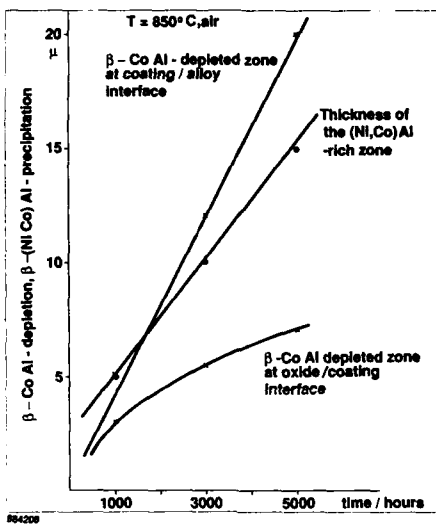


FIG. 9:  $\beta$ -CO AL DEPLETION AND  $\beta$ -(Ni, Co) AL PRECIPITATION AT 850°C IN A Si-MODIFIED COCrAlY-COATING

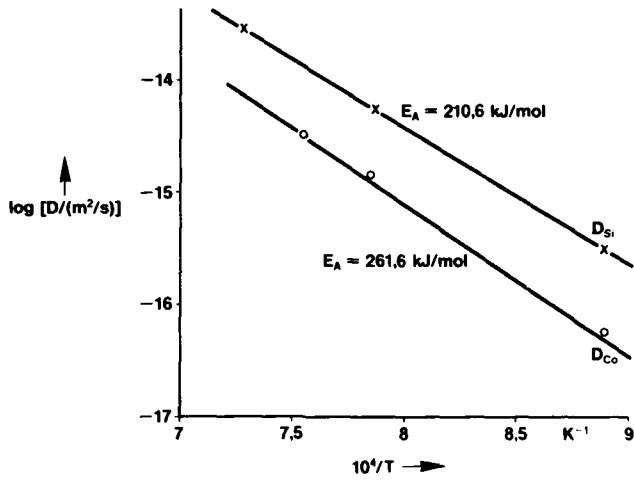


FIG. 10: ARRHENIUS PLOT OF CO AND Si DIFFUSIVITY IN MA 6000 AND IN 738 LC

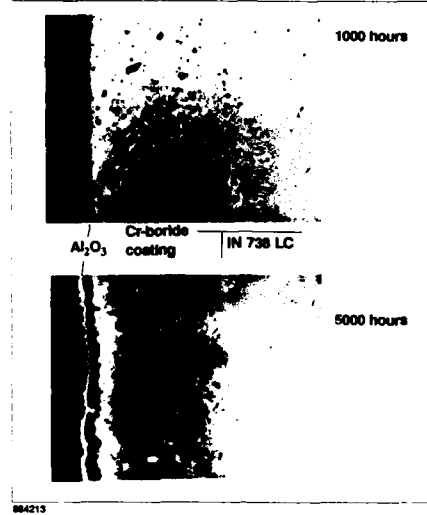


FIG. 11: Si-MODIFIED NiCrAlY-COATING ON IN 738 LC  
(1000°C, AIR)

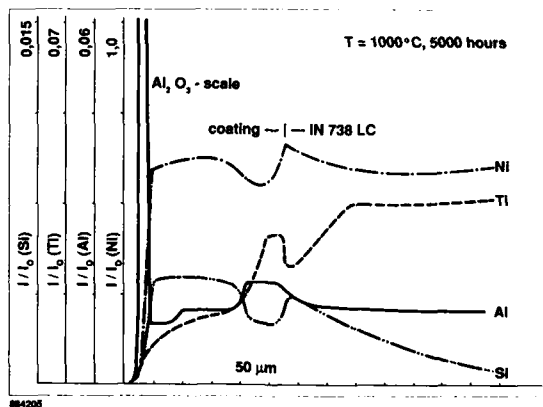


FIG. 12: EDX-PROFILES OF NI, Ti, AL AND SI IN THE NiCrAlY-COATING  
AND IN 738 LC AFTER 5000 HOURS, 1000°C, AIR

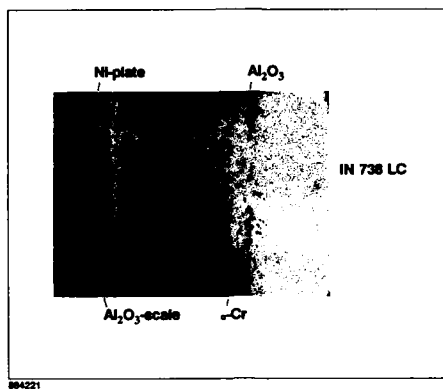


FIG. 13: MICROSTRUCTURE OF SI-MODIFIED NiCrAlY  
IN 738 LC (5000 HOURS, 850°C, AIR)

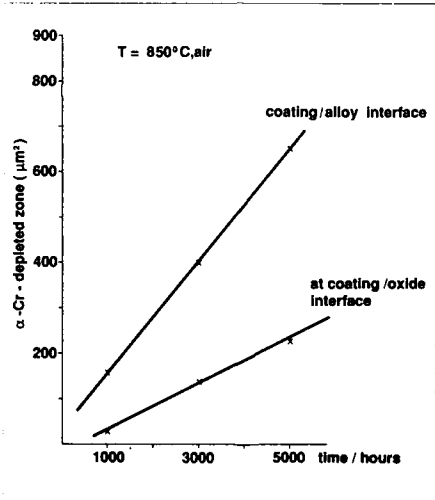


FIG. 14: PARABOLIC PLOT OF  $\alpha$ -Cr DISSOLUTION AT THE COATING SURFACE AND THE COATING/ALLOY INTERFACE AT 850°C

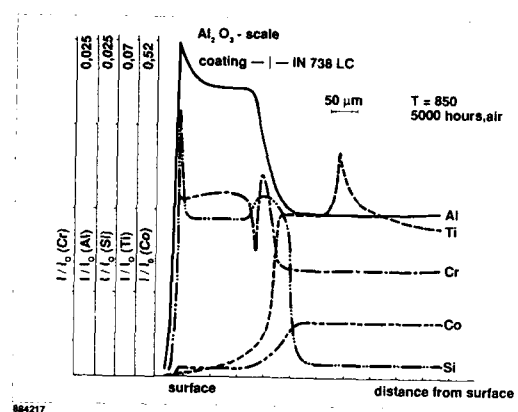


FIG. 15: EDX-PROFILES OF AL, TI, CR, CO AND SI IN A SI-MODIFIED NiCrAlY AND IN 738 LC (5000 HOURS, 850°C, AIR)

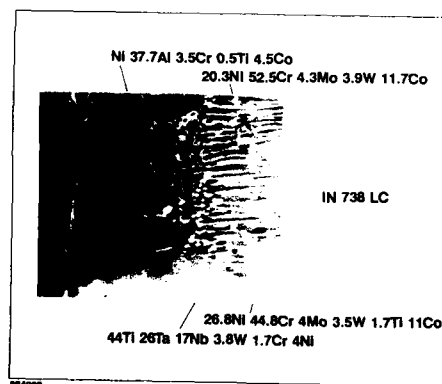


FIG. 16: MICROSTRUCTURE AND COMPOSITION OF ALUMINIZED IN 738 LC (1100°C, 20 HOURS,  $P_{TOT} = 100$  MBAR,  $P_{\text{ALCl}_3} = 2$  MBAR)

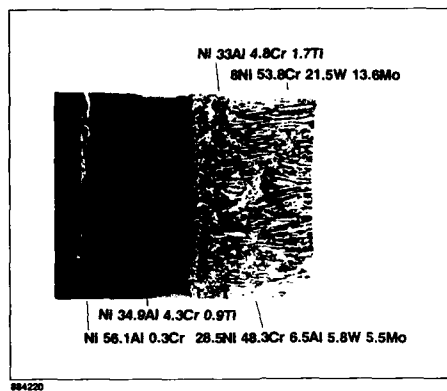


FIG. 17: MICROSTRUCTURE AND COMPOSITION OF ALUMINIZED MA 6000  
(1100°C, 20 HOURS,  $P_{TOT} = 100$  MBAR,  $P_{ALCL_3} = 2$  MBAR)

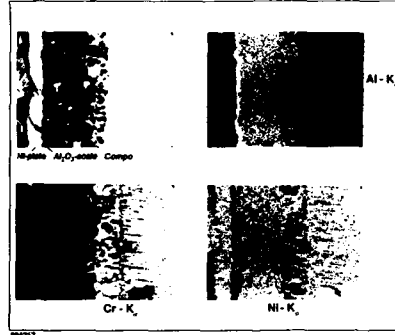


FIG. 18: METALLOGRAPHIC CROSS SECTION AND X-RAY MAPS OF AL, CR, NI  
OF ALUMINIZED IN 738 LC (300 HOURS, 1100°C)

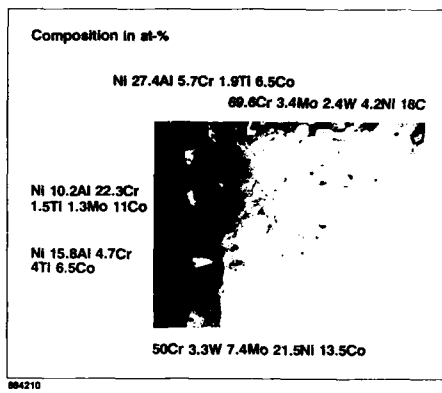


FIG. 19: ALUMINIDE COATING ON IN 738 LC (6000 HOURS, 1000°C, AIR)

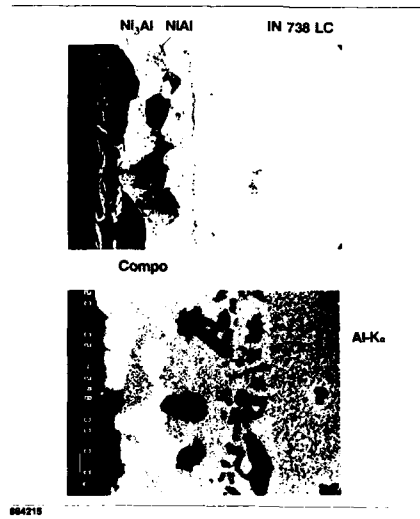


FIG. 20: DEGRADATION OF AN ALUMINIDE COATING ON IN 738 LC  
AT 1100°C (1000 HOURS, AIR)

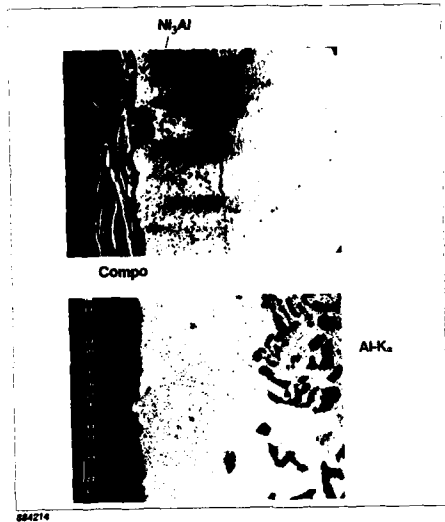


FIG. 21: DEGRADATION OF AN ALUMINIDE COATING ON IN 738 LC  
AT 1100°C (3000 HOURS, AIR)

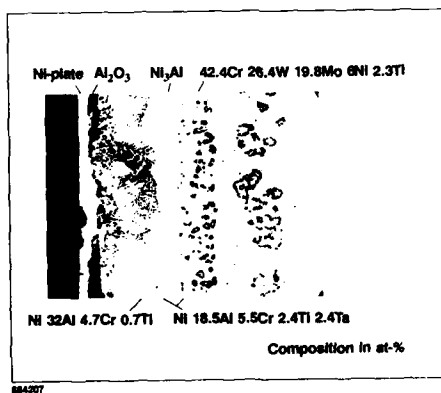


FIG. 22: DEGRADATION OF ALUMINIDE COATING ON MA 6000 AT 1100°C  
(600 HOURS, AIR)

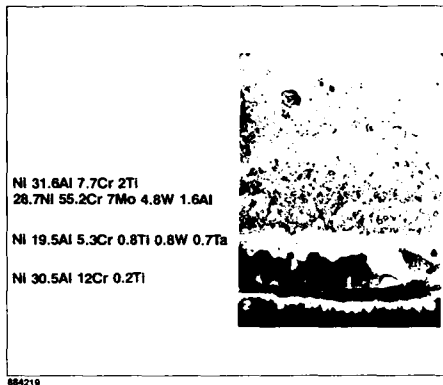


FIG. 23A: METALLOGRAPHIC CROSS SECTION OF ALUMINIZED MA 6000  
AFTER 6000 HOURS EXPOSURE AT 1000°C IN AIR

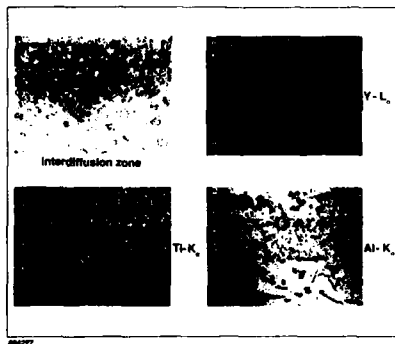


FIG. 23B: METALLOGRAPHIC CROSS SECTION OF THE INTERDIFFUSION  
ZONE OF AL-COATED MA 6000 AND X-RAY MAPS OF AL, TI  
AND Y (6000 HOURS, 1000°C, AIR)

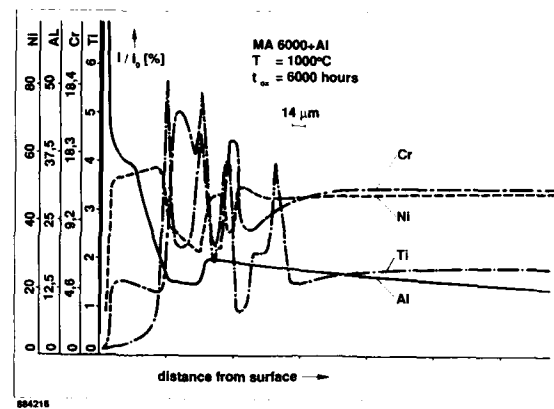


FIG. 24: EDX-PROFILES OF Ti, Al, Ni AND Cr OF AL-COATED MA 6000 AFTER 6000 HOURS EXPOSURE AT 1000°C IN AIR

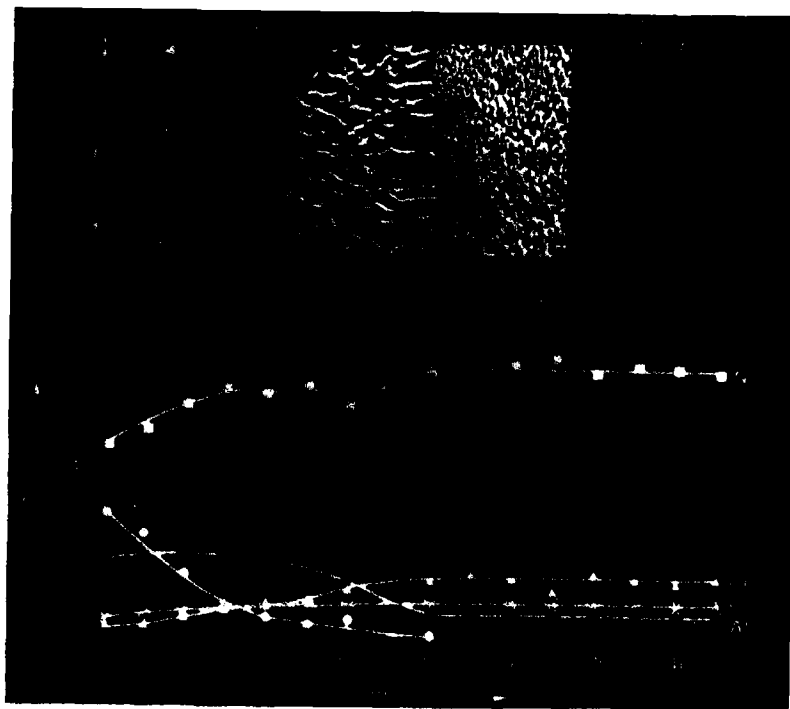


FIG. 25: RT 22-COATING ON IN 738 LC (INITIAL CONDITION)

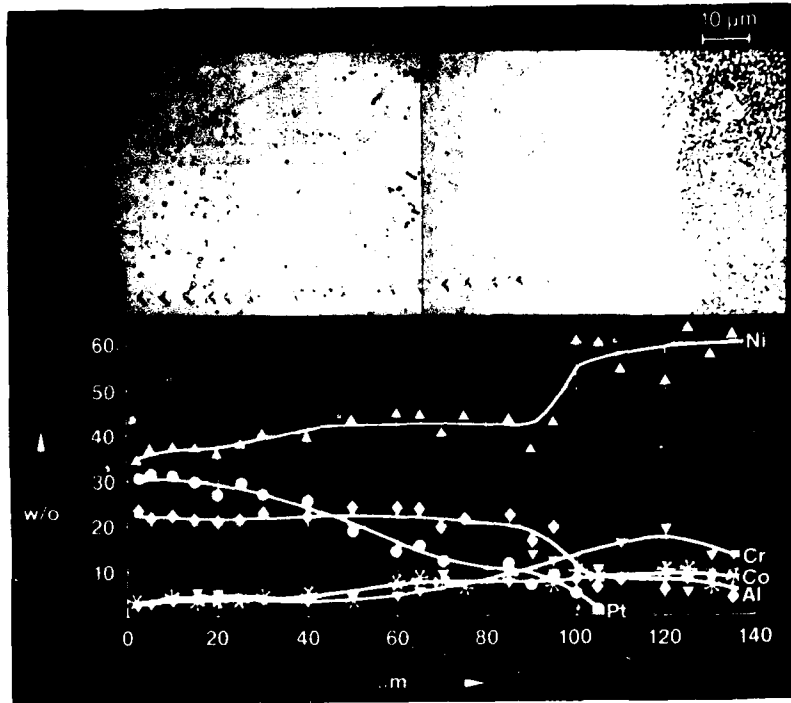


FIG. 26: RT 22-COATING ON IN 738 LC AFTER 5180 HOURS OPERATION AT 950°C

coating	diffusion	superalloy
reduced oxidation resistance	Al—>	increased N <sub>v</sub> -number
change of microstructure	Co—>	precipitation of (Ni,Co)Al
increased oxidation rate	Si—>	increase of N <sub>v</sub> -number, decrease of solidus temperature
increased Al-solubility increased critical Al-concentration for Al <sub>2</sub> O <sub>3</sub> -formation	Cr—>	increase of N <sub>v</sub> -number, σ'-phase formation
increased oxidation rate	<—Ti	decrease of γ-prime
increase of N <sub>v</sub> -number	<—W,Mo	decrease of N <sub>v</sub> -number
increase of N <sub>v</sub> -number	<—Ta	decrease of γ-prime stability
change of microstructure	<—Ni	increase of N <sub>v</sub> -number

FIG. 27: INFLUENCE OF INTERDIFFUSION EFFECTS ON CHEMICAL PROPERTIES OF COATED SUPERALLOYS

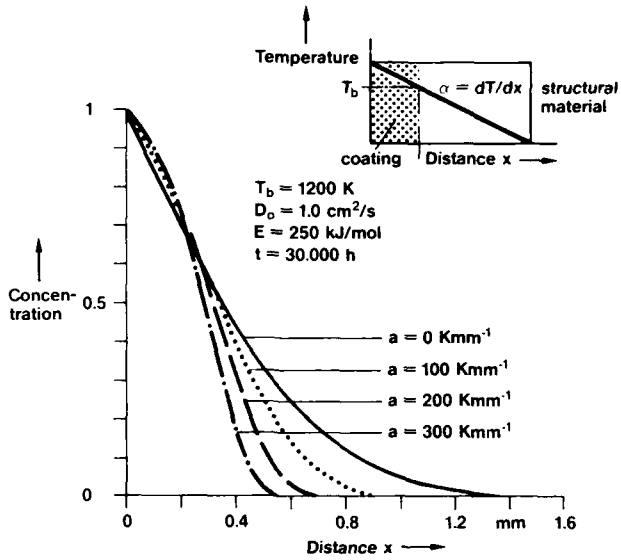


FIG. 28: CALCULATED DIFFUSION PROFILES OF AL UNDER ISOTHERMAL AND NON-ISOTHERMAL CONDITIONS (1200 K AT THE COATING/ALLOY INTERFACE)

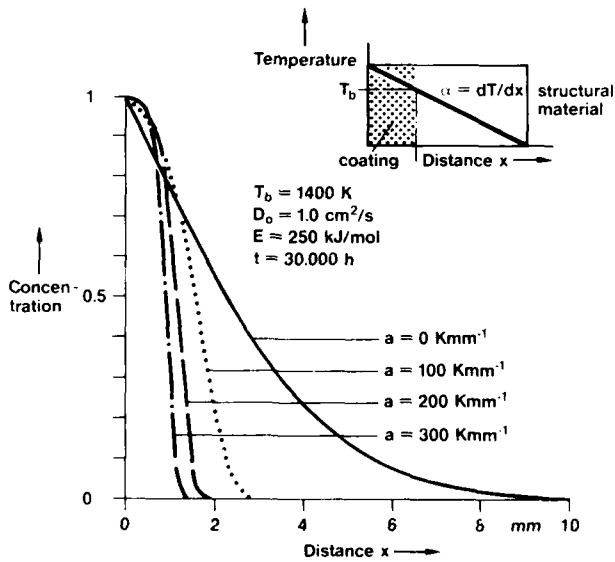


FIG. 29: CALCULATED DIFFUSION PROFILES OF AL UNDER ISOTHERMAL AND NON-ISOTHERMAL CONDITIONS (1400 K AT THE COATING/ALLOY INTERFACE)

### DISCUSSION

E. Thompson, United Technologies Research Center, US. Would you comment further on the precipitation of the yttrium-containing phase in the coated MA 6000 alloy? Is this effect well known?

Mr Singheiser, Brown, Boveri & Cie, FRG. What we observe is agglomeration of yttrium oxide dispersoids in the interdiffusion zone of MA 6000. The dispersoids do not agglomerate in the bulk of the material even after long time exposures at temperature. The phenomenon is not yet fully understood. Yttria agglomeration also occurs during pack aluminizing of MA 754, resulting in poor adherence of the aluminide coating on the alloys. We assume that a gradient in surface tension may be responsible for yttria agglomeration if precipitation of additional phases occurs. The particles can be moved and enriched ahead of the growing precipitate. The higher susceptibility of oxide dispersion strengthened alloys to void formation may be attributed to lower activation energies for condensation of vacancies to form stable voids.

E. Thompson, United Technologies Research Center, US. How deep into the alloy did you see this effect?

Mr Singheiser, Brown, Boveri & Cie, FRG. About 100 micrometers. It depends on time and temperature, and the agglomeration occurs only in the interdiffusion zone.

### VACUUM PLASMA SPRAY COATING

Richard R. Holmes  
 Materials and Processes Laboratory  
 National Aeronautics and Space Administration  
 George C. Marshall Space Flight Center  
 Huntsville, Alabama 35812, USA

and

Timothy N. McKechnie  
 Rocketdyne Division, Rockwell International  
 2227 Drake Avenue SW, Suite 45  
 Huntsville, Alabama 35805, USA

### ABSTRACT

Currently, protective plasma spray coatings are applied to space shuttle main engine turbine blades of high-performance nickel alloys by an air plasma spray process. Originally, a ceramic coating of yttria-stabilized zirconia ( $ZrO_2 \cdot 12Y_2O_3$ ) was applied for thermal protection, but was removed because of severe spalling.

In vacuum plasma spray coating, plasma coatings of nickel-chromium-aluminum-yttrium (NiCrAlY) are applied in a reduced atmosphere of argon/helium. These enhanced coatings showed no spalling after 40 MSFC burner rig thermal shock cycles between 927°C (1700°F) and -253°C (-423°F), while current coatings spalled during 5 to 25 test cycles.

Subsequently, a process was developed for applying a durable thermal barrier coating of  $ZrO_2 \cdot 8Y_2O_3$  to the turbine blades of first-stage high-pressure fuel turbopumps utilizing the enhanced NiCrAlY bond-coating process. NiCrAlY bond coating is applied first, with  $ZrO_2 \cdot 8Y_2O_3$  added sequentially in increasing amounts until a thermal barrier coating is obtained. The enhanced thermal barrier coating has successfully passed 40 burner rig thermal shock cycles.

### INTRODUCTION

Hydrogen fuel is supplied to the Space Shuttle Main Engine (SSME) combustion chamber by the High Pressure Fuel Turbopump (HPFTP). Each turbine blade, about the size of a 25-cent piece and rotating at 34,700 rpm, develops approximately 600 horse power during operation, undergoing tremendous dynamic stress. The blades are heated instantaneously from cryogenic temperatures at engine start-up to the operating temperature with gaseous hydrogen at 1500°F (815°C) in less than one second. After 500 seconds of flight operation, the blades are quenched with liquid hydrogen, -423°F (-253°C) at engine shutdown. The thermal shock at start-up and shutdown plus the dynamic stress of rotation, induce high thermal strains on the surfaces of the turbine blades. This harsh environment causes some of the blades to crack and have to be replaced, realizing a shorter service life than desired.

Baseline coatings for thermal protection were applied initially to the SSME turbine blades by air plasma spray coating with both NiCrAlY (Ni-16Cr-5.6Al-0.6Y) bond coating, and yttria stabilized zirconia ( $ZrO_2 \cdot 12Y_2O_3$ ), thermal barrier top coating. The zirconia coating was deleted immediately from the application procedure because of severe spalling or flaking away of the coating in turbine engine test firings. Although some thermal protection was realized by the air plasma NiCrAlY bond coating, this coating also spalled in the harsh environment of the SSME.

The objective of this investigation was to demonstrate that durable Thermal Barrier Coatings (TBC's) could be applied to the SSME by Vacuum Plasma Spray coating (also referred to as Low Pressure Plasma Spray, LPPS, coating). Vacuum plasma spray coating offered the following advantage over air plasma spray coatings:

- (1) Exclusion of oxides (stronger bond)
- (2) Denser, less porous coating
- (3) Reverse polarity transferred arc cleaning
- (4) Mach 3 velocities (better adhesion)
- (5) Improved coating thickness uniformity
- (6) Part can be preheated and coated at its operating temperature.

The next milestone in this program will be to utilize the improved coating adhesion/durability of the thermal barrier coating, to realize improved engine performance, longer turbine blade life and reduced maintenance costs. These improvements will be demonstrated in a Turbine Engine Rainbow Wheel Test followed by Certification Engine Tests.

### PROCEDURE

All vacuum plasma coatings were developed in the Vacuum Plasma Spray Facility at Marshall Space Flight Center. The equipment was purchased from Electro Plasma, Inc., Irvine, California, and consists of a 5-ft diameter vacuum chamber with a 120 KW EPI-03 plasma head. Five axes of motion are provided by the plasma head in conjunction with the target or workpiece. Minus 200/+325 or -400 mesh powder was supplied to the plasma head by four powder feeder hoppers. An inert gas mixture of 80% argon and 20% helium was used

as the plasma arc gas while pure argon was used as the powder carrier gas. Oxygen was purged from the system by pulling a vacuum to 50 microns two times and back filling with 99.999% pure argon. The second time, the chamber was flushed, it was back filled to a 20-60 Torr level and operated at that level by regulating the vacuum. Vacuum was pulled by a 300 cfm Stokes vacuum pump in tandem with a second 300 cfm vacuum pump with a 1600 cfm roots blower. The plasma gun, workpiece motion, powder feeder, primary and secondary gas flow, and other essential process parameters were controlled automatically by an Allen Bradley microprocessor.

After the chamber was back filled the second time and regulated at a low pressure of 20-60 Torr, the workpiece was preheated to 1500° to 1700°F with the plasma gun regulated between 80 and 90 kW. During the preheat cycle, the turbine blades were transferred arc cleaned by negatively biasing the workpiece relative to the gun anode. Powder particles injected into the plasma arc stream were melted/softened and simultaneously accelerated toward the workpiece where they adhered on impact. Bond coating was 0.002 in. with the thermal barrier top coating 0.004 in., both coatings applied with an accuracy of  $\pm 0.0015$  in. The bond coating was 0.006 in. when applied as the only coating.

The Thermal Barrier Coatings (TBC's) were applied by Vacuum Plasma Spray (VPS) or Air Plasma Spray (APS) onto MAR-M-246(Hf) turbine blades and tested for adherence in the MSFC Burner Rig Thermal Shock Tester. In addition, the thermal conductivities of the coatings were measured and the densities calculated.

The materials used for TBC's were: Ni-16.5 CR-5.5 Al-0.55Y and  $ZrO_2-8Y_2O_3$ , and combinations of both materials.

The VPS coatings were applied in the VPS Facility of NASA's MSFC. The APS coatings were applied by an SSME approved vendor, Plasma Coating Corporation.

#### RESULTS

##### Thermal Shock Adhesion

SSME HPFTP First Stage MAR-M-246(Hf) turbine blades were tested in the MSFC Turbine Blade Thermal Shock Tester for coating adherence by thermal cycling from 1700°F (927°C) to -350°F (-212°C). Test cycling has been described in earlier literature [1]; the tester operates between environments of burning H<sub>2</sub> gas at 1700°F (927°C) and quenching liquid hydrogen at -423°F (-253°C). Six blades are tested each time. A normal test is 25 cycles of 15 seconds duration each. The coated blades are examined after a total of 5, 15, and 25 cycles. The coating adherence found is listed in Table 1 [2]. The APS coating of NiCrAlY and NiCrAlY/ZrO<sub>2</sub> spalled randomly during testing; some coatings spalled after 5 cycles while others produced in the same batch exhibited a life of 25 cycles. Some vacuum plasma coated blades tested 40 cycles without spalling, when they were used to replace air plasma coated blades that failed. The poor APS coating adhesion and poor repeatability were both unacceptable. The VPS coatings of NiCrAlY, NiCrAlY/ZrO<sub>2</sub>.8Y<sub>2</sub>O<sub>3</sub> mixture, and NiCrAlY with APS ZrO<sub>2</sub>.8Y<sub>2</sub>O<sub>3</sub> topcoat showed no signs of spalling in the typical 25 cycle testing, or the extra 40 cycle testing, but APS zirconia topcoats did show signs of erosion. These thermal shock tests demonstrated the large increase in coating adherence due to the VPS process as compared to APS. The attributes of VPS are an oxide free bond coating and coating/substrate interface, greater density and uniformity. These attributes are well described in the literature [3-5].

##### Thermal Conductivity

Thermal conductivities of six coatings, 0.010 in. thick, were calculated from specific heat ( $C_p$ ), density ( $d$ ), and thermal diffusivity ( $\alpha$ ) measurements [2]. The thermal conductivity ( $\lambda$ ) was found by taking the product of the measurements according to:

$$\lambda = C_p d \alpha .$$

The measurements were determined by:

$C_p$  - differential scanning calorimetry

$\alpha$  - laser flash technique

$d$  - bulk density from geometry and mass.

All thermophysical measurements were conducted at the Thermophysical Properties Research Laboratory at Purdue University [6]. The thermal conductivities are plotted in Figure 1 in the temperature range of -200° to 1000°C. The thermal conductivities in descending order of conductivity are:

VPS NiCrAlY  
 VPS 70% NiCrAlY/30%  $ZrO_2-8Y_2O_3$  (by volume)  
 APS NiCrAlY  
 APS 70% NiCrAlY/30%  $ZrO_2-8Y_2O_3$  (by volume)  
 APS  $ZrO_2-8Y_2O_3$ .

These data clearly show that thermal conductivity is related to both the material properties and the processing. The same NiCrAlY/ZrO<sub>2</sub>8Y<sub>2</sub>O<sub>3</sub> mixture applied by the two different processes gave different thermal conductivities as well as different thermal shock performance lives.

#### Density

The bulk densities of each coating are shown in Figure 2. It is quite evident that the thermal conductivity is also directly related to density of the material [2]. With increased oxide and porosity content, the density and thermal conductivity become lower.

#### DISCUSSION OF RESULTS

The thermal conductivity of Thermal Barrier Coatings has been found to directly relate to:

- (1) Coating application
- (2) Coating adhesion
- (3) Coating density
- (4) Material properties

and indirectly relate to:

- (1) Amount of oxide content
- (2) Porosity.

The VPS coatings with higher thermal shock adhesion and density had higher thermal conductivities. The APS coatings of the same materials were more porous and oxidized, and therefore had lower thermal conductivities. The difference between APS and VPS coatings illustrates the tradeoffs encountered in the design of TBC's between thermal conductivity, density, and coating life. The more insulative coatings do not have the life of less insulative coatings.

With the flexibility of VPS, coatings can be tailor made for the application. Since the coating adherence problem has been overcome with the VPS process, more insulative coatings are now being developed. VPS coatings containing greater volumes of ceramics are being developed, and these are thought to increase the thermal dampening capability past those tested in this study.

#### CONCLUSION

Durable thermal protective coatings and application processes have been developed and demonstrated that withstand the rigorous environment of the SSME, based on results from the MSFC Burner Rig Thermal Shock Tester. Insulative VPS (vacuum plasma spray) TBC's (Thermal Barrier Coatings) have been shown to adhere to the SSME turbine blades for 40 thermal shock cycles without any signs of spalling. Existing APS (Air Plasma Spray) coatings spall after as few as 5 cycles. The TBC's can increase the thermal low cycle fatigue life of SSME HPFTP (High Pressure Fuel Turbopump) turbine blades and nozzle/stators (vanes that direct the flow of gaseous hydrogen fuel onto the blades) by affording thermal protection from severe thermal shock.

The methods of application of TBC's has a significant effect on the life and thermal conductivity of the coating, in addition to the effect realized from the properties of the coating material. Coatings applied by the Vacuum Plasma Spray Process, while uniform, dense and durable, also show greater thermal conductivity than porous, non-durable APS coatings. To obtain the equivalent reduced thermal conductivity of APS coatings, it is necessary to increase the ceramic, ZrO<sub>2</sub>.8Y<sub>2</sub>O<sub>3</sub>, content of the VPS coatings. New coatings are currently being developed that extend the ceramic content of VPS coatings from 30 volume percent ceramic to 70 volume percent.

Preliminary tests in the MSFC Burner Rig Thermal Shock Tester indicate that the 70% ceramic by volume coatings will be as durable as demonstrated by the 30% ceramic by volume coatings reported on in this paper. This current work will be expedited and reported at a later date.

#### REFERENCES

1. Richard R. Holmes, "Vacuum Plasma Coating for Turbine Blades," Advanced High Pressure O<sub>2</sub>H<sub>2</sub> Technology, NASA Conference Publication 2372, 1985, pp. 74-90.
2. R. R. Holmes and T. N. McKechnie, "Vacuum Application of Thermal Barrier Plasma Coatings," 1988 Conference on Advanced Earth-to-Orbit Propulsion Technology, May 10-12, 1988, NASA/University of Alabama in Huntsville.
3. H. Gruner, "Vacuum Plasma Sprayed Composite Coatings," Advances in Thermal Spraying, ITSC 1986, Pergamon Press, Welding Institute of Canada, pp. 73-82.
4. D. Houck, "Thermal Spray: Advance in Coatings Technology," Proceedings of National Thermal Spray Conference, 1987, ASM International.
5. S. Shankar, D. E. Koenig, and L. E. Dardi, "Vacuum Plasma Sprayed Metallic Coatings," Journal of Metals, Vol. 33, No. 10, October 1981, pp. 13-20.

6. R. E. Taylor, H. Groot, and J. Larimore, Thermophysical Properties of Coatings, 1988, Purdue University.

TABLE 1. Thermal Shock Cyclic Testing Between 927°C and -212°C

BOND COATING*	THERMAL BARRIER COATING (.004 IN)	NUMBER OF CYCLES	COMMENTS
VPS NiCrAlY	--	40	NO SPALLING
APS NiCrAlY	--	5-25	SPALLING
VPS NiCrAlY	VPS NiCrAlY/ZrO <sub>2</sub> · 8Y <sub>2</sub> O <sub>3</sub>	40	NO SPALLING
VPS NiCrAlY	APS ZrO <sub>2</sub> · 8Y <sub>2</sub> O <sub>3</sub>	25	NO SPALLING, EROSION OF POROUS ZrO <sub>2</sub> · 8Y <sub>2</sub> O <sub>3</sub>
APS NiCrAlY	APS ZrO <sub>2</sub> · 8Y <sub>2</sub> O <sub>3</sub>	5-25	SPALLING

\* BOND COATING ONLY: 0.006 IN. THICKNESS

BOND COATING BEFORE ADDING THERMAL BARRIER COATING: 0.002 IN. THICKNESS

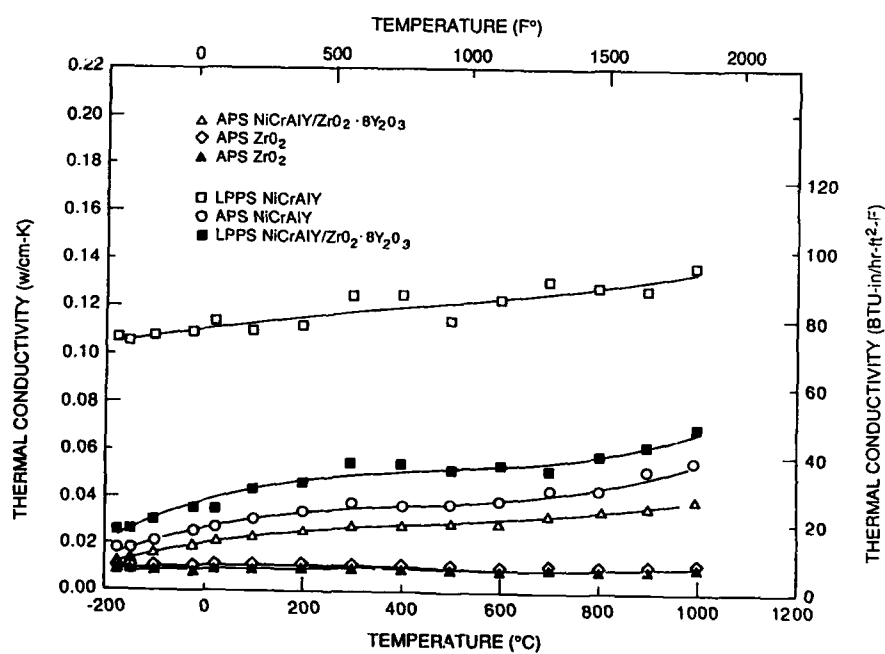


Figure 1. Thermal Conductivity of Coatings

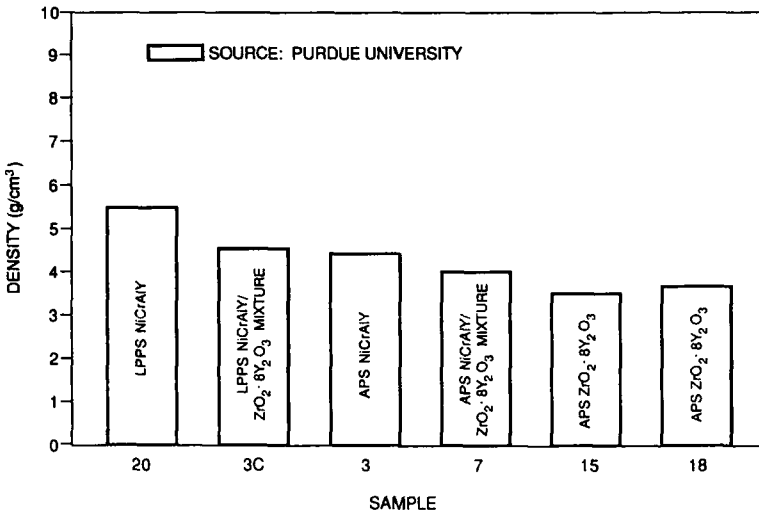


Figure 2. Density of Plasma Coatings

#### DISCUSSION

R. Eck, Metallwerk Plansee, Austria. In one of your diagrams you showed absolute densities of low pressure plasma sprayed materials. What is the residual porosity of the densest material and what do you consider an average density?

R. Holmes, NASA-Marshall, US. The air plasma sprayed material is a little less than 90% dense and the low pressure plasma sprayed material is greater than 99% dense.

Unidentified Questioner

Have these coatings been flown on the shuttle yet?

R. Holmes, NASA- Marshall, US. We have 400 flight quality turbine blades on order at the moment. They'll be coated at a vendor, then go into a rainbow-wheel turbine engine test, from there they'll go into a certification engine test, and then into the engine. That will take about two years. The titanium main fuel valve housing that I showed will be tested and should go into shuttle use in April 1989.

J-M. de Monicault, SEP, France. After coating, do you need to remachine the blade?

R. Holmes, NASA-Marshall, US. No, but we do polish them to improve operating efficiency.

## THRUST CHAMBER THERMAL BARRIER COATING TECHNIQUES

Richard J. Quentmeyer  
 National Aeronautics and Space Administration  
 Lewis Research Center  
 Cleveland, Ohio 44135 U.S.A.

### SUMMARY

Methods for applying thermal barrier coatings to the hot-gas side wall of rocket thrust chambers in order to significantly reduce the heat transfer in high heat flux regions has been the focus of technology efforts for many years. This paper describes a successful technique developed by the Lewis Research Center that starts with the coating on a mandrel and then builds the thrust chamber around it by electroforming appropriate materials. This results in a smooth coating with exceptional adherence, as has been demonstrated in hot fire rig tests. The low cycle fatigue life of chambers with coatings applied in this manner has been increased dramatically compared to uncoated chambers.

### INTRODUCTION

High pressure, reusable rocket thrust chambers, such as the Space Shuttle Main Engine (SSME), encounter a progressive deformation and thinning of the cooling passage wall during engine operation. The deformation is caused by a large, thermally induced, plastic strain that occurs in the hot-gas side wall during each thermal cycle. This phenomenon is known as plastic ratcheting and, after numerous thermal cycles, causes cracks to form in the cooling passage wall.<sup>1-6</sup>

One method of reducing, or eliminating the plastic strain, is to apply a thermal barrier coating (TBC), such as zirconium-oxide ( $ZrO_2$ ), to the combustion-side wall of the thrust chamber. The use of TBC's to increase thrust chamber life is not a new concept. And many experimental programs have been conducted to perfect TBC's for use on rocket engines.<sup>7-12</sup> However, their use has been limited due to the tendency of the TBC's to spall after repeated thermal cycles. This is caused by the inability of the relatively brittle TBC to absorb the compressive strain that occurs in the coating during engine operation.

Most of the experimental work with TBC's was done with coatings greater than 0.25 mm thick, which is too thick for use on high pressure rocket thrust chambers. The TBC thickness required for use on a rocket thrust chamber where the throat heat flux is in the range of 80 to 160 MW/m<sup>2</sup>, is 0.12 to 0.012 mm,<sup>12</sup> depending on the effective thermal conductivity of the coating. Experience has shown that the thinner the coating, the better is its ability to absorb the compressive strain and remain bonded to the substrate.<sup>13</sup> Therefore, the use of TBC's on high pressure rocket thrust chambers offers the potential of substantially increasing life.

The normal procedure of applying TBC's is to apply a bond coat, such as nickel-chromium or nickel-chromium-aluminum-yttrium, onto the inner wall of an already fabricated thrust chamber liner, and then plasma spray the TBC layer over the top. Problems associated with this method of application include oxidation of the substrate, especially copper, during the application of the bond coat, a residual compressive stress which develops in the ceramic coating after the coated chamber returns to room temperature, and a relatively rough coating surface which increases the hot-gas-side heat transfer coefficient during engine operation. All of these phenomenon are detrimental to coating endurance.

Another method of applying a TBC, which reduces or eliminates the phenomenon described above, is to fabricate the thrust chamber inside out (i.e., start with the TBC and fabricate the chamber liner around it). A method of fabricating coated chambers by this technique, called the "electroform pickup process," was developed by the Lewis Research Center.<sup>14</sup> The process consists of plasma spraying the TBC onto a mandrel, applying the bond coat to the TBC, and then electroforming the thrust chamber liner around the coating. A 0.203-mm-thick  $ZrO_2$  TBC applied to a subscale rocket thrust chamber with this technique demonstrated excellent performance during cyclic testing.<sup>15</sup> However, there remained a need to evaluate thin TBC's with this technique for application on high pressure rocket thrust chambers.

At Lewis, there has been an ongoing program to develop techniques for applying thin TBC's to rocket thrust chambers, both by applying coatings to already fabricated chambers,<sup>16</sup> and by applying coatings by using the electroform pickup process. The objective of the effort described in this report was to evaluate the performance and durability of thin TBC's applied to rocket thrust chambers by the electroform pickup process. The results reported herein are for a nominally 0.076-mm  $ZrO_2$  coating applied to a subscale annular rocket thrust chamber by the electroform pickup process. The chamber was cyclically tested at a 4.14-MPa chamber pressure with liquid oxygen and gaseous hydrogen as propellants, and liquid hydrogen as the coolant. The experimental results are compared with an identical chamber tested without the TBC applied to the inner wall.

## APPARATUS AND TEST PROCEDURE

### Annular Rocket Thrust Chamber Assembly

Figure 1 shows a schematic of the annular rocket thrust chamber. The apparatus consisted of an annular injector; a contoured centerbody, which formed the combustion chamber, throat, and nozzle sections of the thrust chamber; and an outer cylinder, which served as the test section. The thrust chamber had a contraction and expansion area ratio of 1.79. At a chamber pressure of 4.14 MPa the thrust was approximately 5.34 kN with gaseous hydrogen and liquid oxygen as propellants. The cylindrical test section was separately cooled with liquid hydrogen, and the centerbody was cooled with water. Figure 2 shows the thrust chamber assembly with a cutaway of the cylindrical test section.

#### Injector

The injector was designed to operate with liquid oxygen and gaseous hydrogen. The oxygen was injected through 70 showerhead tubes arranged in two circular rows, 36 in the inner row and 34 in the outer row. The tubes were made of 0.23-cm-o.d. stainless steel having a 0.03-cm-thick wall. Two chamber pressure taps were located in the outer row of oxidizer tubes. All of the gaseous hydrogen was injected through the porous Rigmesh face plate. The face plate was removable, so that it could be replaced if damaged. The characteristic exhaust velocity efficiency averaged 95 percent.

#### Centerbody

The contoured centerbody was fabricated from copper with 40 rectangular cooling passages running axially throughout its length. The diameter in the combustion zone was 4.06 cm and 5.33 cm at the throat. The centerbody was 15.24 cm in length with a 7.5° half-angle conical expansion section. It was inserted through the injector and bolted into place from the back side.

A 0.076- to 0.127-mm zirconium-oxide coating was applied by conventional flame spray techniques to the outside surface to reduce the heat load and prolong the centerbody life. Water entered the centerbody from behind the injector, passed through the cooling passages, and was dumped at the thrust chamber exit.

#### Cylindrical Test Section

The conventional method of fabricating high pressure rocket thrust chambers is to machine cooling channels into a copper alloy liner and then close out the cooling channels by electro-deposition. If a coating (TBC) is to be used, it is normally applied to the chamber after fabrication. However, the cylindrical test section used in this program was fabricated by starting with the TBC and then building the chamber around it.

The cylinder was 15.24 cm in length and had an inside diameter of 6.60 cm. The fabrication sequence is shown figure 3. The process was started by machining an aluminum mandrel to the desired cylindrical shape. The TBC, in this case, an yttria-stabilized zirconia, was plasma sprayed onto the mandrel to a nominal thickness of 0.076 mm. A nickel-chromium bond coat was sprayed over the zirconium-oxide to a nominal thickness of 0.025 mm. The bond coat served not only to protect the copper substrate, but also rendered the surface electrically conductive. The mandrel assembly was then placed in a copper sulfate bath where it was continuously rotated during the plating operation. After a sufficient layer of copper was plated to the surface, the assembly was removed from the plating bath and the copper surface was machined to the proper diameter. Following this operation, 72 constant area cooling channels, 0.169 cm wide and 0.127 cm high, were milled into the copper liner. After machining, the cooling channels were filled with wax and the assembly placed back into the plating bath to electro-deposit the copper closeout. The wax was then removed from the cooling channels and the aluminum mandrel removed chemically. Final machining was performed and the manifolds added. This method of fabrication produced a smooth and even TBC having a surface finish of 0.7  $\mu\text{m}$  rms. Figure 4 shows a cross-section of the cylinder wall with the cooling channel dimensions.

#### Instrumentation

The instrumentation of the cylindrical test section consisted primarily of chrome/constantan thermocouples. Eight thermocouples were located in the cooling passage ribs, four at one depth and four at another depth. Eight thermocouples were also located on the cylinder backside wall. The thermocouples were equally spaced circumferentially and all were located at the thrust chamber throat plane. The rib thermocouples were spring loaded against the bottom of the rib holes while the backside thermocouples were peened into the surface. Figure 5 shows typical thermocouple locations and figure 5 shows a coated cylinder with the instrumentation installed. In addition to the instrumentation described above, the liquid hydrogen inlet and outlet temperatures and pressures were also measured.

### Test Facility

The tests were conducted at the Lewis Research Center rocket engine test facility. This is a 222 410-N sea-level rocket test stand equipped with an exhaust-gas muffler and scrubber. Propellants and coolants are supplied to the test stand using pressurized tanks. The liquid hydrogen used to cool the cylindrical test section was disposed of through a burn-off stack. The thrust chamber exhaust gas and the centerbody cooling water were expelled into the scrubber. Because of the small volume of the thrust chamber combustion zone, an external torch using gaseous hydrogen and gaseous oxygen was used to back-light the combustion chamber.

### Data Recording

All pressures and temperatures were recorded in digital form on a magnetic tape. The digital recording system was set at a basic rate of 2500 samples per second. After processing, all of the data and calculations performed on the data could be printed out on the control room terminal.

### Test Procedure

The cyclic tests were conducted so that the heat-up portion of the cycle was long enough for the hot-gas side wall temperature to reach steady-state, and where the chill-down portion of the cycle was long enough to bring the entire cylinder back to liquid hydrogen temperature. Total cycle time was 3.5 sec, 1.7 sec of burn time and 1.8 sec of chill-down time.

In order to create the maximum thermal strain in the cylinder wall, the liquid hydrogen flowed continuously for the entire cyclic test series. During the first cycle of any given test, a liquid hydrogen precool was used to bring the entire cylinder to liquid hydrogen temperature prior to ignition of the propellants. Short tests, consisting of just two cycles, were made before a cyclic test series in order to establish the desired chamber pressure and liquid hydrogen weight flow. After the desired test conditions were achieved, the thrust chamber was continuously cycled until the supply of liquid hydrogen was depleted. Generally, 70 to 90 cycles could be achieved on one tank of hydrogen. Figure 6 shows a computer plot of chamber pressure and liquid hydrogen weight flow for a typical cycle. Figure 7 shows the annular thrust chamber during cyclic testing.

A controller was used to control mixture ratio and chamber pressure. The liquid hydrogen flow was controlled by tank pressure and valve position. Water flow for the centerbody was set to the maximum obtainable and flowed continuously throughout the cyclic tests. All testing was monitored by closed-circuit television and a test cell microphone. The television and audio outputs were recorded on magnetic tape. After each test series, the cylinder was inspected to observe the condition of the coating.

### TEST RESULTS

The objective of the program was to thermally cycle the coated cylinder to evaluate the performance and durability of the coating and its effect on cylinder life. After 1450 cycles, the testing was terminated due to the large amount of liquid hydrogen being consumed. The coating sustained only minor damage and proved to be very effective.

#### Post-test Destructive Analysis

After the testing was terminated, the cylinder was sectioned to study the coating morphology and to determine the amount of damage to the wall of the cooling passages.

Figure 8 shows the two halves of the cylinder after longitudinal sectioning. One half of the cylinder was also sectioned at the throat plane to examine a cross section of the coating and cylinder wall in the high heat flux region. It can be seen that there was no coating loss in the throat region, but some delamination of the ceramic layer occurred in the low heat flux region of the combustion zone. However, this delamination did not extend down to the bond coat, indicating a good bond between the ceramic layer and the bond coat.

The entire coating surface exhibited a micro-crack morphology, with the surface texture of the zirconia varying from relatively smooth in the throat region, shown at 500x in figure 9, to a rougher surface in the combustion zone upstream of the throat, shown at 250x in figure 10. The micro-crack morphology for the throat region is shown in cross section in figure 11. These surface cracks act as stress relieving locations and tend to prevent the coating from spalling. This phenomenon has been observed on ceramic coated turbine blades and attempts have been made to precrack the coating to provide these stress relieving sites before testing.<sup>17-18</sup>

The cylinder was also sectioned in the region upstream of the throat, where the coating delaminated. The coating surface is shown in figure 12 at a point where the delamination occurred. Note the micro-crack morphology in the upper portion of the figure where the coating remained intact. This same location is shown in cross section in figure 13. It can be seen that a layer of ceramic remains adhered to the bond coat.

Delamination of the coating within the ceramic layer is typical of the coating failure mechanism when there is good adhesion between the ceramic and the bond coat.<sup>15,19</sup> However, if a sufficient layer of ceramic remains, the substrate may still be adequately protected. An identical chamber, with a 0.2 mm zirconium-Oxide TBC, was tested at the same conditions.<sup>15</sup> Seventy percent of the ceramic layer delaminated to a uniform thickness of approximately one-third of the original thickness after 80 thermal cycles. However, there was no loss of the coating down to the bond coat or substrate, and the cylinder wall remained well protected for an additional 579 cycles with no further delamination. The most significant point is that the cylinder tested in this program had no coating loss at the throat after 1450 cycles, which indicates that the thinner coating is more strain tolerant.

The effectiveness of the coating is exhibited in figure 14. This is a cross section of the cylinder wall at the throat plane. The original geometry of the cooling passages is still intact, and there is no apparent damage to the wall. This is in contrast to a typical thrust chamber wall failure as shown in figure 15. This figure shows a throat plane cross section of an uncoated cylinder which had an original cooling passage geometry identical to the coated cylinder.<sup>4</sup> The liner of this cylinder was fabricated from 1/2-hard Amzirc (Cu-0.15%Zr), which has significantly more strength than electroformed copper. A crack developed in the wall of one of the cooling passages after 393 thermal cycles. The deformation and thinning of the wall of the cooling passages is typical of the damage caused by plastic ratcheting. This demonstrates the dramatic effect a TBC can have on thrust chamber life.

#### Thermal Analysis

A TBC is very effective in increasing the life of a thrust chamber because it substantially reduces the operating temperature of the metal substrate and the thermal strain in the wall. In order to quantify this effect, a thermal analysis was performed, using the experimental temperature measurements to generate a thermal profile of the cylinder wall. The following procedure was used to perform the analysis: (1) a thermal model of the cylinder wall was developed, (2) the measured rib and backside wall temperatures were plotted as a function of time, and (3) a two-dimensional conduction analysis was performed, using the SINDA thermal analyzer program,<sup>20</sup> until a best fit of the experimental temperature measurements could be achieved.

Figure 16 shows the model used for the thermal analysis. Because of symmetry, only one-half of a cooling channel wall cross section is required, see figure 4. Also shown on the model are the two depths at which rib thermocouples were located circumferentially around the cylinder, denoted as T.C.1 and T.C.2. The backside thermocouples are denoted as T.C.3.

Input to SINDA requires the hot-gas side and coolant side boundary conditions as a function of time and the thermal conductivity of the copper substrate, the bond coat, and the ceramic as a function of temperature. The steady-state hot-gas side heat transfer coefficients were obtained with a water cooled calorimeter for the annular thrust chamber configuration. The steady-state coolant-side heat transfer coefficients were calculated from empirical correlations which best describe convective heat transfer to liquid hydrogen. The hot-gas side and coolant side transient heat transfer coefficients were not available from experimental data; therefore, as an initial input, they were assumed to vary from their steady-state values in proportion to variations in chamber pressure and liquid hydrogen weight flow for each time slice. This procedure did a reasonable job of fitting the temperature data, although minor adjustments were made in the boundary conditions, where needed, to best fit the experimental data.

Since the measured parameters remained essentially the same throughout the cyclic testing, the data from any cycle was considered to be representative of the data from all cycles. Figure 17 shows a plot of the experimental temperature data from the 861st cycle of the coated cylinder. The data shown for T.C.1, T.C.2, and T.C.3 represent the averaged temperature measurements of the thermocouples at those locations. Also shown on this figure are the calculated matching temperatures of the experimental data at T.C.1, T.C.2, and T.C.3; the calculated temperature at the interface of the substrate and the bond coat; and the calculated hot-gas side wall temperature. Although not shown on this figure, the temperatures for every nodal point in the model were also calculated.

The reason a TBC can be so effective, especially on a high pressure rocket thrust chamber, is because a very large temperature drop can be achieved across the wall of a relatively thin coating. This is due to the high heat flux associated with a high pressure rocket thrust chamber and the extremely low thermal conductivity of the ceramic coating. This effect is readily apparent in figure 17. Although the steady-state hot-gas side wall temperature is nearly 2000 K, reflecting the higher operating temperature of the TBC, the temperature drop across the coating, which includes the bond coat, is nearly 1670 K. In order to show the effect the TBC has on the substrate wall temperatures, a comparison of wall temperatures is made with an identical uncoated copper cylinder tested at the same conditions.<sup>4,15</sup> The results are shown in table I. It can be seen that the copper substrate wall temperature was reduced from 844 K, which is the hot-gas side wall temperature for the uncoated cylinder, to 334 K for the coated cylinder. The temperature drop across the copper wall was reduced from 556 K to 194 K, respectively. These are substantial reductions in the cylinder wall operating temperatures. Since the tensile strength of the material varies inversely with temperature and the thermal strain varies directly with temperature difference, a

TBC can have a profound effect on the operating stresses and strains within a thrust chamber wall. This is apparent in the life of the two cylinders. The uncoated cylinder developed cracks in the wall after only 210 cycles, which was the typical life of cylinders with OFHC (oxygen-free high conductivity) copper liners.<sup>4</sup> The coated cylinder showed no damage to the wall after 1450 cycles, demonstrating that the effects of plastic ratcheting were eliminated as shown in figure 14.

#### CONCLUSIONS

The life of reusable, high pressure rocket thrust chambers can be significantly increased through the use of thermal barrier coatings (TBC's) on the chamber wall. A TBC can reduce the substrate wall temperatures and the thermal strain in the wall to the extent that the damage caused by cyclic plastic ratcheting can be virtually eliminated.

A TBC used in a high heat flux environment must be thin to keep the coating temperature within its operating limits. Based on the results of the fabrication and cyclic testing of an annular rocket thrust chamber, it has been demonstrated that a thin, durable TBC can be applied to a chamber wall by the electroform pickup process. This technique of applying TBC's needs to be validated on a high pressure, contoured rocket thrust chamber.

#### REFERENCES

1. Fulton, D.: Investigation of Thermal Fatigue in Non-Tubular Regeneratively Cooled Thrust Chambers, Vol. 2. R-9093-VOL-2, Rockwell International Corp., Canoga Park, CA, AFRL-TR-73-10-VOL-2, May 1973. (Avail. NTIS, AD-760583).
2. Posttest Metallurgical Analyses of 40 K Subscale Chamber. MPR-76-2304, Rockwell International, Rocketdyne Division, Dec. 6, 1976. (Primary Source - Cook, R.T.; Fryk, E.E.; and Newell, J.F.: SSME Main Combustion Chamber Life Prediction. (RI/RD83-150, Rockwell International Corp.; NASA Contract NAS3-23256) NASA CR-168215, 1983.)
3. Hannum, N.P.; Kasper, H.J.; and Pavli, A.J.: Experimental and Theoretical Investigation of Fatigue Life in Reusable Rocket Thrust Chambers. AIAA Paper 76-685, July 1976. (NASA TM X-73413).
4. Quentmeyer, R.J.: Experimental Fatigue Life Investigation of Cylindrical Thrust Chambers. AIAA Paper 77-893, July 1977. (NASA TM X-73665).
5. Hannum, N.P.; Quentmeyer, R.J.; and Kasper, H.J.: Some Effects of Cyclic Induced Deformation in Rocket Thrust Chambers. Conference on Advanced Technology for Future Space Systems, AIAA, 1979, pp. 290-299. (NASA TM-79112).
6. Cook, R.T.; Fryk, E.E.; and Newell, J.F.: SSME Main Combustion Chamber Life Prediction. (RI/RD83-150, Rockwell International Corp.; NASA Contract NAS3-23256) NASA CR-168215, 1983.
7. Lewis, W.J.: Coatings for Regenerative Engines. (REPT-28238T, Aerojet-General Corp.; NASA Contract NAS3-7955) NASA CR-72413, 1968.
8. Lewis, W.J.: Coatings for Advanced Thrust Chambers. NASA CR-72604, 1968.
9. Stubbs, V.R.: Development of a Thermal Barrier Coating for Use on a Water-Cooled Nozzle of a Solid Propellant Rocket Motor. NASA CR-72549, 1969.
10. Schacht, R.L.; Price, H.G. Jr.; and Quentmeyer, R.J.: Effective Thermal Conductivities of Four Metal-Ceramic Composite Coatings in Hydrogen-Oxygen Rocket Firings. NASA TN D-7055, 1972.
11. Curren, A.N.; Grisaffe, S.J.; and Wycoff, K.C.: Hydrogen Plasma Tests of Some Insulating Coating Systems for the Nuclear Rocket Thrust Chambers. NASA TM X-2461, 1972.
12. Price, H.G. Jr.; Schacht, R.L.; and Quentmeyer, R.J.: Reliability and Effective Thermal Conductivity of Three Metallic-Ceramic Composite Insulating Coatings on Cooled Hydrogen-Oxygen Rockets. NASA TN D-7392, 1973.
13. Sheffler, K.D.; and DeMasi, J.T.: Thermal Barrier Coating Life Prediction Model Development. NASA CR-179508, 1986.
14. Hammer, S.; and Czacka, Z.: Development of Advanced Fabrication Techniques for Regeneratively Cooled Thrust Chambers by the Electroforming Process. NASA CR-72698, 1968.
15. Quentmeyer, R.J.; Kasper, H.J.; and Kazaroff, J.M.: Investigation of the Effect of Ceramic Coatings on Rocket Thrust Chamber Life. AIAA Paper 78-1034, July 1978. (NASA TM-78892).
16. Batakis, A.P.; and Vogan, J.W.: Rocket Thrust Chamber Thermal Barrier Coatings. (SR85-R-5052-16, Solar Turbines International; NASA Contract NAS3-23262) NASA CR-175022, 1985.

17. Sumner, I.E.; and Ruckle, D.: Development of Improved-Durability Plasma Sprayed Ceramic Coatings for Gas Turbine Engines. AIAA Paper 80-1193, July 1980. (NASA TM-81512).
18. Anderson, N.P.; and Sheffler, K.D.: Development of Strain Tolerant Thermal Barrier Coatings Systems. (PWA-5777-29, Pratt & Whitney Aircraft Group; NASA Contract NAS3-22546) NASA CR-168251, 1983.
19. Liebert, C.H.; and Miller, R.A.: Ceramic Thermal Barrier Coatings. Ind. Eng. Chem. Prod. Res. Dev., vol. 23, no. 3, Sept. 1984, pp. 344-349.
20. Smith, J.P.: Systems Improved Numerical Differencing Analyzer (SINDA): User's Manual. (TRW-14690-H001-R0-00, TRW Systems Group; NASA Contract NAS9-10435) NASA CR-134271, 1971.

Table I

Configuration	Hot-gas side wall temperature, $T_{gw}$ , <sup>a</sup> K	Copper substrate wall temperature at bond coat interface, $T_{cw}$ , <sup>a,b</sup> K	Backside wall temperature of cylinder, $T_{bw}$ , <sup>a</sup> K	Temperature difference across copper wall, $T_{cw} - T_{bw}$ , <sup>a</sup> K	Number of cycles	Remarks
Coated cylinder <sup>c</sup> (Electroformed copper liner)	2000	334	140	194	1450	No damage to the wall of the cooling passages.
Uncoated cylinder <sup>d</sup> (OFHC copper liner)	844	844	288	556	210	Cracks in the wall of the cooling passages, severe deformation and thinning of the wall due to plastic ratcheting.

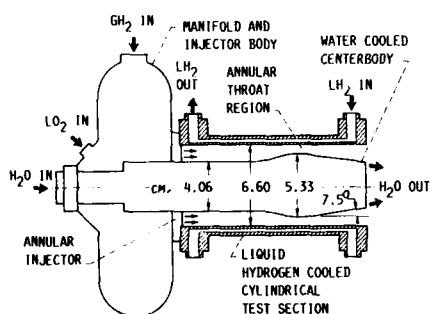
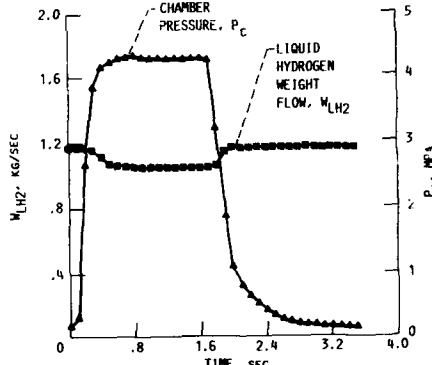
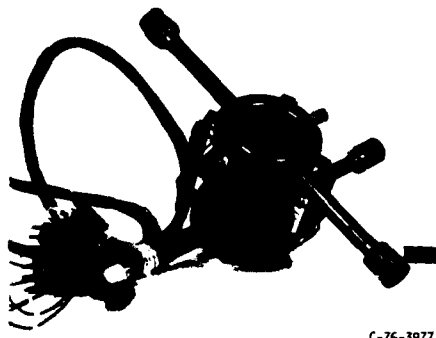
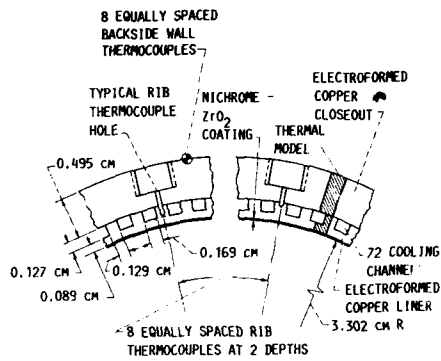
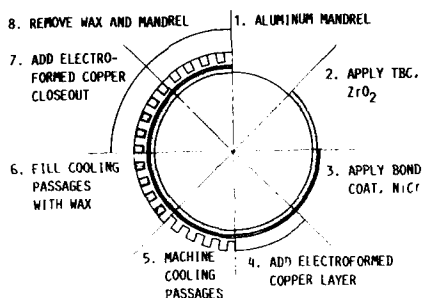
<sup>a</sup>Calculated temperature locations shown on fig. 16.<sup>b</sup>Or the copper hot-gas side wall temperature of the uncoated cylinder.<sup>c</sup>See fig. 17.<sup>d</sup>See ref. 15.

FIGURE 1. - SCHEMATIC OF ANNULAR ROCKET THRUST CHAMBER ASSEMBLY.



FIGURE 2. - ANNULAR THRUST CHAMBER ASSEMBLY.



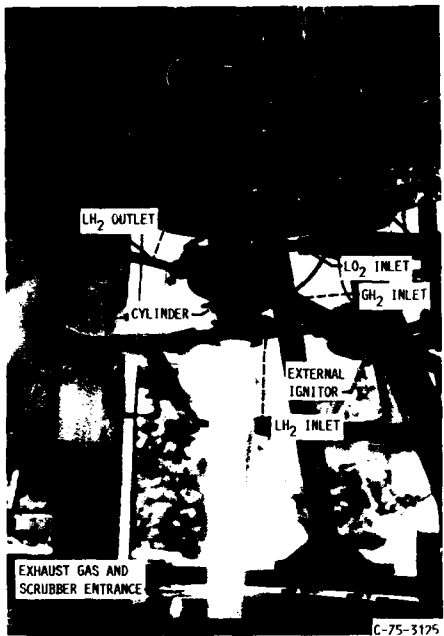


FIGURE 7. - ANNULAR THRUST CHAMBER DURING CYCLIC TEST.

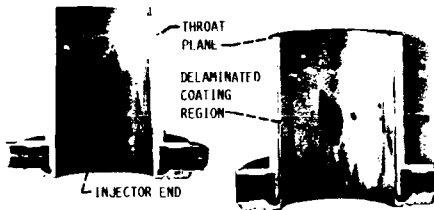


FIGURE 8. - POST-TEST SECTIONS OF CYLINDRICAL TEST SECTION.

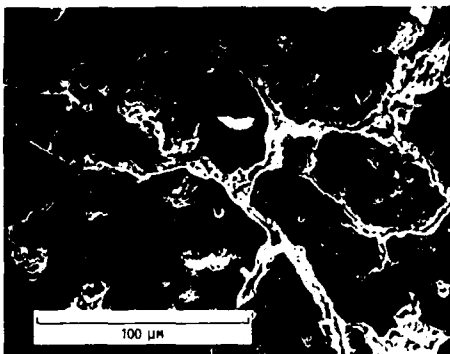


FIGURE 9. - MICRO-CRACK MORPHOLOGY IN THROAT REGION. 500x.

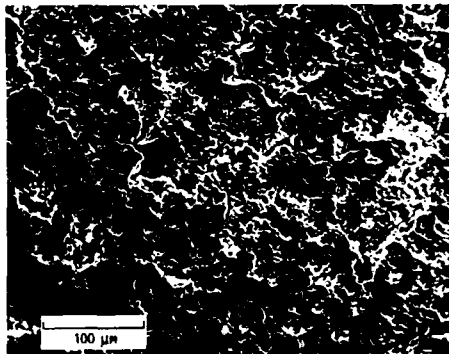


FIGURE 10. - MICRO-CRACK MORPHOLOGY IN COMBUSTION ZONE. 250x.

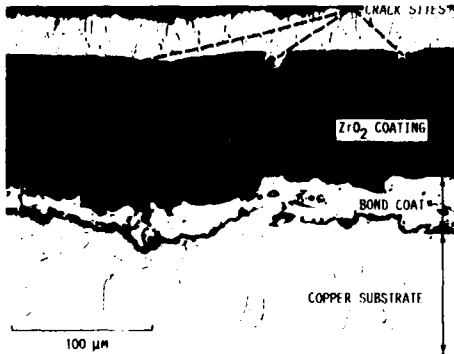


FIGURE 11. - CROSS SECTION OF CRACK MORPHOLOGY IN THROAT REGION. 400x.

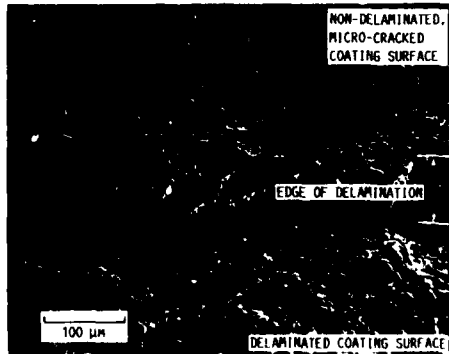


FIGURE 12. - OBLIQUE VIEW OF COATING SURFACE AT THE LOCATION OF DELAMINATION. 200x.

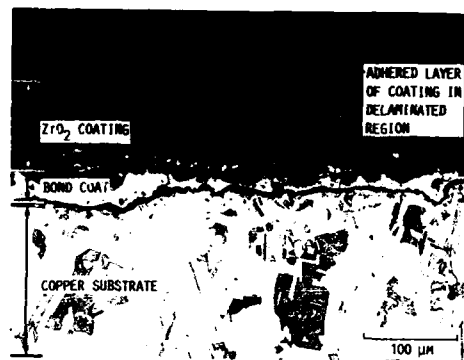


FIGURE 13. - CROSS SECTION OF COATING AT THE LOCATION OF DELAMINATION. 200x.

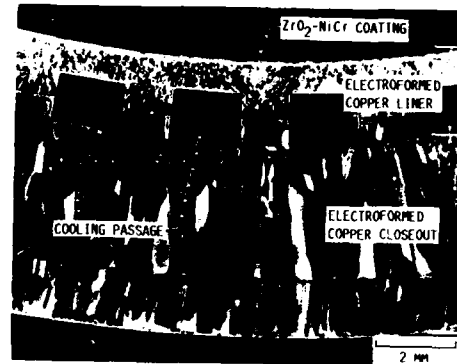


FIGURE 14. - CROSS SECTION OF COATED COPPER CYLINDER AT THE THROAT PLANE AFTER 1450 THERMAL CYCLES. 10x.

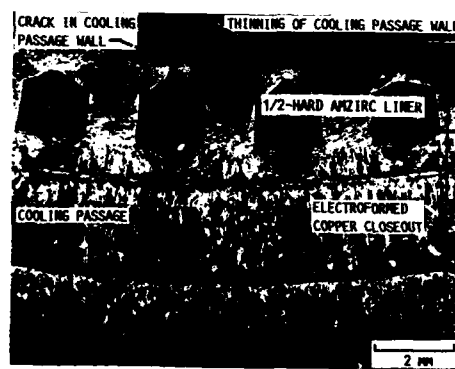


FIGURE 15. - CROSS SECTION OF 1/2-HARD ALNICO CYLINDER AT THE THROAT PLANE AFTER 393 THER. CYCLES. 10x.

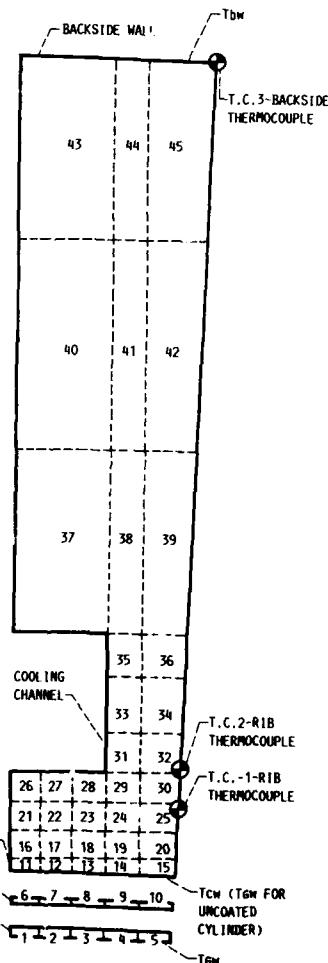


FIGURE 16. - 45 ELEMENT THERMAL MODEL.

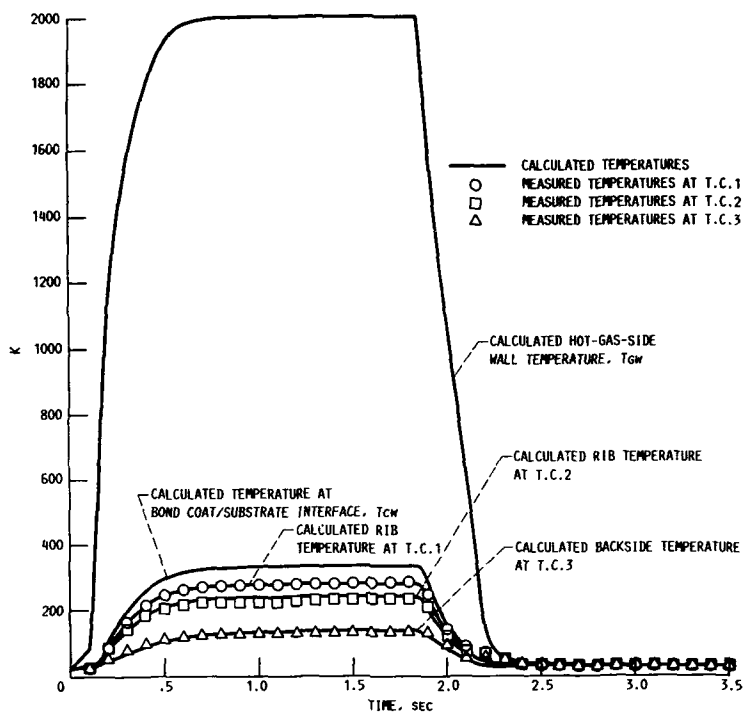


FIGURE 17. - MATCHING OF CALCULATED TEMPERATURES WITH EXPERIMENTAL TEMPERATURE MEASUREMENTS.

#### DISCUSSION

R. Kochendorfer, DFVLR, FRG. It is rather astonishing that you've reduced the temperature at the metallic chamber wall so much with such a thin thermal barrier coating. Did I understand correctly that this is associated with a large reduction in heat flux to the internally cooled metallic structure?

R. Quentmeyer, NASA-Lewis, US. It is the combination of the very low thermal conductivity of the thermal barrier coating and a relatively high wall heat flux that results in such a large reduction in the chamber metal wall (substrate) temperature. It's true that the heat flux has been substantially reduced, due to the high operating temperature of the coating. But it is still sufficiently high to result in a large temperature drop across the coating, even though the coating is very thin. Therefore, the temperature of the metallic substrate is greatly reduced. The reason a thermal barrier coating can be so effective in a high heat flux environment is the large temperature drop that can be achieved across a very thin coating.

**SILICON-CARBIDE COATED CARBON-CARBON – AN ADVANCED MATERIAL  
FOR ROCKET SYSTEMS**

by

E.v.Gellhorn  
U.Gruber  
SIGRI GmbH, Meitingen  
and  
H.Leis  
Messerschmitt Bölkow-Blohm  
Postfach 80 11 09  
8000 München 80  
Federal Republic of Germany

**1. Summary**

To increase the resistance of rocket systems, materials have to be used which can withstand temperatures above 2000°C, as well as erosion and corrosion attack. Carbon fibre-reinforced carbon coated with silicon carbide seems to be the outstanding material suited to resist temperature as well as mechanical requirements.

The first part of this paper describes the manufacture of the nozzles. Carbon fibres are impregnated with resins, the resins are carbonized to form a closed carbon matrix and the shaped body is coated with silicon carbide.

The nozzles were tested for up to 300 seconds in a semi-free jet and a connected pipe test rig for the ramrocket under regular operating conditions. The tests proved the excellent thermal shock resistance of the material, as well as its oxidation resistance. A better understanding of the material properties demanded has been obtained.

**2. Introduction**

In guided missile development there is a worldwide trend towards marked increases in flight speeds aimed at achieving adequate penetration against improved defence systems.

For tactical reasons, neither range nor missile compactness can be sacrificed; so a need exists for rocket systems with improved economy. One type of power unit capable of meeting the demands for economy and simple handling is the solid-propellant rocket engine. This can fulfill the military requirement for high flight speed and, simultaneously, a long range.

These engines for ramrockets impose stringent and highly specific demands on materials technology. The materials problems existing relate primarily to the hot gas valve, the combustion chamber and associated equipment such as the gas generator.

Any material for combustion chamber linings will be subjected to the following demands:

- oxidation resistance up to 2000 K
- high bursting strength (for rings)
- ablation and creep resistance at 2000 K for up to 250 seconds

In a research program being sponsored by the Federal Ministry of Defence, investigations are being conducted into materials characterized by high specific heat resistance up to 2000 K, low thermal expansion, thermal shock resistance and resistance to oxidation.

One material being tested to determine its suitability for combustion chambers is C/C, a composite material consisting of a carbon matrix reinforced by carbon fibres.

The following tests were conducted on the C/C specimens:

- a) determination of thermal shock resistance ( $\Delta T$  2000 K)
- b) bond strength measurements
- c) ceramographic investigations
- d) determination of characteristic properties (bulk density, thermal conductivity, flexural strength on laboratory samples, tensile strength on small annular samples)
- e) oxidation resistance
- f) testing under conditions similar to those in practical use, both in the test rig (Fig. 1) and in the simulator (Fig. 2)

**3. Production of C/C thrust nozzles**

**3.1 Materials development and manufacturing**

For more than 12 years now, carbon fibre-reinforced carbons have been manufactured at SIGRI for rocket engine components subjected to high thermal stress. Over this period there has been a continuous development in manufacturing processes for two-dimensionally reinforced C/C components, although, as the test series was only small, it was not possible to develop a larger series production (Table 1).

Material and component tests were successful for the most part, both in longterm trials (ramrocket engines, 300 s, 1800 K) and on systems subjected to higher thermal stresses (liquid propellant, 10 s, 3000 K).

Marked progress in materials development had been evident since the start of the 1980s because the production processes were changing. Component size and shaping were no longer limiting factors in production processes. Stress distribution in a component could be influenced by specific fibre orientation and concentration. Also improvements were achieved in the ceramic coating methods.

Generally, to generate the carbon matrix there are applied impregnation processes using liquid or gaseous (CVD) impregnants. In table 2 an attempt is made to contrast the advantages and drawbacks of the two types of material, one with the other. The choice of manufacturing technique among the various ones available for the two-dimensional C/C grades hitherto produced at SIGRI was a clear decision in favour of the autoclave method. Compared with grades produced by the methods previously used, these display the following advantages:

- higher interlaminar shear strength (30 - 40 %)
- better impact resistance (about 50 - 70 % higher)
- higher strain at break (0.6 - 0.7 %)
- lower bulk density (1.4 g/cm<sup>3</sup>) compared to wound material (1.5 - 1.6 g/cm<sup>3</sup>)
- simpler shaping
- reinforcement adaptable to requirements
- better reproducibility, especially dimensional stability
- good machinability
- any form of shaping possible, no joint needed

### **3.2 Laminate structure**

The component design was derived from tests on laminates and prototype components. The nozzle contour was reinforced with a twill-weave carbon fibre fabric. The laminate, provided as a phenolic resin prepreg, was in tape form. The tapes, cut into conical shapes, were laid up axially (0°), edge to edge, on a graphite mandrel. Several incisions were made in the flange region to ensure that there were no creases in the lay-up. Each subsequent prepreg layer was placed so that the lamination extended over the butt joints of the preceding layer (Fig. 3). In the flange region, two rings cut out of prepreg were applied as lateral reinforcement after every sixth layer. Fig. 4 shows the laminate structure schematically. Cold intermediate compaction or moulding was applied after each second laminate layer and intermediate curing after every sixth layer.

### **3.3 Curing**

The resin was cured by heating the laminated component at between 90°C and 130°C and a pressure of 0.5 bar. After each curing stage the pressure had to be reduced. The time schedule is shown in Fig. 5. When final curing was completed, the vacuum bag was removed and the component then post-cured for several hours at atmospheric pressure of up to 150°C or more. The component was removed from the laminating mandrel after curing was completed.

### **3.4 Carbonization**

In the pyrolysis of cured carbon fibre-reinforced components it should be kept in mind that the temperature ranges through which polymers pass during the carbonization process may lead to non reversible deformation (eg ovalization). To prevent deformation in the flange area of the nozzle, a graphite plate was screwed on to it. The inner contour of the nozzle was filled with a conical graphite mandrel. By the end of the first pyrolysis stage it is already apparent whether changes are occurring in the geometry of the component or whether cracking or delamination is taking place. Consequently, the first carbonization step is critical, especially the resin matrix undergoes a weight loss of some 50 % during pyrolysis and becomes porous. Processing techniques have been developed which allow components up to 1 m diameter and 2.5 m length to be pyrolysed without loss of shape.

The thrust nozzles were pyrolysed at up to 1000°C. Any dimensional changes that occurred had to be taken into account at the component design stage. The shrinkage in wall thickness was manifested as a slight reduction in the outer diameter and increase in the inner diameter.

### **3.5 Impregnation**

Carbonization of the cured matrix produces a porous carbon body which is then densified by impregnation and re-carbonization processes. Impregnation is carried out with thermosetting phenolic resin systems. The impregnation and carbonization process was carried out three times in succession. Major factors affecting impregnation are:

- the wetting behaviour of the resin system employed
- the viscosity of the impregnating resin
- pore size and pore distribution (open or closed pores)
- pressure, vacuum and impregnation time

### **3.6 Graphitization, machining**

In principle, graphitization is characterized by a structural rearrangement. In the graphitization treatment carried out at 2000°C or more for the C/C nozzle, there were no appreciable changes either in the dimensions or in the mechanical properties. Before ceramic coating, the thrust nozzle was graphitized, then machined in order to get the final shape. Machining was carried out by turning and grinding.

#### 4. Ceramic coating

##### 4.1 Coating process

C/C materials oxidize in air at temperatures above 400°C [1]. To allow use at higher temperatures of the various C/C which properties are better than those of brittle, though oxidation-resistant ceramics, namely:

- resistance to thermal shock
- high sublimation temperature
- toughness
- specific strength
- ease of manufacture and machining,

it is necessary to improve oxidation resistance. So far, despite considerable success, and did not succeed to develop impermeable ceramic coatings offering permanent protection against oxidation. Coatings containing SiC have proved successful for short-term applications. Various authors report the use of SiC-coated C/C components in hot-gas turbines, space shuttles and rocket sections [2,3,4], in which C/C components have been successfully protected against oxidation for several hours at temperatures of up to 1700°C. This progress was achieved only when microfine cracks on the ceramic protective coating were successfully closed with orthosilicates. In the presence of oxygen and at a sufficiently high temperature, silicon forms glasslike protective coatings of SiO<sub>2</sub>, which afford long-term protection at temperatures of up to 700 - 800°C. Even better protection is provided by B<sub>2</sub>O<sub>3</sub> glasses, as reported in recent publications [5].

In the case of a re-entry vehicle the C/C component is in contact with air exposed to high temperatures as a result of friction-induced heat. However, a rocket nozzle may also suffer erosion due to impact by solid particles of propellant. Consequently, the development of protective coatings will depend on the particular burden.

Various publications dealing with the coating of 2-dimensional or 3-dimensional C/C materials exist. In principle, two different processes are available:

1. coating from the gas phase (CVD process)
2. chemical reaction with liquid silicon.

Both processes are basically suitable, though the second is harder to control. Experience has shown that the coatings produced by CVD-processes are more uniform and that the decrease in strength after the application of the protective coatings is smaller. This provided confirmation of references [6] where this process is described as being less aggressive than the liquid phase process. The literature includes statements that liquid silicon reacts very rapidly with the substrate, eventually destruct the reinforcing fibres and hence to a decreases in the strength of the composites [6,7].

For more than ten years now, 2-dimensional C/C components have been coated by SIGRI both under normal pressure and in a vacuum. Coatings can now be produced with diameters up to a maximum of 800 mm in special high-temperature furnaces. Good results have been obtained in tests with SiC coatings of 50 - 100 µ thickness which do not penetrate into the shape.

In practice, components of this type have been used successfully for thrust nozzles and thrust deflectors.

Fig. 5 shows in principle the coating process. The C/C nozzle was mounted in the furnace above the silicon powder, after which the furnace temperature was raised to 1700 to 2000°C. At these temperatures silicon vapour reacts with the carbon of the C/C component to produce silicon carbide (SiC). Difficulties may occur owing to the anisotropy of the C/C material. Because of differences in thermal expansion in the C/C-laminate below the coating plane, micro cracks may form in the SiC coating. The coefficients of thermal expansion of carbon and SiC (isotropic) are almost identical perpendicular to the plane of coating (CTE - C/C 4-6 x 10<sup>-6</sup>/K, CTE - SiC 4.2-4.5 x 10<sup>-6</sup>/K), while in the plane the CTE value C/C is distinctly lower (CTE - C/C 1 x 10<sup>-6</sup>/K). Despite this it is still possible to apply SiC coatings which adhere well and are reproducible. The following process factors are crucial to the production of coatings with good adherence:

- the temperature cycle during the coating process (heating up rate, cooling, residence times, max. temperature, temperature distribution)
- the inert gas, flow distribution and rate
- the mounting of the C/C component in the furnace
- the geometry of the component to be coated (angle of incidence of gas flow)
- the proportion by weight of silicon powder and its distribution in the furnace
- the density of the C/C component to be coated and hence the surface porosity
- the structure and type of the composite material, i.e. types of fibre and matrix and alignment of fibre in the composite.

##### 4.2 Machining

As a general rule machining must be avoided due to its costs. Only diamond tools (polycrystalline diamond) can be used for SiC. The most suitable process is grinding. As the SiC coatings are only 50 to 100 µ thick on average, the coating is at risk of being damaged, with a resultant loss of its protective action against oxidation.

#### **4.3 Structural investigations and quality control**

The only final checks that can be carried out on the coated components are the measurement of dimensions. Structural examinations to determine the thickness of the ceramic coating or strength analyses are possible only on specimens produced and coated in parallel with the components. Exceptions are possible if the C/C component has to be only partially coated, in which case areas not coated can be removed for test purposes. In practice, however, partial coating is difficult; so all-over coating is used even for components not requiring it (eg combustion chamber components where oxidative attack occurs only on the inner face). Hence, the quality of such components can be tested only indirectly by measuring said "parallel" shapes. NDT methods should be developed.

#### **5. Characteristic materials data and component tests with C/C nozzles in the engine test rig**

##### Method

The annular and cylindrical test items made of C/C were tested in three different test rigs. The test parameters chosen resembled the conditions of an original ramrocket burn as closely as possible.

##### a) The simulator/hot-gas generator, Fig. 2

was powered by a kerosine-air mixture.

Test conditions:

- Pressure: 15 bar
- Temperature: 1800 K
- Test duration: 250 s

##### b) The simulator/combustion chamber, Fig. 6

was powered by a liquid fuel ram combuster propellant.

Test parameters:

- Pressure: 5 bar
- Mass flow: 4.4 kg/s
- Propellant mass flow: 0.35 kg/s
- Temperature: 1700 K
- Specific thermal loading of the chamber wall: 1.6 MW/m<sup>2</sup>

##### c) The engine test rig, Fig. 1

was powered by high-particle-content solid propellant.

Re a) In the simulator/hot-gas generator, tests were conducted on the annular test specimens.

In the kerosine-powered test rig, ignition nozzles with stabilizers were mounted in the four air-feed ducts to ensure continuous combustion.

The necessary test rig length to accommodate the mixing and combustion sections is formed by two water-cooled jacketed tubes to which the test section with the interchangeable combustion chamber section and the thrust nozzle mounting are attached.

Re b) Fig. 7 shows in schematic form the mechanical structure of the combustion chamber simulator. The hot gas needed for the test is generated in the water-cooled combustion chamber (not illustrated on the figure). It flows through the test items in the condition required and passes out into the open air via the C/C nozzle, which likewise has to be tested. The values for pressure, temperature and speed can be varied over a wide range by adjusting the air and propellant throughput rates, as well as by choosing appropriate end nozzles.

The C/C test items are secured in the simulator in such a way that none of the effects that might falsify the test result can occur. The thermal expansion is taken up by a 4 mm-wide gap which is filled with a heat-resistant ablation compound. The hot gas flows in smoothly /9/.

Re c) The sonic nozzels were tested under original conditions in a solid-propellant engine.

Fig. 1 illustrates an engine of this type which differs from the test unit previously described only in that the hot gas is produced with the aid of propellant of the type used in a ramrocket. The trials with original propellants were important because the test specimens for investigation were exposed to erosive particle impact as well.

#### **6. Thermal and oxidation resistance of C/C test bodies during testing under conditions resembling those in actual use**

##### a) Tests in the hot gas generator

Without exception, the manufactured parts displayed good creep behaviour up to a maximum of 300 seconds. After intervals of 100 seconds with a thermal loading of 1.6 MW/m<sup>2</sup> the test samples were dismantled from the hot gas generator and examined for both stress cracks and damage to the anti-oxidation layer. The condition of a sonic nozzle after thermal loading of 1.6 MW/m<sup>2</sup> and a dwell time of 2-3 times 100 seconds is shown in Fig. 8.

b) Simulator - combustion chamber and test rig

The results of the visual assessment of all annular test specimens from the simulation tests with a combustion chamber or stationary ramrocket engine can be summarized as follows:

- No cracks indicative of thermal shock failure were discernible either in the C/C composite or in the oxidation protective coating.
- Under the given test conditions the coating was adequate to perform its function throughout an entire burn lasting 300 seconds.

Despite the good overall impression, some minor defects were observed, but a comparative assessment of these was made difficult by the inability to maintain constant test conditions in the power unit tests.

**7. Schedule of requirements imposed on C/C materials for use in combustion chambers**

This program of tests described, in which specimens are tested under conditions of practical use and characteristic material values are ascertained separately, enables us to compile a schedule of optimum material properties for C/C heat-resistant materials for combustion chambers in test rocket engines (Table 3).

**8. Literature**

- |  |  |
|--|--|
| /1/ D.W. McKee                         | OXIDATION BEHAVIOR AND PROTECTION OF CARBON/CARBON COMPOSITES<br>in: Carbon Vol. 25, No. 4, pp. 551-557/1987   |
| /2/ L. Davis, S.Cruzen,<br>W. Schimmel | CARBON/CARBON COMPONENTS FOR ADVANCED GAS TURBINE ENGINES<br>in ASME: The American Society of Mechanical Engineers, Houston, Texas<br>Gas Turbine Conference & Products Show, pp. 1-8, 9-12th March, 1981  |
| /3/ Paul R. Becker                     | LEADING-EDGE STRUCTURAL MATERIAL SYSTEM OF THE SPACE SHUTTLE<br>in: American Ceramic Society Bulletin Vol.60, No.11, 1981, pp.1210-1214  |
| /4/ Allen J. Klein                     | CARBON/CARBON COMPOSITES<br>in: Advanced Materials & Processes Inc., Metal Progress 11/86, pp.64-68  |
| /5/ James E. Sheeham                   | CERAMIC COATINGS FOR CARBON MATERIALS<br>GA-Technologies Inc., San Diego, Cal.92138<br>in: Proceedings of the Fourth Annual Conference on Materials Technology,<br>5th May 1987  |
| /6/ C.C. Evans, A.C. Parmee            | SILICON TREATMENT OF CARBON-FIBRE - CARBON COMPOSITES,<br>4th Lond. Conference on Carbon and Graphite, 1974, pp.231-235  |
| /7/ R. Kochendörfer                    | HEISSE TRAGENDE STRUKTUREN AUS FASERVERBUND-LEICHTBAUWERKSTOFFEN,<br>DFVLR, Stuttgart<br>German Research and Experimental Institute for the Aerospace Industry,<br>Stuttgart<br>in: DGLR-Tagung (Congress of the German Society of the Aerospace<br>Industry), Berlin, 1987. |
| /8/ H. Henkel                          | MBB report No. TN-RT 31-2/79   |
| /9/ H. Keller                          | MBB report No. TN-RT 34-11/81  |

	Date	Advantages	Disadvantages
	1975	inexpensive technique for series production - tubes easy to manufacture	delamination and crack formation due to uncontrollable stresses during winding; power flux (excessive stresses) in the component cannot be allowed for as only circumferential winding possible; only suitable for the production of simple shapes (no flanges)
Winding of carbon fabric tapes			
	1978-1982	production of standard sheets, inexpensive technique, good mechanical properties, controllable, measurable, reproducible for series production; suitable for machining	nozzles of diam. 80 to 100 mm need to be jointed; only suitable for the production of simple shapes (no flanges); considerable waste when machined unless the core is drilled out in one piece; reinforcement not variable, flexural stresses in axial direction must be avoided during incorporation of the nozzle; incorporation under compressive stress
Compression moulding of C fabric sheets / jointing technique			
	1982-1984	inexpensive technique for the production of cylinders; fast production	- conical mandrels difficult to wind - each must be individually wound - poor interlaminar shear strength and impact resistance - difficult machining - limited shaping possibilities, production of flanges impossible
Winding of C rovings			
	since 1984	- any kind of shaping possible - fibre reinforcement variable by choice of laminating technique (prepregs) - good mechanical properties	- expensive technique owing to need for individual production - time-consuming
Prepreg processing with autoclave techniques			
Lamination of fabric tapes			

Table 1 Manufacturing techniques for C/C thrust nozzles

Properties and comparable characteristics	Liquid impregnation process (two-dimensional)	CVD process (three-dimensional)
Bulk Density (g/cm <sup>3</sup> )	below 1.4	1.5 to 1.7
Thermal shock resistance	better because of open porosity	worse
Abrasion, erosion	higher	lower
Price	cheaper	more expensive
Manufacturing	hand lay-up moulding with autoclave technique easy to control, reinforcement feasible as specified	shaping more difficult, prolonged pore diffusion, reinforcement not feasible as specified
Structure	anisotropic	isotropic
Thermal conductivity	controllable by fibre direction and polymer system, lower, insulating properties	more suitable for thermal expansion and oxidation, more homogeneous very high because of pyrographite properties

**Table 2** Production of C/C nozzles by liquid impregnation (two dimensional) and CVD process (three-dimensional)

Properties	Unit	Direction	Internal measurements	External measurements	Requirement
Bulk Density	g/cm <sup>3</sup>	-	1.47 - 1.62	1.5 - 1.8	1.5 - 1.7
Fibre content	% by vol.	x, y	-	45	35
Porosity	% by vol.	-	-	1 - 5	1 - 5
Flexural strength	N/mm <sup>2</sup>	x, y	100 - 246	120 - 300	180 - 250
Young's modulus	kN/mm <sup>2</sup>	x, y	-	13 - 55	40 - 60
Tensile strength	N/mm <sup>2</sup>	x, y	100 - 640	40 - 700	100 - 700
Tensile modulus	kN/mm <sup>2</sup>	x, y	-	20 - 30	30 - 50
Compressive strength	N/mm <sup>2</sup>	x, y	-	80 - 160	100 - 300
Shear strength	N/mm <sup>2</sup>	z	5.2 - 15	10 - 30	15 - 30
Thermal conductivity					
carbonized	W/(K.m)	z	2 - 5	8 - 10	15
graphitized	W/(K.m)	z	-	90 - 100	100
Coefficient of thermal expansion					
1000°C	10 <sup>-6</sup> 1/K	x, y	-	0.03-0.05	1
2500°C	10 <sup>-6</sup> 1/K	x, y	-	2 - 3	4
1000°C	10 <sup>-6</sup> 1/K	z	-	6	1 - 10
2500°C	10 <sup>-6</sup> 1/K	z	-	8	1 - 10

The properties measured and required relate to a structure of fabric laminates (0°, 90°) or a combination of fabric laminates (0°, 90°) and unidirectional wound layer (0°)

**Table 3** Schedule of requirements imposed on C/C materials for combustion chambers in test rocket engines



Fig. 1

Engine Test Rig



Fig. 2

Simulator / Hot-Gas Generator



Fig. 3 a

Laminating of the C/C Nozzle

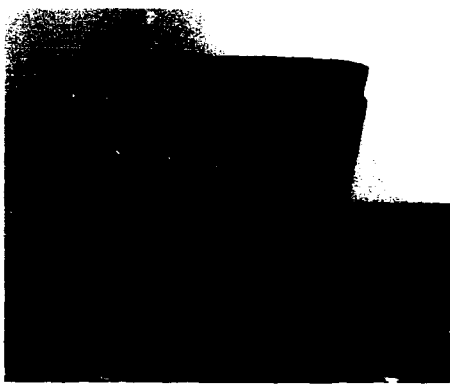


Fig. 3 b

Laminating of the C/C Nozzle

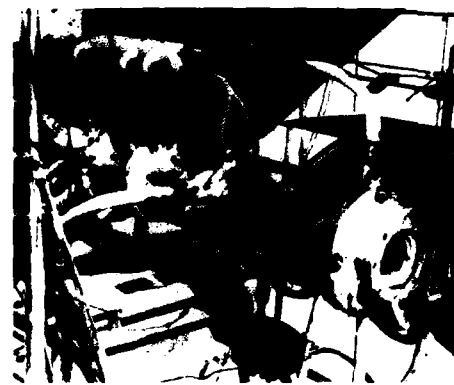


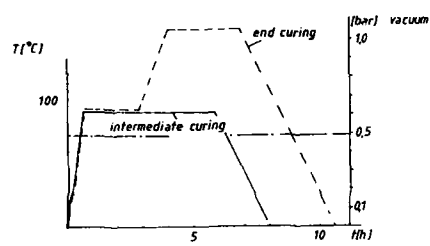
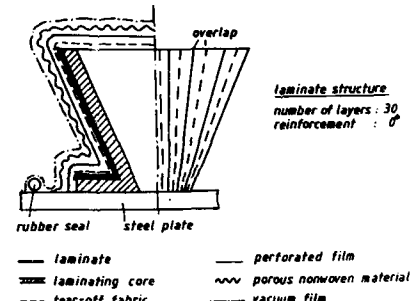
Fig. 6

Simulator / Combustion Chamber

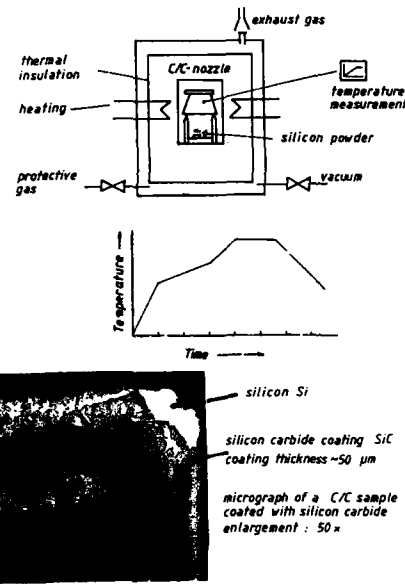


Fig. 8

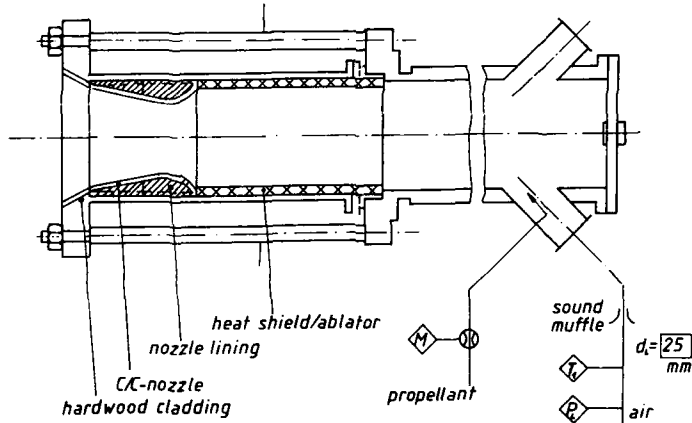
Sonic Nozzle after testing

Fig. 4

Production of the C/C Nozzle

Fig. 5

SiC Coating of the C/C Nozzle

Fig. 7

Sketch of the Combustion Chamber Simulator

#### DISCUSSION

R. Pickering, Royal Ordnance, UK. What were the test conditions, pressures, flame temperatures and burn times in the solid propellant motor tests you referred to in Fig. 1?

B. Crispin, MBB, FRG. The pressure in the combustion test was 8 bars, the flame temperature was above 3000°K and the burn time was 250 seconds.

R. Pickering, Royal Ordnance, UK. How did the silicon carbide coated material compare to an uncoated composite under identical test conditions?

B. Crispin, MBB, FRG. The uncoated composite oxidized within 10-30 seconds.

## FIBER REINFORCED SUPERALLOYS FOR ROCKET ENGINES

Donald W. Petrasek and Joseph R. Stephens  
National Aeronautics and Space Administration  
Lewis Research Center  
Cleveland, Ohio 44135 U.S.A.

### SUMMARY

High-pressure turbopumps for advanced reusable liquid-propellant rocket engines such as that for the Space Shuttle Main Engine (SSME) require turbine blade materials that operate under extreme conditions of temperature, hydrogen environment, high-cycle fatigue loading, thermal fatigue and thermal shock. Such requirements tax the capabilities of current blade materials. Based on projections of properties for tungsten fiber reinforced superalloy (FRS) composites, it was concluded that FRS turbine blades offer the potential of a several fold increase in life and over a 200 °C increase in temperature capability over the current SSME blade material. FRS composites were evaluated with respect to mechanical property requirements for SSME blade applications. Compared to the current blade material, the thermal shock resistance of FRS materials is excellent, two to nine times better, and their thermal fatigue resistance is equal to or higher than the current blade material. FRS materials had excellent low and high-cycle fatigue strengths, and thermal shock-induced surface microcracks had no influence on their fatigue strength. The material also exhibited negligible embrittlement when exposed to a hydrogen environment.

### INTRODUCTION

The need for improved performance and longer life in advanced liquid propellant rocket engines has stimulated interest in the potential benefits of advanced high-temperature structural materials for rocket engine turbopump turbine blades. Historically, the rocket engine industry has relied on aircraft gas turbine materials; however, there are significant differences in the requirements placed on blade materials in rocket engine turbines compared to aircraft gas turbines, as shown in Table I. It has become apparent that the blade materials developed by the aircraft gas turbine industry do not necessarily meet some of the operating requirements of liquid propellant rocket engines, such as very severe thermal start/stop transients, high operating speeds, and hydrogen environments. These conditions result in unique requirements including: high thermal strain low-cycle fatigue strength; high mean stress high-cycle fatigue strength; resistance to hydrogen environment embrittlement; thermal shock resistance; and relatively short time stress-rupture/creep strength.

Currently the most advanced large, liquid propellant rocket engine in service is the Space Shuttle Main Engine (SSME) and it utilizes directionally solidified hafnium-modified MAR M246 (MAR M-246 (Hf) (DS)) for the high pressure fuel turbopump and the high pressure oxidizer turbopump turbine blades. In this instance the fatigue requirements on the alloy are particularly severe as evidenced by the fact that the MAR M-246 (Hf) (DS) turbine blades in both turbopumps are subjected to life-limiting fatigue cracking. There is thus a need to improve turbine blade materials for increased life under current SSME operating conditions and to increase the temperature capability for future rocket engines.

A study was conducted to identify those materials that would provide the greatest benefits as a turbine blade material for advanced liquid propellant rocket engine turbines, Ref. 1. The candidate materials were selected from six classes of materials: fiber reinforced superalloys (FRS), single crystal superalloys (SC), oxide dispersion strengthened superalloys (ODS), rapid solidified processed superalloys (RSP), directionally solidified superalloys (DSE), and ceramics. Mechanical and physical properties were compiled and evaluated, and improvements were projected approximately 5 years into the future for advanced versions of the materials. The estimated values were used in a turbine blade structural analysis based on the design and operating conditions of the SSME and the configuration and operating conditions of the SSME high pressure fuel turbopump first-stage turbine blade where the temperatures of interest ranged from 870 °C, the approximate steady-state operating temperature of turbine blades in the SSME, to approximately 1100 °C. Based on these calculations, development plans were prepared, and benefit analyses were performed to permit the identification of those materials offering the best balance in terms of gains to the system, risk, and development costs. It was concluded that the materials which warranted development were the single crystal superalloys for use at 870 °C, the FRS composite for use at 870 and 1100 °C, and the ceramics for use at 1100 °C. At 1100 °C the FRS composite stood out as being the only one of five metallic classes of materials studied to have the properties to provide adequate rocket engine turbine blade life and was regarded as the leading candidate for this application.

Fiber reinforcement of superalloys has a long history and is a relatively mature technology. Tungsten fiber reinforced superalloy composites have been of interest for air breathing gas turbine blade application for more than 20 years in the United States, Great Britain, Sweden, and the USSR due to their (1) potential use temperature advantage of over 160 °C above that of conventional superalloy blade materials and (2) capability to provide longer operating life. Work on FRS in the United States has been most actively pursued by NASA Lewis Research Center where emphasis has been on evaluating tungsten fiber reinforced FeCrAlY, Refs. 2 and 3. The feasibility of

fabricating complex shaped blades of FRS composite material has been demonstrated, Ref. 4. A cooled aircraft gas turbine blade that was fabricated as a result of this program is shown in Fig. 1. A comprehensive review of the status of FRS composite materials can be found in Ref. 5.

Both in-house and contractual studies (Refs. 6 to 8) are being conducted to evaluate the use of fiber reinforced superalloys for rocket engine turbopump turbine blades. The first-stage blades of the high pressure fuel turbopump of the SSME were chosen as the reference system and a preliminary analysis was undertaken based on the use of high strength tungsten alloy fibers in a ductile superalloy matrix. This analysis included modeling to estimate mechanical and physical properties as well as experimental measurements of critical properties. For purposes of comparison to existing technology, estimated and measured behavior of the FRS composite is contrasted with that determined for MAR M-246 (Hf) (DS) at 870 °C. Additionally the properties of fiber strengthened alloys are projected for use at 1100 °C in advanced rocket engines.

#### ANALYSIS

##### Materials

Due to their combination of high-strength, high temperature capability and good ductility, tungsten alloy fibers have been favored as the reinforcement for FRS composites. Because the current SSME blades experience a high tensile stress due to a combination of high centrifugal forces and gas bending loads, a high value of specific strength (strength/density) is desirable. Thus the strongest tungsten wire that has been fabricated to date is the W-4Re-0.38Hf-0.02C (weight percent), Ref. 9, which was selected as the reinforcing fiber to be used in the analysis.

The consideration for selection of the matrix material to be reinforced included:

- (1) Compatibility with the environment; hydrogen and/or hydrogen/steam
- (2) Compatibility with the tungsten alloy fiber
- (3) Thermal fatigue resistance
- (4) High-cycle fatigue behavior
- (5) High tensile ductility

Based on these criteria three iron base alloys (Incoloy 903, FeCrAlY, and 316L stainless steel) and the nickel base superalloy, Waspaloy had potential as matrix alloys. The chemical composition of the matrix materials are shown in Table II. These materials are different in many respects and each has attractive features for use as a matrix material. Waspaloy is representative of a ductile nickel base superalloy that maintains high tensile strength up to 870 °C. Incoloy 903 (IN 903) is one of several austenitic iron alloys (IN 903, 905, 907, 909) developed by INCO for low thermal expansion properties and is resistant to hydrogen environment embrittlement. The commercial 316L austenitic stainless steel is also resistant to hydrogen environment embrittlement. Finally, the FeCrAlY and FeCrAl alloys have been shown to have excellent compatibility with tungsten alloy fibers and tungsten fiber reinforced FeCrAlY has also been shown to have very good thermal fatigue resistance properties.

The FRS system projected for the advanced version of the SSME turbine blade was a composite comprising 50 vol % of W-4Re-0.38Hf-0.02C fibers embedded in a ductile matrix of the compositions indicated previously. Unfortunately experimental property data for these composite systems are limited; therefore, it was necessary to estimate behavior from data and predictive techniques developed under previous metal-matrix composite programs.

##### Mechanical Properties

Figures 2 and 3 show projections of tensile and specific tensile strengths of candidate FRS composite systems based upon incorporation of W-Re-Hf-C fibers in various matrix alloys. In all cases the composites have an advantage in tensile strength (Fig. 2) over the MAR M-246 (Hf) (DS); however, if specific strength is the critical criteria improvement below 870 °C depends on the matrix alloy (Fig. 3). In terms of expected long term life at elevated temperature, stress rupture projections (Fig. 4) indicate at least a 100 percent advantage in load bearing ability for the FRS system over the conventional superalloy.

The projected high-cycle fatigue behavior of W-Re-Hf-C/Waspaloy composite is contrasted with that of the current SSME blade alloy in Fig. 5. For similar test conditions, the high-cycle fatigue life of the FRS composite is estimated to be three orders of magnitude higher than that for MAR M-246 (Hf) (DS) at 870 °C. Using available fatigue data for FRS composites, Ref. 10, a Goodman diagram has been calculated (Fig. 6) which shows the projected fatigue behavior of W-Re-Hf-C/Waspaloy composites as a function of combined axial and flexural stresses for a fatigue life of  $10^8$  cycles at 870 and 1100 °C. Additionally the calculated stress at the root of the FRS airfoil designed for this application is also shown in Fig. 6. These data indicate that fiber reinforcement can offer a potential of over 200 °C increase in use temperature.

Although very little strain-controlled, low-cycle fatigue data have been generated for FRS composites, an attempt has been made to estimate a range of low cycle fatigue behavior using the Manson-Coffin approach Ref. 6, and the results for 50 volume fraction content W-Re-Hf-C fibers in a Waspaloy matrix for 870 °C are shown in Fig. 7.

Clearly the low-cycle fatigue behavior for the FRS composite falls within the range obtained for the current SSME blade alloy material.

#### Blade Redesign

A major feature of the investigation of Ref. 6 involved preliminary design of turbine blades fabricated from advanced materials for the SSME. Because of the high strengths of FRS structures, it was found that the SSME airfoil could be redesigned from the current solid airfoil to a hollow thin-wall member, thereby reducing the mass of the turbine blade. This feature, combined with the relatively high thermal conductivity of FRS composites (Fig. 8), which is approximately double that of MAR M-246 (Hf) (DS) at 870 °C, is a distinct advantage in reducing the thermal strains that accompany engine start and shutdown transients.

#### VERIFICATION OF FRS PROPERTIES

The results of the turbine blade structural analysis showed that FRS composites have a highly attractive combination of properties for advanced rocket engine turbopump turbine blade applications. In order to develop the FRS composite for use as advanced rocket engine turbine blades however, development of a data base is needed with particular attention to areas such as thermal fatigue, thermal shock and hydrogen environmental embrittlement effects. The first priority was therefore to produce an adequate supply of FRS materials and to measure the key design properties of those materials. Thus a program (Ref. 7) was conducted to evaluate four candidate fiber reinforced superalloy composite systems with respect to mechanical properties required for SSME blade application. The tests included: tensile, ductile-brittle transition temperature determination; thermal shock under SSME start transient conditions; thermal fatigue; low and high-cycle fatigue; and hydrogen environmental embrittlement.

#### Materials

As the high strength W-Re-Hf-C fiber was not commercially available, a weaker tungsten-1.5 percent thorium oxide fiber was substituted since it is the strongest readily available tungsten alloy fiber. Following the general recommendations of Ref. 6, Waspaloy, 316L stainless steel, Incoloy 907, and FeCrAl (Table II) were utilized as the matrix materials.

For ease of fabrication, FRS composites containing 40 vol % fiber contents rather than 50 vol % were fabricated using an arc-spray process (Ref. 11) to produce monofilament tapes. These were subsequently hot pressed into composite panels 50 mm wide, 150 mm long and 1.5 mm thick with the fiber's length parallel to the panel length. The microstructure of a typical FRS composite is shown in Fig. 9. It is evident that the fibers are evenly distributed within the matrix (Fig. 9(a)) and that there is little evidence of a deleterious reaction between the two components, (Fig. 9(b)). To provide a basis for comparison for the FRS composites in the thermal shock and thermal fatigue tests, MAR M-246 (Hf) (DS) and Alloy 1480 (single crystal) panels were also fabricated. The nominal compositions for MAR M-246 (Hf) (DS) and Alloy 1480 are shown in Table II.

Due to the use of a lower volume fraction, lower strength fiber, mechanical and physical properties of the tungsten-1.5 percent thoria reinforced composites were projected utilizing the same methodology developed for the W-Re-Hf-C strengthened materials. Comparisons of these estimated values to the measured property data were made to assess the potential of FRS composites for use as SSME turbine blades and to assess the validity of projection methodology.

#### Tensile Testing

Tensile test were conducted using flat sheet specimens fabricated from composite panels by wirecut electro discharge machining. The specimens had a 12 mm gauge length with fibers oriented parallel to the longitudinal axis of the specimens. Tensile tests were undertaken at -196°, 20°, 870°, and 1100 °C and the ductile-brittle transition temperature was estimated from the reduction in area data. Results for the 870 °C ultimate tensile strengths are presented for three FRS composite systems in Table III. The measured values for the 40 vol % tungsten-1.5 percent thoria reinforced materials compare well with the estimated strengths; hence it is concluded that the methodology for projecting tensile strengths is valid and that the ultimate tensile strengths of the W-Re-Hf-C reinforced composites should thus also be equal or higher than the estimates given in Table III.

As temperatures can drop to the cryogenic during engine shut down in liquid propellant rocket engines based on oxygen/hydrogen fuels, the ductile/brittle transition temperatures (DBTT) for the composite is of interest. None of the three composite systems examined (Waspaloy, 316L stainless steel, and IN 907 matrices) exhibited a ductile-brittle transition temperature from -196 to 1100 °C which is consistent with the matrix alloys. Reduction in area values for the composites range from 5 to 17 percent at -196 °C and 9 to 20 percent at 1100 °C.

#### Thermal Shock Testing

Figure 10 illustrates the high-pressure fuel turbine inlet gas temperature transients that produce the thermal transient in the turbopump turbine blades of the SSME. Two high-intensity spikes occur within 2 sec of start-up and yield severe thermal shock

loadings. After this initial period there is a gradual rise in temperature which leads to thermal fatigue damage. In order to simulate these thermal shock transients, a programmed computer-controlled, high-intensity electron beam was utilized to repeatedly heat a square area centrally located on polished FRS and superalloy test panels (Fig. 11). A typical time-temperature profile is shown in Fig. 12; in general the maximum temperature ranged from 870 to 980 °C during each thermal shock cycle. The panels were heated from 90 to 870 °C within 0.3 sec.

The number of thermal cycles required to generate surface microcracking for the FRS composites and superalloys are shown in Fig. 13. The FRS composites have excellent thermal shock resistance compared to the present SSME material MAR M-246 (Hf) (DS), which cracked after 1 to 6 cycles, while the single crystal Alloy 1480 was better than MAR M-246 (Hf) (DS), microcracks were still observed after 6 to 11 cycles. In contrast to the unreinforced materials, the worst composite life was 20 cycles (Waspaloy, 316L stainless steel and FeCrAl matrices) while the IN 907 composite resisted over 45 cycles before any signs of microcracks were observed. The thermal shock damage in the FRS composites and superalloys occurred primarily in the surface of the panels. The superior thermal conductivities of the FRS composites readily dissipated the heat generated by the thermal shock cycles. This minimized the temperature gradient and consequently the thermal strains were less severe in the FRS composites than in the superalloy panels. A significant improvement in thermal shock resistance can thus be gained using this class of materials for rocket engine turbine blades.

#### Thermal fatigue Testing

In order to simulate the thermal transients that occur after 2 sec of SSME engine start-up which leads to blade thermal fatigue damage, a programmed computer-controlled high-intensity electron beam was utilized to heat polished test panels. A thermal analysis of the SSME airfoil indicated that the average heating rate for the airfoil occurring from 2 to 5 sec after engine start was about 220 °C/sec. To produce the same heating rate in the FRS composite test panels as in similar panels machined from superalloys, the power input into the FRS composites had to be increased because of their higher thermal conductivity: for example the 870 °C peak temperature tests required 66 percent more power to produce the desired heating rate in the FRS composite panels as compared to the superalloys, while the 1100 °C peak temperature tests required 38 percent more power. All panels were cycled 55 times before the thermal fatigue tests were terminated. The test results for the thermal fatigue experiments are given in Table IV. In the 870 °C tests, the unreinforced superalloys performed well and in some cases better than a few of the composites. The single crystal Alloy 1480 and the tungsten/Waspaloy composite showed no indications of microcrack initiation after 55 thermal fatigue cycles. The MAR M-246 (Hf) (DS) and the tungsten/316L stainless steel composite had microcracks after 45 to 55 thermal fatigue cycles, and the tungsten/Incoloy 907 and tungsten/FeCrAl composites developed microcracks between 11 and 31 thermal fatigue cycles. At the 1100 °C peak temperature all of the materials showed indications of microcracking before the desired 55 cycles were achieved. At this maximum temperature the best performing material was tungsten/316L stainless steel, which cracked between 25 to 40 cycles while the least resistant composite, tungsten/Incoloy 907, showed signs of microcracking in less than 10 cycles. The superalloys performed as well as the tungsten/FeCrAl and tungsten/Waspaloy composites.

#### Low and High-Cycle Fatigue Testing

All low and high-cycle fatigue tests were conducted at 870 °C in a helium atmosphere under tension-tension conditions with a load ratio (minimum stress/maximum stress) of  $R = 0.2$  at 1 and 55 Hz respectively for the low and high-cycle fatigue experiments. The test specimen geometry was the same as that used for tension testing and in all cases specimen fatigue failure was defined as complete separation. Baseline specimens were tested in the as-polished condition. Companion specimens were thermal shock damaged to produce surface microcracks by subjecting the specimens to 55 thermal shock cycles. These samples were also tested to determine the effect of surface condition on cyclic fatigue behavior. The projected upper and lower low-cycle fatigue (strain life) curves for composites reinforced with tungsten-1.5 percent thorium fibers are compared with the experimental data for polished specimens in Fig. 14. The data are within the upper and lower projected bounds except for tungsten/316L stainless steel composites which are more ductile than expected at longer lives. It can be seen that the thermal shock damage to introduce surface microcracks did not have a detrimental effect on the low-cycle fatigue behavior of the composites.

If one makes the assumption that the self imposed stresses in thermal fatigue results in a low-cycle fatigue situation, prediction of life under thermal fatigue behavior can be obtained from the low cyclic test results. For instance, different thermal strains will occur in the blades constructed of different materials when subjected to the same hot gas transient. For a given geometry, the thermal gradients depend on the thermal diffusivity of the material:

$$D_f = K/\rho C$$

where

$D_f$	thermal diffusivity
$K$	thermal conductivity
$\rho$	density
$C$	specific heat

The temperature gradients for a given configuration subjected to the same thermal transient made of different materials were assumed to be proportional to the reciprocal of their diffusivities, Ref. 1. With MAR M-246 (Hf) (DS) as the baseline, the relative thermal transient strains for the composites are given by:

$$\frac{\Delta\epsilon_{\text{composite}}}{\Delta\epsilon_{\text{MAR M-246 (Hf) (DS)}}} = \frac{\alpha_{\text{composite}} (K/\rho C)}{\alpha_{\text{MAR M-246 (Hf) (DS)}} (K/\rho C_{\text{composite}})}$$

where

$$\begin{aligned}\Delta\epsilon &= \text{thermal strain} \\ \alpha &= \text{thermal expansion}\end{aligned}$$

Thus, a thermal strain range of 3 percent for MAR M-246 (Hf) (DS) is reduced to 0.35 percent for a FRS blade because the thermal diffusivity for the composite is almost five times greater than the superalloy, primarily due to the three times higher thermal conductivity. Furthermore the thermal coefficient of expansion of the composite is about 50 percent of that for the superalloy. With the assumption that thermal fatigue can be approximated by low-cycle fatigue testing, the life of a FRS blade subjected to a thermal strain range of 0.35 percent is estimated from Fig. 14 to be  $10^4$  cycles. This is a significant improvement over the current blade material life of less than 10 cycles.

Figure 15 illustrates the low and high-cycle fatigue data for the tungsten/Waspaloy composite plotted with the stress amplitude as a function of cycles to failure. It can be seen that the attempts to induce thermal shock damage did not have a detrimental effect on the low or high-cycle fatigue strength; both the as-polished data and thermal shock damaged data are in excellent agreement and lie on a single curve which has the form:

$$\Delta\sigma/2 = a(N_f)^b$$

where

$$\begin{aligned}\Delta\sigma &= \text{stress range} = \text{maximum stress} - \text{minimum stress} \\ \Delta\sigma/2 &= \text{stress amplitude} \\ a &= \text{constant} \\ N_f &= \text{cycles to failure} \\ b &= \text{power law exponent}\end{aligned}$$

The fatigue curves for three FRS composites and the two superalloys are plotted in Fig. 16. The curves are for the as-polished and thermal-shock-damaged FRS composites while those for the two superalloys are for the as-polished condition. In the high-cycle fatigue regime, the tungsten/Waspaloy composite showed the highest fatigue strength of the three FRS composites tested and it is higher than that for the superalloys above  $10^5$  cycles. The fatigue data indicate that the FRS composites can have superior high-cycle fatigue strength retention as the power law exponents are slightly higher than those for conventional wrought superalloys. This further suggests that the fatigue life of the composite is less sensitive to stress amplitude.

Projected high-cycle fatigue (stress life) curves for a Waspaloy matrix composite reinforced with either tungsten-1.5 percent thoria or W-Re-Hf-C fibers are shown in Fig. 17; clearly there is significant benefit to be gained from the use of the higher strength W-Re-Hf-C fiber. The actual fatigue data for tungsten-1.5 percent thoria reinforced Waspaloy composites is also shown in the figure and it lies above the projected curve which indicates that the methodology of estimating fatigue behavior is conservative. Therefore it is anticipated that the fatigue strength of a Waspaloy matrix composite reinforced with W-Re-Hf-C fibers will also be higher than the projection. The W-Re-Hf-C fiber reinforced composite offers a significant advantage for  $870^{\circ}\text{C}$  high-cycle fatigue conditions compared to the data for MAR M-246 (Hf) (DS).

#### Hydrogen Environment Embrittlement Testing

Notched flat sheet tensile specimens were used for hydrogen environment embrittlement tests. The specimens were tension tested in 6.9 MPa hydrogen at room temperature with additional specimens tested in 6.9 MPa helium to provide a basis for comparison for the susceptibility to hydrogen.

As shown in Fig. 18, the tungsten/Incoloy 907, tungsten/316L stainless steel and the tungsten/Waspaloy composites do not appear to have undergone embrittlement in a 6.9 MPa hydrogen environment at room temperature. The fractography showed that the matrices of the three composites all failed in a ductile manner while the fibers broke in a brittle manner. This behavior was identical to that observed after room temperature helium tests. Although additional testing at higher hydrogen pressures must be conducted, the existing data indicate that the FRS composites should perform well in contrast to the behavior of MAR M-246 (Hf) (DS) and single crystal Alloy 1480 (Fig. 18). The FRS composite materials thus offer an advantage over the current SSME blade material relative to use in a hydrogen environment.

## SUMMARY OF RESULTS

Studies were conducted to determine the potential of fiber reinforced superalloys for rocket engine turbine blade use. The first stage blades of the high pressure turbopump of the SSME have been chosen as the reference system, and preliminary design properties were estimated for FRS composite materials based on the use of 50 vol % fiber content W-Re-Hf-C fibers in ductile superalloy matrices. It was concluded based on these projections that FRS turbine blades offer the potential of significantly improved operating life (three orders of magnitude increase over the current material), higher operating temperature capability (over a 200 °C increase) and reduced strains induced by transient thermal conditions during engine start and shut down. In order to develop the FRS composite for use as advanced rocket engine turbine blade material however, more adequate data base was needed and experimental confirmation of the methodology used to project key design properties for FRS was also required. Research was thus conducted on readily fabricable composites containing 40 vol % tungsten-1.5 percent thoria fibers in several alloy matrices. Experiments were undertaken to evaluate key engineering properties for blade application and to assess the validity of the methodology used in the design property projections. This work yielded the following results:

1. The thermal shock resistance of the FRS composites was excellent, two to nine times better than the current superalloy blade material.
2. The thermal fatigue resistance of the FRS composites was equal to or higher than the current blade material.
3. The tensile and low and high-cycle fatigue strengths were equivalent to greater than the projected properties.
4. Prior thermal shock damage had a negligible influence on the low or high-cycle fatigue behavior of the FRS composites.
5. The FRS composites exhibited negligible embrittlement from a 6.9 MPa hydrogen environment.
6. No ductile brittle transition temperature was observed for FRS materials from -196 to 1100 °C.

Thus the FRS composites have a highly attractive combination of properties for advanced rocket engine turbopump blade application for a temperature range from 870 to 1100 °C. Based on these results continued effort directed towards developing FRS composites for use as rocket turbine blades is underway.

## REFERENCES

1. Chandler, W.T.: Materials for Advanced Rocket Engine Turbopump Turbine Blades. (RI/RD83-207, Rockwell International; NASA Contract NAS3-23536) NASA-CR 174729, 1983.
2. Petrasek, D.W., et al.: Tungsten Fiber-Reinforced FeCrAlY- A First Generation Composite Turbine Blade Material. NASA TM-79094, 1979.
3. Winsa, E.A.; Westfall, L.J.; and Petrasek, D.W.: Predicted Inlet Gas Temperatures for Tungsten Fiber Reinforced Superalloy Turbine Blades. ICCM/2, B.R. Norton, et al., eds., Metallurgical Society of AIME, Philadelphia, PA, 1978, pp. 840-857.
4. Melnyk, P.; and Fleck, J.N.: Tungsten Wire/FeCrAlY Matrix Turbine Blade Fabrication Study. (TRW-ER-8101, TRW Inc.; NASA Contract NAS3-20391) NASA CR-159788, 1979.
5. Petrasek, D.W.; and Signorelli, R.A.: Tungsten Fiber Reinforced Superalloys- A Status Review. Ceram. Eng. Sci. Proc., vol. 2, no. 7-8, July-Aug. 1981, pp. 739-786.
6. Lewis, J.R.: Design Overview of Fiber-Reinforced Superalloy Composites for the Space Shuttle Main Engine. (RI/RD83-152, Rockwell International; NASA Contract NAS3-23521) NASA CR-168185, 1983.
7. Yuen, J.L.: Screening Evaluation of Candidate Fiber-Reinforced Superalloys for Space Shuttle Main Engine Turbopump Blade Application, Part I. (RI/RD85-282, Rockwell International; NASA Contract NAS3-24380) NASA CR-17408, 1986.
8. Yuen, J.L.: Screening Evaluation of Candidate Fiber-Reinforced Superalloys for Space Shuttle Main Engine Turbopump Blade Application, Part II. (RI/RD87-217-PT-2, Rockwell International; NASA Contract NAS3-24380) NASA CR-180838, 1987.
9. Petrasek, D.W.: High-Temperature Strength of Refractory-Metal Wires and Consideration for Composite Applications. NASA TN D-6881, 1972.
10. Fleck, J.N.: Fabrication of Tungsten Wire/FeCrAlY-Matrix Composite Specimens. TRW-ER-8076, TRW Inc., Cleveland, OH, 1979.

11. Westfall, L.J.: Tungsten Fiber Reinforced Superalloy Composite Monolayer Fabrication by an Arc-Spray Process. NASA TM-86917, 1985.

TABLE I. - COMPARISON OF OPERATING PARAMETERS BETWEEN ROCKET ENGINE TURBINES AND AIRCRAFT GAS TURBINES (REF. 1)

Item	Rocket engine turbines	Aircraft gas turbines
Fuel	Hydrogen or CH <sub>4</sub>	Petroleum distillate or Air
Oxidizer	Oxygen	15 000
Operating speed, rpm	36 000-110 000	564 (1850)
Blade tip speed, m/s (ft/s)	564 (1850)	0.47 (630)
Power/blade, MW (hp)	0.15-0.35 (200-470)	870-1205 (1600-2200)
Turbine inlet temperature, °C (°F)	1425 (2600)	870-1205 (1600-2200)
Heat transfer coefficient, W/m <sup>2</sup> C (Btu/ft <sup>2</sup> h °F)	306 000 (54 000)	2840 (500)
Thermal start/stop-transients, °C/s (°F/s)	18 000/2000 (32 000/36000)	56 (100)
Engine starts	55-700	2400
Operational life, hr	7.5-100	8000

TABLE II. - NOMINAL CHEMICAL COMPOSITION OF ALLOYS

Alloy	Element composition, weight percent														
	Ni	Co	Cr	Fe	Mo	Ti	Al	W	Ta	Hf	Nb	Mn	Y	C	B
MAR M-246 (Hf) (DS)	Bal.	10	9	----	2.5	1.5	5.5	10	1.5	1.75	----	----	0.15	----	----
Alloy 1480 (SC)	Bal.	5.2	9.3	----	0.03	1.4	4.8	4.1	11.8	----	----	----	0.08	0.006	0.06
Waspaloy	Bal.	14	20	----	4	3	1	----	----	----	3	----	0.02	----	----
Incoloy 903	38	15	----	Bal.	----	1.4	0.7	----	----	----	4.7	2	0.03	----	----
Incoloy 907	38	13	----	----	1.5	0.03	----	----	----	----	2	0.02	----	----	----
316L Stainless steel	12	----	18	----	3	----	4	----	----	----	1	----	0.03	----	----
FeCrAl	----	----	24	----	----	4	----	----	----	----	----	1	----	----	----
FeCrAlY	----	----	24	----	----	4	----	----	----	----	----	1	----	----	----

TABLE III. - 870 °C ULTIMATE TENSILE STRENGTHS FOR FRS COMPOSITES

Matrix material	Measured ultimate tensile strength for 40 vol % W - 1.5% ThO <sub>2</sub> fibers, MPa	Projected ultimate tensile strength, MPa	
		40 vol % W - 1.5% ThO <sub>2</sub> fibers	50 vol % W-Re-Hf-C fibers
Waspaloy	999	882	1378
316L stainless steel	758	717	1240
Incoloy 907	655	655	1192

TABLE IV. - THERMAL FATIGUE RESULTS

Material	871 °C peak temperature <sup>a</sup>	1093 °C peak temperature <sup>b</sup>
MAR M-246 (Hf) (DS)	45 to 55	10 to 25
Alloy 1480 (SC)	>55	10 to 25
W/FeCrAl composite	11 to 31	10 to 25
W/907 composite	11 to 31	<10
W/Waspaloy composite	>55	10 to 25
W/316L SS composite	45 to 55	25 to 40

<sup>a</sup>Heated to 871 °C at 220 °C/sec FRS composites required more energy input to achieve this heating rate than the cast superalloys.

<sup>b</sup>Heated to 1093 °C at 220 °C/sec FRS composites required more energy input to achieve this heating rate than the cast superalloys.

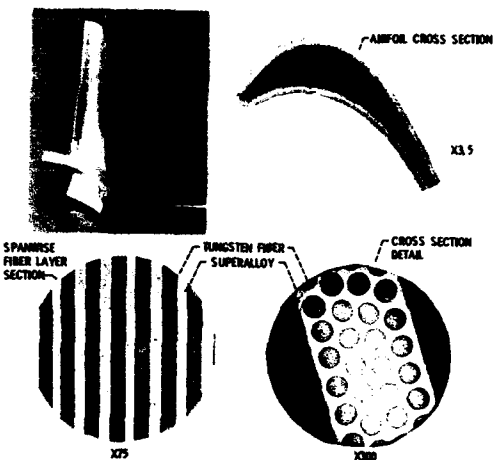


FIGURE 1. - PHOTOGRAPHS AND MICROSTRUCTURE OF A TUNGSTEN FIBER/SUPER-ALLOY COMPOSITE BLADE. (REF. 5).

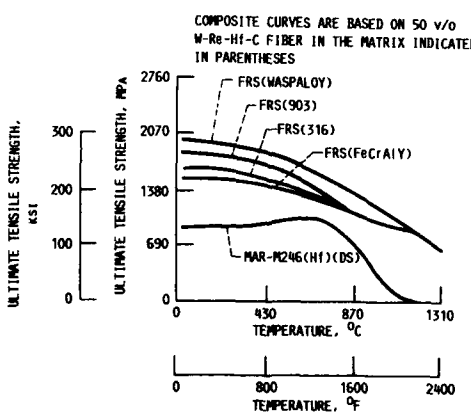


FIGURE 2. - ESTIMATED TENSILE STRENGTH OF CANDIDATE FRS COMPOSITES AS A FUNCTION OF TEMPERATURE COMPARED TO THAT OF MAR-M246 (H1)(DS). (REF. 6.)

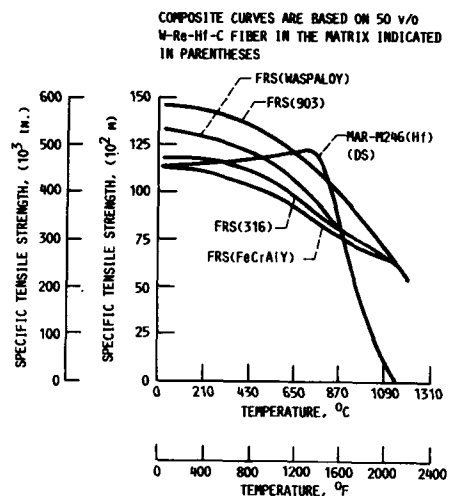


FIGURE 3. - ESTIMATED SPECIFIC STRENGTHS OF CANDIDATE  
FRS COMPOSITES AS A FUNCTION OF TEMPERATURE COMPARED  
TO THAT OF MAR-M246(Hf)(DS). (REF. 6.)

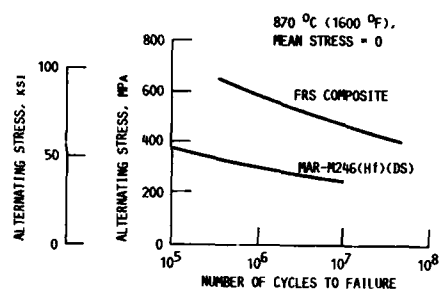


FIGURE 5. - COMPARISON OF THE ESTIMATED HIGH-CYCLE  
FATIGUE STRENGTH OF A 50 VOL PERCENT W-Re-Hf-C  
FIBER/WASPALOY COMPOSITE MATERIAL WITH MAR-M246(Hf)  
(DS). (REF. 1.)

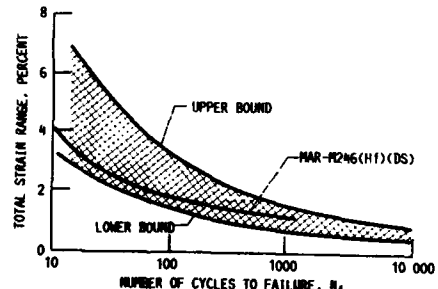


FIGURE 7. - LOW-CYCLE FATIGUE PROJECTION FOR W-Re-Hf-C/  
WASPALOY COMPOSITE AT 870 °C (1600 °F) COMPARED  
TO THE BEHAVIOR OF MAR-M246(Hf)(DS). (REF. 6.)

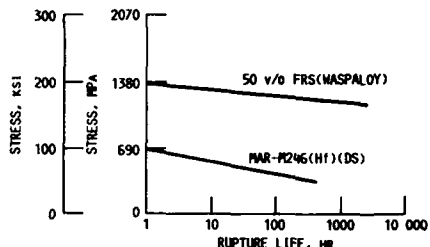


FIGURE 4. - STRESS RUPTURE STRENGTH OF MAR-M246  
(Hf)(DS) AND A FRS COMPOSITE AT 870 °C (1600 °F).  
(REF. 6.)

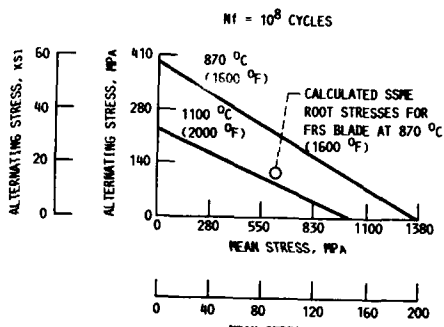


FIGURE 6. - CALCULATED GOODMAN DIAGRAM FOR A  
W-Re-Hf-C/WASPALOY COMPOSITE. (REF. 6.)

- (1) CALCULATED (REF. 3)
- (2) MEASURED (REF. 3)
- (3) MEASURED (REF. 6)

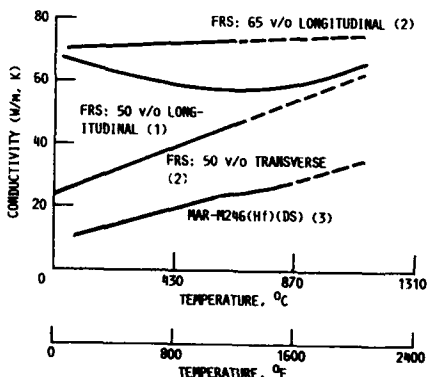


FIGURE 8. - THERMAL CONDUCTIVITY OF A TUNGSTEN  
FIBER/FeCrAlY COMPOSITE AND MAR-M246(Hf)(DS)  
AS A FUNCTION OF TEMPERATURE. (REF. 6.)

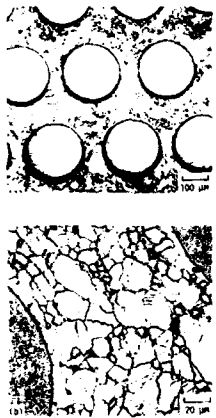


FIGURE 9. - MICROSTRUCTURE OF AN AS-FABRICATED TUNGSTEN-1.5 PERCENT  $TiO_2$ -WASPALOY COMPOSITE. (REF. 8.)

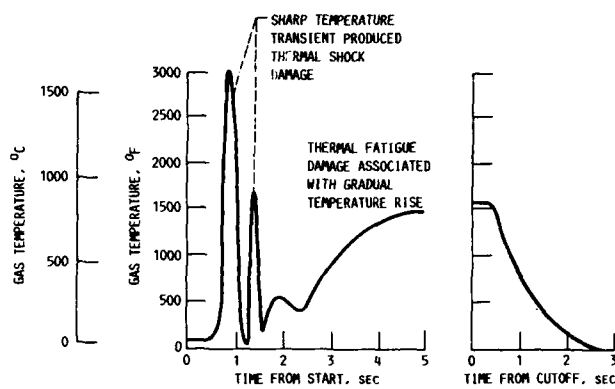


FIGURE 10. - SSME HIGH-PRESSURE FUEL TURBINE INLET TEMPERATURE TRANSIENTS DURING ENGINE START-UP AND SHUTDOWN. (REF. 7.)

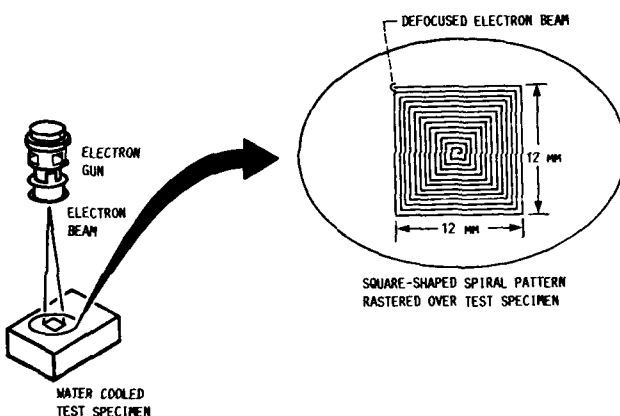


FIGURE 11. - SQUARE-SHAPED SPIRAL PATTERN USED IN THE THERMAL SHOCK AND THERMAL FATIGUE TESTS. (REF. 7.)

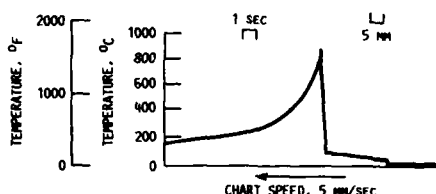


FIGURE 12. - THERMAL SHOCK TEMPERATURE PROFILE SIMULATING THE SSME ENGINE STARTUP TRANSIENT. DURATION OF POWER PULSE IS 0.3 SEC. (REF. 7.)

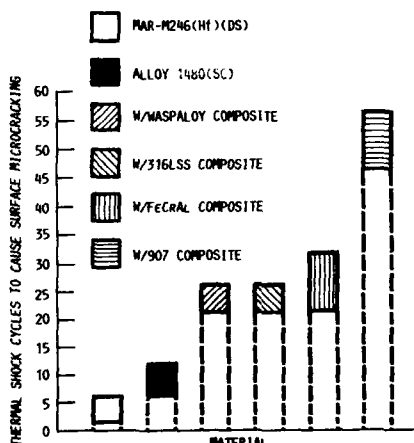


FIGURE 13. - NUMBER OF THERMAL SHOCK CYCLES TO INDUCE SURFACE MICROCRACKING IN FRS COMPOSITES, MAR-M246(H)(DS), AND ALLOY 1480 SINGLE CRYSTAL (REF. 8.)

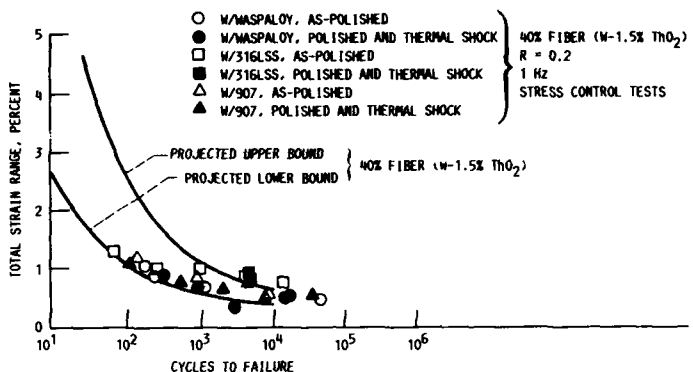


FIGURE 14. - COMPARISON OF 870 °C (1600 °F) ESTIMATED LOW-CYCLE FATIGUE UPPER AND LOWER BOUNDS WITH ACTUAL TEST DATA FOR FRS COMPOSITES. (REF. 8.)

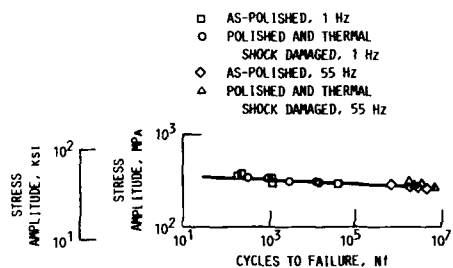


FIGURE 15. - COMBINED LOW AND HIGH-CYCLE FATIGUE DATA FOR A TUNGSTEN-1.5% ThO<sub>2</sub>/WASPALOY COMPOSITE TESTED AT 870 °C (1600 °F). (REF. 7.)

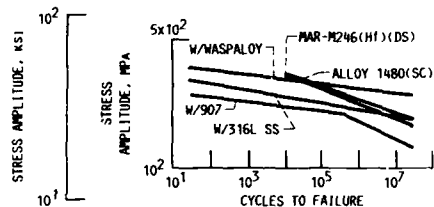


FIGURE 16. - COMPARISON OF THE 870 °C (1600 °F) HIGH-CYCLE FATIGUE BEHAVIOR OF SEVERAL FRS COMPOSITES WITH MAR-M246(H1)(DS) AND SINGLE CRYSTAL ALLOY 1480. (REF. 8.)

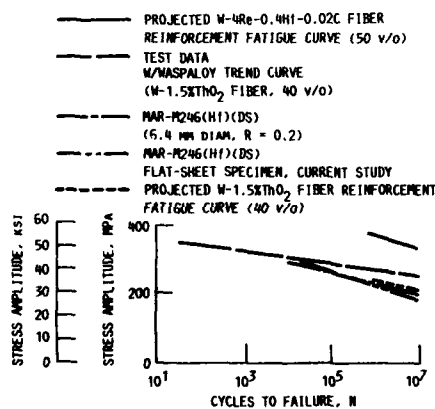


FIGURE 17. - COMPARISON OF THE 870 °C (1600 °F) HIGH-CYCLE FATIGUE DATA FOR A TUNGSTEN/WASPALOY COMPOSITE AND MAR-M246(H1)(DS) WITH PROJECTED CURVES BASED ON SEVERAL TYPES OF FIBERS AND FIBER CONTENTS. (REF. 8.)

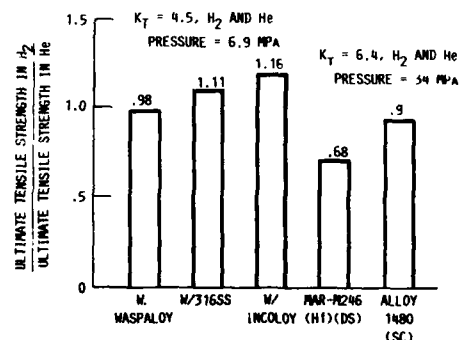


FIGURE 18. - HYDROGEN ENVIRONMENTAL EMBRITTLEMENT RESISTANCE OF FRS COMPOSITES COMPARED TO THAT FOR MAR-M246(H1)(DS) AND SINGLE CRYSTAL ALLOY 1480. (REF. 8.)

## DISCUSSION

R. Eck, Metallwerk Plansee, Austria. You mentioned that you worked with tungsten-1.5% thorium wire. Was that wire aluminum, potassium and silicon-doped wire? Was it used in the as-drawn state or was it recrystallized before processing? What was the diameter of the wire?

D. Petrasek, NASA-Lewis, US. The wire was not doped. It was made by Philips Elmet. It's tungsten with an ultra-fine thorium dispersoid. It was used in the as-drawn state and its diameter was 0.008 inch, 0.02 cm.

P. Ramette, SEP, France. In Fig. 1 of your paper you showed a tungsten fiber reinforced superalloy composite, aircraft engine-type turbine blade with cooling at the trailing edge. Could you comment on the nature of the cooling and the cooling parameters (coolant temperature, mass flow, etc.) for a blade of this type?

D. Petrasek, NASA-Lewis, US. The blade shown was fabricated to demonstrate the feasibility of making complex airfoil structures with this material. This particular blade had an airfoil geometry very similar to that of a JT9D blade. The airfoil was hollow and had trailing edge cooling slots. The cooling process envisioned for this particular blade was impingement cooling. An insert containing holes would be placed within the hollow airfoil cavity. Thermal barrier coatings might also be used. We never actually tested that blade, however. It was fabricated to prove we could make complex shapes.

R. Kochendorfer, DFVLR, FRG. Where are the most critical parts of today's space shuttle main engine (SSME) blades? Are they in the airfoil, where it is relatively easy to use fiber reinforcement, or in the root area where it is almost impossible to use reinforcement?

D. Petrasek, NASA-Lewis, US. The critical part of the SSME blade is dependent upon which stage and which turbopump the blade is being used for. Fatigue cracking in the first-stage blades of the high pressure fuel turbopump occurs in the airfoil at the leading edge near the platform of the blade. Fatigue cracking in the second-stage blades of the high pressure fuel turbopump occurs in the trailing edge shank section of the root. Fatigue cracking in the first-stage blades in the high pressure oxygen turbopump occurs in the trailing edge fir-tree section of the root. Fiber reinforced superalloy composites are being considered for use in the airfoil section of first-stage blades of the high pressure fuel turbopump.

P. Hancock, Cranfield Institute of Technology, UK. Most of the data you presented are short-term data. Have you done any long-term tests at high temperatures and do you find any degradation of properties after long-term exposure?

D. Petrasek, NASA-Lewis, US. Short-term properties are the important ones for the SSME turbine blade application. Exposure times there are likely to be less than ten hours, as opposed to the case of airbreathing turbine engines where exposure times are likely to be hundreds or thousands of hours. Property degradation for short-term exposure is not a problem for these materials. We have looked at longer-term behavior, for example in creep or stress-rupture, but that is not the requirement for this application.

E. Campo, Fiat Aviazione, Italy. In Fig. 7, in which you showed the low cycle fatigue behavior of fiber reinforced superalloys, the fatigue curve was derived on the basis of Manson's 'universal slopes' equation. Since you also have experimental data for the low cycle fatigue of these fiber reinforced superalloys, have you compared them to verify the applicability of the Manson model to these materials?

D. Petrasek, NASA-Lewis, US. The lower bound derived by the Manson-Coffin universal slopes method fit our experimental low cycle fatigue data quite well. I think it is applicable, as a first order approximation, for projections of the behavior of these fiber reinforced superalloys.

E. Campo, Fiat Aviazione, Italy. Since you've used electron beam heated specimens in your thermal shock and thermal fatigue tests, have you performed finite element analyses to derive a relationship between the electron beam test conditions and those that would actually be experienced in an engine? I think the anisotropy of the fiber reinforced superalloys may be a problem in relating electron beam test results and actual engine performance.

D. Petrasek, NASA-Lewis, US. We have found that the number of cycles required for the observation of the first signs of surface microcracking, and the nature of the cracking observed in electron beam damaged specimens were similar to those observed for actual turbine blades run in engine tests. We have not made a direct correlation between electron beam simulation and engine tests, but we believe that the electron beam test can be used to screen candidate materials and provide relative rankings of their thermal shock resistance.

B. Bhat, NASA-Marshall, US. Have you conducted any plastic strain to crack initiation tests in high pressure hydrogen? That gives the strain tolerance of these materials in hydrogen, and that is an important design criterion.

D. Petrasek, NASA-Lewis, US. No, we have not, and some testing should be done. We do not expect hydrogen embrittlement to be a serious problem since the tungsten fibers are not susceptible and we could select matrix materials that are also not susceptible. Even if the matrix material were embrittled and cracks were initiated, the fiber interfaces would blunt such cracks, as evidenced in our fatigue tests on thermally shock damaged specimens.

**"BEHAVIOR OF TUNGSTEN, MOLYBDENUM AND ALLOYS UNDER UNUSUAL HEATING CONDITIONS"**

R. Eck, H. Bildstein, F. Simader, R. Stickler\*, J. Tinzl  
 Metallwerk Plansee GmbH  
 A-6600 Reutte  
 \*University of Vienna, Austria

**1. SUMMARY**

The first part summarizes the state of the art of fabricability of tungsten by powder metallurgy methods for relevant configurations in relation to final properties desired. Effects of unisotropy through metal forming and its relevance to design are discussed. For tungsten-thoria alloys as an example for a refractory ODS alloy mechanical properties such as DBTT for low temperature stresses and strength, ductility and microstructural data at temperatures up to 3000°K are presented and discussed in context with application considerations.

As an alternative tungsten-rhenium alloys containing up to 26 % Re are discussed in comparison with tungsten-thoria emphasizing advantages of ductility at low temperatures.

A simple model of interference of heat dissipation and buildup of thermal stresses in a plate configuration of tungsten is shortly discussed.

Relevant properties of the molybdenum alloys Mo5Re to Mo41Re, a selection of Ti, Zr, Hf carbide-oxide dispersion strengthened alloys and molybdenum tungsten alloys are discussed.

Limitations of erosion and oxidation inhibiting coatings for refractory metals are explained for advanced chemical and physical methods.

**2. INTRODUCTION**

Among materials considered to function at extremely high temperatures under unconventional environmental conditions several powder metallurgical refractory metals and alloys have been found most suitable. Combustion of gaseous, liquid or solid fuel used in propulsion and turbine systems generates temperatures so high that refractory metals have been employed since the early days of this development. Up till now tungsten alloys are standard materials for rocket nozzles and similar devices because of the relatively high ductility compared to advanced non-metallic materials.

We do not want to discuss powder metallurgical methods for refractory metals in detail, because standard literature is available (1-4), but a short summary of the state of the art of PM fabrication for tungsten and molybdenum should be given.

Starting from pure or alloyed powders parts are cold isostatically pressed to configurations that are adjusted to the dimensions of the final part. Pressed molybdenum parts can be machined to close tolerances, tungsten and tungsten alloy parts only if presintered in hydrogen. Sintering is performed at temperatures of 2000°C for molybdenum and 2500°C for tungsten based alloys under hydrogen as a protective and reducing atmosphere to densities above 95 %. Standard deformation processes for tungsten and molybdenum involve all kinds of rolling, forging and swaging. For production of radially symmetric parts such as cylinders, cones and rings forging methods are the preferred operations. Depending on the ratios of OD, ID and height these parts are prepared mostly by upset forging of discs and further forming operations to achieve tube like configurations.

Differing from nearly all other groups of metals where the final grain structure primarily depends on various heat treatments with more or less complete phase changes, refractory metals with b.c.c crystal structure achieve their final grain structure through deformation and subsequent recrystallization heat treatment.

**3. FORGING OF TUNGSTEN, MOLYBDENUM AND ALLOYS**

**3.1 MOLYBDENUM ALLOYS**

To demonstrate the influence of massflow dependent on forging procedure on the properties of an upset forged disc produced out of a sintered TZM (Mo-0,5Ti-0,08Zr-0,01...C) cylinder, Fig. 1 shows ultimate tensile strength and elongation in three possible directions for 50 % and 70 % deformation (5) (Deformation is defined as change of crosssection or height expressed as percentage of

starting section or height). Increasing degree of upset forging increases tensile strength and elongation in tangential and axial direction, but reduces axial strength. Axial elongation was found zero, independent of degree of forging, measured at ambient temperature.

### 3.2. TUNGSTEN THORIA ALLOYS

The diagrams in Fig. 2 demonstrate which strength and ductility values can be achieved by unidirectional forming of W-2ThO<sub>2</sub> using swaging and drawing as forming methods. The increase in strength up to 1400°C with increasing deformation is a logarithmic dependency especially at temperatures below the recrystallization temperature. Increase in deformation also improves ductility measured as DBTT in standardized bending tests, but only at more than 20 % deformation the DBTT reaches ambient temperature and elongations of several % can be measured. Increasing elongations at a test temperature of 300°C shows, that the DBTT is exceeded. The decrease in elongation at 800° and 1400°C for deformation at and above 90 % may be explained by changes in the deformation mechanisms for ODS (oxide dispersion strengthened) materials such as W-ThO<sub>2</sub>. For jet propulsion applications forged rings or tube like configurations weighing several kg are usual. For such forgings deformation between 50 and about 90 % are possible. Forgings of WThO<sub>2</sub> are brittle at room temperature and reach ductility at temperatures between about 100°C and 300°C dependent on location and direction within the forged and machined part. Fig. 3 shows data of ultimate tensile strength and elongation for a W-2ThO<sub>2</sub> rod 90 % deformed. The highest strength is reached at 350°C, a temperature above the ductile-brittle-transition-temperature range. In this temperature range a pronounced change in the fracture mode can be detected as shown in Fig. 4 (6).

To get information about the effect of heat treatments on ultimate tensile strength and elongation tensile testing has to be performed using specimens heat treated at temperatures between 1000°C and 2400°C. As shown in Fig. 5 a drop in strength and an increase in ductility between 1300°C and 1500°C correlate with the onset and the end of recrystallization. As for all refractory metals strength-ductility ratios can be selected depending on mode of application.

A typical fracture surface of a W-2ThO<sub>2</sub> sample 90 % deformed and tested after recrystallization is shown in Fig. 6. On the predominant intercristalline fracture surface thoria particles are visible. The distribution of particle sizes could be determined using SEM fracture analysis as follows:

< 1 um	: 47 %
1 - 5 um	: 48 %
5 - 10 um	: 1 %

The grain size of this sample is 2500 grains/mm<sup>2</sup> measured by linear analyses. The stability of the grain size of this material is demonstrated by the fact that at 1750°C, which is 450°C above onset of recrystallization, the grains only coarsen to 1000 grains/mm<sup>2</sup> after long time exposure of 4069 hours.

### 3.3 TUNGSTEN AND TUNGSTEN RHENIUM ALLOYS

If low temperature ductility and/or high temperature strength appear to be a problem the only way to succeed is to add rhenium to tungsten. The ductilizing effect of rhenium has been known since many years (7). Low additions of Re to W have been found to be satisfactory only in applications where cyclic heating requires high fatigue strength, e. g. for X-ray rotating anodes. Additions of 3,5 and 10 % Re have been found satisfactory for this application. To improve properties to a larger extent additions of 10 to 26 % Re are necessary. As the following data show, 10 % Re already improves pure tungsten considerably. The alloy W26Re contains the highest possible amount of Re for the formation of the homogenous -phase without brittle -phase. Fig. 7 shows hot strength and ductility data up to test temperatures of 1750°C in vacuum for W, W10Re and W26Re. The test specimens used for the data of Fig. 7 - 9 were radially cut out of a forged disc set up forged 75 % at 1600°C and stress relieved at 1000°C for 6 hours in hydrogen. At test temperatures beyond 1750°C creep processes influence UTS.

Of great interest to users of W- and WRe-alloys are data that answer the question how much ductility remains in a device after a certain time at temperature. Fig. 8 gives information that W26Re stays ductile at room temperature even after heating up to 2900°C, which is near the melting point. The eutectic melts at 3000°C (1) and the solidus temperature for 26 weight % Re is below 3100°C.

From the diagram shown in Fig. 9 an excellent room temperature ductility of W26Re could be determined by measuring DBTT by bend testing. W26Re has a DBTT temperature below 0°C even after a heat treatment of up to 2300°C. A heat treatment at 2900°C shows an increase in the DBTT.

All data determined for W and WRe alloys are valid for specimens cut in radial direction. As demonstrated in Fig. 1 for molybdenum alloys the very important tangential direction exhibits the same distribution of strength and elongation. If axial strength and elongation have to be improved final forming processes have to be adjusted to the configuration of the particular part.

#### 4. THERMAL STRESSES AND STRENGTH OF TUNGSTEN

For standard applications of refractory metals, heating or cooling times are in the range of 1000° per several hours. During fabrication of tungsten heating as well as cooling times can be about 1000° per several minutes, especially during forming operations. To better understand what happens during powerful heat transfer to a cold tungsten or tungsten alloy surface a model shown in Fig. 10 shall be discussed. If a flat surface is in contact with a medium 3000°C hot the surface reaches 3000°C in a short time, but heat dissipation into the tungsten is slow and the inner part stays cold within a distance of centimeters after a time of seconds. Using the elastic modulus and linear thermal expansion (8) stresses can be estimated to be compressive at the hot surface region. Depending on width of tungsten part, being not infinite and within the normal size of rocket nozzles and some centimeters wide, compressive stresses on the hot side are compensated by tensile stresses on the cold side. A comparison of the strength of W-2ThO<sub>2</sub> to stresses created by thermal expansion indicates the probability of cracking. If stresses surpass the yield strength above the DBTT of 350°C, stresses are relieved by plastic flow. The most critical situation for any tungsten part exists when stresses are effective in that section of the part where temperatures are below the DBTT. The part may crack by brittle fracture under thermal stresses.

#### 5. ADVANCED MOLYBDENUM ALLOYS AS AN ALTERNATIVE

For some applications exhaust temperatures and overall conditions are such that also molybdenum based alloys with lower melting points can be considered. Lower melting points (for Mo41Re as low as 2450°C) are compensated by the much lower density of 10,2 g/cm<sup>3</sup> instead of 19,3 g/cm<sup>3</sup> for W. In addition to the lower density, a much better low temperature ductility and strength up to temperatures of 1500°C are desirable advantages of molybdenum alloys.

The diagrams in Fig. 11 compare ultimate tensile strength and elongation of all important high strength molybdenum alloys tested at temperatures up to 1800°C. ZHM is a new Zr and Hf carbide dispersion strengthened molybdenum alloy of the nominal composition Mo-1,5Hf-0,5Zr-0,19C that can be strain-hardened. The ZHM data were determined on radially cut specimens from 75 % forged discs with optimum heat treatment. A new molybdenum alloy that surpasses even W-alloys in high temperature strength is Mo25WH nominally containing Mo-25W-1Hf-0,06C. The Mo25WH disc was forged 60 %, and the specimens were cut in radial direction (9). For comparison tensile strength and elongation of Mo-, Mo5Re- and Mo41Re-alloys were determined on 1 mm sheet of higher reduction rate. The hot strength of ZHM and Mo25WH is superior with sufficient ductility (10).

The excellent strength and ductility characteristics after heat treatment can be seen in Fig. 12 and 13. Mo41Re remains at a RT strength of 800 N/mm<sup>2</sup> even after 1 hour at 2200°C. Optimum ductility can be achieved by heat treating at 1200°C for Mo and MoRe alloys and at 1600°C for ZHM.

Ductility measured as DBTT by bend testing is below -70°C for Mo41Re independent of heat treatment up to 2200°C. There is a minimum for Mo, Mo5Re and Mo41Re at 900°C 1-hour heat treatment which means partly recrystallization, Fig. 14.

#### 6. COATINGS ON TUNGSTEN, MOLYBDENUM AND ALLOYS

Up till now there are no satisfactory methods available to protect molybdenum and tungsten against oxidizing atmospheres. MoSi<sub>2</sub>-, SiC- and Al<sub>2</sub>O<sub>3</sub>-layers deposited by PVD and CVD processes improve oxidation resistance only within a time range of hours above 1000°C. The disadvantage of these layers is brittleness and limited thickness. Noble metals such as Pt deposited by fused salt electrolysis and PVD methods are alternative protection material, as long as molybdenum does not diffuse through these layers. Thicker layers that can be deposited by flame- and plasmaspraying are based on the group of iron metals alloyed with Cr, Al and sometimes Yttria. Also thick glass layers can protect molybdenum to a certain extent.

In summary it can be stated that for medium temperatures no long lasting oxidation protection for molybdenum, tungsten and alloys is established. For very short protection periods the above mentioned groups of metals, alloys and compounds are the basis for further development. Still larger efforts will be necessary to solve the problem of combined oxidation and erosion protection.

## LITERATURE

- (1) Yih W.H. and C.T. Wang: "Tungsten" Plenum Press, New York and London 1979.
- (2) Kieffer R., G. Jangg, P. Ettmayr: "Sondermetalle", Springer-Verlag, Wien New York 1971.
- (3) Internationale Plansee Seminare Nr. 1 bis 11, Reutte - Austria.
- (4) Hagel W.C., J.A. Shields Jr., S.M. Tuominen: Proceedings of Symposium on "Refractory Alloy Technology for Space Nuclear Power Applications" pp. 98, Oak Ridge, Tennessee, August 10 - 11, 1983.
- (5) Eck R., J. Tinzl: "Mechanical Properties of Advanced Molybdenum Based Ti-Zr-Hf-C Alloys" in Modern Developments in Powder Metallurgy, vol 15 - 17, 1985 p. 129 - 143.
- (6) Femböck J., R. Stickler and A. Vinckier: 11. Plansee Seminar 1985 RM 46, p. 361 - 380 Reutte - Austria.
- (7) Gonser B.W.: "Rhenium" Elsevier Publishing Comp., Amsterdam New York 1962.
- (8) Tietz T.E. and J.W. Wilson: "Behavior and Properties of Refractory Metals" Stanford University Press 1965, Stanford California
- (9) Eck R., J. Tinzl: "High Temperature High Strength Molybdenum and Molybdenum-Tungsten Ti-Zr-Hf-C Alloys". PM 88 Conference Orlando FA, U.S.A. 1988.
- (10) Eck R.: 11. Internationale Plansee Seminar 1985, Reutte - Austria, Proceeding Vol 2 RM 4.

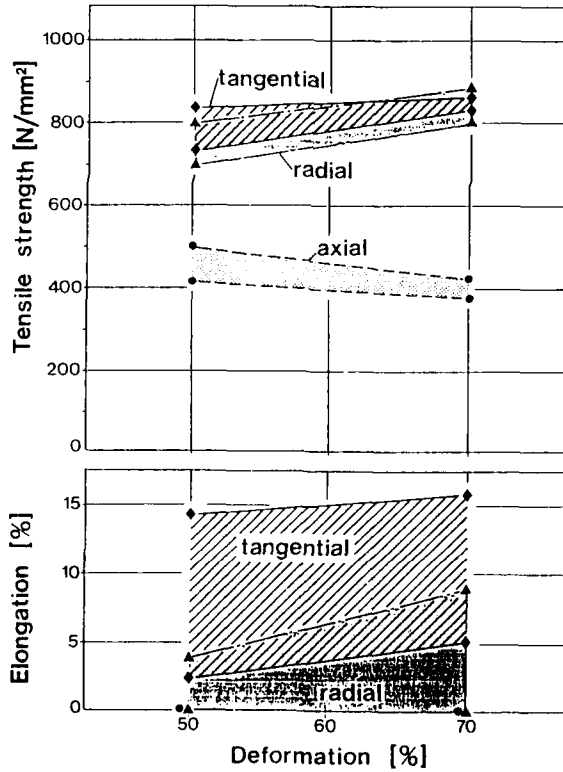


Fig. 1: Ultimate tensile strength and elongation of two ZM discs upset forged 50 and 70 % measured in three directions at 20°C (data-range for the outer section: 204 OD, 160 ID and 246 OD, 200 ID respectively).

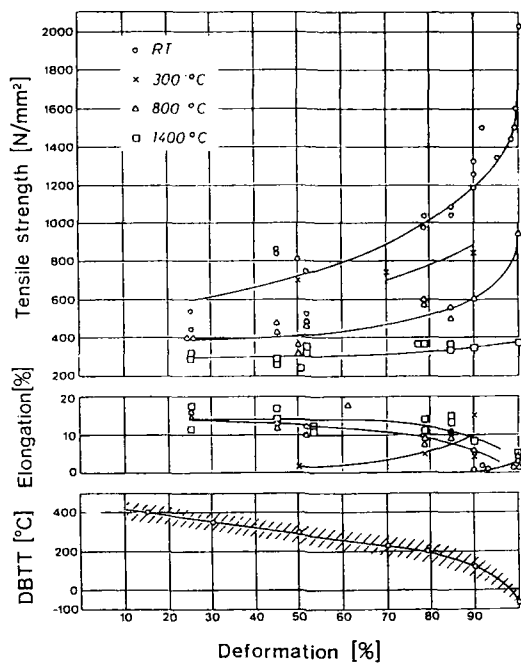


Fig. 2: Ultimate tensile strength, elongation and ductile-brittle-transition-temperature at test temperatures between 20°C and 1400°C dependent on degree of deformation for W-2ThO<sub>2</sub>.

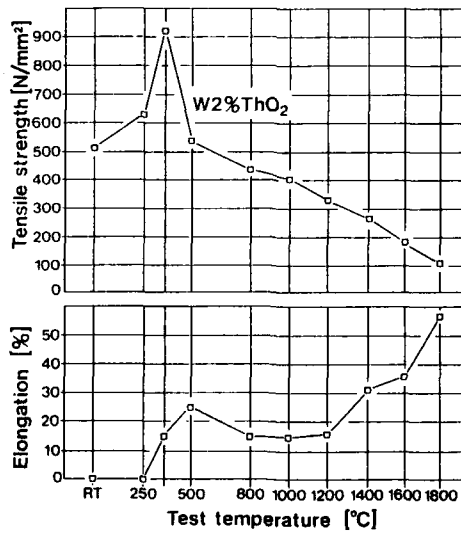


Fig. 3: Ultimate tensile strength and elongation of W-2ThO<sub>2</sub> rod 90 % deformed dependent on test temperature.

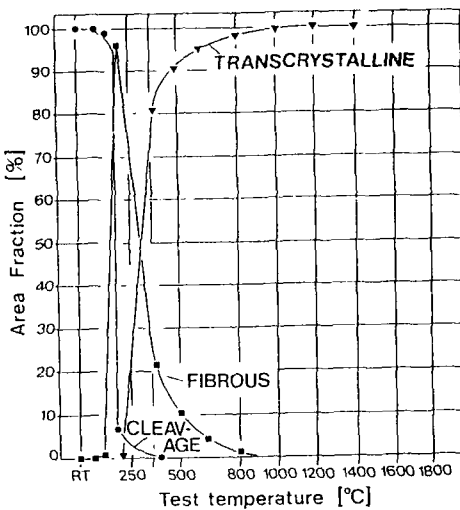


Fig. 4: Fracture mode of W-2ThO<sub>2</sub> rod 90 % deformed dependent on test temperature (6).

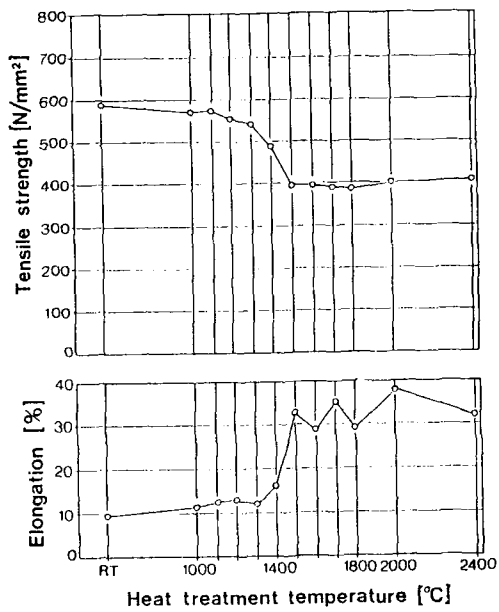


Fig. 5: Ultimate tensile strength and elongation of a W-2ThO<sub>2</sub> rod 90 % deformed and subsequently heat-treated 1 hour in H<sub>2</sub> up to 2400°C tested at 500°C.

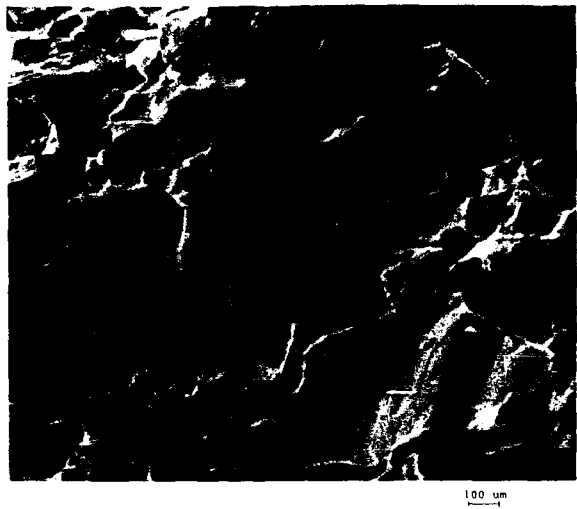


Fig. 6: SEM fractograph of a 90 % deformed W-2TiO<sub>2</sub> rod, recrystallized at 1750°C.

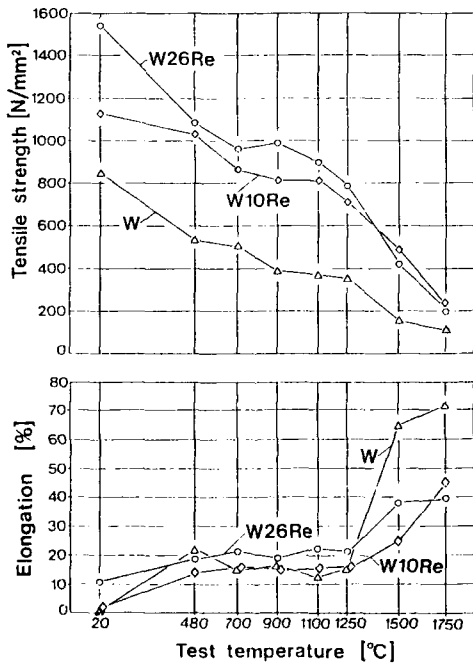


Fig. 7: Ultimate tensile strength and elongation of W, W10Re and W26Re discs forged 75 %, measured in radial direction at temperatures up to 1750°C in vacuum.

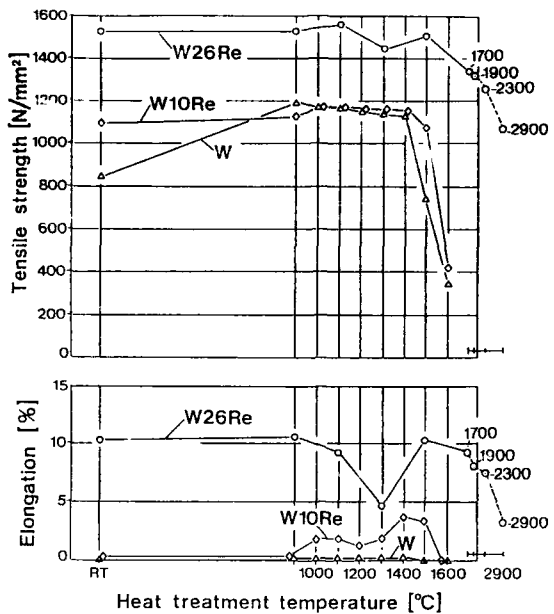


Fig. 8: Ultimate tensile strength and elongation of W, W10Re and W26Re discs forged 75 %, measured in radial direction after 1 hour heat treatment up to 2900°C.

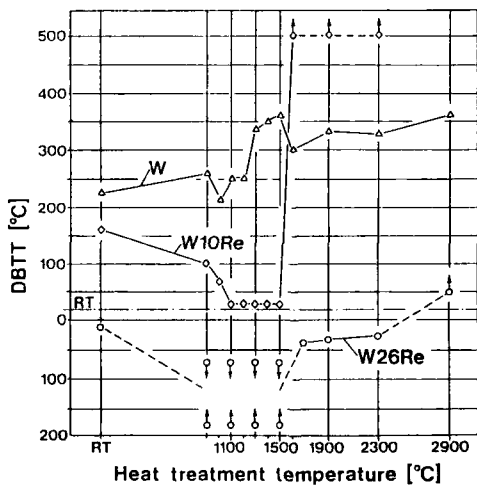


Fig. 9: Ductile-brittle-transition-temperature of W, W10Re and W26Re discs forged 75 %, measured by bend testing in radial direction after 1 hour heat-treatment up to 2900°C.

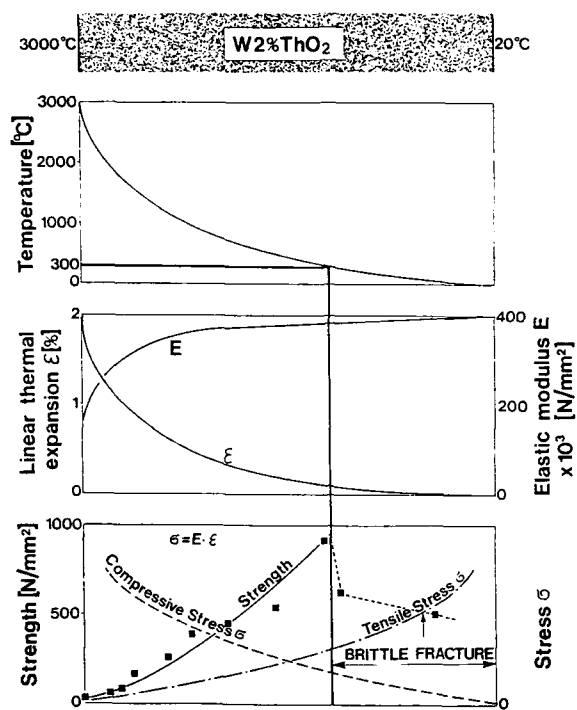


Fig. 10: Schematic model for the distribution of stresses in a Tungsten-part heated rapidly on one side.

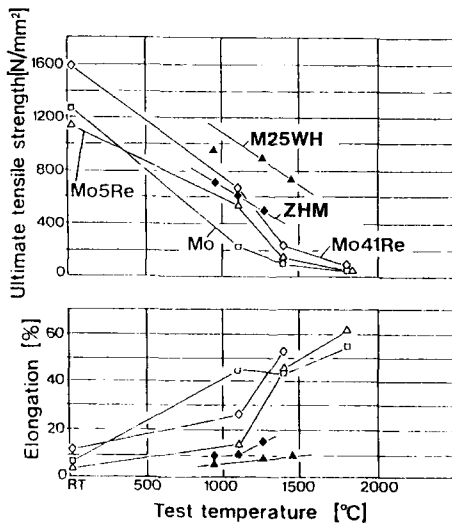


Fig. 11: Ultimate tensile strength and elongation at temperatures up to 1800°C for ZHM discs 75 % and M25WH discs 60 % deformed. Specimens cut in radial direction. Comparison with results from 1 mm thick Mo, Mo5Re and Mo41Re.

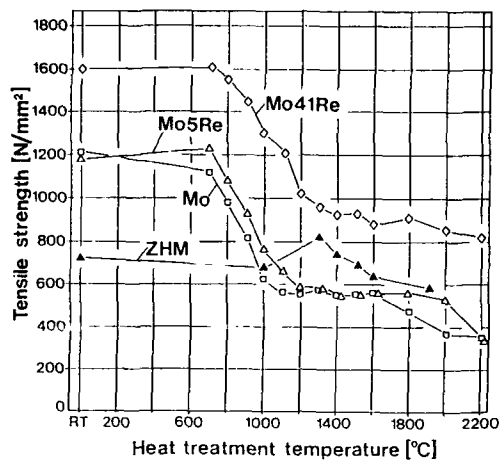


Fig. 12: Effect of 1 hour heat treatment in H<sub>2</sub> on tensile strength at 20°C for the same alloys as in Fig. 11.

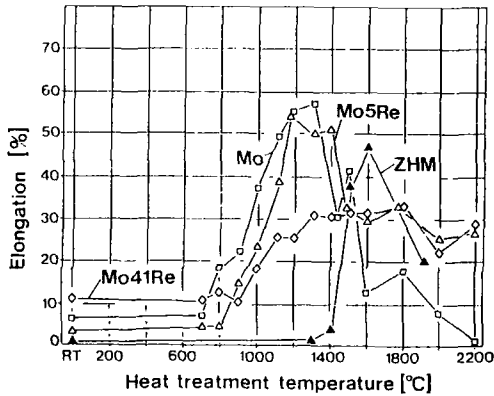


Fig. 13: Effect of 1 hour heat treatment in H<sub>2</sub> on elongation at RT for the same alloys as in Fig. 11.

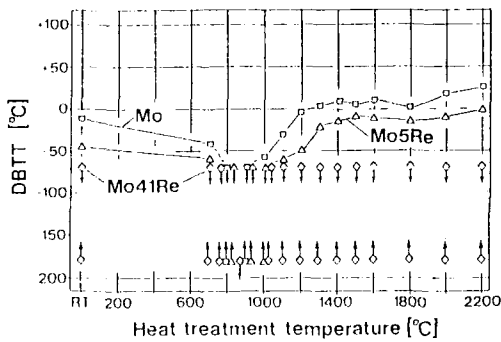


FIG. 14. Ductile-brittle transition temperature dependent on 1 hour heat treatment in H<sub>2</sub> for Mo, Mo<sub>5</sub>Re and Mo<sub>41</sub>Re sheet 1 mm.

#### DISCUSSION

J. Margetson, RARDE, UK. You quoted tensile strength values in your presentation. Did you do tensile tests or did you deduce your tensile strengths from flexure tests? Also, why did you use three-point and not four-point bend tests, where the bending load would have been distributed over a wider area? And third, did you consider both surface and volume defects, and thus surface and volume strengths in your study?

R. Eck, Metallwerk Plansee, FRG. All tensile data were values measured in tension at temperatures ranging between 20 and 1800°C in vacuum. The three-point bend test on unnotched specimens is a standard procedure for the determination of the ductile-brittle transition temperature in refractory metals. As noted in some of our data, there is scatter in the data obtained in the brittle range. Surface defects do influence the tensile test data, especially at low temperatures.

## LES MATERIAUX COMPOSITES REFRACTAIRES A HAUTE PERFORMANCE

A. HORDONNEAU  
Responsable des Recherches  
AEROSPATIALE - ETABLISSEMENT D'AQUITAINE  
ST MEDARD-EN-JALLES 33165 FRANCE

### **RESUME**

Les spécifications de fonctionnement des propulseurs à poudre augmentent régulièrement, poussées par l'accroissement des performances : poussée, manœuvrabilité, température de fonctionnement. Pour les satifaire, il devient nécessaire d'avoir une meilleure adéquation du matériau et du concept. Les matériaux composites carbone et céramique grâce à une grande variété de procédés et une grande plage de caractéristiques thermomécaniques sont bien adaptés pour y répondre. Aérospatiale a développé pour ces besoins des matériaux et procédés originaux, principalement dans le domaine du tissage automatique de préformes fibreuses, de la densification automatisée et du revêtement.

Des applications dans le domaine des missiles ont montré de bons résultats. Des possibilités d'application dans d'autres domaines comme les moteurs et les véhicules de rentrée ont été démontrées.

### **INTRODUCTION**

Aérospatiale par sa division systèmes stratégiques et spatiaux est maître d'œuvre des programmes de la force de dissuasion française, MSBS, SSBS et HADES, fournisseur principal des enveloppes de propulseur à poudre en composite bobiné et responsable de la fabrication des corps de rentrée dans l'atmosphère. Aérospatiale est également maître d'œuvre du système spatial européen Hermès.

La Division Engins Tactiques produit, quant à elle, de nombreux missiles, seule ou en coopération.

Les matériaux composites pour application à très haute température dits "composites chauds" ou "composites thermostructuraux" y ont donc été étudiés depuis de nombreuses années et tout particulièrement par l'établissement d'Aquitaine.

Dans le futur, d'autres systèmes tel que le STS 2000, avion spatial du 21ème siècle, utiliseront ces matériaux, mais les besoins plus proches des systèmes stratégiques ou engins tactiques conduiront à des développements importants.

Initialement utilisés pour leur simplicité de conception et leur facilité de stockage, les propulseurs à poudre ne demandaient que des matériaux rustiques tels que les composites Silice/Résine phénolique et les graphites. L'accroissement des performances, la complexité croissante du système a entraîné l'utilisation de solutions nouvelles comme :

- la tuyère intégrée et les divergents déployables qui exigent des matériaux plus résistants et plus légers.
- une poudre plus énergétique qui entraîne une augmentation des chocs thermiques.

Dans le domaine des engins tactiques, la manœuvrabilité, le pilotage en force ont été à l'origine du développement de nouveaux concepts tels que les déviateurs de jet, systèmes de vannage de gaz et tubes de flamme.

Pour répondre à ces besoins nouveaux, l'Aérospatiale a développé des matériaux répondant aux nouvelles spécifications :

- Haute température d'utilisation jusqu'à 3000°C,
- Résistance mécanique,
- Tenue au choc thermomécanique,
- Légereté,
- Résistance à l'oxydation et à l'érosion,
- Possibilité de réalisation de pièces de grandes dimensions.

Les matériaux traditionnels, métaux réfractaires, graphites, céramiques, répondent partiellement au problème mais aucun ne peut satisfaire l'ensemble des spécifications.

Les métaux réfractaires Tantale, Tungstène, Molybdène sont lourds et peu résistants à haute température.

Les graphites et les céramiques sont fragiles, peu résistants au choc et sont réservés aux petites pièces et aux sous-ensembles massifs.

Par contre, les matériaux composites, à matrice carbone verre ou céramique, permettent d'associer, au sein d'un même matériau, les propriétés de réfractarité et légèreté à une bonne résistance aux charges mécaniques et au choc thermique.

De plus les fibres apportent au matériau la maîtrise des propriétés dimensionnelles et l'augmentation de la tenacité. Cet accroissement des caractéristiques n'est cependant pas obtenu pour tout le domaine de température et dépend beaucoup de l'environnement.

En effet, les fibres carbone conservent leurs propriétés mécaniques à très haute température, plus de 2500°C, en ambiance neutre ou réductrice mais s'oxydent à partir de 400°C.

Les fibres céramiques présentent, soit des impuretés, qui affaiblissent la fibre à haute température, soit des transformations cristallines. Leur température est aujourd'hui limitée aux alentours de 1200°C en utilisation de longue durée.

Les whiskers bien que très imparfaits sont utilisables jusqu'à 1400°C et supportent des températures d'élaboration du matériau plus élevées.

L'Aérospatiale a développé ces matériaux en se focalisant sur leur propriété d'usage et les méthodes industrielles d'élaboration. Ces travaux ont donné naissance à des procédés originaux touchant :

- Le tissage automatique des renforts fibreux destinés à la réalisation de pièces complexes soumises à des contraintes tridimensionnelles.
- La réalisation de matrices carbone, verte, ou céramique par des procédés adaptés au type des pièces à réaliser.
- Les techniques de revêtement. En effet les conditions d'environnement peuvent être telles que les matériaux nécessitent une protection contre l'oxydation et/ou un revêtement résistant à l'érosion comme c'est le cas pour les carbone/carbone dont les propriétés sont conservées jusqu'à 2500°C mais ne peuvent être utilisés en ambiance oxydante.

#### LES PROCÉDÉS DE TISSAGE

Les fibres carbone et céramique utilisées pour la réalisation des composites réfractaires ont un module élevé, sont donc difficiles à manipuler et sont généralement chères. Les pièces sont, quant à elles, de forme complexe ou de grandes dimensions. L'intérêt est donc grand de réaliser les préformes d'une manière automatique, garantissant ainsi la qualité et la rapidité. A titre d'exemple, un bloc de carbone tissé en trois directions est constitué de 450 000 fils ou mèches pour des dimensions de l'ordre de 500 mm de côté. L'automatisation a permis de réduire le temps de fabrication d'un facteur 10 en éliminant tout risque de défaut (désalignement, lacune, rupture...).

Le tissage automatique doit répondre à plusieurs exigences :

- Les fibres doivent être orientées dans la direction des efforts principaux et respecter si possible le profil de la pièce,
- La préforme doit être homogène,
- Le procédé doit respecter la fibre.

On trouvera deux types de procédés selon que :

- Les pièces sont telles qu'elles peuvent être usinées dans la masse, le tissage apporte alors un renfort quasi isotrope et l'opération consistera à tisser des blocs,
- Les pièces sont de faible masse comparées à leur volume, un tissage en forme est alors nécessaire.

Le procédé décrit plus loin permet de tisser des pièces cylindriques circulaires ou à symétrie de révolution, d'autres procédés permettent des formes plus complexes et sont adaptés à des parois minces.

L'association de ces procédés par couture est possible on trouve donc une gamme de procédés adaptés à toutes formes de pièces :

Type de pièce	Procédé	Remarque
Bloc	3 D bloc	Tissage équilibré trioctogonal
Cylindre	3 D circulaire	Cylindre creux
Pièces de révolution	3 D en forme	Adapté à un convergent divergent de tuyère
Plaques minces	2,5 D	Tissu épais indéflamable
Cônes - calottes sphériques	2 D évolutif	Permet un tissage à épaisseur constante

Les procédés sont brevetés par Aérospatiale.

**PROCEDE DE TISSAGE 3 D CIRCULAIRE**

Le procédé est décrit par les schémas en annexe.

La première opération consiste à préparer un outillage constitué d'un panier formé de plaques métalliques percées et de tiges métalliques qui matérialisent la direction longitudinale de la pièce à réaliser.

La deuxième opération consiste à disposer des fibres circonférentielles et radiales.

La troisième, à remplacer chacune des tiges métalliques par des fils.

Le panier constitué une fois pour toutes est alors recyclé.

Pour le tissage en forme le même procédé est utilisé mais de diamètre et l'épaisseur sont réglés en fonction de la cote.

Ces procédés sont tous entièrement gérés par un ordinateur qui assure le contrôle de la pièce et la traçabilité.

**LES MATRICES**

Les blocs ou préformes de fibres, carbone ou céramique, ainsi tissés doivent être densifiés pour en assurer la rigidité.

La résine tout d'abord utilisée a été remplacée par le carbone, le verre et les céramiques.

Les procédés employés sont variés et dépendent du matériau et de la pièce à réaliser. Les propriétés obtenues sont aussi fonction du procédé.

Le tableau ci-dessous résume les principaux procédés utilisés et leurs caractéristiques.

Matrice	Procédé	Pièce type	Caractéristiques
CARBONE	C.V.D	Paroi mince Grandes dimensions	Densité ~ 1,6 Bonne résistance mécanique
	Pyrolyse Brai haute pression 1000 bars	Blocs et pièces épaisses	Densité ~ 2 Bonne résistance à l'ablation Bonne résistance mécanique
	Pyrolyse Brai moyenne pression 100 bars	"	Idem mais procédé plus long
	Pyrolyse résine	Complexé	Densité faible < 1,6 Etanche Moyens peu onéreux
VERRES	Sol/Gel - Pressage	Pièces simples	En développement
CERAMIQUE	C.V.D - C.V.I	Paroi mince	Bonne résistance Procédé long
	Pyrolyse organométallique	Pièces massives Grandes pièces	Bonne homogénéité
	Barbotines - Frittage	Pièces minces	Procédé économique exige des poudres réactives à température compatible avec la stabilité des fibres
	Pressage unidirectionnel à chaud	Petites pièces simples	Renfort whiskers Procédé rapide
	Pressage H.I.P à chaud	Petites pièces complexes	Caractéristiques matériau élevées

Les propriétés mécaniques dépendent fortement de la nature de la matrice, le tableau ci-dessous donne des caractéristiques typiques de quelques matériaux. Ces valeurs sont à corriger du taux de fibre dans la direction de la sollicitation puisqu'elles ont été obtenues pour des matériaux à renfort multidirectionnel généralement équilibré dans les trois directions, soit de l'ordre de 16 % en volume pour chacune d'elle.

Matériau	Densité g (MPa)	Traction E (GPa)	Compression E (GPa)	Température d'emploi		
<b>CARBONE/CARBONE</b>						
BRAI	1,9 à 2	250	100	140	80	2500°C
CVD	1,7	290	85	130	94	"
RESINE	1,5	230	65			"
SiC/SiO <sub>2</sub>	1,8	130	25			800°C
Al <sub>2</sub> O <sub>3</sub> /SiO <sub>2</sub>	1,8	100	25			900°C
Al <sub>2</sub> O <sub>3</sub> /Al <sub>2</sub> O <sub>3</sub>	2,6	80	100			1200°C
SiC/Si <sub>3</sub> N <sub>4</sub> (whiskers)	3	600	350	3000	350	1400°C
V <sub>f</sub> = 25 %						

#### LE TRAITEMENT DE SURFACE

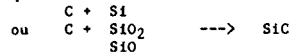
Les céramiques composites sont limitées dans leur développement par la faible température d'utilisation des fibres, le seul matériau utilisable à très haute température reste le carbone/carbone, malheureusement oxydable.

La solution consiste donc à réaliser une protection étanche respectant les conditions :

- compatibilité de dilatation avec le carbone,
- compatibilité chimique avec le carbone à haute température,
- résistance à haute température en ambiance,
- adhérence suffisante,
- étanchéité.

Ces revêtements peuvent être constitués de plusieurs couches, les techniques employées sont :

\* les réactions chimiques du carbone avec des éléments simples ou composés pour donner naissance à une céramique tels que :

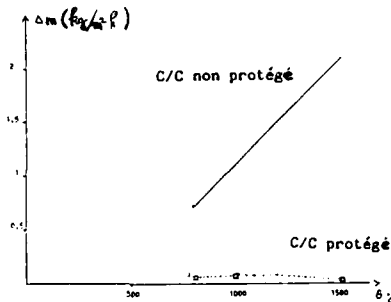


- \* Les revêtements par sol gel
- \* les dépôts P.V.D ou C.V.D.

L'association de ces procédés dépend essentiellement de l'application.

Les résultats obtenus aujourd'hui permettent une utilisation de plusieurs heures à 1500°C sans perte de caractéristiques mécaniques.

Une courbe d'oxydation typique est donnée ci-dessous pour un matériau de 3 mm d'épaisseur.



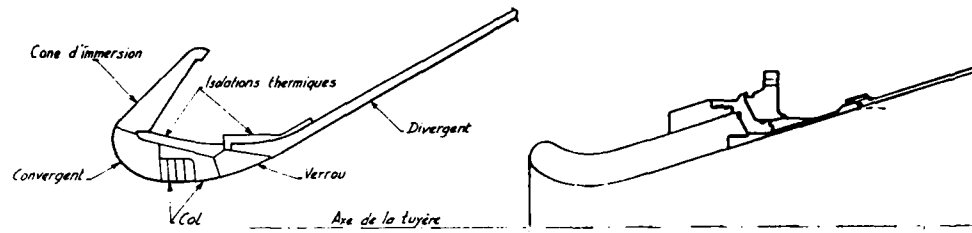
**APPLICATION**

Les carbone/carbone et matériaux composites tissés ont été initialement produits à l'Aérospatiale pour la fabrication des corps de rentrée dans l'atmosphère des systèmes stratégiques et spatiaux. Ils sont depuis utilisés pour les tuyères, pour les systèmes de vannage de gaz et les conduites de gaz chauds. Ils sont aussi utilisés avec les céramiques composites dans d'autres domaines comme les moteurs et les véhicules spatiaux notamment Hermes.

**LES TUYERES**

La technologie de fabrication des tuyères a été le point clé du développement des propulseurs à poudre. Le concept classique est donné ci-dessous. Il fait appel à un assemblage de matériaux divers permettant d'assurer l'intégralité des fonctions. La structure résistante est en acier, le col en graphite, le convergent et le divergent en composite silice/résine phénolique. De plus des protections thermiques sont nécessaires pour protéger l'acier de l'échauffement interne.

La première amélioration a porté sur le remplacement du convergent et du col par une seule pièce en carbone/carbone. Le gain a été double : suppression d'une pièce et amélioration de la qualité du col.



Les pièces suivantes, verrou, divergent ont été progressivement remplacées par des composites carbone/résine, puis carbone/carbone.

Les cols de petit diamètre (quelques cm) ont été réalisés par usinage de blocs 3 D, pour les plus grands diamètres, la technologie de tissage 3 D circulaire a été employée. Dans les deux cas les pièces sont densifiées par la technique de pyrolyse de brai sous haute pression.

Les essais réalisés aussi bien en France qu'aux Etats Unis ont montré d'excellents résultats qualitatifs et une vitesse d'ablation au col inférieure de 20 à 40 % par rapport aux matériaux précédents pour des propulseurs de même nature.

Pour le divergent, le problème s'exprime de façon différente : l'ablation est faible, mais l'échauffement important conduit à un dimensionnement en protection thermique pour des matériaux comme le silice/phénol ou le carbone/phénol puisqu'ils perdent leurs caractéristiques mécaniques au dessous de 300°C.

L'adoption d'un matériau comme le carbone/carbone permet d'élever notablement la température d'emploi et par conséquent d'abaisser le poids des structures par suppression de la couche assurant l'isolation thermique.

Les matériaux carbone/carbone ont été employés initialement avec une architecture de type iris. Cette technologie a montré ses limites par les risques de délamination qu'elle introduit aussi bien en fabrication qu'en utilisation. Le tissage tridimensionnel a permis de s'affranchir de cette difficulté tout en augmentant la résistance mécanique circonférentielle.

Des divergents tissés en 3 D circonférentiel "en forme" ont été densifiés par la méthode C.V.D et essayés avec succès aux Etats Unis par l'US Air Force - Rocket Propulsion Laboratory. Les dimensions du divergent étaient de l'ordre de 1500 mm de long et 1200 mm de diamètre maximum. Ces travaux étaient conduits pour Hercules Inc.

Depuis cette technologie lui a été transférée et de nombreuses pièces ont été produites pour le développement des programmes U.S.

L'avantage majeur de cette technologie réside dans la possibilité de réaliser des structures chaudes auto porteuses ce qui permis la simplification notable des tuyères.

L'assemblage des pièces entre elles (divergent, col) peut s'effectuer par filetage. C'est dans cette configuration qu'ont été effectués les essais.

#### LES CHAMBRES DE COMBUSTION

Dans de nombreux engins tactiques les chambres de combustion sont mixtes et peuvent servir au fonctionnement d'un statot réacteur. Les solutions traditionnelles consistent à utiliser une structure résistante métallique ou composite doublée d'un isolant thermique ablatif.

Ces techniques valables dans le cas d'engins de courte durée de fonctionnement s'avèrent toutefois pénalisantes pour des durées plus longues.

Pour étudier la faisabilité de chambres plus performantes et pour répondre à des besoins plus complexes de conduites de gaz notamment, des pièces cylindriques étanches ont été étudiées. Les technologies de mise en oeuvre de fibres par bobinage et tissage ont été évaluées par la réalisation de cylindres qui ont été testés avec satisfaction en pression interne de plus de 50 bars.

Les applications de propulsion à poudre ne requièrent généralement pas de durée de fonctionnement très longues, les matériaux carbone/carbone y sont donc bien adaptés dans le plupart des cas.

Cependant pour des besoins de propulsion aérobie plus larges comme les missiles de longue portée, les avions hypersoniques civils ou militaires, l'oxydation du carbone deviendrait rédhibitoire. Les solutions consistent donc à utiliser les matériaux carbone/carbone inox développés par ailleurs pour d'autres applications et les matériaux à matrice céramique.

#### MOTEURS A COMBUSTION INTERNE

Les matériaux à matrice céramique ont notamment été essayés dans les conditions de fonctionnement de moteurs diésel, caractérisées par une atmosphère oxydante et un cyclage thermique et mécanique intense. L'isolation de la chambre de combustion a été réalisée à l'aide d'un matériau à matrice silice renforcé par des fibres d'alumine ou de carbure de silicium.

Les essais ont montré une bonne résistance mécanique et chimique aux conditions d'environnement. Une durée de vie de 50 heures a été atteinte malgré une forte porosité du matériau incompatible avec le cyclage dû à la pression.

Ce matériau isolant et résistant est adapté pour la réalisation de pièces travaillant à une température de l'ordre de 800°C.

#### LES STRUCTURES CHAUDES

Les structures du planeur hypersonique Hermes et principalement le nez et les bords d'attaque sont soumises à la rentrée dans l'atmosphère à un échauffement supérieur à 1500°C pour lequel les fibres céramiques ne sont pas adaptées. Dans ces conditions encore seul le carbone/carbone permet de répondre au besoin à condition de le protéger contre l'oxydation.

Dans les systèmes de transport spatiaux futurs comme le STS 2000 le même problème se posera pour les moteurs, les entrées d'air et les structures.

En utilisant les technologies de tissage automatique l'Aérospatiale a créé pour ce besoin un matériau inoxydable indélaminaire dit 2,5 D protégé en surface, par une barrière réfractaire étanche en carbure de silicium lui même revêtu, et à coeur, par un composé qui limite l'oxydation en cas de dommage superficiel.

Si le problème semble se poser comme identique à celui du "shuttle US" il est en effet différent sous deux aspects.

- *Hermès* est trois fois plus petit - les épaisseurs de matériau doivent donc être plus faibles (quelques mm),
- Les températures sont plus élevées en raison des rayons de courbure plus faibles.

La résistance à l'oxydation du matériau est satisfaisante et assure l'utilisation du matériau à 1500°C pendant plusieurs heures dans les conditions de pression de la rentrée dans l'atmosphère.

Les essais d'un bord d'attaque Hermès ont été effectués au four solaire d'Almeria dans des conditions représentatives d'une série de 30 rentrées dans l'atmosphère.

Ce succès est à l'origine de la décision du CNES de confier à l'Aérospatiale l'étude des bords d'attaque et du nez d'Hermès.

#### PIECES MECANIQUES

Aussi bien pour la propulsion solide que pour les moteurs à combustible liquide l'accroissement des températures posera le problème des pièces mécaniques.

Dans cet objectif des systèmes de fixation par vis ont été développés incluant la conception de filets spéciaux adaptés au matériau.

Pour ce dernier le choix s'est porté sur un nitride de silicium renforcé par des whiskers.

Les prototypes de vis usinés dans la masse et testés en traction ont donné des résultats peu dispersés centrés sur une valeur de 200 MPa.

Les caractéristiques sont conservées jusqu'à une température de 1400°C. La valeur du  $K_{IC}$  à froid est de 12 soit le double de celle du nitride massif non renforcé.

#### CONCLUSION

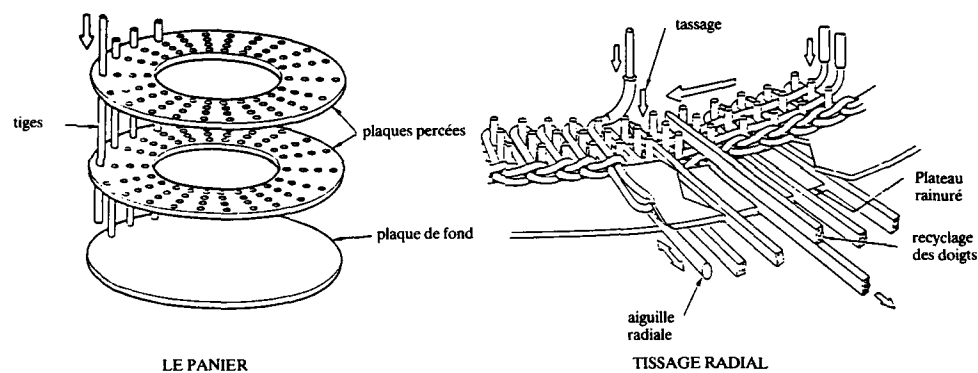
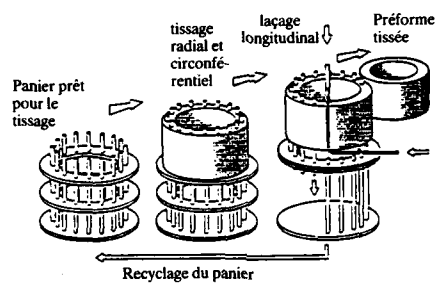
Les matériaux composites réfractaires ont montré un intérêt très grand pour le développement de nouveaux concepts de propulsion mais aussi de structures chaudes.

Cependant, les matières premières disponibles, fibres précurseurs de matrice, ne sont pas encore suffisamment performantes pour permettre la réalisation d'un matériau répondant à l'ensemble des spécifications.

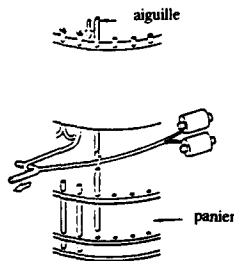
C'est donc à une véritable ingénierie des matériaux que doivent se livrer les concepteurs en relation avec le dessin de la pièce et les technologies de fabrication.

Dans cet objectif Aérospatiale a développé les techniques de base, tissage automatique, matrices, revêtements, qui lui permettent en relation avec les Bureaux d'étude de réaliser des systèmes très avancés.

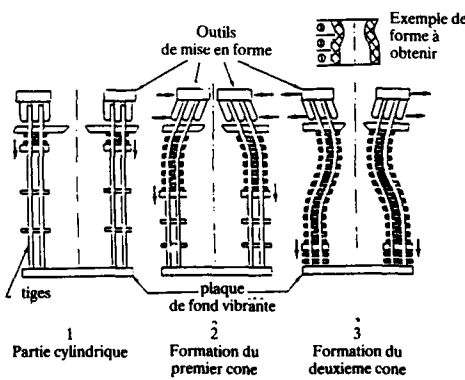
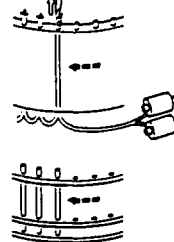
**PRINCIPE DU TISSAGE 3D DE REVOLUTION  
PROCEDE AUTOMATIQUE**



- Détection et chasse de la tige par l'aiguille
- Accrochage du fil



- Remontée de l'aiguille et du fil



LACAGE DIRECTION LONGITUDINALE

MISE EN FORME EN COURSE DE TISSAGE

**DISCUSSION**

R. Kochendorfer, DFVLR, FRG. Regarding the weight loss results you showed for non-protected carbon-carbon and protected carbon-carbon, were the oxidation conditions representative of the upper atmosphere during reentry or oxidation conditions on earth?

A. Hordonneau, Aerospatiale, France. Our results were obtained at laboratory atmospheric pressure. I would expect that above 1500°C, in vacuum or very low pressures, the oxidation would be accelerated by sublimation of the coating and the results would be different, but for temperatures below 1500°C I believe that ours was a good simulation.

## HIGH TEMPERATURE COMPOSITE MATERIALS FOR ROCKET PROPULSION

by

Paul Donguy and Jacques Broca  
Société Européenne de Propulsion  
Le Haillan, BP 37  
33165 Saint Médard en Jalles  
France

### ABSTRACT

The scope of this paper is to show by some examples what are the promises of the composite materials with non degradable matrix like carbon or ceramics in Rocket Propulsion.

From an historical point of view, carbon-carbon materials were first used in solid rocket motor nozzles. More recently, successful all composite hot gas valving systems have incorporated not only carbon-carbon materials, but also thermostable insulators and oxydation resistant materials with silicon carbide matrix. These oxydation resistant materials open the way now for liquid propellant rocket applications such as small thrusters and large nozzle exit-cone.

As concluding remarks, the design philosophy to be followed to reach the best compromise between propulsion requirements and material properties is discussed.

### 1 - INTRODUCTION

Société Européenne de Propulsion (S.E.P) is in France the main rocket motor company. Today, S.E.P. is in charge of all the French ballistic missile motors, is prime contractor of the liquid propellant rocket motors of the Ariane vehicles, and is also involved in many other rocket programs. So, materials with good mechanical properties at high temperature are a key issue, and S.E.P. has been working on thermostable composite materials, sometimes also called refractory composites, for twenty years. Thermostable composite materials mean composite materials reinforced by long fibers embedded in a matrix which does not char or evolve at high temperature. Such a matrix may be carbon or ceramics.

### 2 - SOLID ROCKET NOZZLES

The first materials to be developed were the carbon-carbon for application on rocket nozzles. The Mage 2 motor designed in 1981, which is a high performance European apogee boost space motor, features a very typical nozzle made of such materials. This nozzle is described by Figure 1.

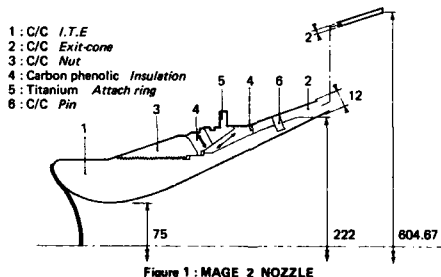


Figure 1: MAGE 2 NOZZLE

The free standing Integral Throat and Entrance (I.T.E) which is the part 1, is made of 4D Sepcarb™ carbon-carbon material. This material is reinforced by a network of rods made of bundled carbon fibers interlaced along the four directions of the long diagonals of a cube (patented arrangement).

This rods network is densified by pitch impregnation and high pressure carbonization. This material multi-directionnaly reinforced, featuring a high density (1.92 g/cc), is used in most of the French nozzles as an I.T.E.

Due to its density, its erosion rate is very low, 0.105 mm/s for the Mage 2 motor. Moreover, this material is very uniform, easy to densify (nearly no rejection during the densification process), and features a high shear strength. The Mage 2 nozzle takes advantage of this high shear strength, the Sepcarb™ 4D I.T.E is linked to the combustion chamber by a Sepcarb™ 4D nut (part 3), the threaded joint conveying the blow-off load of the nozzle to the combustion chamber.

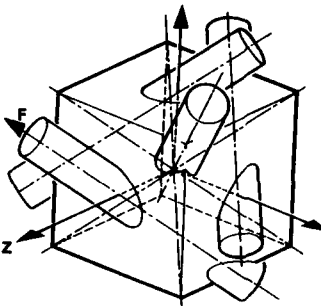


Figure 2 : SEPCARB 4D

The Sepcarb™ 4D material for the Mage 2 nozzle is used in the F direction, i.e., the nozzle centerline is along a long diagonal of the reference cube of the material in order to get enough hoop stiffness.

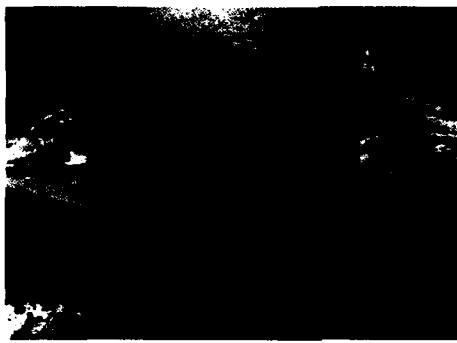


Figure 3 : MAGE 2 NOZZLE SECTION AFTER FIRING

The exit-cone (part 2) is made of 2D involute carbon-carbon material. The wall thickness tapered from 8 mm to 2 mm. The densification is made by a mixed process resin carbonization and chemical vapor infiltration. The final density is 1.45 g/cc.

Due to the involute lay up process limitations, a very simple shape, with a large entrance diameter, was selected for this part, which is nearly conical. So the attachment with the I.T.E is made through a conical joint with carbon-carbon pins. The outside surface is free of any contact to avoid any thermal radial restraint detrimental to such a 2D involute carbon-carbon structure. This carbon-carbon nozzle appears very reliable, in 9 static firing tests (development, qualification and acceptance tests), and 7 operational flights, no failure has been recorded. However, the limitations of the 2D involute carbon-carbon for the exit-cone has imposed a design with a large size I.T.E made of a high performance carbon-carbon which is not cost optimal.

Now a new breakthrough in the carbon-carbon materials field allows to overcome this problem, that is the second generation 3D carbon-carbon materials called Sepcarb Novoltex™. These materials are characterized by a very fine net cell, one of the main features is that the reinforcing carbon fibers perpendicular to the wall are inserted separately instead of being bundled. The resulting properties are :

- high shear strength,
- low wall thickness capability (less than 2 mm),
- complex shape with rapidly evolving thickness capability,
- good ability to be densified by chemical vapor infiltration.

These properties free the design of the nozzle exit-cones.

Figure 4 describes a movable nozzle with a flexible joint which was successfully fire tested in order to demonstrate new technologies for future ballistic missile motors (see Annex B). This is a good example of what is possible to do with Sepcarb Novoltex™ and other thermostructural composite materials.

- 1 : NOVOLTEX Exit-cone  
 2 : C/C E.E.C  
 3 : C/C I.T.E  
 4 : NOVOLTEX INSULATOR  
 5 : FLEXIBLE-JOINT

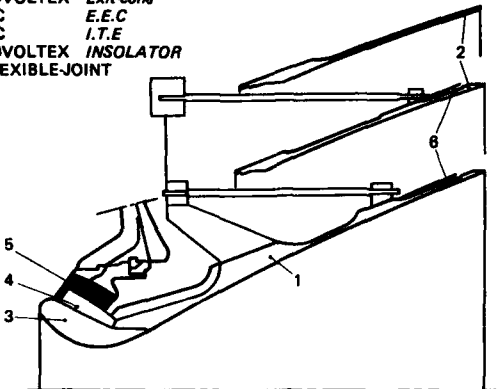


Figure 4 : NOZZLE DESIGN

The exit-cone (part 1), the extendible exit-cone (part 2) and the latching system (part 6) are made of Sepcarb Novoltex<sup>(\*)</sup> carbon-carbon materials. The complex shape of this exit cone fitted with a compliance ring and a threaded joint is noteworthy. The nozzle actuation loads coming from the actuators go through the exit-cone to the flexible joint (part 5). The compliance ring distributes evenly the concentrated loads of the actuators to the exit-cone wall while limiting the distortions. These loads then go through the threaded joint to the Sepcarb<sup>(\*)</sup> 4D I.T.E.

The Sepcarb<sup>(\*)</sup> 4D of the I.T.E has a shear strength consistent with the Sepcarb Novoltex<sup>(\*)</sup> of the exit-cone. In this case the 4D carbon-carbon material is oriented in the Z direction in order to comply with the thermal radial restraints. In this orientation this material presents indeed a lower hoop stiffness and a high hoop strain capability.

This nozzle features also a very promising new class of materials which are the thermostructural insulators. Part 4, which plays a key role in being the mechanical link between the hot structure composed of the I.T.E. (part 3) and the exit-cone (part 1), and the flexible bearing which must remain at low temperature, is a good example of that. State of the art insulators, made of carbon or silica-phenolic tape-wrapped material, have very limited structural capabilities because the charring of the phenolic resin matrix begins at about 300°C. Moreover, resulting outgassing and thermal expansion make the real behaviour of such part very difficult to predict and analyze. The material of the part 4 is a composite material with a 3D carbon reinforcement Novoltex<sup>(\*)</sup> type filled with an alumina matrix.

Such a material features mechanical properties which are nearly constant between the room temperatures and 1500°C with a high shear strength. The insulative properties are lower than the carbon-phenolic one, but good enough to reduce the temperature from 1300°C on the I.T.E. side to 200°C on the flexible side after a 40 second firing.



Figure 5 : POSTFIRE VIEW OF THE NOZZLE

### 3 - HOT GAS VALVING

Figure 6 shows a hot gas valving system which has been demonstrated in view of an application on a ballistic missile post boost system. The firing test conditions are presented in annexe C.

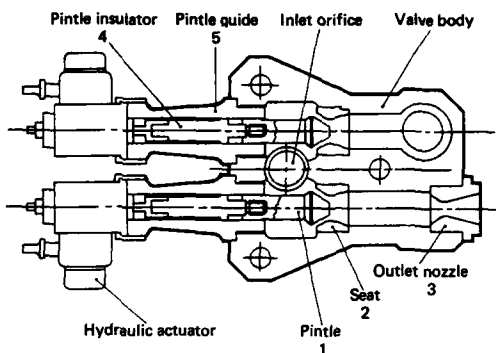


Figure 6 : VALVE SCHEMATIC CONCEPT

This system controls the flow of hot gases coming from a solid propellant gas generator through two proportional pintle valves during five minutes. These gases have a flame temperature of 2100°C and behave as an oxydiser.

In the areas where no erosion is allowed, like the valve pintles, seats and the throats of the outlet nozzles (part 1 - 2 - 3), an oxydation resistant material is needed. The selected material is a composite material with a 3D carbon reinforcement Novoltex™ type and a mixed matrix of carbon and silicon carbide. The silicon carbide is a real matrix embedded in the material and not only a coating which would have not withstood the shocks between the pintle and the seat. The 3D carbon reinforcement gives the high shear strength needed for the threaded joints and good mechanical properties at high temperature.

The design of this hot gas valving system has also been made possible by the use of thermostructural insulators. The pintle insulators and pintle guides (parts 4 and 5) are made of such a material. This is a very simple way to link the hot parts of this system with the actuators. The selected material is a 3D carbon-carbon Novoltex™ type. The insulative properties are obtained by adapting the densification process. The main advantages of these carbon-carbon insulators are a high shear strength, a low density and the possibility of withstanding a very high temperature (> 2000°C) on the hot side.

The valve body is made of carbon-carbon 3D Novoltex™ with a orthogonal reinforcement network, the shear strength of this material allows the use of threaded joints to attach components like the pintle guides and the outlet nozzle



Figure 7 : POST FIRED VALVE

Another interesting feature of this hot gas valving program is the development of hot gas tubings to link two sets of valves in order to equalize hot gas flows between them. A schematic of these tubings is shown in Figure 8.

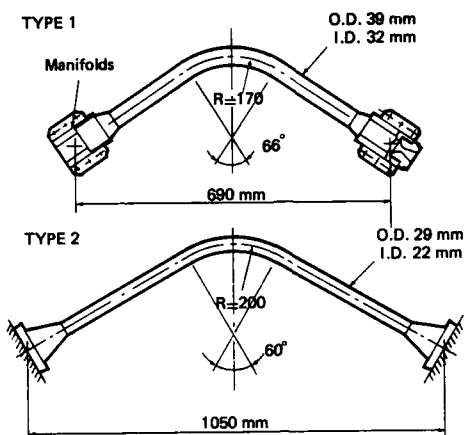


Figure 8 : TUBING SCHEMATIC DESIGN

The reinforcement of these carbon-carbon tubes is made by carbon fibers braiding, the end flanges being made of Sepcarb Novoltex™. These flanges are attached to the tube itself by a special chemical vapor infiltration process which leads to a bonding which can be compared to a metal welding. These tubes have been successfully fire tested for five minutes and under a 2.2 MPa internal pressure of hot gases.

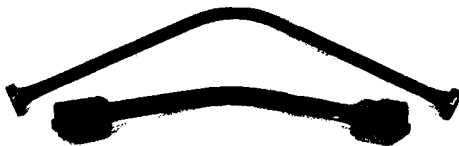


Figure 9 : POST FIRED TUBING

Such a hot gases managing system is not specific of the solid propellant gases, it could be used with a liquid propellants gas generator. In many cases, hot gases coming from the combustion of liquid propellants are similar by their flame temperature and their oxydizing potential.

#### 4 - LIQUID PROPELLANT ROCKETS

The first demonstrations of oxydation resistant thermostable composite materials for liquid rocket applications have been performed on small combustion chambers for satellite thrusters.

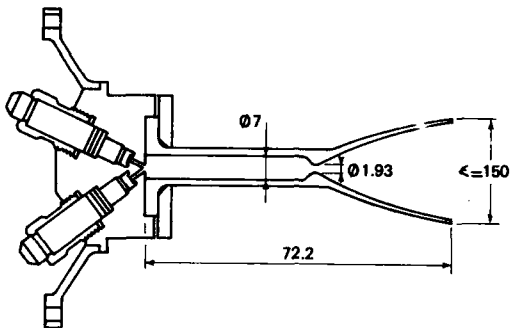


Figure 10 : 5N THRUST CHAMBER

Figure 10 describes a 5N thrust combustion chamber. The propellants are N<sub>2</sub>O<sup>4</sup> and M.M.H. This chamber has been successfully tested under the conditions indicated in Annex E, the total burn time is 7 hours with 400 cycles. In this case the burn time is too long to use a carbon reinforcement with a silicon carbide matrix, due to the oxydation. So a thermostable composite material reinforced by silicon carbon fibers and a silicon carbide matrix has been selected. Such a material can withstand a higher flame temperature than the usual coated Niobium metal, so a more efficient propellant mixture ratio can be selected to increase the specific impulse. Moreover, there is no need for an internal coating, and the reliability is increased.



Figure 11 : 5N THRUST CHAMBER DURING A FIRING TEST

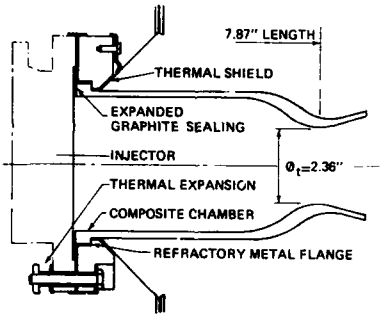


Figure 12 : 6000N THRUST CHAMBER

The 6000N thrust chamber described in Figure 12 has been successfully tested also with N<sub>2</sub>O<sup>4</sup> and M.M.H. propellants. The total burn time was 870 s, the test conditions are indicated in Annex F. In this case, this chamber was made of a material using a 3D carbon reinforcement Novoltex type and with a silicon carbide matrix. Compared to the previous material, this one has a lower oxydation resistance, but also a lower density (2.1 instead of 2.4 g/cc), and better mechanical properties at high temperature. The increased diameter of the 6000 N thrust chamber leads indeed to higher hoop stresses.

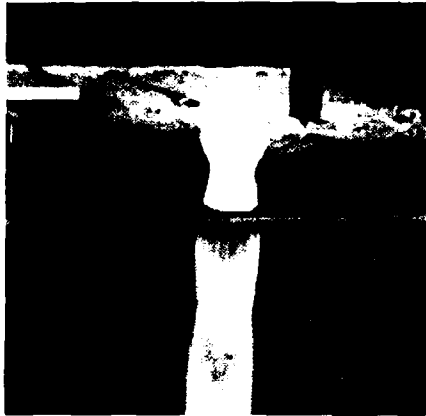


Figure 13 : 6000N THRUST CHAMBER DURING A FIRING TEST

Oxydation resistant materials may be also used for the exit-cone of large liquid propellant rocket nozzles, which will become much simpler, lighter than the State of the art cooled metallic ones. In this case, a material with a 3D carbon reinforcement Novoltex type and a mixed matrix of carbon and silicon carbide will be used. Such an exit-cone will be very similar to the carbon-carbon Novoltex exit-cone or extendible exit-cone already successfully tested on solid rocket nozzles, but will be oxydation-resistant. Preliminary tests have already been performed with a stub nozzle simulating the attachment and the entrance of a complete exit-cone, on a HM7 motor which is the H<sub>2</sub>O motor of the third stage of the Ariane launchers.

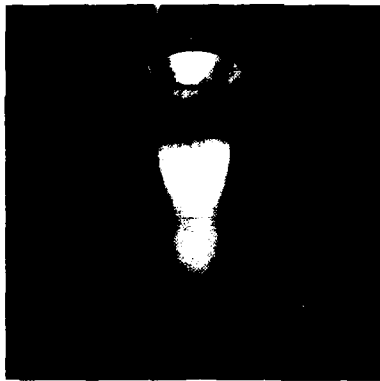


Figure 14 : STUB NOZZLE ON A HM7 MOTOR DURING A FIRING TEST

This stub nozzle performed very successfully, the total test duration was 630 seconds with 6 cycles, without any erosion. A test with a complete exit-cone is now being prepared.

##### **5 - CONCLUDING REMARKS**

These few examples show the new possibilities opened by the thermostable composite materials for rocket propulsion. Obviously designers will find many other applications in the future, in combining the carbon-carbon, the thermostable insulators and the oxydation resistant materials. The main properties of these different materials are given in Annex 1 to 4.

Compared to the state of the art metallic materials, thermostructural composite materials feature mainly higher temperature capabilities combined with higher mechanical properties at high temperature and lower densities. However, it is generally not possible to replace a given metallic part by the same shape part made of a thermostable composite material ; there is, for instance, some process limitation which leads to a redesign, as shown in this presentation. This redesign must be made with an overall view of the system to find the best compromise between the material properties and the mission requirements and so take full advantage of these materials.

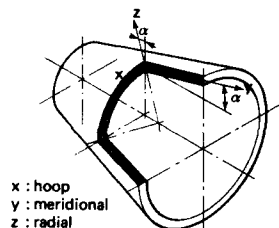
ANNEX 1Carbon-carbon 4D Sepcarb<sup>(\*)</sup>

(1 mm diameter rods)

Specific gravity (g/cc)	1.9 - 1.95
Shear strength at 20°C (MPa)	25
1500°C	45
Tensile strength 20°C (MPa)	120
(F direction) 1500°C	150
Thermal expansion at 500°C (F direction)	0.18 %

ANNEX 2Carbon-carbon Novoltex<sup>(\*)</sup> for exit-cone

T22



Specific gravity (g/cc)	1.7 - 1.8
Shear strength (MPa) MPa)	25 - 30
Tensile strength (MPa) (X direction)	80 - 90
Tensile strength (MPa) (Y direction)	40 - 45
Thermal Expansion at 2400°C (Z direction)	0.9 %

ANNEX 3Thermostable Insulators

Material	Carbon-alumina	Novoltex <sup>(*)</sup> carbon-carbon T29
Specific gravity g/cc	2.3	1.4
Heat diffusivity $10^{-4} \text{ m}^2 \text{ s}^{-1}$	1.8	2
Maximum temperature of use °C	1 800	~ 2500
Hoop tensile shear strength at 1000°C - MPa	80	100
Interlaminar shear strength at 1000°C - MPa	27	30

## ANNEX 4

### Silicon carbide-Silicon carbide (ID)

Specific gravity g/cc	2.4
Tensile strength at 20°C (MPa) at 100°C	500 350
Compression strength at 20°C (MPa) at 1000°C	800 750
Interlaminar shear strength at 20°C (MPa) at 1000°C	60 50

#### - Carbon-Silicon carbide 3D Novoltex type)

Specific gravity g/cc	2.3
Tensile strength at 20°C (MPa)	80
(X direction) at 100°C	100
at 1400°C	140
Compression strength at 20°C (MPA)	650
(X direction) at 1000°C	700
at 1400°C	800
Shear strength at 20°C (MPA)	> 100
at 1000°C	> 40
at 1400°C	> 40

**ANNEX A**

## Mage 2 Firing conditions

- Propellant : CTPB binder, 88 % solids, 16 % aluminium  
- Propellant weight : 490 kg  
- Action time : 43.5 s  
- Average pressure : 3.75 MPa  
- Maximum pressure : 5.125 MPa

**ANNEX B**

### Ballistic missile nozzle firing conditions

- Propellant : HTPB binder, 88 % solids.
  - Action time : 40 s
  - Average pressure : 7.0 MPa

**ANNEX C**

### Hot gas valve operating conditions

- Propellant : PU binder, AP oxydiser,  
flame temperature : 2100°C
  - Operation time : 300 s
  - Mean mass flow rate : 0.35 kg/s
  - Valve internal pressure : between 1.2 MPa and 2.4 MPa

ANNEX DTubing firing conditions

- Propellant : RDX modified cast double base,  
flame temperature : 2010°C
- Operation time : 300 s
- Internal pressure : 2.2 MPa
- Flow rate for tube 1 : 0.1 kg/s
- Flow rate for tube 2 : 0.05 kg/s

ANNEX E5N thrust chamber tests conditions

- Propellant : N<sub>2</sub>O<sup>4</sup> and MMH
- Flame temperature : 3100°K
- Pressure : 1 MPa
- Throat diameter : 1.92 mm
- 400 cycles
- Total burn time : 7 hours

ANNEX F6000N thrust chamber, tests conditions

- Propellant : N<sub>2</sub>O<sup>4</sup> - MMH
- Flame temperature : 3100°K
- Pressure : 1.2 MPa
- Throat diameter : 60 mm
- 7 cycles
- Total burn time : 868 s

ANNEX GHM7 stub nozzle tests conditions

- Propellant : H<sub>2</sub>O<sup>2</sup>, mixture ratio 5.3
- Flame temperature : 3300°K
- Chamber Pressure : 3.5 MPa
- Throat diameter : 108 mm
- Attachment area ratio : 8.2
- 6 cycles
- Total burn time : 631 s

REFERENCES

- (1) - DONGUY, P.J., "Carbon-carbon nozzles for apogee boost motor, Recent evolutions" AIAA Paper N° 82-1187.
- (2) - DELNESTE, L., "Improvements in Mechanical Analysis of multi-directionnal Sepcarb carbon-carbon composites" AIAA Paper N° 84-1308.
- (3) - DONGUY, P.J., "New nozzle concepts allowed by ceramic-ceramic class thermal insulators" AIAA Paper N° 85-1171.
- (4) - SEVELLEC, J.F., "Development and testing of carbon-carbon valves and tubings for hot gas flow control" AIAA Paper N° 87-1820
- (5) - MELCHIOR, A., POULIQUEN, M.F., SOLER, E., "Thermalstructural composite materials for liquid propellant rocket engines" AIAA Paper N° 87-2119.
- (6) - GENTIL, P., "Design and development of a new SRM nozzle based on carbon-carbon and carbon-ceramic materials" AIAA Paper N° 88-3333

#### DISCUSSION

R. Kochendorfer, DFVLR, FRG. There are widely varying results published in the literature regarding the long-term stability of silicon carbide fiber reinforced silicon carbide composites at elevated temperatures in oxidizing environments. In a Bulletin of the American Ceramic Society article (Vol. 65, No. 2, 1986) SEP showed no degradation in bending strength of silicon carbide-silicon carbide composites after 500 hours of exposure in air at 1100°C. On the other hand, the Ecole des Mines published a report in 1986 that showed a drastic decrease in fiber strength after just 12 hours in an argon atmosphere. Can you comment on this, based on your experience with this material?

P. Donguy, SEP, France. Yes. Based on my experience, this is not the only case where we have different results for the composite material than we do for the individual constituents as raw materials. Tests run in real rocket applications with composite materials show good results at temperatures higher than the maximum possible use temperature measured on the fibers alone. This is a fact that still remains to be fully explained, but it has been observed with composites other than silicon carbide-silicon carbide too. An important point for rocket propulsion is that the requirements are not for long lifetimes, but for short to medium lifetimes and high temperatures.

## ÉCHANGEURS DE CHALEUR ET AUBES DE TURBINE EN CÉRAMIQUE THÉORIE ET RÉSULTATS EXPÉRIMENTAUX

par

P. Avran et S. Boudigues  
ONERA  
Fort de Palaiseau  
91120 Palaiseau  
France

### Sommaire

*Cette communication décrit les travaux théoriques et expérimentaux effectués depuis cinq ans par l'Office National d'Etudes et de Recherches Aérospatiales sur deux applications possibles de la céramique à la turbine à gaz : les échangeurs de chaleur et les aubes de turbines (fixes et mobiles).*

### Summary

*Theoretical and experimental research on the use of ceramics in gas turbines developed at O.N.E.R.A (the French Aerospace Research Institute) during the last five years is reviewed and discussed.*

*The two main lines of this research are :*

- ceramic heat exchangers for high efficiency, low specific fuel consumption gas turbine cycles,*
- use of ceramics for fixed or moving turbine blades.*

### Introduction

Les propriétés intéressantes des céramiques, notamment leur faible densité et leur excellente tenue à haute température confère à ce matériau des qualités propres à séduire les motoristes. L'Office National d'Etudes et de Recherches Aérospatiales (O.N.E.R.A) sous l'égide de la Direction des Recherches, Etudes et Techniques (D.R.E.T) s'attache depuis plusieurs années à concevoir des techniques appropriées pour leurs utilisations dans les turbines à gaz, notamment pour la réalisation d'échangeurs de chaleur et d'aubes de turbines fixes ou mobiles.

La première partie de cette communication précise l'intérêt de l'emploi des échangeurs de chaleur dans les turbines à gaz suivant la place qu'ils occupent. Différents échangeurs sont présentés ainsi que les résultats obtenus au banc d'essais, comparés à ceux prévus par un code de calcul simplifié. La seconde partie est consacrée à l'essai d'aubes de turbine en céramique et aux principaux résultats obtenus sur aubes fixes et mobiles.

### Échangeurs en céramique

Le poids et l'encombrement des échangeurs étaient deux obstacles majeurs pour leur utilisation sur véhicule terrestre et plus encore sur les avions. La faible masse volumique, la bonne conductibilité, la tenue aux températures élevées du carburé de silicium permet d'envisager des dimensions et des masses beaucoup plus faibles.

Les échangeurs traditionnels (fig. 1) sont placés en aval de la turbine de puissance, les gaz sont à la pression atmosphérique et l'optimisation du cycle impose une pression relativement faible en sortie de compresseur. Ces deux raisons donnent à l'échangeur un encombrement, une masse et un prix prohibitifs.

Si l'on place l'échangeur entre la turbine de puissance et la turbine du générateur (fig. 2), la pression des gaz vaut alors environ 3 fois la pression atmosphérique. Par ailleurs, l'optimisation du cycle impose une pression plus élevée en sortie de compresseur. Pour ces deux raisons, l'échangeur est environ deux fois moins encombrant, deux fois moins lourd, deux fois moins cher. La performance est moins bonne, le moteur est donc plus important (ce qui pour les faibles puissances est plutôt un avantage) ; il est plus lourd et plus cher mais le plus souvent le bilan global est en faveur de l'échangeur intermédiaire. L'utilisation des céramiques permet de tolérer la température plus élevée imposée à l'échangeur intermédiaire.

Soulignons enfin que l'échangeur intermédiaire peut être court-circuité, fournissant une surpuissance sans augmentation de la température maximum. Cet artifice peut être très utile en particulier pour les turbines d'hélicoptères et pour l'augmentation de poussée que réclament en fin de mission les missiles de croisière.

La planche (fig. 3) compare les consommations spécifiques d'une turbine à gaz pour un cycle simple (CS), pour un échangeur intermédiaire (EI) et pour un échangeur aval (EA). Cette comparaison est faite pour 4 valeurs ( $\epsilon = 0 - 0,6 - 0,7 - 0,8$ ) de l'efficacité de l'échangeur et pour des températures maximum de cycle  $T_{5i}$  variant de 1100 K à 1700 K. On voit qu'aux faibles températures, l'échangeur apporte un gain de  $C_S$  avec en plus une très forte diminution du rapport de pression optimum. Aux fortes températures, le gain de consommation est très faible mais la diminution du rapport de pression optimum est très importante.

La planche (fig. 4) montre, pour un double flux volant à  $M = 0,8$  et  $Z \geq 11$  km, les gains obtenus par un échangeur placé entre la turbine HP et la turbine entraînant la soufflante, la comparaison est faite pour 4 valeurs de l'efficacité  $\epsilon = 0 - 0,6 - 0,7 - 0,8$  et pour trois températures maximum  $T_{5i} = 1200 - 1400 - 1600$  K. Là encore, plus que le gain possible de  $C_S$ , on notera la forte diminution du rapport de pression optimum. Le taux de dilution  $\lambda$  est abaissé par la présence de l'échangeur.

En résumé, on peut dire que pour une turbine à gaz, les échangeurs (intermédiaire ou aval) apportent un léger gain en consommation mais surtout qu'ils permettent d'obtenir la même consommation avec des rapports de pression et des taux de dilution plus faibles. On échange le poids, l'encombrement, le prix de l'échangeur contre le poids, l'encombrement, le prix des étages de compresseur et de turbine. Notons que pour les faibles débits ( $< 3$  kg/s), la voie des échangeurs paraît la seule possible pour tirer parti des fortes températures.

La Société Céramiques et Composites a mis au point un procédé d'extrusion qui permet d'obtenir des tubes nervurés (fig. 5). Des cylindres coaxiaux sont ainsi réunis par des nervures radiales. Les fluides circulent à contre-courant dans les alvéoles (trapèzes curvilignes) délimités par des nervures et des cylindres successifs. On peut en compliquant les entrées et sorties de l'échangeur, multiplier le nombre de cylindres concentriques, afin de gagner en contrainte thermique, en encombrement frontal, en masse, en prix. Nos réalisations actuelles ont été limitées à 3 et 4 cylindres concentriques. Dans ces tubes, l'essentiel de l'échange thermique est réalisé par les nervures prévues en nombre et en épaisseur suffisants pour transmettre les flux thermiques.

En jouant sur le nombre de tubes, sur le nombre de nervures, sur leur épaisseur, on peut obtenir le meilleur compromis entre la masse, la longueur, l'encombrement frontal, la perte de charge (fig. 6). Cette planche est relative à un débit de 1,6 kg/sec d'air. Les pressions sont de 3 et 8 bars, les températures sont de 580 K et 1150 K pour les flux froids et chauds respectivement. La puissance thermique échangée est de 450 kw. L'efficacité de l'échangeur est 0,7. On voit que suivant le nombre de tubes  $t$  et le nombre de nervures  $n$ , la longueur  $L$ , les rayons extérieurs  $R$ , les masses et les pertes de charge varient dans une très large plage. Avec un petit nombre de tubes et de nervures on a de faibles rayons (200 mm) mais des masses importantes (75 kg) et de fortes pertes de charge (environ 6%). A l'opposé avec un grand nombre de tubes et de nervures, on a de faibles longueurs (250 mm), de faibles masses (45 kg), de faibles pertes de charge (4%) mais de grands rayons (450 mm). On a donc une très grande plage de choix et ceci pour des nombres de Mach imposés sur chaque flux. Notons que la masse du moteur est d'environ 90 kg.

Les calculs sont conduits à partir des formules de Kays et London [1] pour la détermination du coefficient d'échange et du document Idel'cik [2] pour les pertes de charge. On suppose les températures uniformes dans un plan normal à l'axe, on raisonne sur les valeurs moyennes des coefficients d'échange et des pertes de charge. Le code de calcul malgré toutes les hypothèses simplificatrices recoupe très bien les résultats expérimentaux. Le calcul donne l'évolution des températures d'une part le long du tube, d'autre part le long des nervures et des cercles dans chaque plan normal à l'axe. On en déduit les contraintes thermiques dans les nervures et dans les cylindres.

Parallèlement à ces études théoriques, l'O.N.E.R.A s'est attaché depuis plusieurs années sous l'égide de la D.R.E.T. et le concours de la Société Céramiques et Composites à concevoir des techniques appropriées pour la réalisation de modules d'échangeurs, de les qualifier au banc d'essais, afin d'aboutir à terme à leurs implantations sur machines réelles. Ces différentes configurations sont présentées ci-dessous :

#### 1) Echangeurs type barillet deux circuits (chaud, froid)

Ces modules constitués principalement (fig. 7) de 8 tubes nervurés en carbure de silicium disposés en barillet sur deux flasques en SiAlon qui a la propriété d'avoir une bonne résistance mécanique à chaud et une excellente tenue aux chocs thermiques.

#### 2) Echangeur type barillet, 5 tubes, trois circuits (chaud, froid, chaud) (fig. 8)

##### Installation d'essais

Le dispositif d'essai (fig. 9) permet de recevoir indifféremment les types d'échangeurs décrits précédemment. Il permet d'alimenter indépendamment en air froid et en gaz chaud celui-ci avec les possibilités suivantes :

- 1) en respectant uniquement le gradient thermique,
- b) en restituant à la fois le gradient thermique et progressivement les niveaux de températures désirés,
- c) en créant les conditions précédentes mais avec chocs thermiques obtenus par la mise en service d'un foyer de combustion placé en amont de l'échangeur. Les niveaux de pression et de températures restitués sont ceux habituellement rencontrés sur machines.

##### Résultats d'essais

La mise au point technologique des modules d'échangeurs nervurés (2 ou 3 circuits) a été effectuée sur des maquettes de 330 mm de longueur totale. Progressivement, on a pu améliorer la tenue des tubes en optimisant leur profil, obtenir une meilleure résistance thermomécanique des flasques par le choix du matériau (SiAlon) mais également par l'amélioration des facteurs de forme, enfin au niveau de la liaison flaque-tube, une mauvaise adhérence du liant dans le temps et sa porosité étaient une source croissante de fuite des gaz froids vers les gaz chauds. Un travail important a été entrepris sur ce point particulier par la Société Céramiques et Composites et l'O.N.E.R.A ; de nouveaux liants ont été élaborés et des progrès significatifs ont été obtenus tant du point de vue tenue mécanique (meilleure adhérence) que du point de vue étanchéité en agissant à la fois sur leurs compositions chimiques, leurs procédés d'élaboration et les modes d'application. Enfin dans la mesure où les taux de fuite restaient faibles, ces essais préliminaires ont permis également de valider nos codes de calculs.

L'expérimentation s'est poursuivie sur des maquettes de plus grandes longueurs (450 mm), afin de se placer dans une configuration réaliste d'échangeur susceptible de s'implanter sur machine, les efficacités recherchées étant voisines de 0,70. On a pu ainsi les éprouver durant plusieurs heures sans dégradation, les taux de fuite enregistrés restant inférieurs à 2%.

Le tableau I donne à titre indicatif, avec les conditions d'essais les principaux résultats relevés sur l'échangeur deux circuits (C.F) et trois circuits (C.F.C) au point nominal. Comparées aux valeurs obtenues à l'aide de notre code de calculs, on note un très bon recouplement des efficacités (mieux que 2%), par contre l'écart existant entre les pertes de charge mesurées et calculées est imputable à une mauvaise estimation de celles-ci à l'entrée et à la sortie de chaque circuit.

Une expérimentation complémentaire sur l'échangeur deux circuits a permis en élargissant son domaine de fonctionnement, de valider, pour une plage plus grande du nombre de Reynolds, notre code de calculs comme le montre la figure 10 où sont portées respectivement les efficacités et pertes de charge relevées pour ces différentes conditions.

#### Aubes en céramique

L'utilisation d'aubes de turbine en céramique permet de diminuer ou même de supprimer le débit de refroidissement. Il en résulte un gain sur la puissance par unité de débit et une légère amélioration du rendement. Par ailleurs la faible masse volumique du carbone de silicium permet un gain de masse sensible sur les aubes elles-mêmes et sur les disques qui les supportent.

Les essais avaient pour but de connaître les performances thermomécaniques d'aubes en céramique de conceptions diverses. Les températures, les pressions, les vitesses de gaz étaient représentatives des conditions réelles de fonctionnement sur banc statique. Le banc dynamique ajoutait la contrainte centrifuge mais à la pression atmosphérique.

#### Conception des aubes en céramique

Le comportement relativement médiocre de la céramique aux efforts de traction nous a amenés à concevoir une technologie nouvelle d'aubes enveloppes qui permet de soumettre la céramique uniquement à des efforts de compression. L'enveloppe céramique (fig. 11) s'appuie sur une plate-forme située en tête d'aube et solidaire d'une lame métallique, l'aube comporte ainsi deux éléments distincts :

- a) l'enveloppe céramique qui au contact de l'écoulement accepte un niveau de température nettement supérieur à celui des alliages connus ;
- b) l'âme métallique qui assure la résistance aux efforts centrifuges lors de la rotation et évacue le flux de chaleur transmis par rayonnement grâce à une faible ventilation.

Le profil céramique est de forme elliptique (grand axe = 30 mm, petit axe = 6 mm, hauteur = 30 mm). L'épaisseur de l'enveloppe est égale à 1,2 mm. Les matériaux utilisés sont soit monolithiques (carbone de silicium de la Société Céramiques et Composites), soit composites (toile SiC, tissus C10, satin SiC de la Société Européenne de Propulsion).

#### Résultats d'essais

Les aubes enveloppes (monolithiques et composites) ont été dans un premier temps éprouvées sur un montage statique en jet libre, soit une aube isolée, soit en grille d'aubes pour une température des gaz de combustion de 2173 K. On a noté une bonne tenue thermomécanique des maquettes, ainsi qu'un bon comportement aux chocs thermiques obtenus à l'aide de cycles successifs d'allumage et d'extinction d'un foyer de combustion. Trois thermocouples contrôlent la température de l'âme métallique et permettent d'ajuster en conséquence le débit de refroidissement, la température de surface de l'aube est enregistrée en différents points, côté intrados et côté extrados à l'aide d'un pyromètre optique infrarouge [3], ce qui permet d'établir une cartographie du champ de température de l'aube. Il est à remarquer que compte tenu des conditions d'essais (température des gaz de combustion égale à 2100 K) et d'un débit de refroidissement de l'âme métallique faible, la température maximale atteinte a été de 1450 K sur l'intrados au bord d'attaque. On peut noter un gradient supérieur à 400 K entre l'intrados et l'extrados. Après plusieurs heures d'essais, aucun dommage n'a été décelé.

Les essais ont été poursuivis sur un montage statique en pression qui limite la température des gaz de combustion à 1800 K et la pression dans la veine à 6 bars. On note que pour les mêmes conditions de température et de vitesse d'écoulement et pour le même débit de refroidissement de l'âme métallique, la pression a pour effet de réduire de 50% environ l'écart qui existe entre la température des gaz et la température de surface (1150 K à la pression atmosphérique et 1450 K à 6 bars). Par contre, la différence de température entre la céramique et l'âme métallique reste la même (300 K). Après plusieurs heures d'essais, pour les conditions citées plus haut, on constate que le bon comportement thermomécanique et aux chocs thermiques se confirme pour les aubes en carbone de silicium ; par contre, pour les trois types d'aubes composites qualifiés, on relève une érosion progressive en surface, ce qui dans l'état actuel des choses condamne ce matériau pour des applications de longue durée.

Une dernière campagne d'essais a été menée sur le montage tournant, afin de soumettre ces mêmes aubes (calées à 60° par rapport à la direction de l'écoulement) à la force centrifuge. Pour une pression voisine de la pression atmosphérique (1,3 bars) et une température de l'écoulement égale à 1800 K, la vitesse linéaire en bout de pale a atteint 270 m/s. Une bonne tenue thermomécanique a été observée aussi bien pour les aubes enveloppes en carbone de silicium que pour les aubes en matériaux composites. Sur ce même montage, on a également qualifié des aubes massives dites en traction en matériaux composites. Des résultats aussi prometteurs ont été enregistrés.

Conclusions

Aidé par un support financier de la D.R.E.T, l'O.N.E.R.A depuis cinq ans a consacré une forte activité pour introduire les céramiques dans les turbines à gaz. L'activité à dominante expérimentale était guidée par des codes de calculs simplifiés du fait des données imprécises des caractéristiques du matériau dans des assemblages complexes. Les résultats sur les échangeurs de chaleur à tubes nervurés sont très encourageants et moyennant quelques progrès sur les assemblages, on peut d'une part modifier très sensiblement les bilans de masse et de volume qu'offraient les échangeurs métalliques mais également envisager leur emploi dans une gamme de température plus élevée.

Les aubes enveloppes ont fourni de bons résultats mais dans un domaine limité en pression (6 bars) et en effet centrifuge (270 m/s), les aubes fibrées ne peuvent être envisagées que pour des missions de faible durée (missile) ou en présence de gaz non oxydants.

Références

- [1] M. Kays et A.L. London : Compact heat exchangers.
- [2] I.E. Idel'cik : Memento des pertes de charge. Eds. Eyrolle.
- [3] M. Charpenel et J. Wilhem : Pyromètre infrarouge pour la mesure des températures d'ailettes de turbine. T.P. ONERA 1976-38.

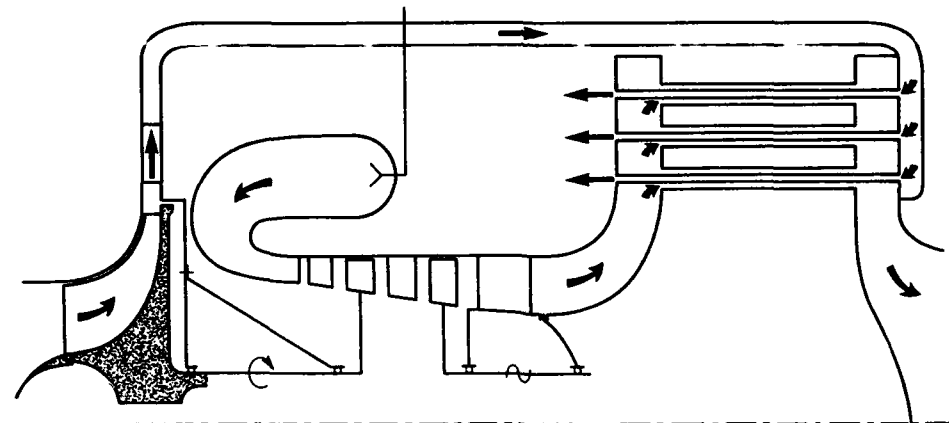


Fig. 1. Echangeur aval.

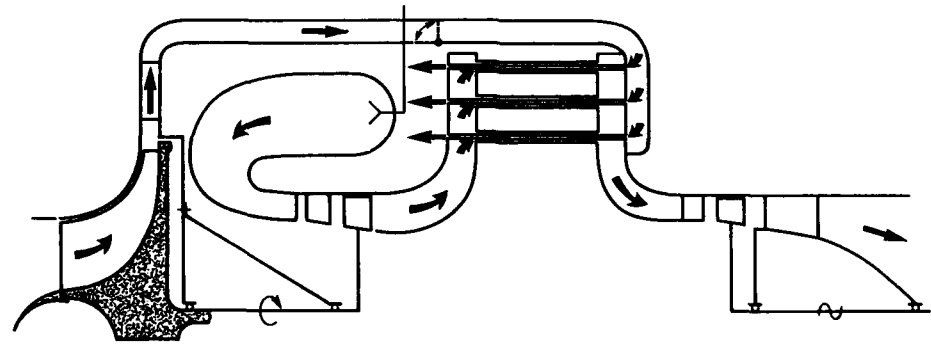


Fig. 2. Echangeur intermédiaire.

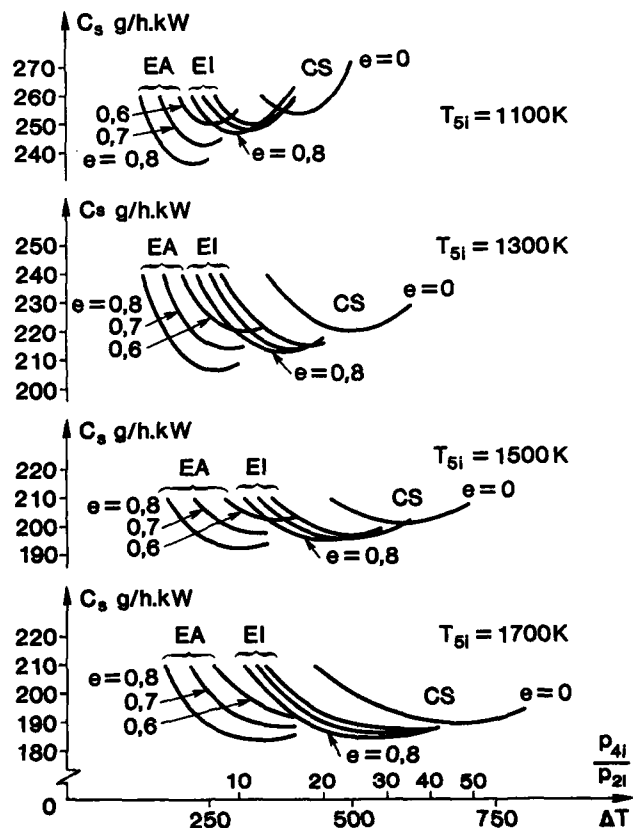


Fig. 3. Influence de l'efficacité de l'échangeur.

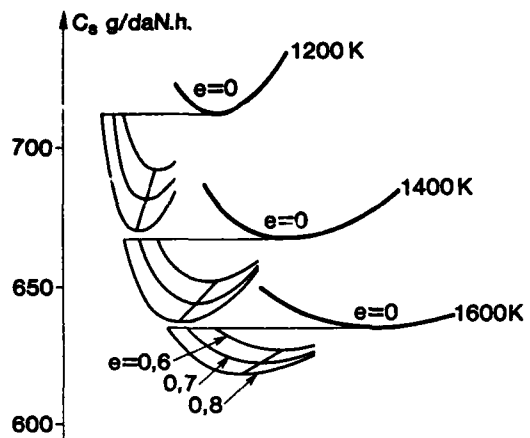


Fig. 4. Influence de l'efficacité de l'échangeur.

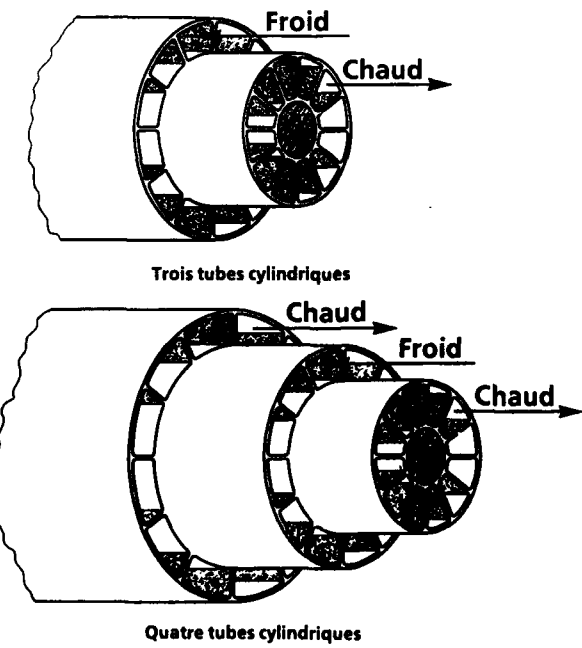
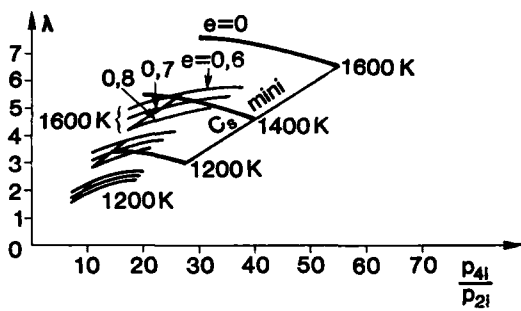


Fig. 5.

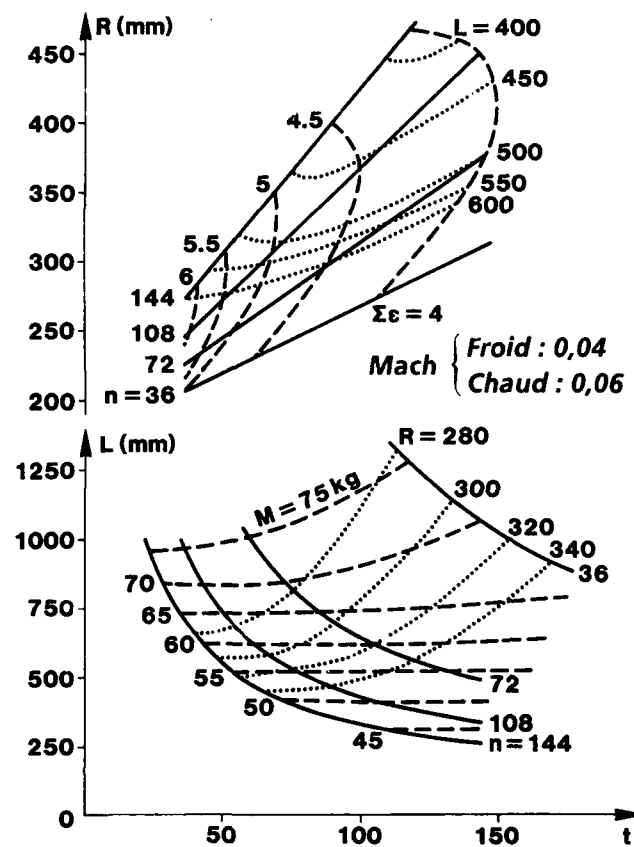


Fig. 6.

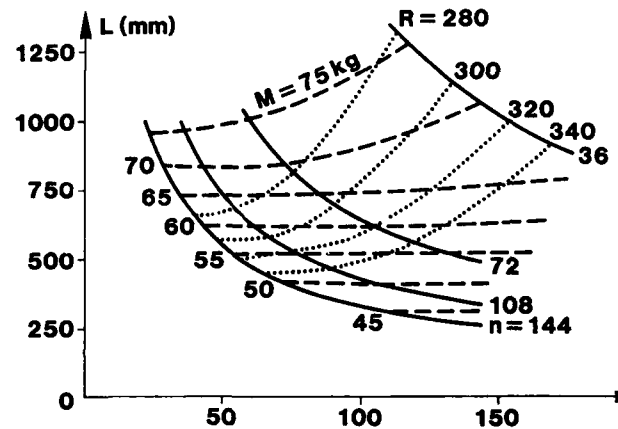


Fig. 7. Echangeur 2 circuits.



Fig. 8. Echangeur 3 circuits.

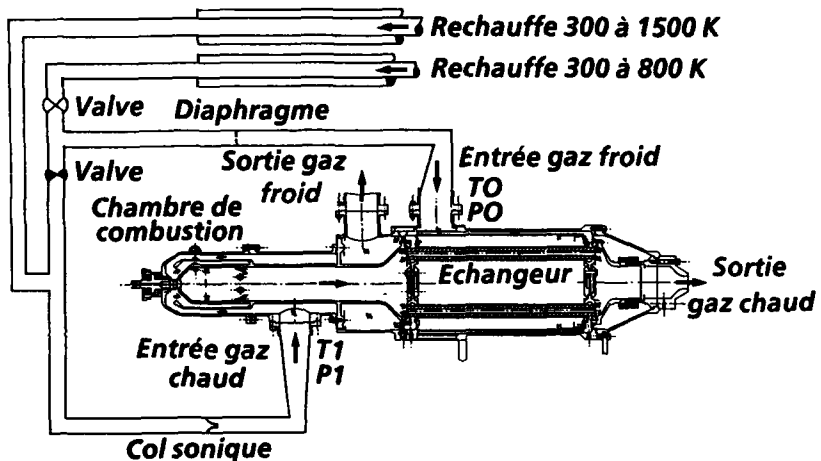


Fig. 9. Banc d'essais.

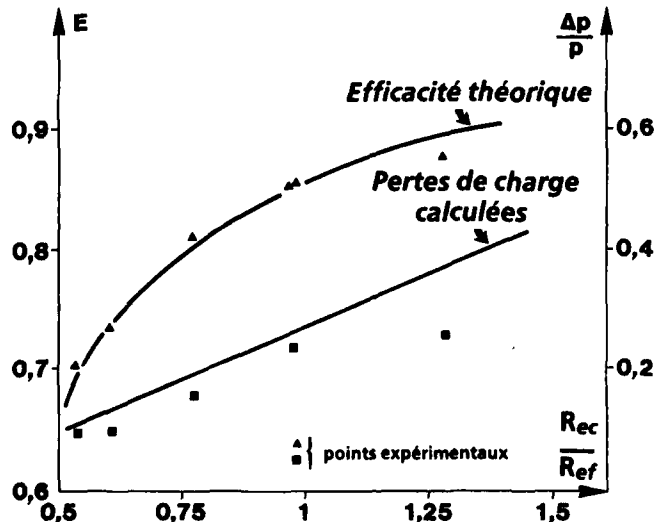


Fig. 10. Echangeur céramique (deux circuits) - Efficacité et pertes de charge.

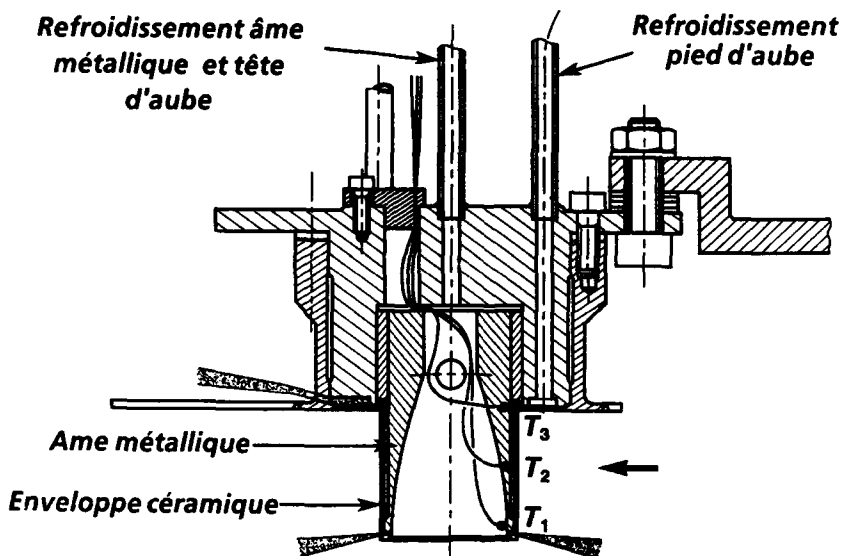


Fig. 11. Représentation schématique d'une aube enveloppe en céramique.

	ECHANGEUR DEUX CIRCUITS		ECHANGEUR TROIS CIRCUITS	
	Froid	Chaud	Froid	Chaud
DEBIT (g/s)	105	103	137	66 75
PRESSION D'ENTREE (bar)	9.61	2.85	8.55	3.05
TEMPERATURE D'ENTREE (°K)	574	878	574	881
PERTES DE CHARGE (%)				
EXPERIENCE	4.2	10	8.2	13.1
CALCUL	3.5	12.1	4.0	6.9
EFFICACITE				
EXPERIENCE	0.701		0.720	
CALCUL	0.695		0.707	

Tableau I. Echangeur céramique : résultats.

**DISCUSSION**

R. Jacques, Ecole Royale Militaire, Belgium. At one point you mentioned rotary heat exchangers as well as stationary ones for use in turbine engines. Do you envision a competition arising between these two types, since the rotary exchangers may have a more rapid recuperation cycle?

P. Avran, ONERA, France. Many people are working on the development of rotary exchangers. Their main advantage is that their efficiencies are close to 96%, but the main problem with them is that inevitably, because of the rotation, there are leaks between the two circuits. There have been some reports of reduced leakage in rotary exchangers, for example some Japanese publications report 6% leakage, but all of the results I have seen up until now put the leakage at close to 10%. Thus, the problem at the moment with rotary exchangers is their even short-term, 5-10 minute, performance and reliability, and their deterioration with time and loss of efficiency. Although the efficiency of stationary heat exchangers is lower, they run for several hours with nearly zero leakage, and for cryogenic applications, for example, one cannot have leakages.

## CRYOGENIC TURBOPUMP BEARING MATERIALS

Biliyar N. Bhat

Materials and Processes Laboratory  
 NASA George C. Marshall Space Flight Center  
 Marshall Space Flight Center, Alabama 35812 USA

Summary

Materials used for modern cryogenic turbopump bearings must withstand extreme conditions of loads and speeds under marginal lubrication. Naturally, these extreme conditions tend to limit the bearing life. It is possible to significantly improve the life of these bearings, however, by improving the fatigue and wear resistance of bearing alloys, and improving the strength, lox compatibility and lubricating ability of the bearing cage materials. Improved cooling will also help to keep the bearing temperatures low and hence prolong the bearing life.

Introduction

Modern cryogenic turbopumps used in rocket engines operate at high speeds. The turbopump bearings carry heavy loads, necessitated by high efficiency designs. Bearing materials are highly stressed, and are subjected to wear more than conventional oil lubricated bearings. As a result, bearing life is limited. This paper presents the life limiting factors in cryogenic turbopump bearings and discusses methods of improving bearing life. Improved bearing materials will also be discussed. Discussions will be limited to liquid oxygen (lox) and liquid hydrogen ( $LH_2$ ) turbopump ball bearings.

Life Limiting Factors in Cryogenic Bearings

Bearing elements are subjected to cyclic stresses, shown schematically in Figure 1. Bearing material is subjected to maximum alternating shear stresses below the surface in a properly lubricated bearing. Cracks are usually initiated in regions of surface contact where these alternating shear stresses acting in the material are at a maximum (Figure 2). Pure rolling loads generate maximum shear stresses slightly below the surface of contacting components (Figure 1). With addition of frictional or sliding forces, maximum shear stresses move closer to the surface. Sliding forces of sufficient magnitude (such as in poorly lubricated bearings) can cause cracks to originate at the surface and can significantly reduce bearing life. Surface cracks grow into spalls (or pits) with metal removal and this represents the end of useful life.

Bearing wear is another life-limiting factor. Wear is a failure mode in which metal atoms are removed from the bearing surface through different mechanisms of wear such as adhesive wear and oxidative wear. In adhesive wear there is metal-to-metal contact at the asperites. The two surfaces bond together locally. When relative motion occurs between the two surfaces, material is removed from the contact area and wear debris is produced. This type of wear can occur in turbopump bearings when there is a lack of lubrication in the presence of relatively high loads.

Lox turbopump bearings are susceptible to oxidative wear. In this mechanism, bearing material is oxidized by oxygen in the cooling system. Lox cooling is necessary for satisfactory operation of the bearing. If cooling is reduced because of insufficient flow rate or reduced vapor margin in the lox, heat generated in the bearing will not be completely dissipated and bearing operating temperatures will rise. Cooling will change from lox to gox (gaseous oxygen). Gox is not as good a coolant as lox, and therefore bearing temperatures rise further to the point where oxidation begins to occur. Oxide film is readily removed by friction and fresh surface is exposed to gox and the process continues, resulting in bearing wear.

Corrosion is another life limiting factor for cryogenic bearings because the bearings are not always protected from corrosive environment. Since lubricating oils cannot be used to protect from general corrosion, corrosion resistant bearing material such as 440C are used for making cryogenic bearings. In addition, bearings must resist stress corrosion cracking. If not, press-fitted bearings will crack and failure of the inner race will result.

Another bearing element with a life limitation is the bearing cage (or retainer). Cages are subjected to ball forces, especially when there is uneven wear of the balls (or cage). Failure mode is either by fatigue or by overload. Bearing cage is also a source of lubricants such as PTFE (polytetrafluoroethylene), which is transferred to the balls by rubbing action. Once the available supply of PTFE in the composite is exhausted, there is no replenishment and the bearings essentially run unlubricated. This results in a significant reduction in bearing life. Furthermore, the present cage material is often reinforced with glass fibers for strength. These fibers tend to remove some of the PTFE transfer film lubricant and to cause abrasive wear of the rolling elements, and further reduce the bearing life.

#### Materials Requirements for Improved Bearing Life

Advanced cryogenic bearing materials are expected to improve bearing life through improved resistance to wear and rolling and sliding contact fatigue. At the same time, they must maintain good resistance to general corrosion and stress corrosion. Alloy 440C, which is an iron-chromium-carbon martensitic stainless steel, is the most commonly used cryogenic bearing material today. However, 440C is not the best bearing material in terms of bearing load capacity and wear resistance; it is used primarily because of its corrosion resistance. Rolling contact fatigue (RCF) life of a bearing can be improved by improving the strength and hardness of the bearing material. Such bearing alloys are available today (e.g., M-50) but are not corrosion resistant and, therefore, are unsuitable for cryogenic applications. Hence, the main thrust of bearing alloy development is to improve the RCF properties without sacrificing corrosion resistance.

Wear resistance is another important requirement for cryogenic turbopump bearings. Both adhesive wear and oxidative wear must be considered. There is an inherent adhesive wear rate characteristic of the bearing material, and it decreases as the operating temperature of the bearing falls. Bearing hardness and load-bearing capacity are generally higher at cryogenic temperatures than at room temperature. Therefore, bearings do not seem to degrade readily at LH<sub>2</sub> temperatures. As the bearing temperatures increase, however, bearing properties go down and so does the bearing life. In the lox pumps, there is a potential for oxidation of the bearing alloy. Oxidation rates are negligible at room temperature, but increase dramatically as the bearing temperatures rise. This could result in severe bearing wear. Hence, it is important to keep the bearing operating temperatures as low as possible. This goal can be attained by reducing the bearing friction coefficient, which means use of lox friction materials and improving lubrication. To resist oxidation wear, bearing alloys must have good oxidation resistance and hot hardness. The latter is required to maintain good bearing properties even at elevated temperatures.

Lox pump bearing materials are required to be lox compatible, i.e., they must have high resistance to ignition and combustion in an oxygen environment. Lox compatibility generally decreases with increasing lox pressures. Today operating pressures of lox turbopump bearings are limited by the lox compatibility of the bearing cage material. The present bearing cage material used in lox turbopump is a fiberglass reinforced polymer called armalon. The lox compatibility of armalon is limited to about 6.9 MPa (1000 psi). Higher lox compatibility will permit the use of higher lox pressures in the bearing section, which in turn, improves the cooling of the bearings through increased vapor margins. Improved cooling helps to prolong the life of the bearings.

Bearing lubrication is yet another important consideration in cryogenic bearings. Conventional lubricants freeze at cryogenic temperatures and cannot be used. The present practice is to coat the bearings with MoS<sub>2</sub> solid lubricant. However, this lubricant wears off rapidly and metal-to-metal contact occurs. Coefficient of friction goes up. When armalon cage is used, some transfer occurs when the bearing balls rub against the cage and the transfer film provides lubrication. Even this film transfer process stops when the polymer is used up. Then the bearings run essentially unlubricated. There is no reservoir of fresh lubricant to draw from. When the lubricants are exhausted, bearing temperatures tend to go up resulting in increased wear rates and, hence, a relatively short service life results. Therefore, any effort to improve bearing life must address the lubrication problem.

#### Evaluation of Cryogenic Bearing Materials

Cryogenic turbopump bearing materials require special evaluation techniques because of the unique operating conditions. Conventional testing methods used for oil lubricated bearings are not generally good enough for cryogenic applications. Several bearing materials test procedures are described below. The tests include rolling contact fatigue, wear, stress corrosion, lox compatibility, and rolling and sliding friction.

##### Rolling Contact Fatigue (RCF)

The purpose of RCF testing is to determine the resistance of bearing material to rolling contact fatigue relative to a standard such as 440C or M-50. Several test arrangements are in use. One such arrangement is shown in Figure 3. The test specimen is in the form of a cylinder, 9.5 mm (0.375 in.) in diameter. Load is applied through a set of three bearing balls. The test specimen is rotated and is subjected to cyclic loading. The number of cycles to failure by spalling is taken as the RCF life for the specimen. The tests can be run either with a lubricant at room temperature or without lubricant at cryogenic temperatures, using LN<sub>2</sub> as the cooling medium.

Five-ball testing is another way to determine RCF life of bearing alloys. The test arrangement is shown in Figure 4. Here only bearing balls are used. The test is generally run with a lubricating oil. The fifth ball in the center is the first to fail.

##### Wear Testing

Bearing wear can occur during both rolling and sliding. Wear rates are generally lower with pure rolling, and the highest with pure sliding. In most bearings, wear process is a combination of both rolling and sliding. A schematic of wear test arrangement is shown in Figure 5. It consists of two cylinders, one stationary and the other rotating in contact at right angles. A predetermined load is applied and the test is run for a

predetermined period of time. The amount of material removed by wear is taken as a measure of wear susceptibility of the alloy. A large weight loss is indicative of poor wear resistance. The test is capable of being run at room temperature and also at elevated temperatures. The environment can be either air or gox.

Three ball and a cone arrangement is also used for wear testing (Figure 6). Here, the cone acts as a bearing raceway. This tester can be operated at ambient or cryogenic temperatures. Both lox and gox can be used as cooling media.

#### Stress Corrosion

Stress corrosion susceptibility of bearing alloys is determined by stressing a small tensile test specimen in a stress frame (Figure 7) and subjecting it to 100 percent humidity environment. Time and stress to failure are taken as figures of merit. The threshold stress level below which the bearing alloy does not crack is a useful number which can be used as a limit for pre-stress in press-fitted bearings.

#### Coefficient of Friction

Coefficient of friction ( $\mu$ ) is an important factor that influences the heat generation rates in cryogenic turbopump bearings. The goal is to reduce the coefficient of friction. Coefficient of rolling friction is generally much smaller than the coefficient of sliding friction. There are several different methods of measuring  $\mu$  in combinations of rolling and sliding. One example of determining sliding friction coefficient is shown schematically in Figure 8. Coefficient of sliding friction ( $\mu_s$ ) is given by

$$\mu_s = \frac{\text{tangential force}}{\text{normal force}}$$

#### Lox Compatibility

Lox compatibility of bearing materials (balls, races, and cages) is tested in a lox impact tester, shown schematically in Figure 9. Developed at Marshall Space Flight Center, this tester uses a small disc-shaped specimen which is placed in a cup in contact with a striker head. A 9.1-kg weight is dropped from a height of 1.1 meters onto the striker. If the specimen does not burn, it is considered acceptable for lox service. The test is then repeated at different lox pressures. The tests can also be run in a gox environment at elevated temperatures. Oxygen compatibility generally decreases with increased oxygen pressure and temperature in both lox and gox. The lox compatibility testing helps to determine an upper limit for operating lox pressures in the lox pump bearings. However, such a limit does not exist for LH<sub>2</sub> pump bearings.

#### Full Scale Bearing Testing

Full scale bearings are tested for performance in a specially built Bearings and Seals Materials Tester (BSMT) designed and developed by Marshall Space Flight Center (Figure 10). The BSMT is fully instrumented to measure bearing loads and speeds, coolant flow rates and temperatures, and friction and wear in bearings. Any new or improved bearing designs or improved bearing materials can be tested in the BSMT and their cryogenic performance can be evaluated. The BSMT is capable of operating in lox, LN<sub>2</sub>, or LH<sub>2</sub>. Promising bearing materials can be further tested and validated in an actual turbopump.

#### Improved Materials for Cryogenic Turbopump Bearings

Materials & Processes Laboratory of Marshall Space Flight Center is working towards the goal of improving cryogenic turbopump bearing life through improvements in bearing materials, especially in the lox pump bearings. Some of the work is described in the following paragraphs.

Powder metallurgy (PM) techniques allow the formation of very fine microstructure compared with conventional wrought alloys such as 440C (Figure 11). This is particularly true of carbides. Carbides are an essential ingredient of bearing alloys. High volume fraction of carbides improves the hardness without sacrificing toughness and improves bearing properties, especially the wear rates. The wrought process tends to produce relatively large carbides whereas the PM technique produces highly desirable fine carbides (Figure 12). Bearing alloy powder is consolidated at elevated temperatures by hot isostatic pressing to give 100 percent density. Laboratory tests run on PM bearing alloys show significant improvement in RCF life and wear resistance without sacrificing corrosion resistance.

Bearing surfaces can be modified to improve fatigue and wear resistance. Ion implantation, for instance, is capable of introducing wear resistant combination of atoms on the surface and to a depth of about 10<sup>-8</sup> m. Ion implantations of CrN and TiC appear to offer improved wear resistance. Ion plating is another physical vapor deposition process which is capable of depositing adherent coatings that are either soft and lubricating (e.g., gold or copper) or hard and wear resistant (e.g., dense chromium). Both ion plating and ion implantation tend to reduce the coefficient of rolling and sliding friction.

Improved bearing cage materials are also required to prolong bearing life, in addition to improving the rolling elements. Improvements are possible in the areas of lox compatibility and strength-to-weight ratio. In addition, it is desirable to have the cage as a source of lubricant. Materials and Processes Laboratory of MSFC is developing a

bronze-filled graphite fiber reinforced PTFE. The goal is to improve the strength-to-weight ratio by 50 percent and lox compatibility by 100 percent. These improvements will allow the bearings to operate at higher lox pressures. All ingredients of the composite, viz: graphite, PTFE, and bronze, act as lubricants to varying degrees. The overall effect is to reduce the coefficient of friction and heat generation during operation.

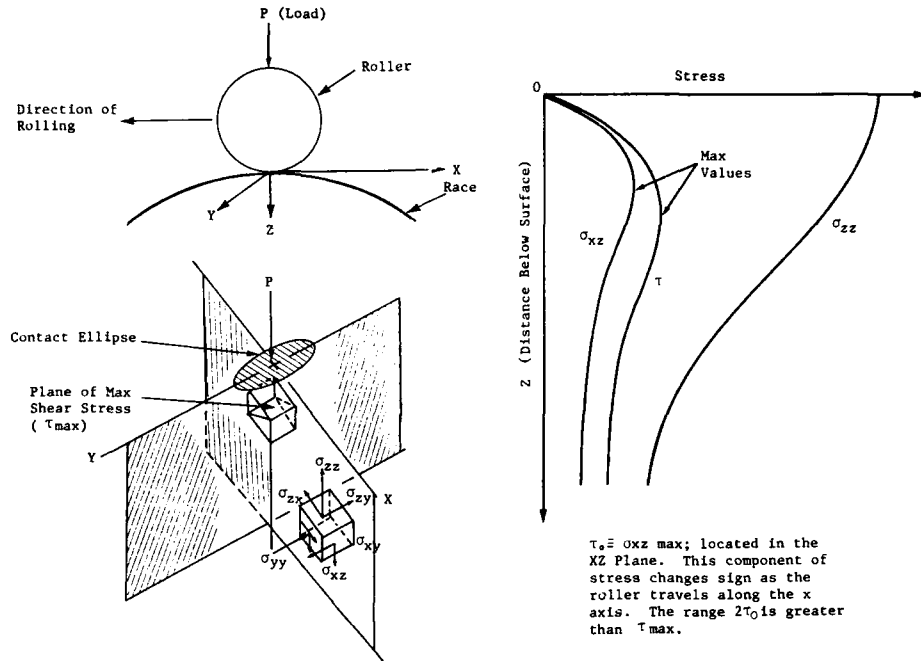


Figure 1. Bearing Stress Diagram

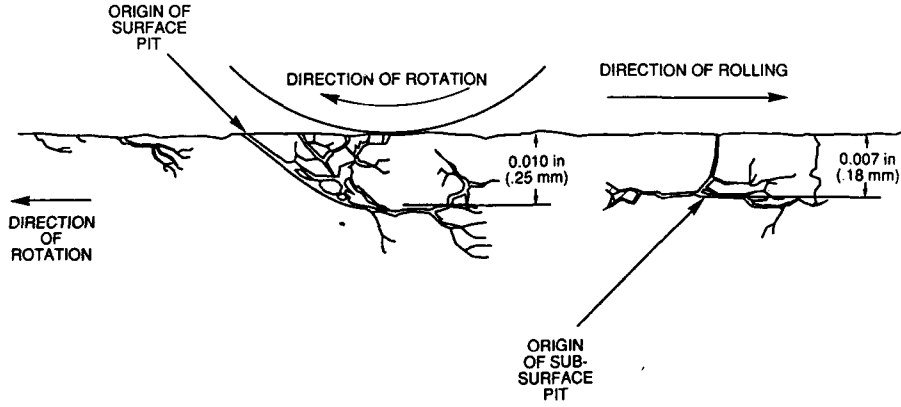


Figure 2. Diagrams of incipient pitting (spalling) caused by contact fatigue. Cracking is parallel and perpendicular to the surface (right) typical of well-lubricated bearings. Crack initiates at the surface for poorly-lubricated bearings (left).

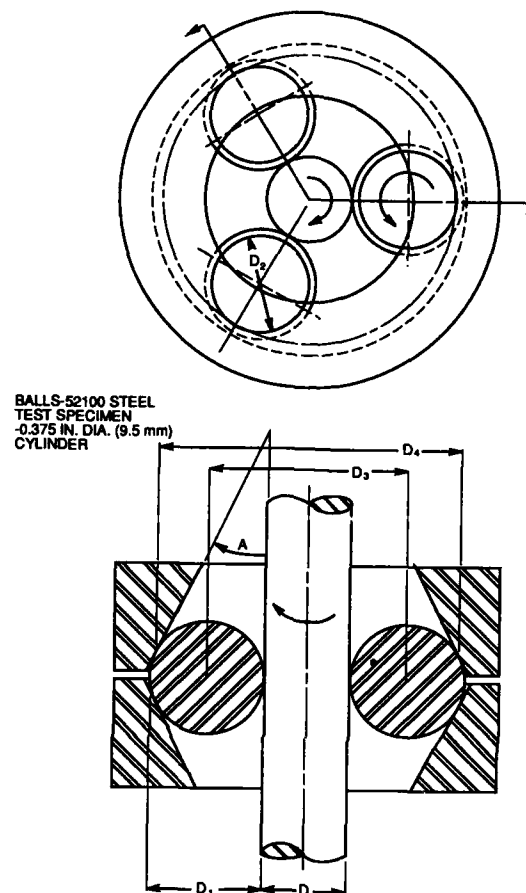


Figure 3. RCF Test Arrangement

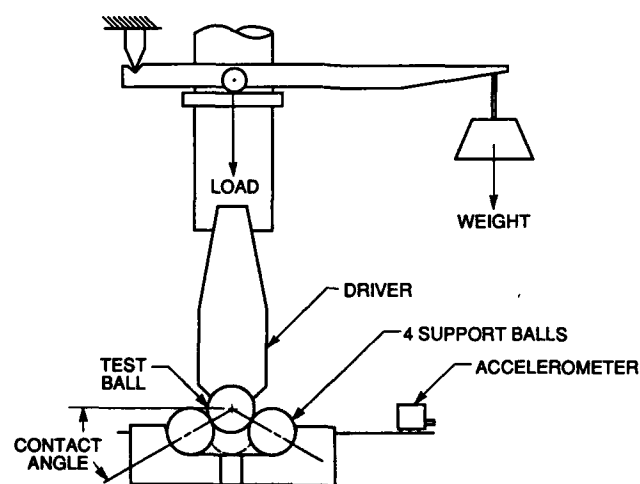


Figure 4. Schematic of Five Ball Testing Apparatus

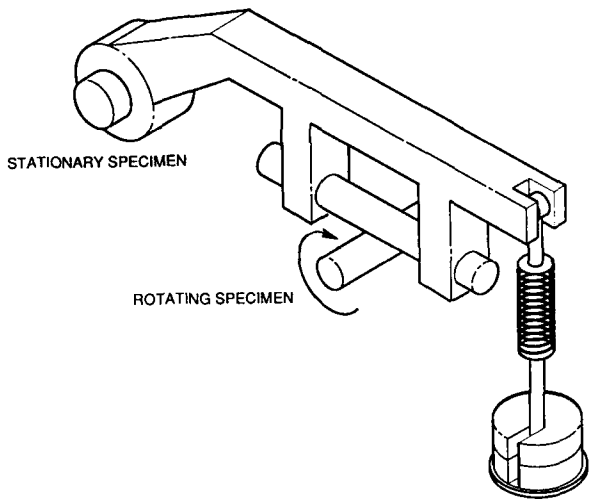


Figure 5. Schematic of Cross-Cylinder Wear Testing Apparatus

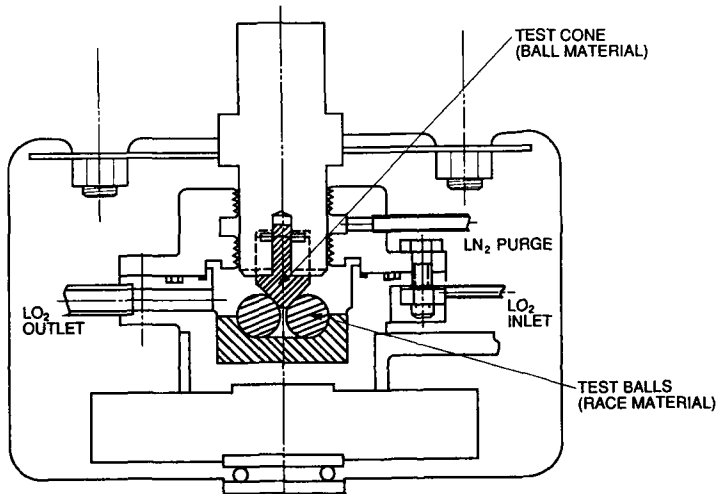


Figure 6. Cone-Three Ball Tester

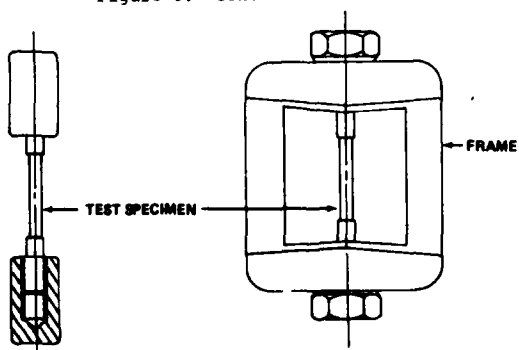


Figure 7. SCC Test Specimen, Frame and Assembly

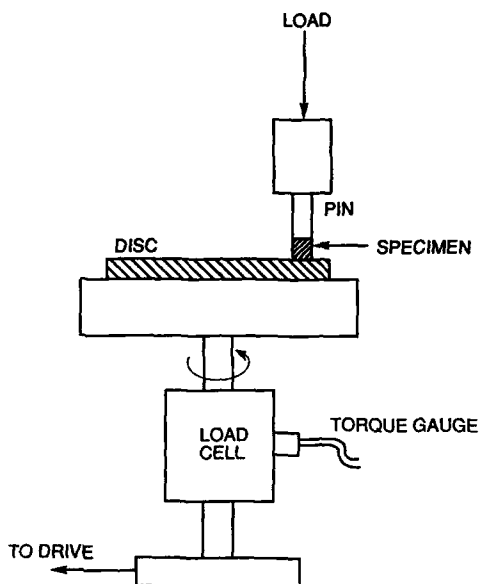


Figure 8. Schematic of Pin-on-Disc Friction Apparatus

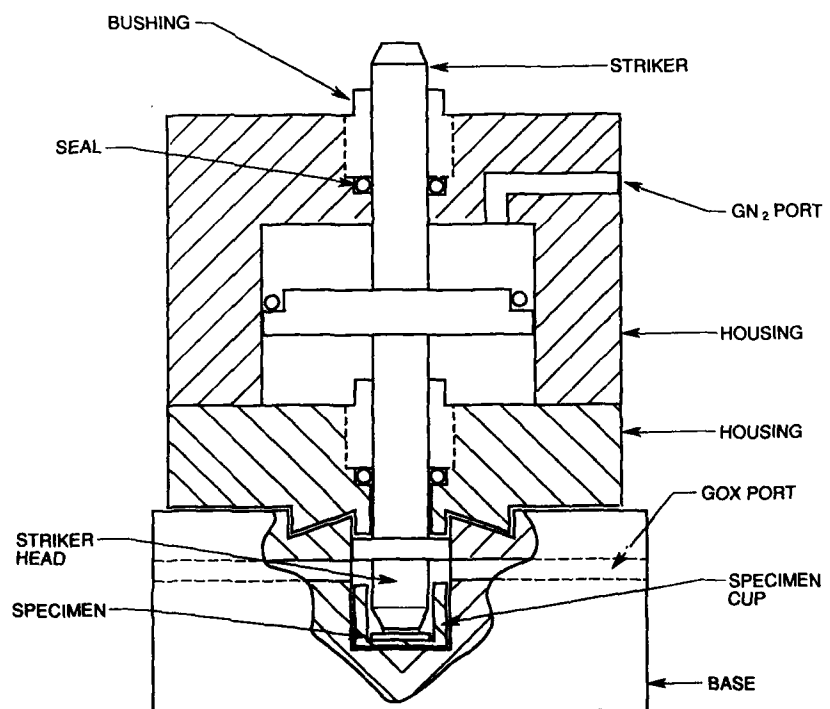


Figure 9. High-Pressure O<sub>2</sub> Impact Test Arrangement

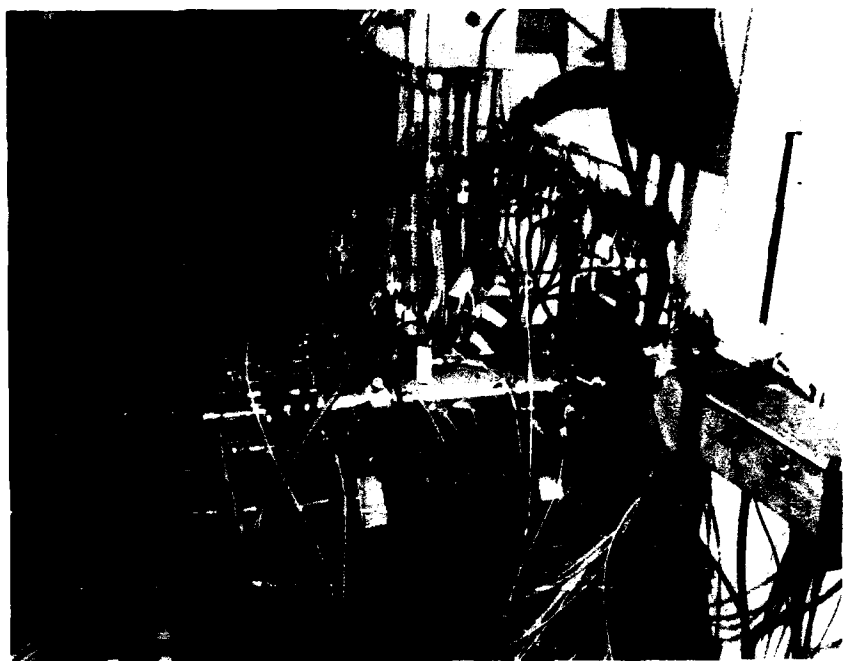


Figure 10. Bearings and Seals Materials Tester

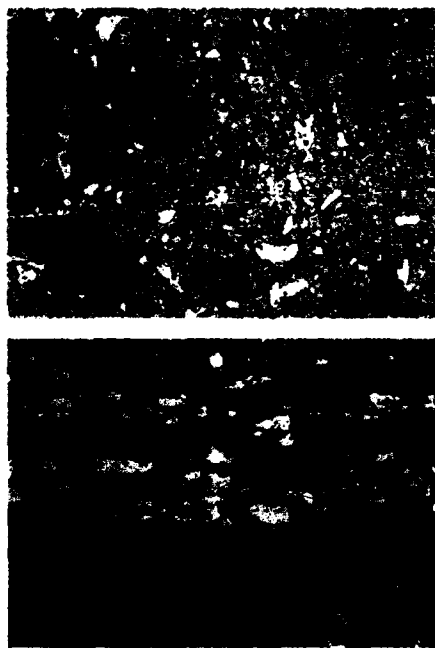


Figure 11. Transverse (top) and Longitudinal (bottom) Sections Taken from the Currently Used 440C Bearing Material. Original Magnification 500X.

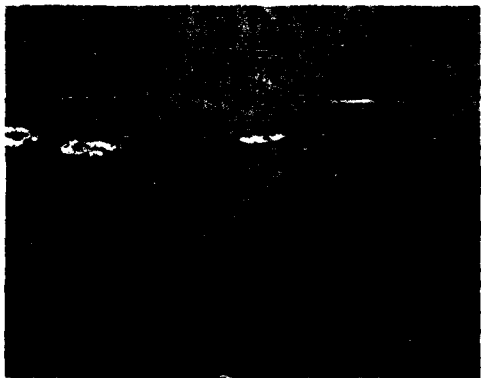
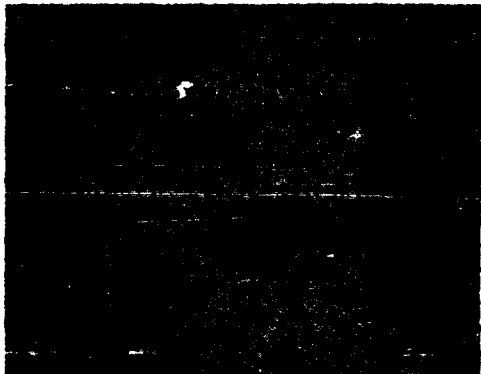


Figure 12. Photomicrographs of Candidate PM Bearing Alloys Being Developed at MSFC. Original Magnification 500X.

### DISCUSSION

R. Kochendorfer, DFVLR, FRG. I wonder why you didn't mention ceramic bearings in your presentation. Silicon carbide bearings and carbon-carbon cages have been fabricated and tested, with potential for some applications and perhaps an advantage in lower friction. Could you comment on that?

B. Bhat, NASA-Marshall, US. We've tested silicon nitride ball bearings and we were hoping for a low coefficient of friction, but we did not get it and were disappointed. There are other considerations too, however, for example such bearings might give us better wear resistance. We don't think we can use silicon nitride races, just silicon nitride bearing balls. That seem's to be where they perform best, and we plan to test them there.

J-M. de Monicault, SEP, France. In your paper you mentioned bronze-filled graphite fiber. Can you tell us about the process used to make that fiber?

B. Bhat, NASA-Marshall, US. The process is proprietary to the vendor, so I really can't comment on it.

E. Campo, Fiat Aviazione, Italy. You mentioned the problem of liquid oxygen compatibility and a test you use that is useful in assessing the compatibility of specific materials. Do you use it as an empirical test or can you correlate your test results with actual service conditions? In your test you have an impact with some fixed energy, but I would think that to simulate service conditions you would include the nature of the debris, operating speed, and so on. Do you have analytical tools for predictions in this area?

B. Bhat, NASA-Marshall, US. I did not have time to cover all of the details in my presentation, but we do vary the energy of the impact. If we start with a 10 kg impact and it passes, then we feel we don't have a problem. If the material doesn't pass that impact, then we go to lower impact levels and find out where it does pass. Then we go back to our application and see how much impact loading we expect on the bearing and use our best judgment.

R. Thamburaj, Hawker Siddeley, Canada. You mentioned that ion implantation is in use now for main bearings in the space shuttle. Can you tell us what the bearing material is and what ion species are used in the implantation?

B. Bhat, NASA-Marshall, US. There are different materials for the bearing and the raceway. I believe the materials are silicon carbide and chromium nitride, but at the moment I don't remember which is which.

R. Thamburaj, Hawker Siddeley, Canada. Also, you mentioned the bearing material M-50 in your paper. There is a modification of that, M-50Nil that is replacing M-50 in some engines at this time. Could you comment on any observations you've made on M-50Nil vs. the M-50?

B. Bhat, NASA-Marshall, US. We're looking at it, but I don't have any information available at the moment. We'd be interested ourselves in knowing if anyone has had any experience with it in actual applications and what their results have been.

**DEVELOPMENT OF AN ASBESTOS-FREE INSULANT  
FOR ROCKET MOTORS**

D. Sanschagrin and G. Couture

Defence Research Establishment Valcartier  
2459, Pie IX Blvd., North (P.O. Box 8800)  
Courchelette, Quebec  
Canada, G0A 1R0

As a result of concerns about restrictions on the industrial use of asbestos, DREV initiated a research project aimed at replacing asbestos in the rocket motor insulant designated RF/B. RF/B is a polymer composite consisting of a carboxyl-terminated polybutadiene filled with asbestos. While retaining the same polymeric resin, a combination of fibers (Kevlar, Refrasil and Pyron) and fillers (kaolin and Mg(OH)<sub>2</sub>) was used to obtain formulations compatible with the processing of RF/B, which is based on the use of a sigma-blade mixer and two-roll mills. The mechanical properties of the new material and its suitability in CRV7 rocket motors were assessed.

**BACKGROUND**

In the late 1960s, DREV developed a laminated insulant for solid rocket motors made up of 70% asbestos solids and 30% butadiene binder (Ref. 1). Since then this insulant, designated RF/B, has been used successfully in the RDT&E, MDSS, CL289, Black Brant and CRV7 rocket. However, since the early 1980s, its use has been brought into question because of the health hazards associated with asbestos. Specifically, it was feared that regulations governing the use of asbestos would become more stringent, thus driving up its cost (or preventing its use altogether) and that the presence of asbestos would restrict export sales of Canadian rocket motors. Consequently, in 1982, DREV initiated a project to develop a replacement insulant containing non-toxic fillers.

**TECHNICAL REQUIREMENTS**

The primary application for the new insulation is as a replacement for RF/B in the CRV7 rocket motor (Ref. 2). It was therefore decided that the processing (mixing and laminating operations), installation and mechanical properties of the new insulant should resemble as closely as possible those of RF/B in the CRV7. The only significant difference would be the type and amount of solid fillers in the insulant itself.

The formulation of RF/B is shown in the third column of Table I. The binder consists of the carboxyl-terminated polybutadiene HC-434 and the multifunctional epoxy Araldite MY 0510; iron octoate is used as curing catalyst. This polymeric mixture is filled with two grades of asbestos, which are in the form of fibers and floats.

The solid charge is dispersed into the resin according to the sequence described in Figure 1. First, the ingredients are mixed in a double-arm sigma blade mixer and the resultant dough is cured for approximately two hours at 60°C. The cured material is then mixed further by means of a differential speed two-roll mill. Finally, when the dough no longer sticks to the rolls, the material is passed through another two-roll mill to form insulant sheets; this last step is called laminating. The flexible, self-adhesive RF/B sheet covered with an aluminum foil liner is bonded to the casing using a pressurized rubber bag. During this operation, the temperature is maintained at 60°C and pressure at 900 kPa. Shredded RF/B is also compression-moulded at room temperature to produce the head-end insulator.

The mechanical properties of the material should comply with the requirements shown in Table II (Ref. 3). The aging periods appearing in this table correspond to meaningful intervals during the manufacturing of CRV7 motors. The one-hour period corresponds to the duration of the bonding process for the insulant-to-casing bond. The 5-day period is the length of time required to cure the propellant. It should be pointed out that these mechanical properties were established from numerous experimental results obtained with RF/B and are not the result of structural integrity calculations.

Since the tensile test and the bond test are non-standard, they will be described briefly. The former consists of stretching insulant samples (2.5 cm x 10 cm x 0.6 mm) in an Instron machine at a crosshead speed of 10 mm/min. Since the fibers contained in the insulant are not randomly oriented due to the action of the roll mills, the tensile test is carried out in two directions: machine direction, which is in the same direction as the rolls motion, and cross machine direction. For the bond test, the insulant is first

punched into discs and the test specimens are then prepared by pressing the samples between two aluminum cylinders ( $9.0 \text{ cm}^2$ ) at a pressure of 900 kPa for 1 h at  $60^\circ\text{C}$ . The test is carried out at a crosshead speed of 5 mm/min.

TABLE I  
Insulant Formulations

Ingredient (Grade)	Manufacturer	Formulation (%)			
		RF/B	1005	1175	1279
Binder as below	Johns Manville Johns Manville Du Pont Company Evans Clay Company Armco Inc. Stackpole Fibers Co. Anachemia Canada (1)	30	43	40	30
Asbestos fibers (3412)		52.5			
Asbestos floats (7TFL)		17.5			
Kevlar 29 (dry pulp type 979)			20	10	8
Kaolin (Snobrite)			20	33.5	44
Refrasil (F-100-A-25)			17		
Pyron (1/2-inch cut fibers)				15	8
Mg(OH) <sub>2</sub> (AC-5544)				1.5	10
Water (on a dry-weight basis)				1.0	0.5
Polybutadiene (HC-434)					
Epoxy (Aralidite MY 0510)	Thiokol Corporation CIBA-GEIGY Corporation Nuodex	94.1	93.1	94.0	94.0
Iron octoate (iron 6%)		4.9	4.6	4.8	4.8
		1.0	2.3	1.2	1.2

(1) Supplier

TABLE II  
Mechanical Properties Requirements of the RF/B Insulant at  $20^\circ\text{C}$

Aging period at $60^\circ\text{C}$	Tensile test				Bond to aluminum (MPa)
	Machine direction $\sigma_m$ (MPa)	$\epsilon_m$ (%)	Cross-machine direction $\sigma_m$ (MPa)	$\epsilon_m$ (%)	
1 h	0.55	10	0.35	20	1.0
5 days	4.5	5	2.2	10	1.7

$\sigma_m$ : Maximum tensile strength  
 $\epsilon_m$ : Elongation at maximum tensile strength

#### PRELIMINARY SCREENING

The preliminary screening tests consisted of an evaluation of more than 100 formulations that included various combinations of fibers and fillers; these ingredients are presented in Table III. This initial study was oriented towards defining the composition of the solid charge required to match the processing characteristics of RF/B, adjusting the curing catalyst content, and evaluating the mechanical properties.

TABLE III  
Ingredients Investigated During Preliminary Screening

Fibers	Kevlar 29 Refrasil Saffil Fiberfrax Fiberglass Pyron	Aromatic polyamide fibers Silica fibers Alumina fibers Aluminum silicate fibers Glass fibers Heat stabilized polyacrylonitrile fibers
Fillers	Kaolin, Mg(OH) <sub>2</sub> , talc, mica, TiO <sub>2</sub> , ZnO, magnesium, and ZrSiO <sub>4</sub>	

It quickly became apparent during the preliminary screening tests that predicting the curing periods of the new formulations was a problem. The insulants were passed through the differential speed roll mill on a trial-and-error basis until they came off the rolls easily; in some cases the insulants were taken out of the oven for laminating too late and became too brittle and consequently useless. In order to overcome this drawback a Shore-A durometer was used to determine the state of cure of the insulants; the higher the Shore-A hardness, the more vulcanized the insulant. Readings were taken on an insulant sheet obtained from the first pass on the differential speed roll mill. Afterwards the hardness was evaluated on a regular basis (without any additional laminating) until it reached approximately 45, which is a typical value obtained with the standard RF/B.

With time, the curing periods of the preliminary formulations started fluctuating, all things being apparently equal. After completion of an investigation concerning the nature of the different ingredients used in these formulations, it was discovered that Kevlar, as shipped, contained absorbed moisture to prevent the accumulation of a high static electricity charge during handling. In addition, the evaluation of Kevlar moisture content using a Mettler LP 15 infrared dryer revealed significant differences from one bag to another. As a result, a series of batches was made to isolate the effect of these variations on the curing period. These tests demonstrated that the curing period was inversely proportional to the moisture content of the Kevlar. Thus driving off the moisture led to reproducible results. Even though lots of Kevlar were more susceptible to variations in moisture content than any other materials, it was decided to dry all the solid ingredients, fibers as well as fillers, to ensure that moisture-related problems would not reoccur. To this end, all the solid ingredients were brought to a close-to-zero moisture content by conditioning at 100°C for 15 h (overnight).

#### INITIAL OPTIMIZED FORMULATION

After completing the preliminary screening, the formulation exhibiting the best overall results, formulation 1005 (see Table II), was chosen for a more complete evaluation. The latter included the determination of its long-term mechanical properties, evaluation of its performance in live motor firings, and scale-up in industry. Compared to RF/B the solid charge of formulation 1005 is lower, whereas the curing catalyst (iron octoate) content is more than twice as high. The change in solid charge is due to the low densities of Kevlar and Pyron, which are respectively 1.44 and 1.35 g/cm<sup>3</sup>; the density of asbestos is about 2.5 g/cm<sup>3</sup>. The replacement of asbestos reduced significantly the curing rate of the material. In spite of conditions that would normally speed up the curing rate, namely a higher iron octoate content and a higher curing temperature, the curing period of formulation 1005 was still 1.25 h longer than that of RF/B (see Table IV).

The mechanical properties of formulation 1005 are presented in Table V. The one-hour aging test mentioned in the requirements was replaced by an evaluation of the material obtained immediately after laminating. This was done because the mechanical properties of this fresh material do not change significantly after one hour.

TABLE IV  
Insulant Characteristics

Characteristics	Formulation			
	RF/B	1005	1175	1279
Curing temperature (°C)	60	71	82	92
Curing period (h)	2	3.25	2.25	1.00
Density (g/cm <sup>3</sup> )	1.688	1.26(1)	1.328	1.52(1)

(1) Calculated density

All the requirements were met except the elongation of the fresh material in the machine direction. Since the mechanical properties of the asbestos-free insulants were on occasion inferior to those of RF/B, especially in terms of elongation, a structural integrity analysis was carried out based on linear-elastic and thin-walled cylinder theories. Thermal and pressurization loadings were considered. Mechanical properties were calculated in the hoop direction, which experiences the greatest stresses. According to the analysis the minimum tensile strength required is 841 kPa and the minimum elongation is 0.4%. Therefore, even if the mechanical properties of formulation 1005 did not match those of RF/B, they were nevertheless sufficient for the CRV7 application.

Six CRV7 rocket motors insulated with formulation 1005 and loaded with a low smoke propellant were static-fired. Two were fired at room temperature while the others were submitted to thermal shock cycling (5 cycles, -54°C to 65°C); of these, two were fired at -54°C and two at 65°C. According to X-ray examination, the thermal shock treatment did not damage the insulation of the motors.

TABLE V  
Mechanical Properties of Experimental Formulations

Formulation	Aging period at 60°C	Machine direction σ <sub>m</sub> (MPa)	Machine direction ε <sub>m</sub> (%)	Cross-machine direction σ <sub>m</sub> (MPa)	Cross-machine direction ε <sub>m</sub> (%)	Bond to aluminum (MPa)
1005	Fresh material 5 days	1.8 5.2	9 8	0.49 2.2	21 22	-- 3.7
1175	Fresh material 5 days	0.91 9.4	9.5 4.0	0.19 1.6	31.2 9.0	-- 2.6
1279	Fresh material 5 days	3.2 11.9	6.8 3.7	1.0 5.1	22.8 6.1	-- 4.6

σ<sub>m</sub>: Maximum tensile strength

ε<sub>m</sub>: Elongation at maximum tensile strength

Although tests conducted in another study revealed that this asbestos-free insulant did not match RF/B in terms of resistance to erosion, formulation 1005 successfully withstood the conditions prevailing in the CRV7 motor during firing and there was no evidence of excessive erosion in any of the fired motors.

At the end of 1983 DREV provided Bristol Aerospace Ltd (BAL) with a data package for asbestos-free insulants in which formulation 1005 was selected for full scale evaluation. BAL processed several batches of insulant and lined a number of CRV7 motors with the formulation. They concluded that the formulation was unacceptable because it was impossible to process without tears and holes in the finished sheets and because of separation in filled motors between the insulant and aluminum foil liner. As a result of these problems, DREV undertook a project to improve the insulant formulation and processing.

#### IMPROVEMENT OF INSULANT PROCESSING

The processing problems encountered during the full-scale evaluation were closely related to the binder system, to which a large amount of curing catalyst had to be added to maintain a reasonably short curing period. This behaviour was related to the chemical structure of asbestos. Since the chrysotile type asbestos used in RF/B was known to be covered with layers of brucite (Ref. 5) or magnesium hydroxide, Mg(OH)<sub>2</sub>, the latter was introduced into formulations. The brucite also accelerated the curing rates, but only in the presence of water; as a result, a given amount of water was added directly into the polymer. Based on formulation 1175, shown in Table I, a series of batches was made varying the Mg(OH)<sub>2</sub> and water contents. The quantity of Mg(OH)<sub>2</sub> was increased at the expense of the amount of kaolin, whereas the amount of water was determined on a dry-weight basis.

These tests showed that the addition of water and Mg(OH)<sub>2</sub> did not affect the mechanical properties of the insulant. Therefore, both ingredients can be used to adjust curing rates without adversely affecting the material. Figure 2 shows combinations of water and Mg(OH)<sub>2</sub>, yielding identical curing periods. The 2-hour curve corresponds to the target values, and the 0-hour curve represents the boundary beyond which the material is too hard to be laminated and becomes brittle. The main effect of the introduction of Mg(OH)<sub>2</sub> and water, aside from the faster curing rates, was a decrease in the hardness required for laminating. Consequently, the resulting material was easier to process. In formulation 1175, Refrasil fibers were replaced by Pyron fibers to alleviate a problem which occurred when softer materials were processed. During laminating these materials had a tendency to form air pockets located on the surface.

In addition to changing the binder system, the mixing cycle was modified because the Kevlar formed agglomerates in the insulant sheet. This is because that dry Kevlar fibers tend to cling together and are difficult to wet with the polymer. To obtain a better dispersion of Kevlar fibers the period of time allowed for the mixing of Kevlar and the binder was extended till all the fibers were wetted; the entire step required fifteen minutes. Since the agglomerates prevented all the fibers from acting as reinforcement, their elimination permitted us to reduce the Kevlar content, which in turn improved wetting by increasing the polymer to Kevlar ratio. Therefore the total amount of fibers in formulation 1175 is lower than that of formulation 1005.

The mechanical properties of formulation 1175 are shown in Table I. Even though they do not match those of RF/B, they are nevertheless beyond the calculated requirements presented in the previous section. The introduction of the new binder system made formulation 1175 behave like RF/B. Compared to formulation 1005, this translates into larger differences between the mechanical properties of 5-day-aged material and fresh material. These fluctuations indicate that the insulant can be laminated when its stage of cure is less advanced; in other words, this material needs little curing time to gain enough cohesion to be converted into sheets in the roll mill. The new binder system imparts a better shelf-life to formulation 1175. The bond strength to aluminum remains steady even after a 56-day storage period at -15°C.

In order to complete the evaluation of formulation 1175, CRV7 rocket motors were insulated. Once in place, however, the insulant exhibited bumps, as shown in Figure 3. When the sheet was removed from the motors, most of the bumps proved to be separations between the casing and the insulant sheet. These bumps appeared either immediately after removing the pressure bag or very slowly afterwards.

#### STUDY OF BUMP FORMATION

To determine if the problem of bumps was associated with the generation of gases within the insulant, a vacuum stability test was performed. A 5 g shredded sample was maintained at 100°C for four days; the material was shredded to increase the surface area. It should be pointed out that these conditions are severe compared to those taking place while insulating a rocket motor. In the latter instance the material is maintained at 60°C for one hour only. Extreme conditions were chosen during the test for the purpose of amplifying the amount of gas released.

The gaseous compounds obtained were analysed by infrared spectroscopy. Figure 4 shows the infrared spectrum of formulation 1175 superimposed on that of RF/B. These spectra present only sharp absorption bands: carbon dioxide at 2300 and 3700  $\text{cm}^{-1}$ , carbon monoxide at 2100  $\text{cm}^{-1}$ , and water at 3400 and 1650  $\text{cm}^{-1}$ . Since both the standard RF/B and formulation 1175 give off  $\text{CO}_2$ , its presence cannot explain the formation of the bumps. As well, the carbon monoxide bands are negligible compared to the  $\text{CO}_2$  bands and can be ignored. The major difference is the presence of strong water absorption bands for formulation 1175. This situation is consistent with the fact that water is a constituent of the new composition. However, this water is an essential ingredient of the binder system, and there is no way of eliminating it without degrading the processing of the insulant. Nonetheless, it was decided to reduce the water content as much as possible in order to diminish the influence that water could exert on the material, especially during aging. Notwithstanding the evolution of water vapour during the vacuum stability test, it was concluded that the bumps could not be due to gas produced by incompatibility between the ingredients in the insulant.

Because of the Kevlar agglomerates encountered previously, a few attempts were made to improve the homogeneity of the dough. It was thought that some other ingredients could be unevenly dispersed, thus producing a non-uniform distribution of the stresses in the material. Periods of mixing were extended, and the dispersion step using the differential roll mill, was performed immediately after mixing. Of these two modifications, the latter gave the best results in terms of homogeneity. After mixing, the dough is still soft which facilitates dispersion of the solid charge; moreover lamination can be extended.

Many other modifications were made to the new insulant system. For instance, the installation conditions were altered. Bonding pressures ranging from 150 to 900 kPa were used, the curing temperature was varied from 20 to 60°C, and finally the length of time under pressure was extended to 3 days. Furthermore, the stiffness of the insulant itself was changed, either by increasing its hardness through longer post curing periods or by increasing its solid charge. To help incorporate the extra solid charge, modifications were made to the mixer to increase its efficiency. A teflon piston was positioned above the blades of the mixer to force the ingredients down into the dough. Formulation 1279, shown in Table I, was made using this technique. It should be pointed out that the  $\text{Mg(OH)}_2$  content was increased to 10% in order to reduce the amount of water. The calculated density of formulation 1279 is 1.52  $\text{g/cm}^3$ , which approaches 1.69  $\text{g/cm}^3$ , the density of RF/B. Unfortunately, while many of these modifications resulted in a better, more homogeneous sheet of insulant, none eliminated the bumps when the sheet was installed in the rocket motor. We therefore turned our attention to the installation procedure itself.

In order to better understand the way the bump formed, the insulant surface was examined using a scanning electron microscope at a magnification of 540X. Figure 5a is a photograph of a fresh insulant sheet prior to installation, and 5b shows another one which was removed from a motor. In this latter case, the photograph shows the internal surface of one bump, i.e. the surface between the insulant and motor casing. On average the surface of the fresh material has a smooth finish. However the sheet exhibits holes, as shown in Figure 5a. Since fresh RF/B contains similar perforations, they probably form because of the action of the roll mills. In opposition to the fresh insulant sheet, that removed from the motor (Fig. 5b), is characterized by a jagged surface. The lighter zone in the photograph represents one particular area where the insulant was stretched. These photographs suggest that the material initially adheres to the casing and gradually starts to come off the wall to produce the bumps. It should be pointed that the bumpy surface does not exhibit any signs of chemical degradation. To explain these phenomena, it was hypothesized that air was entrapped during the installation process and prevented the material from bonding to the casing. Once the pressurized rubber bag was removed, the insulant could then deform freely and detach from the casing. Such an hypothesis is reasonable since the 1-meter long rubber bag pushes the insulant over the entire length of the casing wall simultaneously, thus ensuring the entrapment of some air.

Based on this assumption, two groups of six motors were insulated under vacuum with formulation 1279 in the following manner. The insulation sheets, wrapped around the unpressurized rubber bag, were inserted into the motor casing. The casing were then placed, one at a time, in a 1.5-meter high vacuum bell. The vacuum was drawn in the rubber bag first, and then in the motor. Thereafter the rubber bag was inflated to the

standard insulation pressure, and the motor was maintained under pressure for one hour at 60°C. After curing, there were no bumps in the surface of the insulation. It was therefore concluded that the bumps were due to the entrapment of air during the installation process.

#### CONCLUDING REMARKS

A new asbestos-free insulant for rocket motors has been developed. The processing and installation are slightly different from that of the original RF/B: the water content of the ingredients has to be precisely controlled to obtain reproducible curing periods, and the length of the mixing cycle and lamination must be extended to better disperse the solid charge into the polymeric matrix. The new insulant must be installed under vacuum to prevent entrapping air between the insulant sheet and motor casing wall.

Future work will involve testing a vacuum adaptor for individual motors which will permit higher production rates, and humidifying the solid ingredients in an environmental chamber prior to mixing to control the moisture content more precisely. Notwithstanding these two minor modifications, the new formulation and installation methods are ready for transfer to industry.

#### REFERENCES

1. Ratté, J. and Bigras, J., DREV, Development of Roll-Formed Type B Insulants for Rocket Motors, 1969, R-607/69.
2. Jackson, F., et al., An Improved Canadian 2.75-Inch Rocket Motor, Canadian Aeronautics and Space Journal, Vol. 24, No. 1, January/February 1978.
3. Bristol Aerospace Limited, Specification for Rollform Butadiene, 1981, ER 73553/B.
4. Lazar, J., Bristol Aerospace Limited, Final Report Asbestos Substitution in RF/B, 1985.
5. Nadeau, R., L'amiante, 1st ed., Quebec, Grammatika inc., 1986, p. 37.

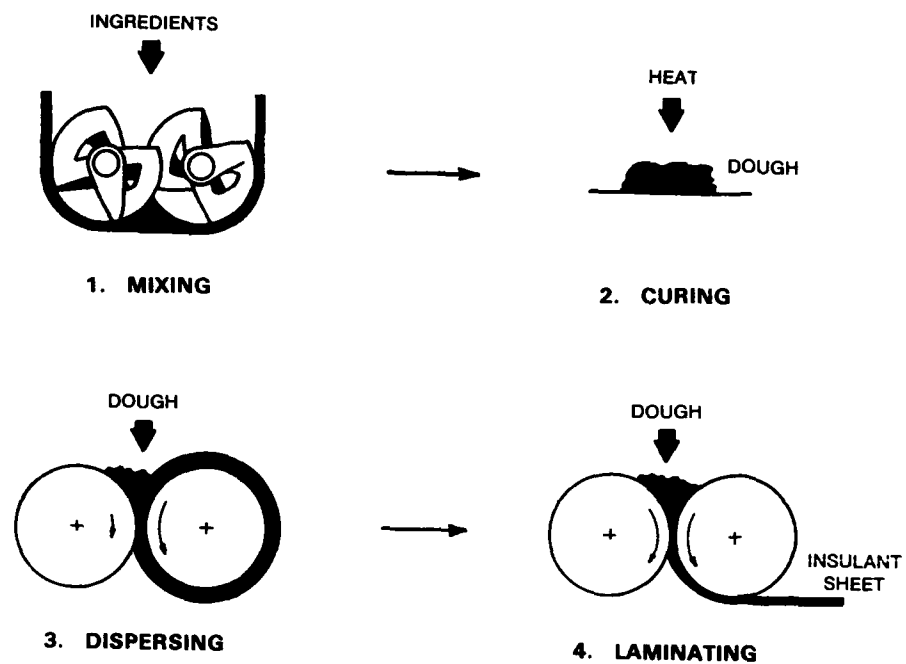


FIGURE 1 - Processing of RF/B

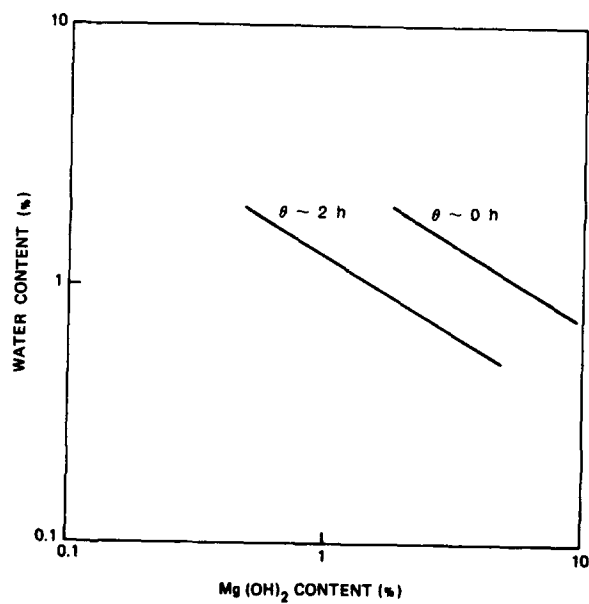
FIGURE 2 - Combinations of water and Mg(OH)<sub>2</sub> yielding similar curing periods ( $\theta$ ) based on formulation 1175



FIGURE 3 - Inside wall of an insulated CRV7 casing exhibiting bumps

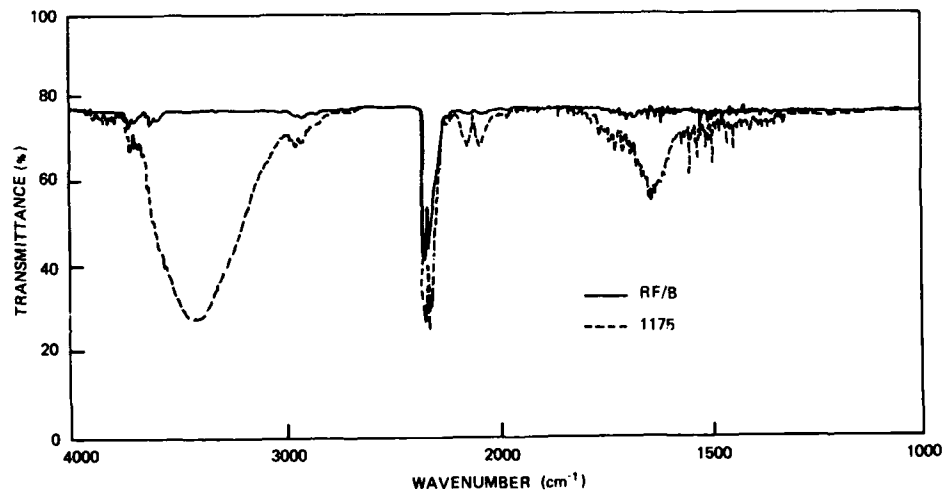
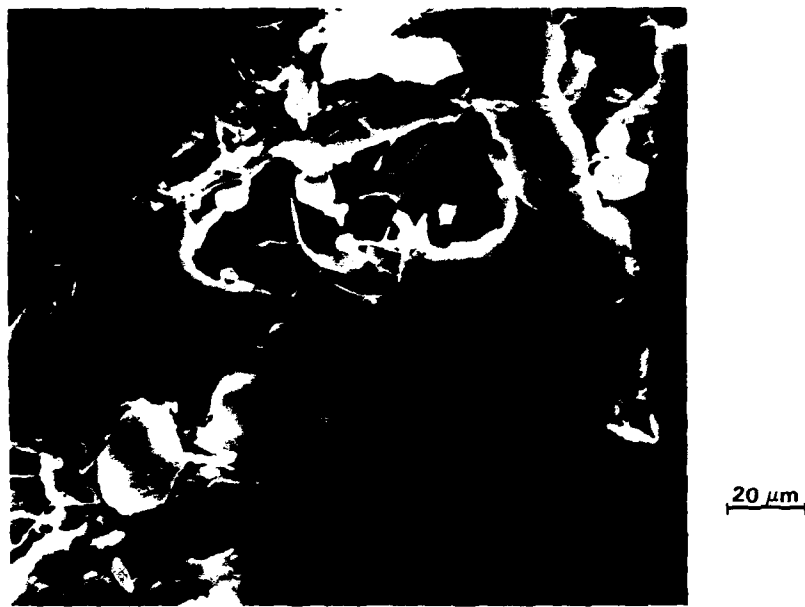
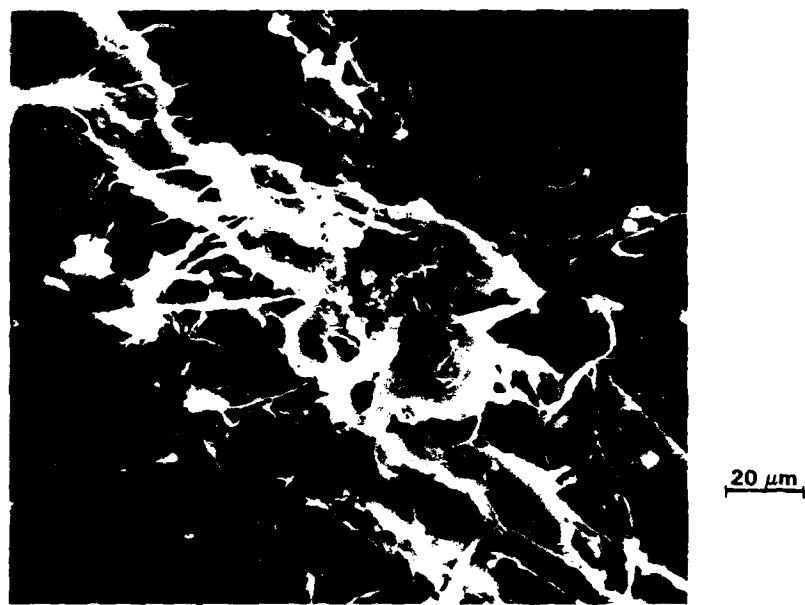


FIGURE 4 - Infrared spectra of RF/B and formulation 1175



a) fresh insulant sheet prior to insulation



b) internal surface of one bump

FIGURE 5 - Scanning electron micrographs

**DISCUSSION**

R. Pickering, Royal Ordnance, UK. Have you carried out a similar program to replace asbestos fiber in rigid ablative phenolics?

D. Sanschagrin, Defense Research Establishment, Canada. No, we have not.

## METALLURGICAL STUDY OF SUPERALLOY BRAZING ALLOYS

Ch. Lecomte-Mertens  
C.R.M.  
Rue E. Solvay, 11 - B 4000 Liège  
  
W. BEX, Chef de Service  
FN Moteurs  
Route de Liers, 121 - B 4411 Mimont  
BELGIUM

### ABSTRACT

For a better understanding of the new superalloy repair or joining process, it is important to know the metallurgical behaviour of more conventional brazing alloys more or less doped with melting point depressants such as aluminum boron and/or silicon especially during the diffusion-brazing treatment.

Therefore, the brazing results on calibrated slots of different widths were metallographically compared after variable brazing and diffusion time-temperature cycles. The composition of the different phases present in the tested brazing alloys were also determinated with the scanning electron microscope

Moreover, evaluation testings as fatigue and thermal shocks were performed to compare new and repaired parts.

Finally, it was possible to evaluate the best time-temperature cycles bringing a satisfactory homogenisation, while keeping them compatible with the eventual subsequent heat treatments and with the requirements of an economical industrial production.

### INTRODUCTION

Study and design of new turbine parts are conducted during the engine development phase in order to achieve optimized performances and to insure the longest life as possible. In this respect, designers have to deal with parameters such as material composition, microstructure, heat treatment, protective layers, shape, etc... which will give the best behavior of the materials at high turbine temperature. Consequently, it is obvious that at the beginning of its life, each part represents the best possible compromise for all parameters. Later, during service condition, parts are subject to deterioration. For example, the hot section of a gas turbine is the most highly stressed part of the machine and the turbine components suffer from different kinds of damages. Consequently, the part which was initially optimized, has lost that advantage and is now life limited, which depends mostly on operating conditions. Replacement costs of such components are very high and this encourages the practice of repairing the original parts to extend their life. Moreover, strategical reasons become more and more important.

The damages caused to the metal can be divided into two groups : internal and external damages. As internal damages, we can understand structural microscopic damages inherent to superalloys at high temperature : carbide degeneration, unwanted phase formation, gamma prime coarsening, creep... External damages are geometrical degradations caused by low cycle fatigue, foreign object, corrosion, erosion, thermal shocks...

The external type of damages can be repaired by welding or brazing techniques. The welding of superalloys has some well known limitations, such as high susceptibility to hot cracking, postweld heat treatment cracking etc. Diffusion brazing obviates those phenomena and has moreover many advantages. The most important are :

- the brazing cycle can combine external crack healing with internal damage rejuvenation.
- the repair is theoretically superior to welding in that thermal stresses and distortions are avoided.
- the fine cracks, which may not have been identified during a typical inspection cycle, would have been healed by applying surplus filler metal around the primary cracks.
- the parts could also be batch processed, which leads to unit cost reduction.

The study reported in this paper, undertook to examine the metallurgical phenomena occurring when brazing IN 792 or HA 188 superalloys with different filler metals.

The aim was to determine the maximum gap which could be brazed with satisfaction. Furthermore, the time-temperature brazing cycles and their influence on the result were investigated.

### EXPERIMENTAL PROCEDURE

#### 1. Specimen preparation

Two types of superalloys were used as base metal to fabricate the test pieces. The first one is IN 792, a nickel base alloy and the second one is HA 188, a cobalt base

alloy. The former was cut from cast piece and the later from sheet metal.

The thickness of the specimens is 1.5mm. Three slots were electrodischarge-machined in each test piece. All are 25mm long but have a width of respectively 0.36, 0.52 and 0.75mm.

After machining, the specimens were vapor degreased, nitric-hydrofluoric acid cleaned, then either H<sub>2</sub> treated (for HA 188) or fluoride treated (for IN 792). Both heat treatments were conducted at 1080°C for one hour with a cooling rate equivalent to a forced air cooling. Finally, the specimens were acetone degreased just prior to brazing.

## 2. Brazing

The nominal chemical compositions of the base metals and of the brazing filler metals are given in table I

TABLE I - Nominal chemical compositions

Alloy	C	Si	Cr	Ni	Co	Mo	W	Ti	Al	B	Zr	Fe	Ta	Hf	La	Y
IN 792	0.14	-	12.7	bal	9	2	4.2	4.1	3.4	0.015	0.05	-	4.2	1.0	-	-
HA 188	0.08	-	22	22	bal	-	14	-	-	-	-	1.5	-	-	0.08	-
DF4a	-	-	14	bal	10	-	-	-	2.7	-	-	2.5	-	-	0.02	-
DF4b	-	-	14	bal	10	-	-	-	3.5	2.7	-	-	2.5	-	-	0.02
S57a	-	-	25	10	bal	-	-	-	2.5	3	-	-	5.0	-	-	0.25
S57b	-	3	21	10	bal	-	-	-	2.5	3	-	-	5.0	-	-	0.2

Differential thermal analysis (DTA) of the brazing metals yielded melting ranges as listed below in table II.

TABLE II - Second heating DTA

Alloy	Solidus (°C)	Liquidus (°C)
DF4a	1057	1112
DF4b	1064	1122
S57a	1133	1211
S57b	1046	1128

From these data, the braze schedules given in tables III and IV were constructed.

The brazing was performed in a vacuum furnace at about 10<sup>-4</sup> to 10<sup>-5</sup> torr according the cycle illustrated at Fig.1. The specimen is flat in the furnace with the brazing paste downside.

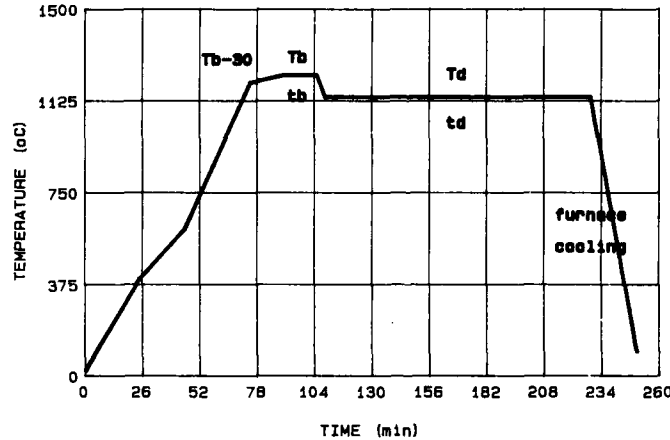
TABLE III - HA 188 Brazing parameters

Cycle Nr.	Filler metal	Brazing temperature liquidus T° +	Holding time	Diffusion temperature solidus T° -	Holding time
1		30°C	15'	10°C	3h
2	S57 a			20°C	3h
3		60°C	15'	10°C	3h
4				20°C	3h
5		30°C	15'	10°C	3h
6				20°C	3h
7		60°C	15'	10°C	3h
8	S57 b			20°C	3h
9		90°C	15'	10°C	3h
10				20°C	3h
11				-	-
12		60°C	15'	10°C	18'
13				10°C	30h

TABLE IV - IN 792 Brazing parameters

Cycle Nr.	Filler metal	Brazing temperature liquidus T° +	Holding time	Diffusion temperature solidus T° -	Holding time
14	DF4 a			10°C	
15	DF4 b	30°C	15'		3h
16	DF4 a			20°C	
17	DF4 b				3h
18	DF4 a			10°C	
19	DF4 b	60°C	15'		3h
20	DF4 a			20°C	
21	DF4 b				3h
22	DF4 a			10°C	
23	DF4 b	90°C	15'		3h
24	DF4 a			20°C	
25	DF4 b				3h
26				-	-
27	DF4 a	60°C	15'	10°C	18'
28				10°C	30h

After brazing, each specimen was sectioned perpendicularly to the middle of the brazed slot. Microstructural examinations were conducted with the optical microscope and the scanning electron microscope (SEM). Phases containing the various constituents of the braze alloys were identified using EDAX or X-ray mapping.

Figure 1 - Brazing cycle

#### RESULTS AND DISCUSSION

Typical results are shown in fig.2 where the four brazes are illustrated. It can be seen that these results are quite different in shape of the gap, diffusion zone, or microconstituent distribution. But it is also interesting to know that visual inspections performed before microscope examinations revealed that the widest slot always showed random material filling on the length.

The optical micrographs show at figure 2 that S57b braze with silicon as melting point depressant has a well defined interface. This is not the case for S57a braze where the braze-base metal transition is not so evident. This phenomenon increases more with the

brazing temperature than with the diffusion temperature. In fact, rapid diffusion of the smaller interstitial atoms occurs during heating to the brazing temperature. Silicon, although of relatively small atomic radius, does not diffuse as rapidly as boron, and takes place with the formation of intermetallic and solid solution (see S57b).

In the nickel base alloy IN 792, the DF4a joint is better defined than the DF4b. Moreover, longer and higher dwell times and temperatures result in better homogenisation in DF4b-IN 792 interface. That is not so true for the DF4a braze even with 30 hours diffusion. The explanation is easy : the DF4b braze has a chemical composition closer to IN 792 than that has the DF4a braze.

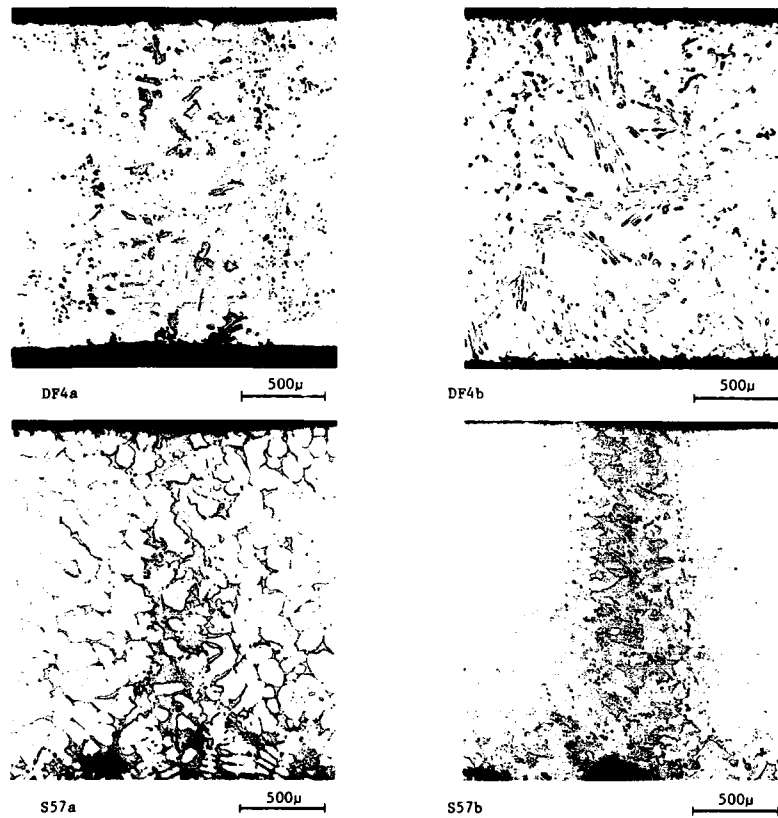


**Figure 2** Optical metallographies - (initial gap : 0,36 mm)

Joints brazed with different brazing temperatures showed significantly different widths. In other words, the base metal dissolves in molten braze and simultaneously, the molten braze penetrates into the base metal and the interface is displaced into solid. This phenomenon is enhanced by the temperature. Thus, it was interesting to establish a relationship between the brazing temperature and the width of the melted zone. The filler metal-base metal interfaces were determined on optical microographies : the metallographic examinations showed the presence in the joint of different intermetallic phases. The distance between the most external points of these phases was defined as the melted zone. Thus, those measures are plotted in fig.3 versus the temperature over the filler metal liquidus. This figure 3 shows that an increase of brazing temperature results in an increase of melted gap and a parabolic relationship was fitted on these data with a very good degree of confidence.

The difference between the structure of the two cobalt brazes is illustrated at Fig.4. Contrary to the S57a braze where the dendritic phase is more important, the S57b braze offers a more eutectic structure which coalesces when the diffusion time increases. This coalescence is more important between 0 and 18 minutes than between 18 and 1800 minutes (Fig.5). The electron microscopy and the energy dispersion analysis (EDAX) show the presence of at least three different microstructure components in both brazes : the Co-Ni-Cr solid solution, the chromium + tungsten carbides and the tantalum rich carbides.

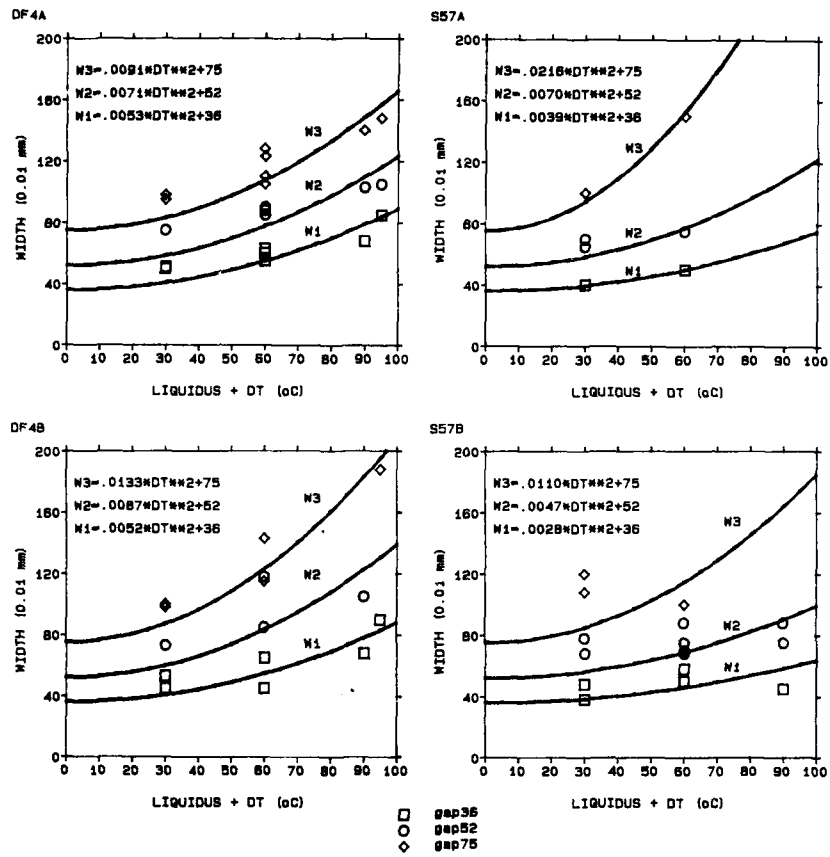


Figure 3 - Parabolic fitting on brazing results

In the silicon containing S57b braze, a fourth phase was observed, which appears brighter on a back scattered electron image. Cobalt, chromium, tungsten and silicon are present in this phase. The concentration of silicon was found to have decreased and that of tungsten to have increased when the diffusion time has increased.

The influence of the brazing temperature is shown by the nickel braze alloy microstructure : more this temperature increases, better is the homogeneity of the microstructure which seems to be a eutectic mixture of a number of phases (Figs.6,7). In both brazes, four microstructure constituents were identified by EDAX analysis combined with BSE images. The two first are gamma solid solutions Ni 70%, Co 10%, Cr 10% for the darker which also contains 4% aluminium in DF4b braze. The two other identified components are (Ta, Ti, Hf) carbides in white and, in black, chromium carbides. In comparing figure 6 to 7, we can see the difference of microstructures between the two nickel braze alloys, DF4b shows more homogeneity and is not underlined as DF4a at the braze-base metal interface by gamma layer which may soften the joint (see also fig.2). For these metallographical reasons, DF4b seems superior.

#### APPLICATIONS

##### 1. Fatigue

Bend fatigue tests were performed on duct supports in HA 188 alloy. These pieces were repaired by diffusion brazing after service.

Their fatigue properties were determined at room temperature under stresses which induced failure in a short time. As comparison, tests were performed on new segments in the same conditions (Frequency 1800 RPM, load - 170 to + 560 kg).

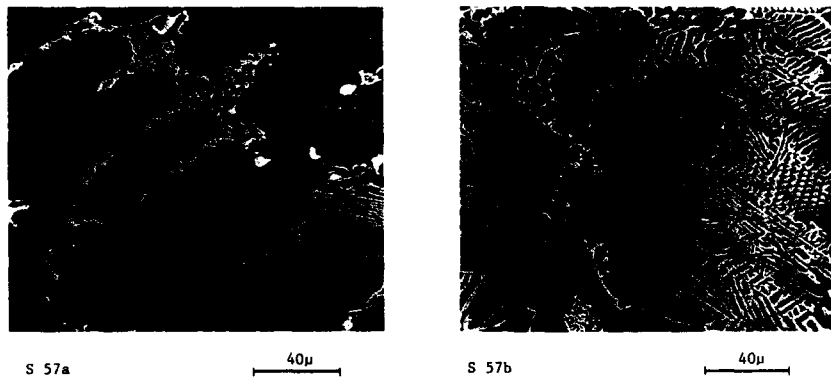


Figure 4 - Microstructures of cobalt brazing alloys

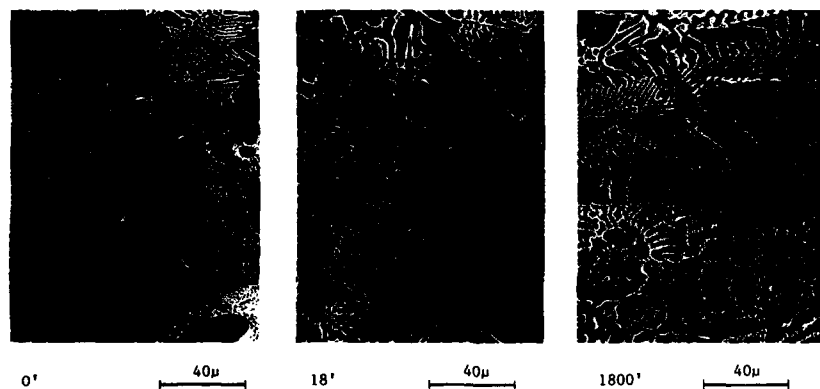


Figure 5 - Influence of diffusion holding time on cobalt S57b braze

The results are summarized in the following table.

	Cycle to crack				
	1	2	3	4	average
New parts	441200	409200	397600	421300	417325
Braze repaired parts	324200	270300	240100	286100	280250

It is to be observed that the number of cycles to crack of repaired blade is about 2/3 of that of a new part, but we must note that surface finish of the new part is fine due to machined grinding, while for the repaired specimen, it is a coarse manual finish which is more detrimental to fatigue testing.

Metallographic examinations were performed on cross cut specimens on a plane perpendicular to the crack direction. New part and repaired part were examined.

The crack propagation is intergranular or transgranular. It can also be observed (figure 8) that the new part have a f.c.c. structure with a fine carbides precipitation in grain boundaries while on repaired specimens the grain boundaries are more marked with a coarse carbides precipitation. This carbide precipitation is due to the service life at high temperature.

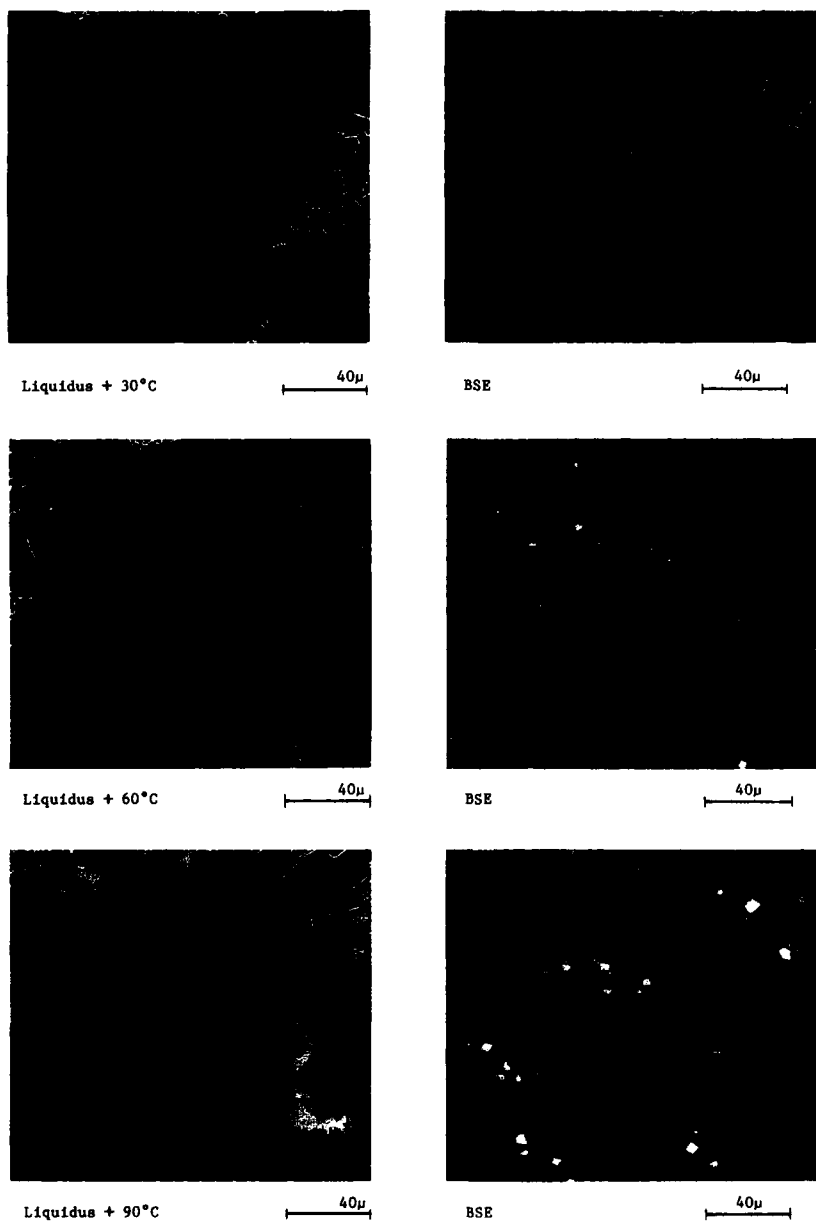


**Figure 6 - Effect of brazing temperature on DF4a braze microstructures**

**2. Thermal shocks**

Fig. 9 shows a picture of the apparatus used to perform the thermal fatigue tests. The specimen is heated to 1000°C in 20 seconds by an oxyacetylenic flame and then cooled at room temperature in 10 seconds by a water jet. The temperature of the piece is measured by an Ircon infrared pyrometer. Meanwhile, internal cooling passages, if present, are maintained at 500°C by a hot air flow.

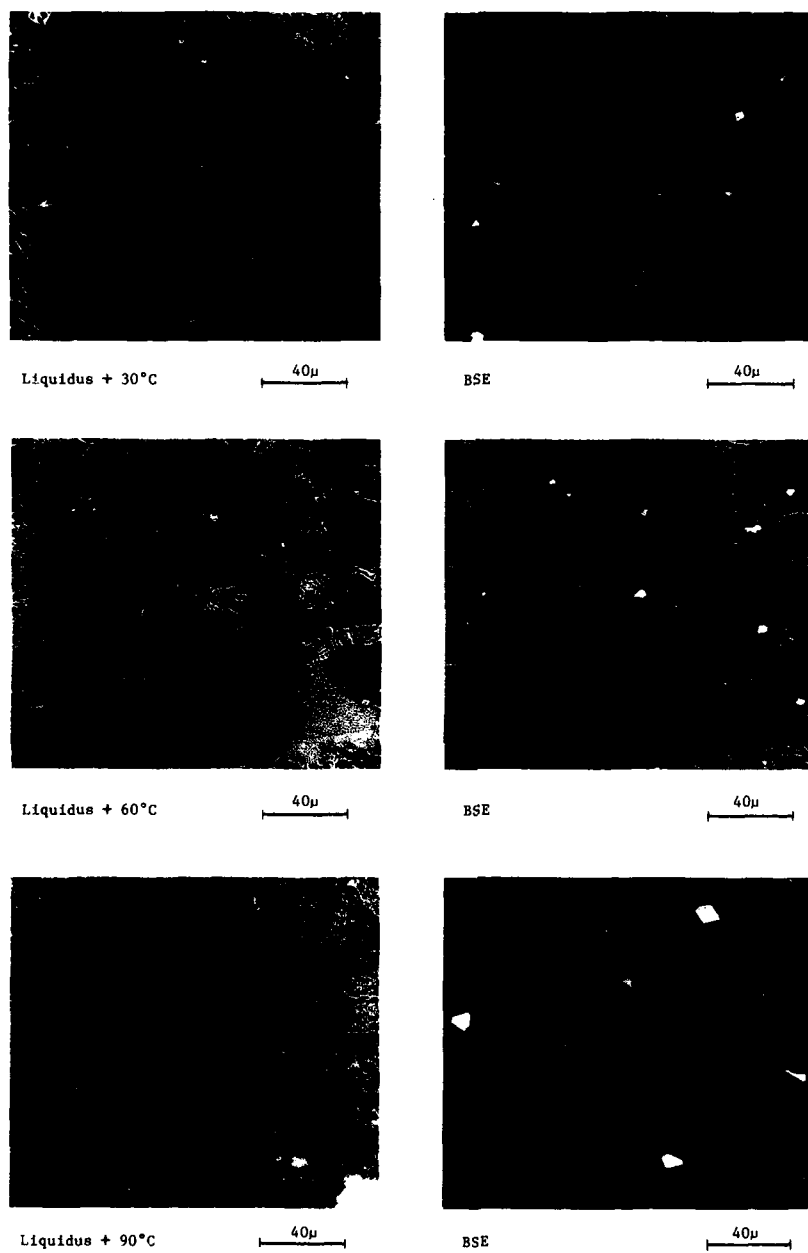


**Figure 7 - Effect of brazing temperature on DF4b braze microstructures**

a) Nozzle guide vane in X-40 alloy : thermal shocks were performed on different vane : new parts, repaired welded parts and diffusion brazing repaired vanes.

The tests were conducted up to 260 cycles with an optical examination each 20 cycles to eventually determine the crack initiation. The crack length was determined by an optical microscope at a magnification of 10x.

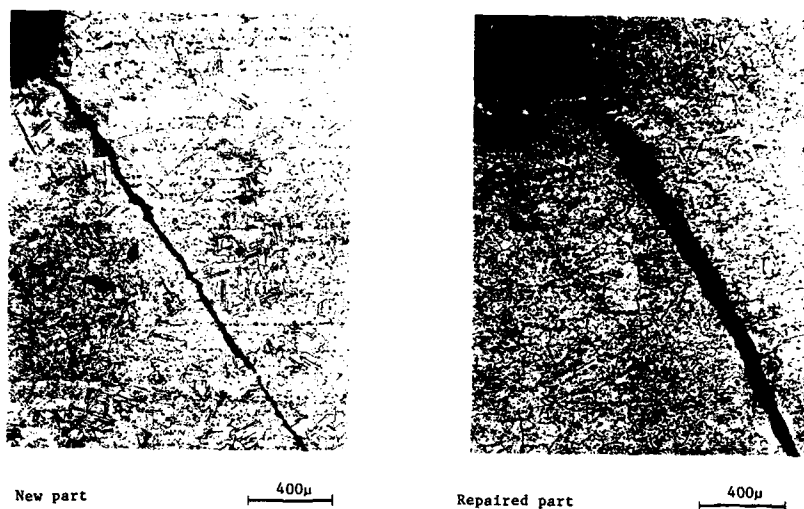


Figure 8 - Cracks in HA188 after fatigue testing

Three vanes of each series were tested. In the case of the repaired brazed vanes two filler brazing metal were used, first a Ni-20Co-2.7B-4.0Si alloy and second a Ni-14Cr-3.3B-4.5Si-4Fe alloy. Table V summarizes the results observed after 260 cycles. This table gives the number of cracks, the cumulated cracks and the average cracks length.

TABLE V

	Number of cracks	Total cracks length (mm)	Average length (mm)
New parts	40	287	7,2
Repaired welded parts	36	168	4,7
Repaired brazed parts alloy II	39	218	5,6

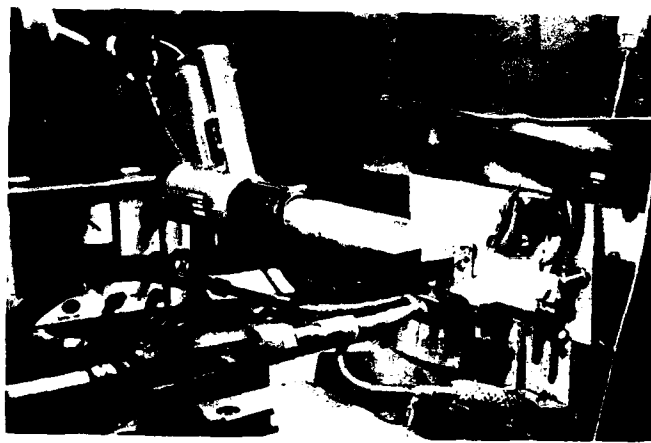


Figure 9 - Thermal shock apparatus

It has been observed that the first brazing filler alloy which does not contain chromium element, has a poor oxidation resistance ; due to this fact, a heavy oxide peels immediately off during the fast cooling giving rise to a large defect on the repaired zone. The results show that the number of cracks, the average crack length and the total crack length are of the same order for the three other types of tested vanes.

Metallographic examinations on a cross section perpendicular to the crack direction for weld repaired vanes and braze repaired blades show that the crack initiation is not related to the repaired cracks.

- b) Nozzle guide vane in Mar-M-200 + Hf: Nozzle guide vanes were submitted to a complete sequence including stripping, cleaning, welding, brazing and recoating.

Thermal shocks were performed on these repaired vanes : test went on until a crack of 1 inch in length is observed perpendicular to the leading edge at the pressure side. Similar tests were performed on new vanes for comparison with the repaired vanes. A Weibull statistical analysis made on the thermal fatigue results gives 254 cycles for the new vanes and 193 cycles for the repaired vanes as warranted minimal value under which no crack will be longer than 25mm.

Metallographic examinations performed in the cracked zone on these two series of vanes revealed (figure 10) that the cracks propagate as well in the repaired area as in not repaired area.

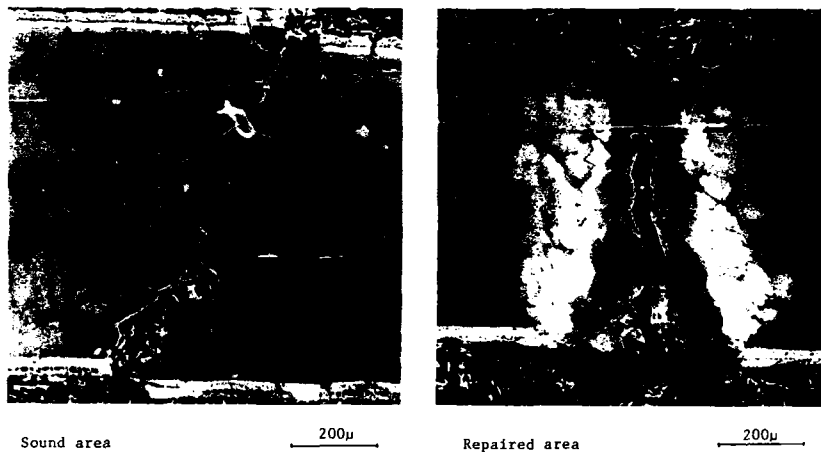


Figure 10 - Repaired vane after thermal shocks

### 3. Field experience

Repaired flameholders were engine tested in flight to verify the acceptability of this repair technique. Four flameholders were so tested. The numbers 1 and 2 are classically weld repaired, number 3 braze repaired, number 4 weld (for cracks wider than 0.5mm) and braze repaired. Before testing, these components were found acceptable, based on dimensional, visual and fluorescent penetrant inspection. It must also be noted that the welded flameholders were found repairable before repair, although the two brazed had to be scrapped because repair was not economical.

The conditions of those four components were monitored by periodic inspections when they were returned to service. The brazed area were found to be in serviceable conditions, after extended engine operations. The results illustrated at Fig.11, indicated that "weld + braze" repair procedure added an acceptable number of hours of service life to the component.

Fig.11 does not show the difference between the crack paths on the repaired components. In fact, after inspection the cracks on flameholder number 1 weld repaired are almost (90%) located in the heat affected zone. On the other hand, on 24 cracks found in flameholder number 4 weld + braze repaired, 12 are located in heat affected zone, 2 in braze and 10 in base metal.

### CONCLUSION

Two important facts result from this study. First, cracks wider than 0.5mm are not always completely filled by braze and have to be repaired by another method. Second, dwell time at diffusion temperature are not as important as supposed. Thus, they can be combined with the other heat treatments of the component.

On another side, it is evident that closer to the base metal composition is the braze analysis, better is the result. This has been demonstrated with the cobalt braze without silicon for HA 188 and with the aluminum containing nickel braze for IN 792.

#### FLAMEHOLDER

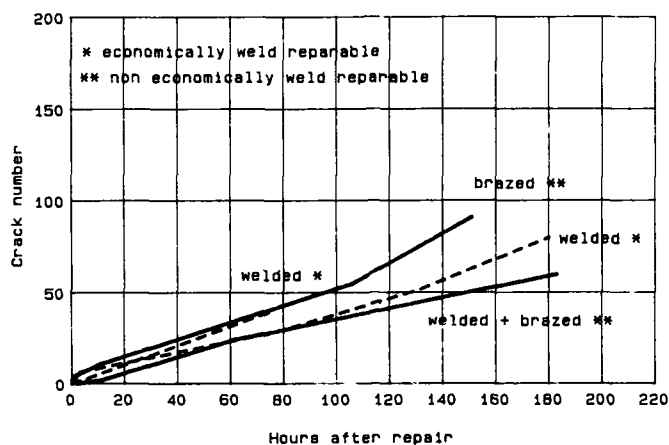


Figure 11 - Effect of service life on repaired parts.

Moreover, in evaluating the acceptability of this repair technique, emphasis must be placed on engine testing and actual service experience of repaired hardware rather than on mechanical specimen testing, because the defects are not only structural.

The development of repair brazing provided a useful and viable method that can be considered as a solution to certain problem. It has also shown itself in many cases as a worth-while alternative to some of the established techniques that are used for repairing parts. The financial benefits alone that are derived from this process are considerable and have more than justified its adoption.

#### REFERENCES

1. O. Knotek, E. Lugscheider. "Brazing filler metals based on reacting Ni-Cr-B-Si alloys". Welding research supplement, 314s-318s, october 1976.
2. F.J. Hermanek, M.J. Stern. "Turbine component restoration by activated diffusion brazing". 84 Westec, Los Angeles, California, March 19-22, 1984. ASM 8407-004.
3. B. Grushko, B.Z. Weiss. "Structure of vacuum brazed BNi-5 joint of Inconel 718". Metallurgical Transactions A, vol.15A, April 1984, 609-620.
4. I. Oestberg, C. Persson. "Braze repair of turbine vanes in cobalt alloys". FFV, Sweden.
5. S.R. Bell. "Repair and rejuvenation procedures for aero gas turbine hot section components". Materials Science and Technology. August 1985, vol.1, 629-634.
6. W. Lee, J.H. Mc Murray, J.A. Miller. "Development of a new brazing technique for repair of turbine engine components". Welding Journal, October 1985, 18-21.
7. A. Davin, Ch. Leconte-Mertens, P. Vierset, P. Louis. "Microstructural damages induced during the repair process ; the influence of service life". Proceedings of "High temperature alloys for gas turbines and other applications". October 6-9, 1986.
8. M. Lamberigts, C. Leconte-Mertens, P. Vierset, P. Louis. "Structural damage rejuvenation of used turbine blades". Proceedings of "High temperature alloys for gas turbines and other applications". October 6-9, 1986.

#### DISCUSSION

R. Thamburaj, Hawker Siddeley, Canada. Your comparison of welding, brazing and welding plus brazing indicates that with conventional welding or brazing you get around 80 cracks at about 150 hours after repair. With welding plus brazing you get about 50-60 cracks. In practical terms, does this difference constitute a useful life extension? Would significant economic benefits be obtained by welding plus brazing as opposed to either welding or brazing alone?

C. Lecomte-Mertens, Centre Recherches Metallurgiques, Belgium. Figure 11 shows that the welded flameholder has around 80 cracks at about 150 hours after repair, and that the welded (for cracks wider than 0.5 mm) plus brazed flameholder has around 50 cracks after the same number of service hours. Moreover, it must be noted that this last flameholder had to be scrapped because the classical weld repair was not economical ( $\pm$  300 cracks).

In addition, it should be noted that cracks in weld repaired flameholders are almost all (90%) located in the heat affected zone. Therefore, if we had repaired the 'welded plus brazed' flameholder by welding alone, we would have had much more than 80 cracks after 150 hours.

In fact, 80 cracks are obtained for a weld repairable flameholder with few cracks before repair. We therefore have to compare 50 cracks for the new method to more than 80 cracks for the classical method. In conclusion, even if the life extension is not considered a useful improvement, the financial benefits alone are sufficient for us to prefer the more economical welding plus brazing repair over the classical, more expensive weld repair, especially when we are dealing with a large number of cracks.

R. Thamburaj, Hawker Siddeley, Canada. Have you considered applying any cobalt-based braze alloys to nickel-based parent material?

C. Lecomte-Mertens, Centre Recherches Metallurgiques, Belgium. We conducted tests applying nickel-based braze alloy to cobalt-based parent material, but not the opposite.

REPORT DOCUMENTATION PAGE			
<b>1. Recipient's Reference</b>	<b>2. Originator's Reference</b>	<b>3. Further Reference</b>	<b>4. Security Classification of Document</b>
	AGARD-CP-449	ISBN 92-835-0498-4	UNCLASSIFIED
<b>5. Originator</b>	Advisory Group for Aerospace Research and Development North Atlantic Treaty Organization 7 rue Ancelle, 92200 Neuilly sur Seine, France		
<b>6. Title</b>	APPLICATION OF ADVANCED MATERIAL FOR TURBOMACHINERY AND ROCKET PROPULSION		
<b>7. Presented at</b>	the Propulsion and Energetics Panel 72nd Specialists' Meeting, held in Bath United Kingdom, 3—5 October 1988.		
<b>8. Author(s)/Editor(s)</b>	Various		<b>9. Date</b> March 1989
<b>10. Author's/Editor's Address</b>	Various		<b>11. Pages</b> 296
<b>12. Distribution Statement</b>	This document is distributed in accordance with AGARD policies and regulations, which are outlined on the Outside Back Covers of all AGARD publications.		
<b>13. Keywords/Descriptors</b>	Turbomachinery Rocket engines Spacecraft propulsion	Aircraft engines Heat resistant materials	
<b>14. Abstract</b>			
<p>The Conference Proceedings contain 25 papers presented at the Propulsion and Energetics Panel 72nd-A Specialists' Meeting on 'Application of Advanced Material for Turbomachinery and Rocket Propulsion', which was held 3—5 October 1988 in Bath, UK.</p> <p>The Specialists' Meeting was arranged in the following sessions: Overview and Combined Applications (3); Gas Turbine Applications (11); Rocket Applications (7); and Special Applications (4). The Technical Evaluation Report is included at the beginning of the Proceedings. Questions and answers of the discussions follow each paper.</p> <p>The aim of the Specialists' Meeting was to review the advances made in the field of material applicable in the hot parts of aerospace propulsion systems during the last few years. The Specialists' Meeting offered a forum for the users of new material in the fields of turbomachines and rockets to report on recent achievements and to discuss the various applications. The Specialists' Meeting also stimulated the information exchange between the turbomachinery and the rocket community.</p>			

<p><b>AGARD Conference Proceedings No.449</b>  <b>Advisory Group for Aerospace Research and Development, NATO</b>  <b>APPLICATION OF ADVANCED MATERIAL FOR TURBOMACHINERY AND ROCKET PROPULSION</b>  <b>Published March 1989</b>  <b>296 pages</b></p>	<p><b>AGARD-CP-449</b>  Turbomachinery  Rocket engines  Spacecraft propulsion  Aircraft engines  Heat resistant materials</p> <p>The Conference Proceedings contain 25 papers presented at the Propulsion and Energetics Panel 72nd-'A Specialists' Meeting on 'Application of Advanced Material for Turbomachinery and Rocket Propulsion', which was held 3-5 October 1988 in Bath, UK.</p> <p>The Specialists' Meeting was arranged in the following sessions: Overview and Combined Applications (3); Gas P.T.O.</p>	<p><b>AGARD Conference Proceedings No.449</b>  <b>Advisory Group for Aerospace Research and Development, NATO</b>  <b>APPLICATION OF ADVANCED MATERIAL FOR TURBOMACHINERY AND ROCKET PROPULSION</b>  <b>Published March 1989</b>  <b>296 pages</b></p>	<p><b>AGARD-CP-449</b>  Turbomachinery  Rocket engines  Spacecraft propulsion  Aircraft engines  Heat resistant materials</p> <p>The Conference Proceedings contain 25 papers presented at the Propulsion and Energetics Panel 72nd-'A Specialists' Meeting on 'Application of Advanced Material for Turbomachinery and Rocket Propulsion', which was held 3-5 October 1988 in Bath, UK.</p> <p>The Specialists' Meeting was arranged in the following sessions: Overview and Combined Applications (3); Gas P.T.O.</p>
<p><b>AGARD Conference Proceedings No.449</b>  <b>Advisory Group for Aerospace Research and Development, NATO</b>  <b>APPLICATION OF ADVANCED MATERIAL FOR TURBOMACHINERY AND ROCKET PROPULSION</b>  <b>Published March 1989</b>  <b>296 pages</b></p>	<p><b>AGARD-CP-449</b>  Turbomachinery  Rocket engines  Spacecraft propulsion  Aircraft engines  Heat resistant materials</p> <p>The Conference Proceedings contain 25 papers presented at the Propulsion and Energetics Panel 72nd-'A Specialists' Meeting on 'Application of Advanced Material for Turbomachinery and Rocket Propulsion', which was held 3-5 October 1988 in Bath, UK.</p> <p>The Specialists' Meeting was arranged in the following sessions: Overview and Combined Applications (3); Gas P.T.O.</p>	<p><b>AGARD Conference Proceedings No.449</b>  <b>Advisory Group for Aerospace Research and Development, NATO</b>  <b>APPLICATION OF ADVANCED MATERIAL FOR TURBOMACHINERY AND ROCKET PROPULSION</b>  <b>Published March 1989</b>  <b>296 pages</b></p>	<p><b>AGARD-CP-449</b>  Turbomachinery  Rocket engines  Spacecraft propulsion  Aircraft engines  Heat resistant materials</p> <p>The Conference Proceedings contain 25 papers presented at the Propulsion and Energetics Panel 72nd-'A Specialists' Meeting on 'Application of Advanced Material for Turbomachinery and Rocket Propulsion', which was held 3-5 October 1988 in Bath, UK.</p> <p>The Specialists' Meeting was arranged in the following sessions: Overview and Combined Applications (3); Gas P.T.O.</p>

<p>Turbine Applications (1); Rocket Applications (7); and Special Applications (4). The Technical Evaluation Report is included at the beginning of the Proceedings. Questions and answers of the discussions follow each paper.</p> <p>The aim of the Specialists' Meeting was to review the advances made in the field of material applicable in the hot parts of aerospace propulsion systems during the last few years. The Specialists' Meeting offered a forum for the users of new material in the fields of turbomachines and rockets to report on recent achievements and to discuss the various applications. The Specialists' Meeting also stimulated the information exchange between the turbomachinery and the rocket community.</p>	<p>Turbine Applications (1); Rocket Applications (7); and Special Applications (4). The Technical Evaluation Report is included at the beginning of the Proceedings. Questions and answers of the discussions follow each paper.</p> <p>The aim of the Specialists' Meeting was to review the advances made in the field of material applicable in the hot parts of aerospace propulsion systems during the last few years. The Specialists' Meeting offered a forum for the users of new material in the fields of turbomachines and rockets to report on recent achievements and to discuss the various applications. The Specialists' Meeting also stimulated the information exchange between the turbomachinery and the rocket community.</p>	<p>Turbine Applications (1); Rocket Applications (7); and Special Applications (4). The Technical Evaluation Report is included at the beginning of the Proceedings. Questions and answers of the discussions follow each paper.</p> <p>The aim of the Specialists' Meeting was to review the advances made in the field of material applicable in the hot parts of aerospace propulsion systems during the last few years. The Specialists' Meeting offered a forum for the users of new material in the fields of turbomachines and rockets to report on recent achievements and to discuss the various applications. The Specialists' Meeting also stimulated the information exchange between the turbomachinery and the rocket community.</p>
<p>ISBN 92-835-0498-4</p>	<p>ISBN 92-835-0498-4</p>	<p>ISBN 92-835-0498-4</p>